CHARACTERISATION AND OPTIMISATION OF BIOFILM AND PELLICLE FORMATION BY *ESCHERICHIA COLI* K-12

By

Stacey Ruth Golub

A thesis is submitted to the University of Birmingham for the degree of DOCTOR OF PHILOSOPHY

School of Chemical Engineering

College of Engineering and Physical Sciences

University of Birmingham

July 2019

ABSTRACT

Bacteria form biofilms on solid surfaces by using surface adhesins and by secreting extracellular matrix components. While many biofilms are harmful, for example in clinical and industrial settings, biofilms have been shown to improve yield in biocatalysis reactions generating pharmaceutical precursors. In this work, biofilm formation was studied in *Escherichia coli* K-12 PHL644, which is a known biofilm-forming strain that has been previously used for biocatalysis. In order to generate a physically robust biofilm, promoter-green fluorescent protein reporters were used to optimise the expression of curli, an adhesin important in biofilm formation, in response to a variety of stimuli and physical conditions. Curli expression was greatest in planktonic cells grown in minimal medium supplemented with 10 mM glucose at 30 °C and 70 rpm shaking. The effect of aromatic amino acids on biofilm formation was investigated, and the addition of phenylalanine to cultures was found to increase curli expression and optical density. It was hypothesised that phenylalanine forms amyloid-like fibres which seed curli formation in *E. coli*; however this needs to be investigated further. Potentially, phenylalanine may be used to make biofilm formation a tuneable system. During work to further improve biofilm formation, a biofilm floating at the air-liquid interface, called a pellicle, was observed. *E. coli* K-12 pellicle formation was optimised and characterised in terms of curli expression, motility, and secretion of matrix components and it was found that pellicle formation requires curli. The potential for a biofilm at the air-liquid interface may be advantageous in certain industrial settings.

DEDICATION

I dedicate this entire body of work to my ever-growing family; as with you, this thesis is now a part of me.

To my husband, Callum. A person who has encouraged my dreams as wildly as I encouraged his. I am continued to be struck by your kindness, your understanding, and your passion. The bounds of my love for you are endless.

To my entire family, especially my mother, Ruth, my father, Sandy, and my big brother, Scott, thank you- for everything. For traveling across the Atlantic multiple times to visit me, your unwavering support and for loving me my entire life. Everything good in me was cultivated by you all and I wouldn't be here without you. Words cannot express my gratitude that I have for you, and the fact that I have the best family on the planet.

To my mentor, my big sister, Kristina, for teaching (making) me dream bigger than I was capable of. Without you, I would have never realized my full potential, I would have never gone to graduate school and this thesis would not exist.

To my English mother and father, Dawn and Glen, thank you for everything. Moving to England to achieve this life goal was a dream come true, and I couldn't have done it without you.

To Allison, Collins, Pratt, Fluter, Nagesh, and Charalambous: because every woman needs her own family of amazing women supporting her, defending her, befriending her, cheering for her, and never giving up on her. You all inspire me, and I cannot fathom my life without you. I dedicate this work to you.

And lastly, I dedicate this thesis to women everywhere. This is just but a pebble thrown at the injustice that women, especially women of color and transwomen, face every day. We are not encouraged to enter STEM, we face more scrutiny, and in 2019 we make on average $0.79 to every man's dollar. I am your ally in this struggle. This dedication to you is my vow that I will continue to fight for equal opportunity to education, and I will continue to learn and become a better advocate for you; I will speak up for women without my privilege; and lastly when it is right, I promise to shut up as to not blow away those as they rise.

“We must have perseverance and above all confidence in ourselves. We must believe that we are gifted for something and that this thing must be attained.”

Marie Curie

ACKNOWLEDGEMENTS

I would like to thank my advisor, Dr. Tim Overton, for his guidance and wisdom as well as his endless support. Tim (I finally said it), thank you for the collaboration and for all the conversations about cats. I am truly lucky to have you as my mentor.

None of the work in this thesis could have been achieved without the incredible help of the biochemical engineering technical staff, but I wouldn't have gotten through it with the unwavering support and assistance by the brilliant 'lab moms': Ronnie and Elaine. We would be lost without you.

As with Ronnie and Elaine, I want to thank all my friends in the G20 office past and present, especially those in the Overton research group. You made my time at University of Birmingham unforgettable. Thank you for all your help and most importantly your friendship. You made "the tall American girl" so at home.

I would like to acknowledge the hard work of the master students Rob Millar and Jay Sangha as well as the visiting PhD student, Audum Chhun. I would like to thank Alessandro Di Maio for guidance on the confocal microscope and James Leech for his curli reporter plasmid.

CONTENTS

LIST OF TABLES

LIST OF FIGURES

LIST OF APPENDICES

1 INTRODUCTION

1.1 Biofilms and pellicles

1.1.1 Bacterial biofilms

Contrary to the common conception that bacteria exist singularly and free-floating, bacteria tend to adhere and grow together in a structured communal matrix, called a biofilm (Hall-Stoodley, Costerton and Stoodley, 2004). A biofilm can develop on biotic or abiotic surfaces and consists of single or multiple species of bacteria or other microbes bound together by surface appendages and a self-secreted matrix (Eboigbodin and Biggs, 2008; Coenye and Nelis, 2010; Hufnagel, Depas and Chapman, 2015). Compared to free-floating or planktonic cells, the cells within the biofilm matrix are able to withstand mechanical forces (such as shear), unideal temperatures, changes in pH, nutrient deprivation, exposure to radiation, and antibiotics (Yang *et al*., 2011; Stewart, 2014; Singh *et al*., 2017). While biofilms are notorious in the medical industry as major causes of infection, antibiotic resistance, and death, there is an established and growing industry that utilise biofilms in a variety of applications (Rosche *et al*., 2009; Dewasthale, Mani and Vasdev, 2018).

While a biofilm is most often defined as solid surface-attached, there are suspended filamentous biofilms, called streamers, and biofilms capable of forming at the air-liquid interface, called pellicles (Rusconi *et al.*, 2010). While it is assumed pellicles are a type of biofilm and thus are comprised of the same components, it appears there are differences in the resulting biofilm architecture between a submerged biofilm and a pellicle formed at the air-liquid interface (Hung *et al.*, 2013). As with solid surface-attached biofilms, the role of motility, oxygen tension, shaking, and extracellular organelles appear to also be important in pellicle formation (Andersson *et al.*, 2013).

1.1.2 Biofilm for use in industry

While much of the current biofilm research focuses on prevention and removal of biofilms that plague industries because of their resilient and robust nature, this characteristic has made them ideal for use in harsh conditions where the focus is to improve reactor output by protecting the biocatalytic activity of the cell (Costerton *et al.*, 1994; Winn *et al.*, 2012). Biocatalysis is the use of bacteria and other microbes as living factories; the enzymes within the cell are used to catalyse chemical reactions in order to make a desired product (Sheldon and Woodley, 2018). The potential for biocatalysis is limitless as research is already investigating novel methods to engineer recombinant *Escherichia coli* to produce ethanol as a biofuel, to be used in fuel cells to generate electricity, or to biocatalyse the capture of harmful CO_2 greenhouse gases (Zhang *et al.*, 2007; Shin *et al.*, 2010; Jo *et al.*, 2013). The use of biofilms as a means of protecting cells as they catalyse reactions is also already employed in many scenarios from wastewater treatment and bioremediation to engineering bacteria for the manufacture of various desirable products, such as the compound precursor molecule halotryptophan (Chang and Keasling, 2006; Tsoligkas *et al.*, 2011; Edwards and Kjellerup, 2013; Maksimova, 2014; Ercan and Demirci, 2015). However, as the need for renewable fuels and environmental-friendly chemical and pharmaceutical production increases, so does the importance of further developing this biochemical technology and optimising current practices (Davis, Peters and Caldeira, 2011). Furthermore, the search to find new methods in order to produce more robust biofilms is still in high demand and is therefore still studied (Coenye and Nelis, 2010).

1.1.3 General steps and key constituents

In addition to protection from unfavourable environments, biofilms form to colonise favourable environments and to provide better opportunities for cells. The biofilm creates a bacterial community in which the microbes have the opportunity to exchange genetic material, divide and share metabolic activities, and coordinate gene expression (Li and Tian, 2012). Regardless of the mechanism behind biofilm formation, the bacteria must communicate (via quorum sensing) and coordinate in order to collectively change gene transcription and form a biofilm (Costerton *et al.*, 1995).

Different species of bacteria differ significantly on the exact mechanism of biofilm formation and the resulting biofilm architecture and components. However, there are five general steps necessary to form a biofilm (Fig 1.1): initial reversible attachment; irreversible attachment or adhesion; growth and production of matrix by major EPS secretion; maturation; and dispersion (Palmer, Flint and Brooks, 2007; García-Contreras *et al.*, 2008). All of these steps are dependent on the bacteria's environment, which can greatly affect the expression of required genes and other factors necessary for biofilm formation. Some commonly-studied biofilm-forming species include *Streptococcus pneumonia*, *Salmonella typhimurium*, *Pseudomonas aeruginosa*, *Bacillus subtilis*, and *Escherichia coli*, which require different components and regulatory mechanisms in order to form a biofilm (Davey and O'toole, 2000; Römling and Balsalobre, 2012).

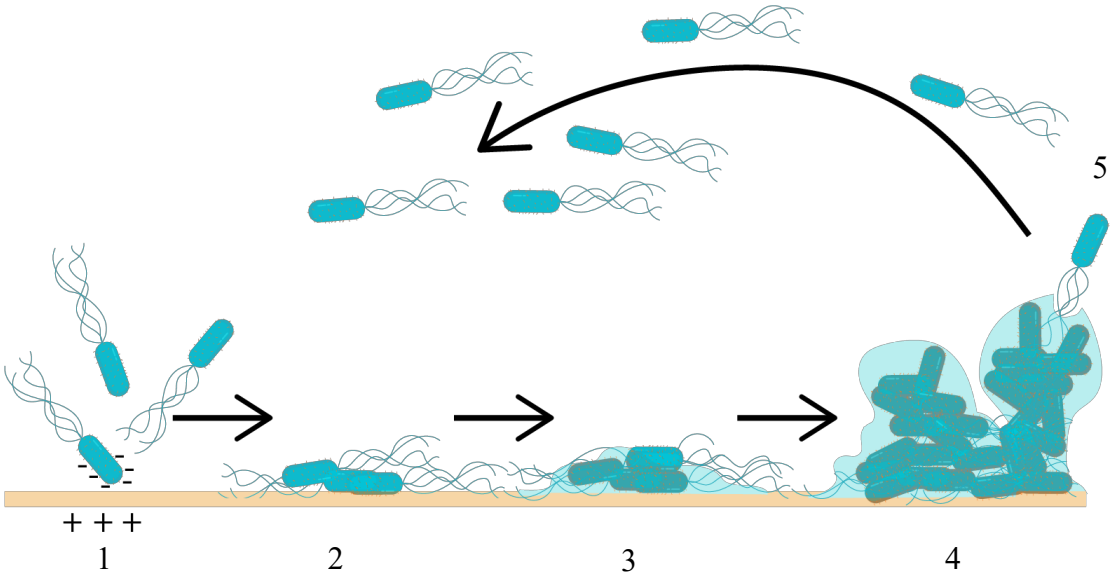

Figure 1.1: Diagram of biofilm formation.

Biofilm formation is generally comprised of five steps: reversible attachment of the cells which involves electrostatic forces (among others); irreversible attachment; secretion of matrix components (light blue); maturation; and dispersion.

The first step of reversible attachment is the act of a cell localising to the surface or zone where the biofilm will form. This step is facilitated by motility via flagellar movement, swarming and/or twitching motility along a solid surface. While motility has been shown to be important in biofilm formation, it is not essential as cells use passive mobility in order to come into contact with a surface. Passive mobility can occur by the natural movement of particles in a fluid (Brownian motion), hydrodynamic forces, and fluid flow by agitation or shaking. The irreversible attachment of a cell to the surface has been found to be a crucial step in order to form a solid surface-attached biofilm. This step can be mediated through a variety of extracellular appendages and adhesins, such as the amyloid fimbriae curli described in section 1.2.2.1 (Reisner *et al.*, 2003). The next step after irreversible attachment is the secretion of Extracellular Polymeric Substances (EPS) to form the matrix. As the matrix forms, the biofilm takes on more defined structure and architecture, which can change shape depending upon the presence of extracellular appendages, such as the flagella. Maturation will continue until

the biofilm is triggered to disperse. Dispersion can occur in two ways: actively, by changing gene expression within the cell, such as increasing levels of the global regulator CsrA that positively regulates motility genes and represses genes for matrix secretion; or passively by the natural sloughing off of cells by shear force and other outside factors (Jackson *et al.,* 2002; Kaplan, 2010).

Alternatively, to solid surface-attached biofilm, pellicles are a subset of biofilms found at the air-liquid interface and thus form differently. A pellicle formation model (Fig. 1.2) by Armitano and colleagues proposed that first cells need to localise to the air-liquid interface (Armitano, Méjean and Jourlin-Castelli, 2014). Next, cells will either attach to the solid surface at air-liquid interface (vessel wall) and grow outward, or cells will form "raft-like" aggregates on the air-liquid interface which will eventually grow together. While pellicle formation is often studied in Gram positive species such as *Bacillus* subtilis, there are Gram negative bacteria, such as *Pseudomonas*, *Salmonella* and *Vibrio* species, among others, that have also been studied for their ability to form a pellicle. The few reports of *E. coli* pellicle formation focus mainly on uropathogenic *E. coli* (UPEC) and enteropathogenic *E. coli* (EPEC), but less is known about *E. coli* K-12 pellicle formation (Lim, May and Cegelski, 2012; Wu *et al*., 2012, 2013).

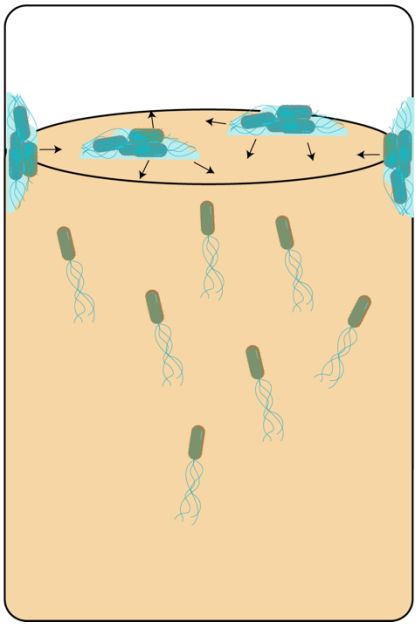

Figure 1.2: Diagram of pellicle formation.

In order to form a pellicle, cells must localise to the air-liquid interface by either active motility or passive movement. Once at the air-liquid interface, it has been proposed that cells either attach to the solid surface at the air-liquid interface and grow outward onto the medium, or cells form floating aggregates which grow together, or both. Diagram is based off model proposed by Armitano and colleagues.

The first step of pellicle formation requires cells to localise at the air-liquid interface. This step is thought to require flagellar motility in most strains and is likely stimulated by the oxygen rich environment at this phase. After localising to the air-liquid interface, the cells multiply, secrete EPS, and form a confluent pellicle. The pellicle will continue to mature and form architecture unique to the bacterial strain. Lastly, similarly to biofilm formation, cells will disperse from the pellicle. Despite some differences between biofilms and pellicles, pellicle formation involves many of the same EPS components and gene regulation as biofilm formation, which has led to the assertion that pellicles are a type of biofilm in a specific ecological niche but need to be studied further (Hung *et al.*, 2013). Research of each step of biofilm and pellicle formation, their components, and the genetics driving the individual systems has revealed a diverse network of complex gene regulation, environmental factors, and signalling, which is discussed later in this introduction.

1.1.4 Physical Conditions

There are many physical and environmental conditions that affect biofilm and pellicle formation (Van Houdt and Michiels, 2005; Renner and Weibel, 2011). While less is known about how these conditions affect pellicle formation, it can be assumed that they are similar to those found in biofilm formation, but this needs to be studied further. In the early stages of biofilm formation, the cell approaches a surface and encounters a number of forces, including electrostatic forces and hydrophobic interactions (Ong *et al.*, 1999). Electrostatic force occurs because both the cell and surface are charged; most bacterial cells, including *E. coli*, are often negatively charged, and thus will experience repulsive forces from negatively charged surfaces and attractive forces to positively charged surfaces (Oh *et al.*, 2007). A hydrophobic surface

will repel water molecules, thus other hydrophobic, nonpolar particles and microorganisms will preferentially bind to this surface (Krasowska and Sigler, 2014). Physical conditions that affect biofilm and pellicle formation also include surface topology; other small interactive forces, such as van der Waals; surface conditioning by molecules and proteins in the medium; and the presence of adhesins on the cell surface (Tuson and Weibel, 2013). Furthermore, temperature and carbon source/nutrient availability also affect biofilm formation and the interaction of all these forces and variables is complex and still not fully understood (Karunakaran *et al.*, 2011).

Generally, *E. coli* K-12, a common laboratory strain, preferentially binds to rough, hydrophobic surfaces; rough surfaces promote bacterial-surface interactions and increase the area on which cells can bind, while hydrophobic surfaces absorb protein which precondition the surface and attract hydrophobic bacterial cells (Lüdecke *et al*., 2014). Moderately or highly hydrophobic bacterial cells, such as *E. coli*, adhered less to hydrophilic materials, such as glass with a water contact angle of ~32°, and more to hydrophobic materials, such as Polytetrafluoroethylene (PTFE) with a water contact angle of ~113.2° (Lüdecke *et al.*, 2014). Additionally, the hydrophobic appendages of *E. coli* K-12, such as type 1 fimbriae and flagellum cause the cell to preferentially bind to hydrophobic surfaces and promote bacterial-surface interactions (Rodrigues and Elimelech, 2009; Friedlander, Vogel and Aizenberg, 2015). Spatial observations of *E. coli* biofilms noted key areas of tangled flagella which indicates these surface organelles may also have a role in the biofilm matrix as well (Serra, Richter and Hengge, 2013). Mobility by orbital shaking and Brownian motion is also important in biofilm formation as it reduces the need of motility by flagellar motion and helps the cell overcome repulsive van der Waals or electrostatic forces. In addition, mobility can increase shear during bacterial-surface interactions, which increases bacterial rolling and surface

contact and has been shown to increase cell surface attachment (Frymier *et al.*, 1995; Liu and Tay, 2002a; Li, Tam and Tang, 2008; Hölscher *et al.*, 2015).

1.2 *Escherichia coli* and biofilm components

1.2.1 Escherichia coli

Escherichia coli is a rod-shaped Gram negative facultative anaerobe predominant in the gastrointestinal tract of warm blooded animals (Conway and Cohen, 2015). Over time, *E. coli* has become a preferred model organism in research ranging from genetics to molecular biology, in part because it is relatively easy and inexpensive to grow and maintain (Son and Taylor, 2012). Additionally, it was the first bacteria to have its genome completely sequenced (Blattner *et al.*, 1997). There are numerous commensal and pathogenic strains and serotypes of *E. coli* and due to this diversity and its robust nature, it can survive in ecological niches in various environments (Katouli, 2010). One such survival method is the formation of a biofilm on biotic, such as an intestinal wall, and abiotic surfaces, such as plastic, and the formation of pellicles at the air-liquid interface as a means of colonisation and/or survival in unideal environments (Jefferson, 2004). To form a biofilm or pellicle, *E. coli* employs surface organelles and EPS matrix components, which is described in the following sections.

1.2.2 Surface organelles of *E. coli*

1.2.2.1 Curli fimbriae

Curli fimbriae are an extracellular amyloid protein ranging from 0.5 to 1.0 μm in length and aid in bacterial attachment to a surface and to other cells which promotes biofilm formation (Tuson and Weibel, 2013). Curli fimbriae are also important in

pellicle formation as UPEC and many EPEC strains require the formation of curli as a means of adhesion and structural support (Hung *et al.*, 2013; Wu *et al.*, 2013; Eberly *et al.*, 2017). While the cross-β structure of amyloid protein is notoriously known for misfolding and its toxic aggregative nature which can lead to neurological disease, there are types of amyloid, like curli, folded into specific structures known as "functional amyloid" (Fowler *et al*., 2007). Not only do curli play a crucial role during irreversible attachment of *E. coli* to a surface during biofilm formation, studies have shown they also influence the biofilm's three-dimensional structure (Kikuchi *et al*., 2005). For these reasons, curli are studied at length in this research. Two operons, *csgBAC* and *csgDEFG*, are required for curli synthesis (Fig. 1.3). The highly-aggregative major subunit, CsgA, is secreted from the cell where it is nucleated and assembled by the minor subunit, CsgB (Hammar, Bian and Normark, 1996). The protein sequence of CsgA and CsgB, respectively:

MKLLKVAAIA AIVFSGSALA GVVPQYGGGG NHGGGGNNSG
PNSELNIYQY GGGNSALALQ TDARNSDLTI TQHGGGNGAD
VGQGSDDSSI DLTQRGFGNS ATLDQWNGKN SEMTVKQFGG
GNGAAVDQTA SNSSVNVTQV GFGNNATAHQ Y

MKNKLLFMML TILGAPGIAA AAGYDLANSE YNFAVNELSK
SSFNQAAIIG QAGTNNSAQL RQGGSKLLAV VAQEGSSNRA
KIDQTGDYNL AYIDQAGSAN DASISQGAYG NTAMIIQKGS
GNKANITQYG TQKTAIVVQR QSQMAIRVTQ R

CsgA consists of 10 negatively charged residues (aspartate and glutamate), and 6 positively charged residues (arginine and lysine). There are 4 phenylalanine residues in CsgA, which makes up 2.6% of the total composition. CsgB consists of 8 negatively charged residues (aspartate and glutamate), and 13 positively charged residues (arginine and lysine). There are 3 phenylalanine residues in CsgB, which makes up 2.0% of the total composition.

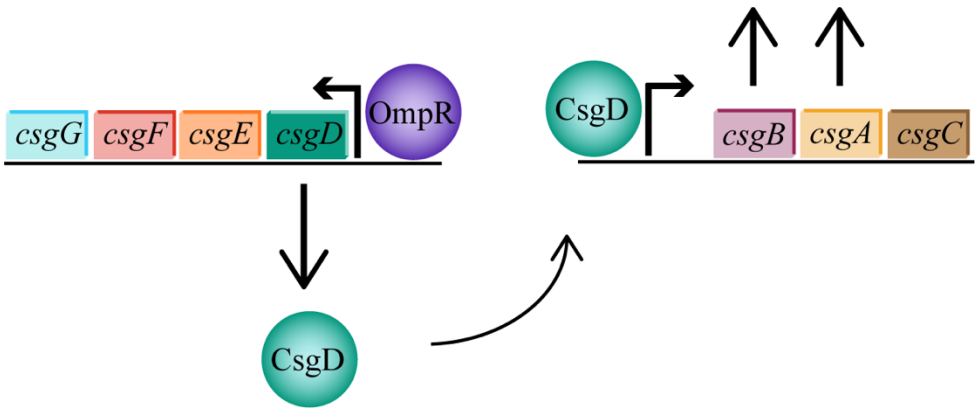

Figure 1.3: Diagram of the genes and proteins necessary for curli expression. OmpR binds to the *csgDEFG* promoter to regulate expression. CsgD, the master curli regulator, binds upstream of *csgBA* and increases expression. Both operons are subject to complex regulation.

Before secretion of CsgA across the membrane, CsgC functions to prevent misfolding of CsgA (Evans *et al*., 2015). Interestingly, CsgA can assemble into functional amyloid fibres without CsgB *in vitro* or by the CsgB of neighbouring cells (Wang *et al*., 2006). Furthermore, amyloid fibres have been shown to have a "seeding" effect on one another, in which subunits will nucleate in the presence of aggregated amyloid (Harper and Lansbury, 1997; Hu *et al.*, 2009). The operon *csgDEFG* is required to produce accessory proteins needed for curli production; CsgD is considered a master biofilm regulator as it is required to regulate *csgBAC* among other genes important to biofilm formation, such as motility (Dudin *et al*., 2014). OmpR is required for production of CsgD. Inside the cell, CsgE helps stabilise and direct soluble CsgA

towards CsgG in the membrane to be secreted across the membrane as an unstructured protein (Andersson *et al*., 2013). On the surface of the cell, CsgG along with CsgF are required for secretion of CsgA and localisation of stable CsgB on the outside of the cell so that it can nucleate CsgA monomers into fibres and anchor it to the cell, which is also known as precipitation-nucleation secretion, or Type VIII secretion (Nenninger, Robinson and Hultgren, 2009, Evans and Chapman, 2014).

The genetic regulation of curli is multifaceted and greatly influenced by the environment, making it a complex and difficult system to understand. Generally, curli are known to be produced maximally in cells in stationary phase and grown aerobically at temperatures less than 30 ºC in minimal media with low glucose concentrations and low salt concentrations (Barnhart and Chapman, 2006). Alternatively, it is important to note that microaerophilic environments were reportedly best for curli production in rich medium (Gerstel, Park and Römling, 2004). Two pathways, CpxAR and Rcs, have been purported to downregulate *csgD* and curli synthesis upon surface attachment (Otto and Silhavy, 2002; Kimkes and Heinemann, 2018). CpxAR has also been shown to downregulate curli expression in high osmolarity, while the EnvZ/OmpR cascade upregulates *csgD* and curli expression in low osmolarity (Raivio and Silhavy, 1997; Dorel *et al.*, 1999). Each of these pathways are described in depth in section 1.3 *E. coli* K-12 biofilm regulation.

1.2.2.2 Antigen 43

Antigen 43 is an autotransporter protein found on the surface of numerous Gram negative bacteria and in most *E. coli* species and is responsible for cell-cell aggregation and autoagglutination (Kjargaard *et al*., 2000). While the aggregative nature of Ag43 has been shown to aid in biofilm formation and plays a role in the three-dimensional architecture, it is not essential in order to form a biofilm (Reisner *et al*., 2003). There are also studies that show that Ag43 can aid in pellicle formation, but are not required in the presence of other surface adhesins (Hasman, Schembri and Klemm,

2000). Ag43 protein is encoded by the *flu* gene and is comprised of an alpha (exposed on the surface) and beta-domain (anchors the alpha-domain) in a distinct L-shape which allows for binding to other Ag43 proteins in a head-to-tail "Velcro-like" manner (van der Woude and Henderson, 2008; Heras *et al.*, 2014). One of the two *E. coli* sensors involved in oxidative stress response, OxyR, was found to repress the *flu* gene by binding to the promoter region, but only when OxyR is in its most common, reduced form (Schembri *et al*., 2003). During moments of oxidative stress, OxyR is oxidised and activated and no longer represses *flu*, indicating that oxidative stress may cause cells to produce Ag43 and form a biofilm (Danese *et al*., 2000). In addition to regulation by OxyR, Ag43 has also been found to be phase variable and can be found in either the "ON" or "OFF" state depending on if the enzyme deoxyadenosine (DAM) methylase or OxyR is recruited to the gene, respectively, after DNA replication (Correnti *et al*., 2002). Studies have shown that phase switching is mainly due to OxyR blocking transcription and can only be relieved after DNA replication and subsequent methylation of the OxyR-binding region by DAM to prevent OxyR binding (Waldron, Owen and Dorman, 2002). While any population of *E. coli* can have cells in either the "ON" or "OFF" state, the majority of cells in biofilms are in the "ON" state, which supports that Ag43 plays a role in biofilm formation (Chauhan *et al*., 2013). However, this is not studied heavily in the following work.

1.2.2.3 Other surface organelles: type 1 fimbriae, F pilus and flagella

In addition to curli fimbriae and antigen 43, there are other surface organelles of note that aid in *E. coli* biofilm formation, such as type 1 fimbriae, conjugative F pilus, and flagella. Type 1 fimbriae and F fimbriae are adhesins and have been shown to aid in irreversible attachment, while flagella typically aid in motility and assist with

early stages of biofilm formation. Although, there have been reports that flagella can help the cell in binding to hydrophobic surfaces and may play a role in the biofilm matrix (Friedlander *et al.*, 2013; Serra, Richter and Hengge, 2013; Friedlander, Vogel and Aizenberg, 2015). All three surface organelles will be discussed in detail in this section.

Type 1 fimbriae are filamentous rods ranging from 0.2 to 3.0 µm long made primarily of repeating FimA units, but with a tip comprised of FimF protein, FimG protein and a FimH adhesin (Jones *et al*., 1995). The FimH adhesin is a lectin located on the outermost end of the tip and is comprised of two domains, one bound to the pili rod and one receptor-binding (Beloin, Roux and Ghigo, 2008). The receptor-binding domain mediates binding to the sugar mannose and allows for attachment to eukaryotic cells (Duncan *et al*., 2005). In addition to biotic surfaces, studies have shown that the presence of type 1 fimbriae changes the propensity of *E. coli* towards propagation which results in an increase in attachment to abiotic surfaces and aids biofilm formation (Orndorff *et al*., 2004). Furthermore, type 1 fimbriae have shown to be important in *S. typhimurium* pellicle formation in static cultures (Old and Duguid, 1970). The *fimAICDFGH* operon is responsible for structural fimbriae formation, while FimB and FimE are recombinases responsible for regulation of the operon (Schilling, Mulvey and Hultgren, 2001). FimB and FimE proteins also regulate a 314 bp "*fim* switch" site which results in phase variability of the FimA promoter; thus type 1 fimbriae can be "ON" or "OFF" in a cell population (Klemm, 1986). The transcriptional regulator LrhA regulates expression of type 1 fimbriae by binding to the *fimE* promoter and downregulating production (Blumer *et al*., 2005). LrhA also reduces biofilm formation by downregulating flagellar motility and chemotaxis, but this is not studied in this work (Lehnen *et al*., 2002).

F fimbriae, or conjugative F pili, connect between cells and function primarily as a method of horizontal gene transfer; however, it has been shown that that they can also aid biofilm formation by initiating surface attachment and stabilising the biofilm during maturation (Ghigo, 2001; Molin and Tolker-Nielsen, 2003). Conjugation (or transfer of DNA through F pili) is also important in biofilm formation as neighbouring cells can share genetic material which can induce biofilm formation (Wuertz, Okabe and Hausner, 2004). While not much is known about conjugation or formation of pilus in pellicles, there are reports that *Bacillus subtilis* cells will share genetic material within a pellicle and *Acinetobacter baumannii* will form pili in their pellicle matrix (Nait Chabane *et al.*, 2014; Lécuyer *et al.*, 2018). Importantly, work by Reisner and colleagues purported that not only are many surface proteins that involve surface attachment, such as type 1 pili, Ag43, and curli, are dispensable when forming a biofilm, but the presence of F fimbriae in the absence of any of these surface proteins produce a similar biofilm (Reisner *et al*., 2003). The F plasmid which encodes F fimbriae, is not present in *E. coli* K-12 laboratory strains after being cured by treatment with acridine orange (Bachmann, Low and Taylor, 1976; Blattner *et al*., 1997). Although, transforming an F plasmid into these strains increases biofilm formation because it stimulates curli production and the synthesis of the matrix component colanic acid, while downregulating genes needed for motility (Domka *et al.*, 2007; May and Okabe, 2008).

Flagella are long, roughly 10 μm in length, complex, propeller-like organelles that rotate multi-directionally to move a bacterial cell (Haiko and Westerlund-Wikström, 2013). The three part flagellum assembles from the inside out, and begins first with the rotary motor in the cell membrane; connected to a hook-like junction; which is connected to the most distal end comprised of flagellin protein in a cylindrical filament (Macnab, 2003). A minimum of 60 genes are required for the synthesis and

regulation of flagella, and the expression is complex and extensive (Chilcott and Hughes, 2000). *E. coli* have multiple flagella on their surface that allow for efficient movement towards nutrients and away from undesirable conditions and repellents (Zhao, Liu and Burgess, 2007). Motility is important during biofilm formation as it allows the cell to overcome counteractive forces (such as hydrostatic forces) and other barriers to attach to a surface; inhibition of flagellar synthesis or presence of dysfunctional flagellum both severely impaired biofilm formation, which indicates that motility must be in part important to biofilm formation (Pratt and Kolter, 1998). However, Prigent-Combaret and coworkers have shown overexpression of curli is one way to alleviate the need for motility in *E. coli* K-12 biofilm formation (Prigent-Combaret *et al*., 2000). Similar to biofilm formation, flagellar motility is important but not necessary for pellicle formation in Gram positive bacterial strains like *B. subtilis* and is also highly regulated (Hölscher *et al*., 2015). Studies using *Pseudomonas aeruginosa* with deleterious mutations in flagellar synthesis and motor function showed pellicle formation was delayed and had altered morphology, indicating that flagellar motility is important but not necessary for pellicle formation and may have a function in the matrix structure (Yamamoto *et al.*, 2012).

In addition to motility, flagella play an important role in attachment and biofilm maturation. Work using confocal microscopy and SEM have identified and described flagella in the *E. coli* biofilm as "cellular tethers" and it has been proposed that flagella function architecturally and structurally in the matrix (Wood *et al*., 2006; Serra *et al*., 2013). Furthermore, it has been shown that *E. coli* flagella bind with an affinity towards hydrophobic surfaces and can aid attachment to rough surfaces (Friedlander *et al*., 2013; Friedlander, Vogel and Aizenberg, 2015). It has even been proposed that flagella may act as mechanosensors that aid in surface sensing and can further regulate genes for biofilm formation (Belas, 2014). In motile cells, FliZ is a

protein coexpressed with flagellar genes which binds to CsgD and downregulates curli, indicating curli and flagellar expression are inversely expressed (Guttenplan and Kearns, 2013).

Once in contact with a surface, flagella and motility are downregulated and biofilm formation begins through a series of regulatory pathways. The surface contact induces the Rcs pathway which stimulates the synthesis of matrix components, such as colanic acid (section 1.2.3.1), while downregulating flagella motility (Guttenplan and Kearns, 2013). As biofilm formation is initiated, the concentration of signal molecules, like c-di-GMP discussed in section 1.3.2, rises which bind and activate proteins YcgR and CsgD. YgcR has been shown to inhibit the flagellar motor thus decreasing motility, while CsgD upregulates curli expression and downregulates flagellar gene expression (Ryjenkov *et al.*, 2006; Ogasawara, Yamamoto and Ishihama, 2011). The role of flagellar motility in biofilm formation is studied in this work.

1.2.3 Matrix Components

The EPS components that comprise the matrix are a hallmark of biofilm development and provide protection and a structured environment in which bacterial cells can thrive (Branda *et al.*, 2005). The production of each component is highly regulated, and is influenced by environmental signals, such as surface contact, which indicates that each matrix component tends to have a specific function in the biofilm (Danese, Pratt and Kolter, 2000; Beloin, Roux and Ghigo, 2008). The matrix composition is species-dependent and is primarily comprised of water, but it can also have polysaccharides, lipids, extracellular DNA, amyloid, and other bacterial fimbriae (Hobley *et al.*, 2015). In *E. coli*, the EPS is primarily comprised of curli and polysaccharides like colanic acid, poly-β-1,6-N-Acetylglucosamine (PNAG), and cellulose; however, *E. coli* K-12 used in the research comprising this manuscript does

not make cellulose (Serra, Richter and Hengge, 2013). The composition of *E. coli* pellicle matrices is not abundant in literature; however, it is proposed that they are similar to solid surface-attached biofilms and are subject to complex regulation (Hung *et al.*, 2013). Other strains, such as *P. aeruginosa*, have been shown to form pellicles comprised of adhesins and various polysaccharides (Laverty, Gorman and Gilmore, 2014; Limoli, Jones and Wozniak, 2015). Colanic acid and PNAG are discussed in detail in the following sections, and are studied in this work.

1.2.3.1 Colanic Acid

Colanic acid is a branched extracellular polysaccharide comprised of repeating units of galactose, glucose, fucose, and glucuronic acid (Stevenson *et al.*, 1996). While colanic acid is loosely associated with the outside of the cell, it has been found to be a key component in the EPS of *E. coli* biofilms and forms a protective capsule around the cell (Danese, Pratt and Kolter, 2000). However, due to its capsule-like position around the cell, colanic acid can reportedly mask surface adhesins that aid in attachment, thus indicating colanic acid likely acts primarily as a structural matrix component rather than a surface adhesion (Hanna *et al.*, 2003). Work with *E. coli* has shown that production of colanic acid is stimulated upon cell attachment to a surface, and rather than aiding in initial surface attachment it is excreted to provide strength and shape to the three-dimensional biofilm matrix (Prigent-Combaret *et al.*, 1999). In addition to surface attachment, production of colanic acid is stimulated during outer membrane stress, such as from osmotic shock or desiccation (Ophir and Gutnick, 1994; Sledjeski and Gottesman, 1996). Colanic acid biosynthetic genes, *cps*, reside in a large (at least 19 but reports vary) gene cluster (Stout, 1996). The various genes are responsible for producing the sugar subunits, and all the necessary proteins for transport and assembly

(Stevenson *et al.*, 1996). The Rcs phosphorelay pathway regulates capsule synthesis and upregulates colanic acid synthesis in response to membrane structural defects and stress, among other signals (Ren *et al.*, 2016).

1.2.3.2 PNAG or PGA

Poly-β-1,6-N-Acetylglucosamine, also termed PNAG or PGA in the literature, is an unbranched surface polysaccharide secreted by bacteria during biofilm matrix development (Agladze, Wang and Romeo, 2005). Unlike colanic acid, PNAG is secreted throughout the biofilm matrix as a means for cell-surface and cell-cell attachment and is considered critical during early biofilm formation (Wang, Preston and Romeo, 2004). Furthermore, due to the increased cohesion that PNAG provides, it has been proposed that PNAG is capable of stabilising the biofilm matrix of *E. coli* and other bacterial species (Wang, Preston and Romeo, 2004). In *Bacillus subtilis*, PNAG is a significant component in both the biofilm and pellicle matrix, but less is known about PNAG in the *E. coli* pellicle matrix (Roux *et al.*, 2015). PNAG secretion is controlled by the operon *pgaABCD*, which encodes PgaA, a transport and docking protein; PgaB, a potential polysaccharide modifier; PgaC, a glycosyltransferase responsible for polysaccharide synthesis; and PgaD, a protein also involved in PNAG synthesis (Wang, Preston and Romeo, 2004; Cerca *et al.*, 2007). NhaR, a transcriptional regulator, can sense monovalent cations (Na^+, K^+, Li^+) and high pH and bind to the *pgaABCD* promoter to upregulate PNAG production (Goller *et al.*, 2006). PNAG synthesis is negatively regulated by CsrA, a global regulator linked to catabolism, which indicates that biofilm formation is partially regulated by growth phase and cell metabolism (Jackson, Simecka and Romeo, 2002; Wang *et al.*, 2005). Work on the effect of glucose, osmolarity and ethanol on PNAG synthesis showed that an increase in *pgaABCD* expression did not necessarily increase biofilm thickness, which may indicate

that PNAG is not the only critical component to the formation of a mature biofilm (Cerca and Jefferson, 2008). However, the various supplements (glucose, ethanol, etc) in this study could have affected other aspects of biofilm formation. Mutant cells unable to synthesise PNAG reportedly could not form permanent surface attachments and thus were unable to form a biofilm (Agladze, Wang and Romeo, 2005).

1.2.3.3 Other matrix components: cellulose

Cellulose is made of glucose subunits polymerised into rigid linear β-linked chains (Ross, Mayer and Benziman, 1991). Cellulose is a polysaccharide secreted during biofilm formation and tends to bind with thin aggregative fimbriae on the outside of the cell to form a structured matrix (Zogaj *et al.*, 2001; White *et al.*, 2003). Cellulose is not necessary for biofilm formation in *E. coli*, but it is unknown the role cellulose plays in *E. coli* pellicle formation. Cellulose appears to be important but not essential in pellicle formation in *Salmonella* strains (Paytubi *et al.*, 2017). The operons *bcsQABZC* and *bcsEFG* are responsible for cellulose production; BcsA is the cellulose synthase protein (Römling and Galperin, 2015). As with curli and colanic acid, c-di-GMP is involved with regulation of cellulose production and BcsB acts as a binding protein to mediate this process (Fang *et al.*, 2014). While cellulose is an important component of many bacterial biofilms, including *E. coli* species, K-12 strains contain a stop codon in *bcsQ* which prevents cellulose production. Thus, the work with *E. coli* K-12 in the following manuscript does not include cellulose (Serra, Richter and Hengge, 2013; Bernal-Bayard *et al.*, 2018).

1.3 *Escherichia coli* K-12 biofilm regulation

The regulation of *E. coli* K-12 biofilm and pellicle formation is vast, complex, and influenced by numerous major regulatory pathways, such as the master curli regulator CsgD and internal signalling molecules c-di-GMP, as well as environmental stimuli such as surface attachment, temperature, and osmolarity. Additionally, the crossover of regulatory networks and interrelated stimulus makes these complexities further convoluted as it appears many of these systems are interlinked. The following sections detail the regulation of biofilm-associated genes in terms of the master curli regulator CsgD; c-di-GMP; cAMP-CRP complex; osmolarity; temperature; entry into stationary phase; and surface attachment.

1.3.1 CsgD

One of the most crucial components of biofilm formation that aid in initial attachment and provide structure for the three-dimensional matrix is curli formation. CsgD, the master regulator of curli expression, is required for curli expression (Barnhart and Chapman, 2006). As with biofilm formation, CsgD is required for formation of a pellicle in curli-producing strains (Grantcharova *et al.*, 2010; Hufnagel, Depas and Chapman, 2015). Composed of a N-terminal (receiver) domain and a C-terminal (DNA-binding) domain, CsgD is a transcriptional regulator involved with mediating the expression of roughly 24 genes (Brombacher *et al.*, 2006). Due to regulation by CsgD, curli are maximally-expressed in cells in stationary phase, grown in microaerophilic conditions, with limited glucose, low temperatures, and low osmolarity (low salt concentrations). CsgD is regulated by a number of pathways and stimuli, including σ^S (RpoS) during stationary phase, the transcriptional regulator OmpR, global regulatory

proteins, and small RNAs. A model was proposed that a combination of these proteins can also regulate CsgD in response to oxygen tension (Gerstel, Park and Römling, 2004a). The model indicates that when aerobic conditions are sensed via an unknown mechanism, increased concentrations of H-NS (a global regulatory protein) are able bind to *csgD* and repress curli expression while also blocking OmpR from binding to *csgD* and upregulating curli expression. Alternatively, when microaerophilic conditions are sensed via an unknown mechanism, it was shown that *csgD* was bound and upregulated by Integration Host Factor (IHF), thus it was proposed that a complex between OmpR, IHF and H-NS forms to upregulate *csgD*.

As described in section 1.3.3, transcription of *csgD* requires OmpR which is influenced by osmolarity and other stimuli (Römling *et al.*, 1998). Glucose deprivation induces curli synthesis, and thus biofilm and pellicle formation via CsgD (Smith *et al.*, 2017). Glucose inhibits synthesis of the global gene regulator cyclic AMP (cAMP), but in low glucose conditions cAMP and the cAMP receptor protein (CRP) are able to positively regulate *csgD* which increase curli formation (Hufnagel *et al.*, 2016). The transcriptional regulator MIrA, which is activated during stationary phase by RpoS, is a positive regulator of CsgD (Brown *et al.*, 2001). RpoS can also form a complex with Crl, a thermal sensor discussed in section 1.3.4, which is thought to increase curli formation in lower temperatures through CsgD (Bougdour, Lelong and Geiselmann, 2004a). CsgD is negatively regulated by the CpxAR and Rcs pathways, which are induced during changes in osmolarity, envelope stress, pH, and so forth (further described in sections 1.3.3 and 1.3.6).

In addition to curli expression, CsgD is important in the regulation of cellulose production. While the regulation of cellulose production is complex by nature, it has been shown that CsgD indirectly increases or decreases cellulose production by activating *adrA*, which synthesises c-di-GMP required for cellulose production and

motility regulation (discussed in section 1.3.2), and *yoaD*, which is thought to degrade c-di-GMP (Brombacher *et al.*, 2006). It is thought CsgD modulate both genes to fine-tune cellulose production as needed. CsgD, in addition to genes associated with curli (*csgBA*) and cellulose (*adrA*), also stimulates *yaiC*, a gene involved with biofilm formation, and downregulates *fecR*, *pepD*, and *yagS*, which negatively affect cell attachment and biofilm formation (Brombacher *et al.*, 2003, 2006). This indicates that CsgD can act as both an activator and repressor of a multitude of genes to induce biofilm formation.

1.3.2 c-di-GMP

Bis-(3-5)-cyclic-di-guanosine monophosphate (c-di-GMP) is a signal molecule that regulates a number of processes throughout the cell, such as motility and cellulose production, in response to environmental stimulus (Povolotsky and Hengge, 2012). Levels of c-di-GMP are modulated through diguanylate cyclase enzymes, which synthesise c-di-GMP from two molecules of GTP, and phosphodiesterases, which hydrolyse c-di-GMP (Jenal and Malone, 2006). There are numerous transcription factors, such as BolA, a protein which induces biofilm formation, able to regulate the expression of these enzymes in order to regulate c-di-GMP levels (Moreira *et al.*, 2017). Originally thought to be involved only in cellulose synthesis, it is now known that c-di-GMP binds to a vast collection of proteins and can rapidly influence numerous pathways involved with biofilm formation in response to an array of environmental signals (Römling, Galperin and Gomelsky, 2013). While little is known about the effect of c-di-GMP on *E. coli* pellicle formation, there is evidence that c-di-GMP can regulate pellicle formation in *B. subtilis* and c-di-GMP is involved with *P. aeruginosa*

polysaccharide excretion and pellicle formation (Ueda and Wood, 2009; Chen *et al.*, 2012; Li *et al.*, 2012).

Generally, low levels of c-di-GMP are associated with higher levels of motility and planktonic lifestyles, while high levels of c-di-GMP actively stimulate biofilm formation through upregulation of curli and EPS matrix secretion (Simm *et al*., 2004). Upon entry into stationary phase, c-di-GMP levels increase, which spur a number of processes; c-di-GMP, along with RpoS, the stationary phase sigma factor, activate YdaM and YciR which increase and modulate *csgD* expression (Weber *et al*., 2006; Pesavento *et al*., 2008). As previously discussed in section 1.3.2, work has shown that CsgD is required for curli synthesis, and indirectly mediates cellulose production by activating *adrA*, which synthesises c-di-GMP required for cellulose production (Brombacher *et al*., 2006). As c-di-GMP concentrations rise, flagellar motility is reduced because the protein YcgR binds specifically with c-di-GMP to downregulate these genes, while c-di-GMP can also interact with the motor protein MotA to slow the flagellar motor (Boehm *et al*., 2010; Paul *et al*., 2010). The Cpx pathway positively regulates c-di-GMP via YdeH (a diguanylate cyclase enzyme), which is induced by a variety of signals, such as envelope disruption, discussed in section 1.3.4 and 1.3.7 *(*Jonas *et al*., 2008).

1.3.3 cAMP and CRP

Another important secondary signal molecule and global gene regulator in *E. coli* is cyclic adenosine 5'-phosphate (cAMP) and the complex it makes with the catabolite receptor protein (CRP) (Botsford and Harman, 1992). CRP is essential in catabolite repression, where the cell is able to adapt to various available carbon sources and regulate gene expression in order to efficiently catabolise sugars for the cell. In the

cell, cAMP levels are mediated by glucose concentrations: when synthesised, cAMP binds to and activates CRP, which is then able to regulate gene expression accordingly (Hogema *et al.*, 1997; Narang, 2009). Activated CRP (or CAP) is necessary for DNA binding in order to activate genes necessary for catabolism of the available carbon source, while repressing unnecessary genes. Glucose and cAMP levels are inversely related because glucose inhibits adenylate cyclase (CyaA) activity so that it cannot synthesise cAMP; subsequently, when glucose is abundant in the environment cAMP-CRP levels are low, but cAMP-CRP concentrations increase in glucose-poor conditions (Ishizuka *et al.*, 1993; Jackson, Simecka and Romeo, 2002). When levels of cAMP are high (low glucose), it forms a complex with CRP which can then bind and upregulate genes for catabolism of alternative sugars and biofilm formation (Zheng *et al.*, 2004; Fic *et al.*, 2009). Specifically, the cAMP-CRP complex positively regulates *csgD* expression which leads to increased curli and cellulose production and promotes formation of a biofilm (Hufnagel *et al.*, 2016). Similarly, cAMP has been shown to stimulate CsgD and induce pellicle formation in *Salmonella* (Paytubi *et al.*, 2017). Work by Hufnagel *et al.* showed that high levels of glucose reduce biofilm and pellicle formation in UPEC because it reduces intracellular cAMP-CRP concentrations (Hufnagel *et al.*, 2016). Similarly to curli in UPEC, the cAMP-CRP complex mediates production of type 1 fimbriae will induce expression and stimulate biofilm formation (Müller *et al.*, 2009). In addition to curli, type 1 fimbriae, and cellulose formation, the cAMP-CRP complex can bind and upregulate genes important for flagellar synthesis, *flhDC*, which aid in motility and can allow the cell to localise to a surface or zone in order to form a biofilm or pellicle (Pratt and Kolter, 1998; O Soutourina *et al.*, 1999). Furthermore, the cAMP-CRP complex activates *flhDC* while also relieving repression by the global regulatory protein H-NS, indicating that cAMP-CRP can activate

transcription and reverse silencing mechanisms (Forsman *et al.*, 1992; O. Soutourina *et al.*, 1999).

1.3.4 Osmolarity

Osmolarity is the concentration of solutes in a solution. In a culture, the osmolarity differs based on location within the environment and is seldom homogeneous; cells are sensitive to osmolarity gradients within the system (Wood, 1999). Additionally, the osmolarity near surfaces is highly variable. As cells approach and adhere to a surface, a microenvironment is produced from small pools of confined molecules and ions that become trapped between the cell body and the surface and thus osmolarity will differ (Tuson and Weibel, 2013). Changes in osmolarity have been found to induce EnvZ/OmpR (also induced by low pH and increased temperature), CpxAR (also induced by envelope stress, denatured proteins and surface attachment), H-NS, and the Rcs phosphorelay (also induced by membrane disturbance) that regulates genes involved in biofilm formation in different ways (Prigent-Combaret *et al.*, 2001; Oshima *et al.*, 2002). Similarly to biofilm, it has been shown in EPEC that pellicle formation occurs in low osmolarity mediums, but less is known about the exact mechanisms (Weiss-Muszkat *et al.*, 2010).

The EnvZ/OmpR pathway is able to mediate two porins, *ompC* and *ompF*, and has also been shown to increase curli expression. When exposed to high osmolarity, the histidine kinase and inner membrane lipoprotein, EnvZ, first senses the change in osmolarity by a conformational change on its cytoplasmic domain (Wang *et al.*, 2012). Next, EnvZ will autophosphorylate its histidine domain and transfer the phosphoryl group to the N-terminal domain of OmpR (Stock, Robinson and Goudreau, 2000; Wang *et al.*, 2012). Phosphorylated OmpR undergoes a conformational change and the C-

terminal domain is able to bind to the DNA on specific promoter and regulatory sites. The surface sensor EnvZ is also a phosphatase and in low osmolarity is able to remove phosphoryl groups from OmpR (Russo and Silhavy, 1991). In low osmolarity there is less phosphorylated OmpR, but sufficient levels to bind to the regulatory region of *ompF* (encodes a porin which increases nutrient uptake in minimal media) and activate transcription. Alternatively, in high osmolarity with high levels of phosphorylated OmpR, *ompC* (a porin which exclude salts) is upregulated and *ompF* is repressed (Huang, Lan and Igo, 1997; Head, Tardy and Kenney, 1998). This two component system also mediates curli production in response to changes in osmolarity, particularly by stimulating *csgD* and thus the formation of curli in low osmolarity environments (Fig. 1.4) (Egger, Park and Inouye, 1997; Vidal *et al.*, 1998). Furthermore, OmpR is required for positive regulation of *csgD* while phosphorylated OmpR has been shown to repress it; thus, OmpR is essential in curli expression and biofilm and pellicle formation. Mutations in position 43 of the *ompR234* gene which results in constitutive expression of OmpR and thus CsgD has shown that upregulated curli expression allows cells to form biofilms in conditions and on surfaces that they normally could not (Vidal *et al.*, 1998). The mutation also upregulates four genes not associated with curli, *gadE*, *yjbR*, *chbG*, and *recT*; however, only GadE may potentially influence biofilm formation via regulation of *rcsA* in the Rcs phosphorelay cascade, described later in this section (Brombacher *et al.*, 2003; Wall, Majdalani and Gottesman, 2018). It should also be noted that while the *ompR234* mutation amplifies curli expression by binding to and upregulating the *csgD* promoter, curli expression is still regulated by numerous other regulatory pathways and environmental stimulus.

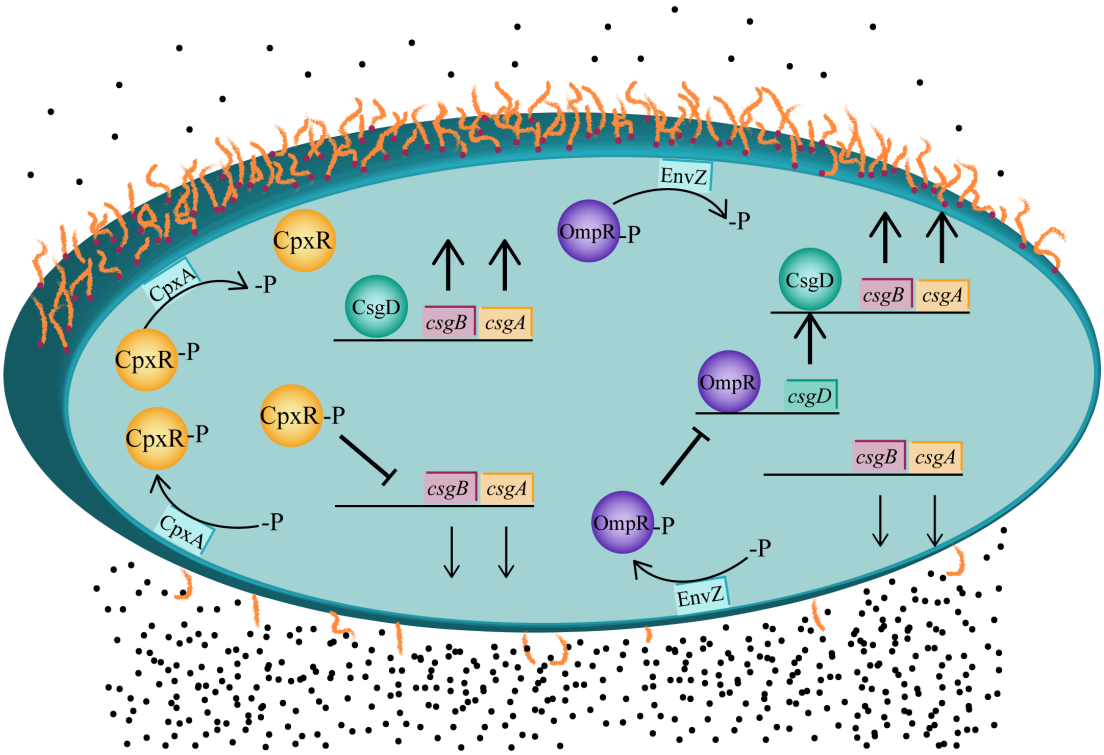

Figure 1.4: Diagram of the regulation of curli expression by the CpxAR and EnvZ/OmpR pathways in response to osmolarity.

Generally in high osmolarity, EnvZ phosphorylates OmpR which undergoes a conformational change, binds to the *csgD* promoter and represses expression. CpxA will phosphorylate CpxR in high osmolarity which then blocks binding of CsgD upstream of *csgBA*. Alternatively in low osmolarity, Both EnvZ and CpxA are phosphatases that can dephosphorylate their respective receptors. Thus, in low osmolarity curli expression increases by allowing OmpR to bind and upregulate *csgD* promoter (EnvZ/OmpR pathway) while dephosphorylated CpxR cannot block CsgD from binding and upregulating curli expression.

A separate histidine kinase phosphorelay, CpxAR, can mediate biofilm formation in response to osmolarity and is responsible for repressing curli expression in high osmolarity and during envelope stress (Fig. 1.4) (Raivio and Silhavy, 1997). It has been hypothesised that proteins are susceptible to denaturing during envelope stress and high osmolarity and thus these denatured proteins also stimulate CpxA so the cascade will repress production and export of proteins like CsgA (Raivio and Silhavy, 1997). Furthermore, Prigent-Combaret *et al*. purported the CpxAR pathway can be induced by

curlin accumulation, which would then repress curli expression (Prigent-Combaret *et al.*, 2001). CpxA is a membrane histidine kinase which directly or indirectly senses high osmolarity via an unknown mechanism and transphosphorylates CpxR (Dong *et al.*, 1993; Raivio and Silhavy, 1997). The phosphorylated CpxR is able to bind upstream of *csgD*, and repress *csgD* expression and curli production, while also blocking OmpR from binding and upregulating *csgD* expression (Dorel *et al.*, 1999; Jubelin *et al.*, 2005). Like EnvZ, CpxA is a phosphatase that is capable of dephosphorylating CpxR in low osmolarity, which has shown to derepress *csgA* (Dorel *et al.*, 1999). Furthermore, the CpxAR cascade is a stress response pathway that can sense high osmolarity in addition to surface attachment, envelope stress, pH, high salt concentration, and so forth and modulate curli expression (Hunke, Keller and Müller, 2012; Weatherspoon-Griffin *et al.*, 2014). Work by Prigent-Combaret and colleagues, showed that overexpression of the *ompR234*, such as in PHL644 in the following work, overcomes the negative regulation of curli in high osmolarity by CpxAR (Prigent-Combaret *et al.*, 2001).

H-NS is a heat-stable global regulatory protein which is responsible for the regulation of numerous genes (roughly 5% of *E. coli* genome), including surface organelles like curli, in response to temperature, oxygen tension (oxygen sensing is via an unknown mechanism) and osmolarity (Arne Olsén *et al.*, 1993; Amit, Oppenheim and Stavans, 2003). The *hns* gene is autoregulated and H-NS levels remain fairly constant in the cell (Atlung and Ingmer, 1997). H-NS preferentially binds to curved and AT rich regions of DNA, commonly promoters, which allow them to regulate transcription (Stella *et al.*, 2006). Generally, H-NS is a repressor of transcription in *E. coli*; however, H-NS has no identifiable binding sequence for *csgD* (curli) and will reportedly activate or repress *csgD* based on the bacterial strain, growth medium, and other factors (Gerstel, Park and Römling, 2004a; Ogasawara *et al.*, 2010). Work with an *E. coli hns* mutant at low osmolarity showed reduced *csgD* expression, which indicates

that H-NS will activate *csgD* in low osmolarity (Jubelin *et al.*, 2005). Furthermore, H-NS has been shown to regulate genes and the global stress response, RpoS, in response to changes in osmolarity and temperature, which indicates the importance of H-NS as an osmoregulatory and thermoregulator (Barth *et al.*, 1995; Stella *et al.*, 2006). In addition to osmolarity, H-NS has also been shown to downregulate type 1 fimbriae at lower (30 ºC) and at higher (37 ºC) temperatures, which is described in section 1.3.5 (Olsen *et al.*, 1998). H-NS is a thermosensor which will bind and regulate DNA expression in response to fluctuations in temperature, purportedly by undergoing conformational changes in response to temperature (Ono *et al.*, 2005).

The Rcs phosphorelay pathway is induced by peptidoglycan layer damage from desiccation, osmotic shock, and other envelope stress, and is required to regulate genes involved in biofilm formation (Ren *et al.*, 2016). Specifically, the Rcs cascade downregulates motility (flagella) and surface organelles used for attachment, such as curli and Ag43, and upregulates genes needed for later stages of biofilm formation, such as colanic acid synthesis discussed in section 1.2.3.1 (Huang, Ferrières and Clarke, 2006). The Rcs cascade is controlled by RcsCDB which have specific functions in the system in response to a variety of signals. When stimulated, RcsF, an outermembrane lipoprotein, signals to RcsC, a transmembrane sensor kinase with a N-terminal in the periplasm and a C-terminal in the cytoplasm, to autophosphorylate; although, RcsC may not necessarily be stimulated only by RcsF (Laubacher and Ades, 2008). RcsC transfers the phosphoryl group first to RcsD, which transfers it to the response regulator, RcsB (Stout and Gottesman, 1990). RcsC can be inhibited by another membrane protein, YrfF/IgaA (Huang, Ferrières and Clarke, 2006). After transphosphorylation, the phosphorylated RcsB can bind to DNA either as a homodimer or a heterodimer with the accessory protein RcsA to mediate gene expression (Majdalani and Gottesman, 2005). It is important to note that H-NS has been shown to be a silencer of *rcsA* (Sledjeski and

Gotresman, 2003). In medium with low osmolarity, a mutation in the Rcs pathway has been shown to increase *csgD* (curli), indicating that RcsB must negatively regulate *csg* gene expression, which was later confirmed by Jubelin and colleagues (Jubelin *et al.*, 2005; Vianney *et al.*, 2005). However, a mutation in *rcsB* did not increase *csg* gene expression in high osmolarity medium, which may indicate many systems control curli expression and biofilm formation in response to changes in osmolarity (Vianney *et al.*, 2005). Other work has shown that not only are RcsB and RcsC required for the regulation of *cps* (colanic acid synthesis), but this pathway is also temperature sensitive (Sledjeski and Gottesman, 1996). Other studies purported that the CpxAR pathway was stimulated more heavily during changes in osmolarity and the Rcs pathway was induced during membrane disturbance; nevertheless, RcsC is required for biofilm formation (Ferrières and Clarke, 2003). While less is known about the exact osmoregulation in *E. coli* pellicle formation, the Rcs phosphorelay has shown to be important in *Salmonella* pellicle formation (Latasa *et al.*, 2012).

It is clear from the literature that there is an intricate and intertwining network of environment-sensing pathways that are induced by changes in osmolarity to efficiently regulate genes involved with biofilm formation, such as curli expression, among many others, and these systems should be studied further (Gerstel, Park and Römling, 2004; Ogasawara *et al.*, 2010; Ogasawara, Yamamoto and Ishihama, 2010).

1.3.5 Temperature

Minute changes in temperature can affect the formation of a biofilm by influencing regulatory pathways that can alter the expression of biofilm and pellicle components curli, flagella and matrix polysaccharides (Donlan, 2002). As discussed in section 1.2.2.1, curli are a crucial component of biofilm formation and are expressed

maximally at lower temperatures. Despite reports that temperatures below 30 °C elicit maximal curli expression in *E. coli* laboratory strains, studies have found that the *csgBA* promoter is activated at 30 °C by a complex between RpoS, a general stress/stationary phase sigma factor, and Crl, a thermosensitive protein (Fig. 1.5) (Bougdour, Lelong and Geiselmann, 2004a; Barnhart and Chapman, 2006; Brombacher *et al.*, 2006). While the binding of the RpoS-Crl complex to the *csgBA* promoter activates expression and relieves H-NS repression of *csgA*, it is influenced by other factors such as osmolarity and the master regulator CsgD (Arnqvist *et al.*, 1992; Arne Olsén *et al.*, 1993).

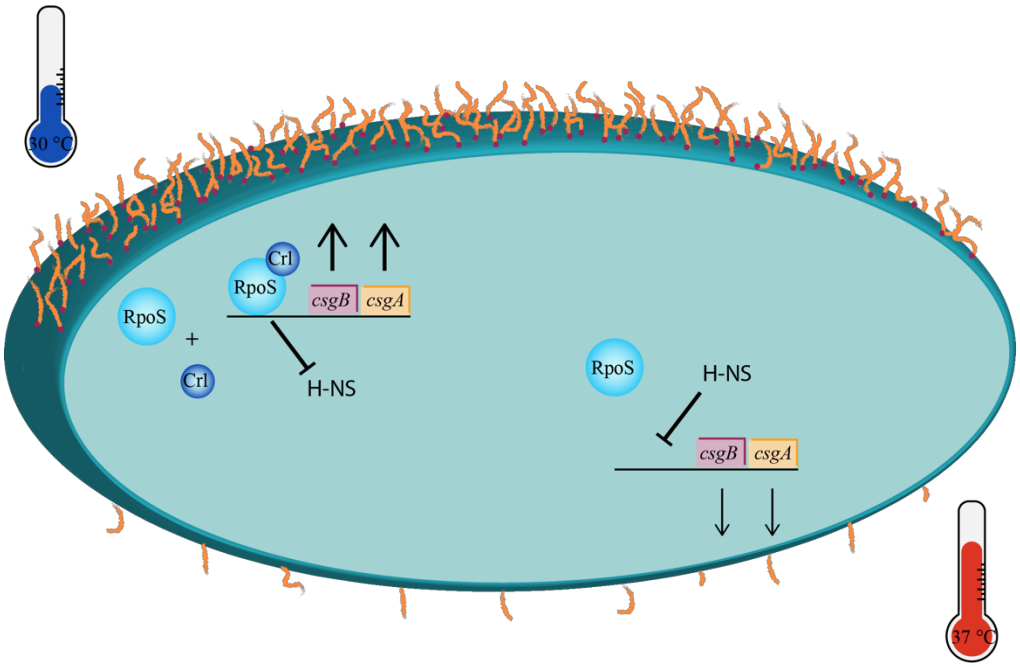

Figure 1.5: Diagram of the regulation of curli expression in response to temperature.

In lower temperatures (~32 °C) the thermosensitive protein Crl makes a complex with RpoS which can upregulate *csgBA* expression. H-NS represses csgBA and blocks binding by other proteins.

In *E. coli*, curli expression was still negatively affected at 37 °C in cells constitutively expressing CsgD, which indicates that CsgD is not temperature-regulated (Brombacher *et al.*, 2003). It is likely that because the thermoregulator Crl protein is not expressed at 37 °C, curli are not highly expressed at these temperatures (Arnqvist *et al.*, 1992). Gualdi and colleagues purported that more curli is expressed in *E. coli* K-12 at temperatures less than 32 °C when compared to 37 °C (Gualdi *et al.*, 2008). Since Crl is required for regulation of curli expression by RpoS in most strains, this indicates the significance of temperature on biofilm formation. Work with a curli-producing strain of EPEC showed that mutations in either the curli gene or *crl* prevented both biofilm and pellicle formation, indicating an importance of temperature in pellicle formation which may also be important in *E. coli* K-12, but has yet to be elucidated (Weiss-Muszkat *et*

al., 2010). It is also important to note that the compound indole, discussed in section 1.4.1, is important in Crl activation (Lelong *et al.*, 2007).

In addition to curli, other surface organelles affected by temperature include flagella and type 1 fimbriae. Work has shown that temperatures above 37 °C are not conducive to flagellar synthesis, and *flhDC* gene expression was reduced in high temperatures which has negative effects on biofilm (Adler and Templeton, 1967; Li *et al.*, 1993; Shi *et al.*, 1993). H-NS has also been shown to downregulate type 1 fimbriae via altering regulatory factors FimB and FimE which affect "ON/OFF" switching of FimA at 30 ºC and at 37 ºC (Olsen *et al*., 1998). Generally, in conjunction with RpoS, H-NS has been proposed to be a major temperature regulator of genes important to *E. coli* K-12 biofilm formation: such as *nhaR*, which encodes a transcriptional regulator needed for PNAG production; *csgA* encoding the major curlin subunit; and *bolA*, which encodes a transcription factor that regulates motility and c-di-GMP levels (White-Ziegler and Davis, 2009; Dressaire *et al.*, 2015; Moreira *et al.*, 2017). These genes that induce biofilm formation tend to be more highly expressed at temperatures closer to 23 °C rather than 37 °C (White-Ziegler *et al.*, 2008).

1.3.6 Stationary Phase

Stationary phase occurs at the end of rapid, logarithmic growth when nutrient sources are depleted, inhibitory by-products increase, and the number of dying and dividing bacterial cells reach an equilibrium (Pletnev *et al*., 2015). This phase is also a result of an increase in stress factors that initiate in response to starvation and change gene transcription. Namely, RpoS concentrations, the stationary-phase sigma factor, increase upon entry into stationary phase and have been found to regulate nearly 10% of the *E. coli* genome (Weber *et al*., 2005). There are regulatory response pathways that

require RpoS, such as the thermosensitive protein Crl, which binds to RpoS and upregulates curli expression at temperatures < 30 ºC. Furthermore, RpoS can positively regulate other regulatory proteins. For instance, RpoS positively regulates MlrA, a transcription factor that upregulates *csgD* expression and curli formation (Brown *et al.*, 2001). The microarray experiment by Weber *et al.* supports that RpoS is considered a general stress response and showed that RpoS is elevated in response to numerous environmental stress stimuli like starvation, high osmolarity, and acidic pH (Weber *et al*., 2005). As previously described in section 1.3.2, c-di-GMP and RpoS are required for regulation of many genes that induce biofilm and pellicle formation, including curli and matrix exopolysaccharides (D'Argenio and Miller, 2004; Klauck *et al.*, 2018). In addition to upregulating genes, RpoS relieves repression by H-NS on *csgA*, a gene encoding the major curlin subunit (Olsén *et al*., 1993). It is important to note that studies by Prigent-Combaret and coworkers reported that strains with an *ompR234* mutation (such as PHL644) obtain greatest expression in stationary phase and can, to an extent, override regulatory mechanisms that decrease curli expression, such as changes in osmolarity (Olsén *et al.*, 1993; Prigent-Combaret *et al.*, 2001).

1.3.7 Surface sensing

NIpE and CpxAR have been proposed as the three-component pathway that regulates curli expression in response to surface attachment (Fig. 1.6) (Otto and Silhavy, 2002). First, hydrophobic surface attachment is sensed by NIpE, an outer membrane lipoprotein, which then activates CpxA, a membrane histidine kinase, which transphosphorylates CpxR (Dong *et al.*, 1993). The phosphorylated CpxR is able to bind and repress *csgD* and *csgB*, which decreases curli formation (Prigent-Combaret *et al.*, 2001; Barnhart and Chapman, 2006). In addition to curli downregulation, NlpE and

CpxAR have also been shown to increase production of PNAG by upregulating DgcZ, a diguanylate cyclase which synthesises c-di-GMP (Lacanna E *et al*., 2016). Opposed to the CpxAR pathway, a study by Kimkes and Heinemann on *E. coli* surface contact found that instead of CpxAR activation, the Rcs pathway was activated and is responsible for downregulating curli expression (Kimkes and Heinemann, 2018). As previous described in section 1.3.3, the Rcs phosphorelay pathway is induced by peptidoglycan layer damage and is required for gene regulation involved in *E. coli* biofilm formation, and potentially *Salmonella* pellicle formation (Latasa *et al.*, 2012; Ren *et al.*, 2016). If the Rcs phosphorelay is induced during surface contact, this is supported by other data that Rcs negatively regulates curli expression (Jubelin *et al.*, 2005). The Rcs cascade is controlled by RcsCDB and when stimulated, RcsF, an outermembrane lipoprotein, induces the cascade that regulates a number of genes. Like CpxAR, Rcs is also responsible for responding to envelope stress but instead of initiating during outer membrane disruptions, Rcs responds to peptidoglycan layer damage (Laubacher and Ades, 2008). Additionally, Rcs upregulates production of colanic acid, which supports the hypothesis that upon surface contact, biofilm formation proceeds by downregulating curli expression and increasing EPS secretion (Majdalani and Gottesman, 2005).

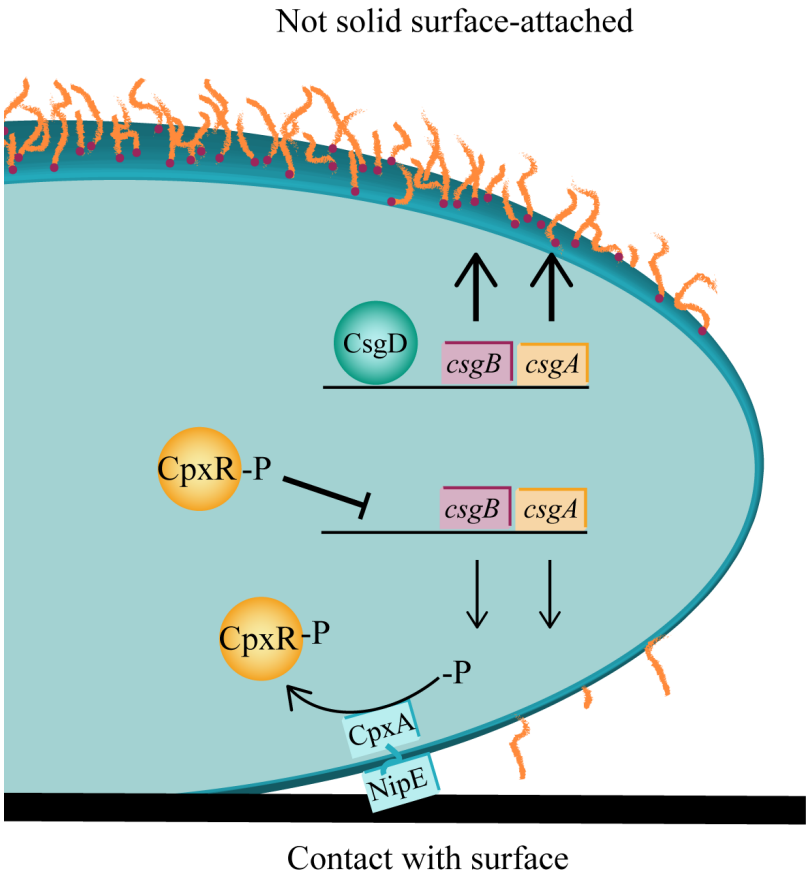

Figure 1.6: Diagram of the regulation of curli expression in response to surface contact (Otto and Silhavy model).

As described by Otto and Silhavy, curli expression is downregulated through a three-component cascade (Otto and Silhavy, 2002). NipE is a surface sensor that (when stimulated) induces the CpxAR pathway which downregulate curli expression. Other models explaining the same phenomena have been proposed (Kimkes and Heinemann, 2018).

1.4 Communication and other factors affecting biofilm formation

1.4.1 Quorum sensing

Quorum sensing is a mechanism where bacteria synthesise, secrete and sense small, diffusible molecules as a means of communicating and coordinating behaviour (Rutherford and Bassler, 2012). Once a density-threshold of the molecule is reached,

hence “quorum,” cells can alter gene expression. These quorum sensing molecules, called autoinducers (AI), are the foundation for purposeful cell-cell communication as they can signal to neighbouring bacteria the cell population and initiate DNA transcription that induce biofilm formation (Miller and Bassler, 2001). Although many quorum sensing molecules can be linked to metabolic processes, this suggests that these signals can also be made for the purpose of communicating the metabolic status of the cell (Pereira, Thompson and Xavier, 2013). There are three classes of autoinducers, AI-1, or Acyl Homoserine Lactone (AHL) in Gram negative bacteria; AI-2, a universal molecule in both Gram negative and Gram positive bacteria; and AI-3, the communication molecule between bacteria and eukaryotes.

While some species of Gram negative bacteria produce AHLs, *Escherichia* does not have an AHL synthase gene, *luxI*, and does not synthesise or secrete this AI. However, *E. coli* do have a LuxR (AHL receptor) homologue, SdiA, and can receive communication from AHL-producing bacteria. In cells that do contain *luxI*, AHL is synthesised and then passively diffuses outside the cell until a high enough level of signal is reached for surrounding AHL-receiving bacteria (Rutherford and Bassler, 2012). Once the AHL levels reach the concentration threshold, it diffuses into the surrounding cells and binds to the N-terminal of LuxR (SdiA), which is both a receptor and transcription factor (Urbanowski, Lostroh and Greenberg, 2004). AHLs are produced during a metabolic process involving S-adenosylmethionine (SAM) and an acyl carrier protein (ACP). However, AHLs are not carelessly synthesised as work with purified Lux-I protein has shown to expressly make AHLs with only specific substrates. (Schaefer *et al.*, 1996). Studies have shown that binding of SdiA to different AHLs induces a “folding switch,” where SdiA changes from an insoluble form to a soluble one, which may act as a way to identify AHLs of different bacterial species (Yao *et al.*, 2006). The C-terminal of SdiA is capable of binding to DNA to regulate target genes

(Henikoff, Wallace and Brown, 1990). Specifically, SdiA was shown to reduce gene expression associated with virulence in Enterohemorrhagic *E. coli* (EHEC) (Kanamaru *et al.*, 2000). AHLs bound to SdiA reduced biofilm formation whereas a mutation in *sdiA* increased biofilm formation, indicating that AI-1 signalling negatively controls *E. coli* biofilm formation (Lee, Jayaraman and Wood, 2007). Additionally, work by Culler *et al.* showed an *sdiA* deletion in EPEC made more compact pellicles, indicating that quorum sensing pathways affect biofilm and pellicles similarly (Culler *et al.*, 2018). Furthermore, there are varying reports on the effects of indole as a signalling molecule on *E. coli* biofilm formation. Indole has also been shown to interfere or bind with SdiA in *E. coli*, which results in markedly reduced biofilm formation via downregulation of motility among other genes, although there are varying reports on the exact mechanism (Di Martino *et al.*, 2003; Lee, Maeda, Hong and Wood, 2009; Sabag-Daigle *et al.*, 2012). One study showed the addition of indole increased *E. coli* biofilm formation and the deletion of TnaA (indole synthase) reduced biofilm formation (Di Martino *et al.*, 2003). Another study purported that indole is imperative for *E. coli* to form a biofilm at temperatures of 30 ºC as indole binds and activates Crl to upregulate curli expression and induce biofilm formation (Lelong *et al.*, 2007). Another study by Domka *et al*. alternatively reported that deletions of genes that regulate indole production and transport (*yliH and yceP*) reduced indole concentrations and increased *E. coli* biofilm formation, and the addition of indole reduced biofilm formation (Domka, Lee and Wood, 2006). However, both YliH and YceP are also involved in the regulation of other genes, such as motility and catabolite repression. It was also reported that the addition of indole synthesised by another bacterial species repressed curli expression and reduced biofilm formation in EHEC (Lee *et al.*, 2012). It is possible indole may upregulate or downregulate biofilm formation in response to a variety of environmental signals, such as culture medium or stress. In *E. coli* cultures, the AHL-SdiA signalling

pathway does not affect biofilm formation as *E. coli* does not synthesise AHLs, but because indole can interact with SdiA it may have an effect on biofilm formation.

It is well-known that AI-2 is used as a means of communication between both major classes of bacteria, Gram negative and Gram positive bacteria, and is thought to be the backbone of multi-species coordinated behaviour (Federle and Bassler, 2003). AI-2 is synthesised by the LuxS enzyme during the Activated Methyl Cycle (AMC) during exponential growth, and upon entering stationary phase the production of AI-2 tapers (Schauder *et al*., 2001; Pereira, Thompson and Xavier, 2013). This may indicate that AI-2 acts as a signal of population density, as well as a sign to prepare for biofilm formation. It has been noted by some papers that AI-2 could be classed as a byproduct of the cycle that turns SAM into homocysteine and 4,5-dihydroxy-2,3-pentanedione (DPD), thus AI-2 could be a necessary signal of metabolic information (Pereira, Thompson and Xavier, 2013). Once AI-2 is synthesised, specific exporters may be required because AI-2 is hydrophilic it is relatively membrane-impermeable, but these means of export are still unknown (Kamaraju *et al.*, 2011). LsrACDB imports AI-2 into the cytoplasm where it is regulated by two proteins LsrK, a kinase, and LsrR, a repressor (Li *et al.*, 2007). LsrK phosphorylates AI-2, and it is the phosphorylated AI-2 that binds to LsrR and stops the repression of the *lsr* genes (Taga, Miller and Bassler, 2003). The upregulation of the *lsr* operon results in the production of more LsrACDB transporter, thus more AI-2 is brought into the cell. Mutations in either *lsrK* or *lsrR* in *E. coli* reduced AI-2 and thus reduced expression of colanic acid and fimbriae (Li *et al.*, 2007). In turn, the biofilm thickness was reduced and had altered morphology. YdgG either exports AI-2 or blocks its uptake, and its deletion increases the formation of *E. coli* K-12 biofilm. Thus internalised AI-2 increases biofilm formation (Herzberg *et al.*, 2006). A microarray study by DeLisa *et al.* showed AI-2 stimulates gene expression associated with fimbriae, curli, and colanic acid production as well as flagellar motor

rotation, while it downregulated genes for flagellar synthesis, which indicates the importance of AI-2 on *E. coli* biofilm formation (DeLisa *et al.*, 2001). Additionally, AI-2 has shown to be a chemoattractant for *E. coli* (Hegde *et al.*, 2011; Laganenka, Colin and Sourjik, 2016). There also appears to be a relationship between AI-2 communication and metabolism: AI-2 is only produced in the presence of glucose, but is not able to be imported because *lsr* is repressed until cAMP-CRP complex (produced in the absence of glucose) upregulates it (Surette and Bassler, 1998; Xavier and Bassler, 2005). This may indicate another regulatory system that induces biofilm formation in nutrient deprivation. Ultimately, AI-2 is not required for biofilm formation in *E. coli* K-12 and cAMP-CRP negatively regulates AI-2 import during stationary phase via RpoS (Reisner *et al.*, 2003).

AI-3 is a unique communication molecule in that it allows communication to occur between *Escherichia* and eukaryotic organisms because AI-3 and human hormones can bind to the same receptor molecule (Kendall and Sperandio, 2014). AI-3 is synthesised by LuxS in *Escherichia coli* which induces a two-component cascade involving QseC, a kinase receptor, and QseB, a transcription factor (Walters, Sircili and Sperandio, 2006; Weigel and Demuth, 2016). The human hormones, epinephrine and norepinephrine, can also bind to the QseC receptor and stimulate the cascade (Sperandio *et al.*, 2003). Once bound, QseC phosphorylates QseB which can then bind to the DNA and regulate virulence genes, such as those involved with motility (Sperandio, Torres and Kaper, 2002). This drives the idea that the not yet known structure of AI-3 must at least be similar to epinephrine and norepinephrine because these hormones also increase motility in *E. coli* K-12 and virulence factors in EHEC (Sperandio *et al.*, 2003; Yang *et al.*, 2014). Like *E. coli* is with AI-2, EHEC is chemoattracted to the human hormones epinephrine and norepinephrine, and when these hormones bind to QseC virulence-associate genes are upregulated (Bansal *et al.*, 2007).

1.4.2 Competition sensing

Alternatively to quorum sensing, there are other molecules produced through a number of processes that are sensed by neighbouring bacteria and cause the formation of biofilms, termed "competition sensing" (Cornforth and Foster, 2013). These signals include all molecules that do not fall under the quorum sensing definition, yet still result in the sensing bacteria to make a biofilm as a means of protection or as a means of colonisation at a food source (Birch, 2002; Li and Tian, 2012; Cornforth and Foster, 2013). One of the most well-studied examples of competition sensing is the biofilm formation/defence response caused by antibiotics sensed in the environment (Kaplan, 2011). Although bacteria produce antibiotics in a defensive manner and not as a way to signal to other cells, these molecules are sensed by other bacteria which then respond in a competitive manner (Hoffman *et al*., 2005; De Lamo Marin *et al*., 2007; Haddadin *et al*., 2010). Much of the antibiotic-induced biofilm formation research supports the theory that bacteria use molecules released by competing bacteria in their surroundings as signals to alert the sensing bacteria of fellow competitors (Nadell, Xavier and Foster, 2009). Another example of competition sensing comes from observations of mixed cultures that often show one type of bacteria overtaking another at different developmental stages (Kolenbrander *et al*., 2002). These observations may suggest more environmental or non-quorum sensing communication is possibly playing a role in biofilm formation. Further examples of competition sensing come from a report that bacteria can sense nucleotides from other bacteria as 'danger signals' and induce biofilm formation (Kolenbrander *et al*., 2002). While competition sensing is key in bacterial colonisation and defence mechanisms, quorum sensing results in cooperative behaviour; both are needed for biofilm formation and both sensing pathways are

considered heavily linked (De Lamo Marin *et al*., 2007; von Bodman, Willey and Diggle, 2008).

1.4.3 Phenylalanine, tyrosine, and tryptophan import/export mechanisms

Biofilms can be used to protect biocatalytic reactions occurring within cells; furthermore, it is important to understand the effect that the products of biocatalysis have on biofilm formation and other gene expression. Previous work in the Overton laboratory introduced the plasmid pSTB7, encoding a tryptophan synthase, into *E. coli* K-12 which allows the biocatalysis of haloindole and serine into halotryptophan, an important precursor molecule that can be used in other reactions (Tsoligkas *et al.*, 2011; Perni *et al.*, 2013). However, transforming pSTB7 into *E. coli* reduces the formation of a biofilm. Potentially, transporters of halotryptophan and similar amino acids in the cell membrane could be importing the excess halotryptophan being overproduced by pSTB7. Once inside the cell, the halotryptophan is degraded into haloindole by tryptophanases and gene expression and biofilm formation are affected. Thus, it is important to understand the import/export mechanisms of tryptophan and similar amino acids and the effect of these amino acids on *E. coli* K-12 biofilm formation.

Phenylalanine, tyrosine, and tryptophan are all aromatic amino acids and are grouped together due to their nonpolar, hydrophobic and neutral side chains which make them insoluble or only slightly soluble in water (Lodish *et al.*, 2000). While tryptophan can be metabolised as a carbon/nitrogen source by the *E. coli*, phenylalanine and tyrosine cannot. However, the means of their import and export are important in understanding their effect on the cell as research expands into engineering bacterial strains to produce these amino acids for commercial use (Rodriguez *et al.*, 2014). Phenylalanine, tyrosine, and tryptophan are imported into the *E. coli* by AroP, but they

can also be imported by PheP, TyrP, Mtr, and TnaB, respectively as seen in Fig. 1.7 (Wookey and Pittard, 1988; Honoré and Cole, 1990; Heatwole and Somerville, 1991; Pi, Wookey and Pittard, 1991; Yanofsky, Horn and Gollnick, 1991). Tryptophan can be used as a carbon source by *E. coli*; consequently, when grown in tryptophan, the *tna* operon will induce expression to import and degrade tryptophan as needed (Yanofsky, Horn and Gollnickt, 1991). The membrane protein YddG is responsible for exporting aromatic amino acids, like phenylalanine, in *E. coli* (Doroshenko *et al.*, 2007). The Mtr permease largely exports indole, a byproduct of tryptophan being broken down by tryptophanase (TnaA) for use as a carbon or nitrogen source in *E. coli* (Heatwole and Somerville, 1991).

Indole can act as a signal molecule in *E. coli* which can affect biofilm formation (section 1.4.1) (Di Martino *et al.*, 2003). Also, the addition of the amino acids to the growth medium changes the *E. coli* gene expression and regulatory mechanism of amino acid transporters. One microarray study in *E. coli* found that, while the *tnaAB* operon is normally activated by cAMP-CRP during nutrient depletion/stationary phase and is responsible for the conversion of tryptophan to indole, the addition of phenylalanine to the medium induced *tnaAB* expression eight fold (Polen *et al.*, 2005). The study also found the addition of phenylalanine decreased expression of genes associated with flagella, which may correspond with an increase in biofilm formation.

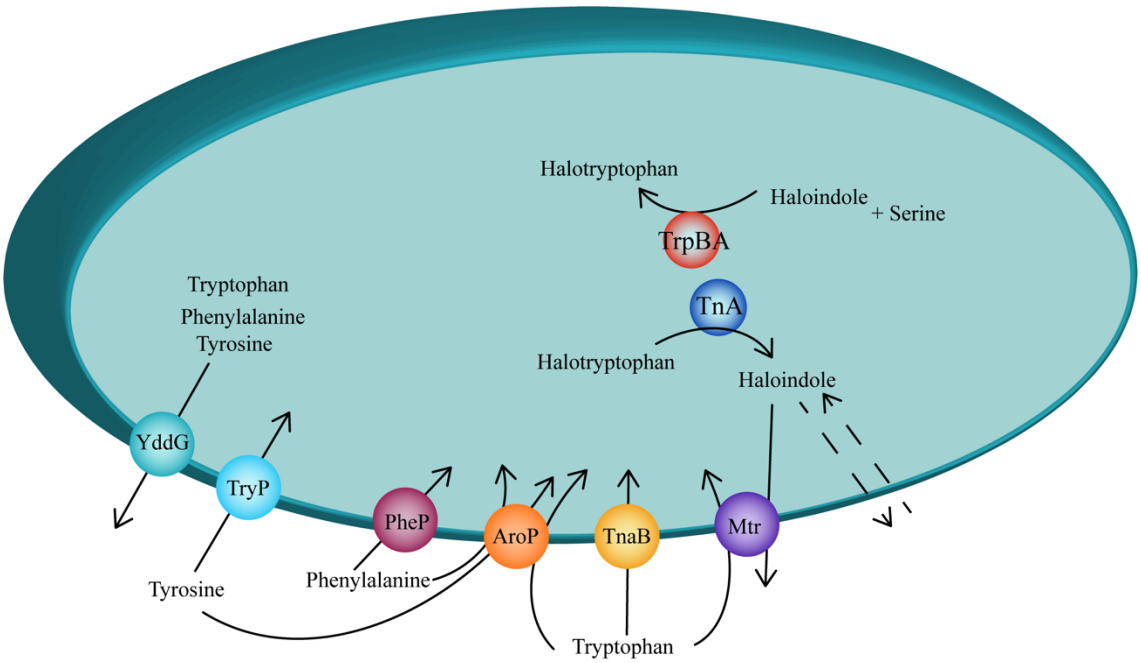

Figure 1.7: Import and export mechanisms of aromatic amino acids.

YddG is responsible for export of aromatic amino acids. While AroP can import phenylalanine, tyrosine, and tryptophan, these amino acids can also be imported by PheP; TryP; TnaB and Mtr, respectively. There are reports that indole can freely disuse (dotted line) or is exported by Mtr. TnA breaks down halotryptophan into haloindole, while TrpBA can synthesise halotryptophan from haloindole and serine.

1.5 Aims and objectives

The primary aim of the following work is the characterisation and optimisation of *E. coli* K-12 biofilm formation with the objective to generate a robust *E. coli* K-12 biofilm capable of industrial applications in biocatalysis. To achieve this goal, crystal violet assays were employed to measure biofilm accumulation, and viability assays were used to measure alive, dead, and injured cells. Additionally, a *csgB::gfp* reporter plasmid was used to measure curli expression by flow cytometry and visualise curli expression by confocal laser scanning microscopy. Stains were also used to visualise matrix components. Specific objectives are as follows:

1) Characterise curli expression in response to changes in osmolarity and surface sensing as well as elucidate and optimise curli expression in response to a variety of physical conditions, such as temperature (chapter 3).
2) Investigate the effect of competition sensing on *E. coli* K-12 biofilm formation in response to spent medium and individual compounds found in spent medium (chapter 3).
3) Study the effect of aromatic amino acids, specifically phenylalanine on *E. coli* K-12 curli expression and biofilm formation (chapter 4).
4) Develop a pellicle generation model and characterise *E. coli* K-12 pellicle formation in terms of curli expression, motility, and matrix components (chapter 5).

1.6 Outline

The following manuscript is organised into eight chapters: the first chapter consists of a literature review covering current knowledge of biofilms, crucial aspects of biofilm formation pertinent to this research, and so forth; the second chapter is a detailed materials and methods of all experiments performed. Chapter three, four, and five are results chapters covering biofilm generation optimisation via curli expression and competition sensing; the effect of aromatic amino acids on biofilm formation specifically detailing the effects of phenylalanine; and a characterisation of *E. coli* K-12 pellicle formation, respectively. Each of these three results chapters contain an introduction with a brief literature review, a general materials and methods section, results and discussion, and a brief conclusion. Each results chapter can be read individually or in the manuscript as a whole. After the final results section, there is an overall conclusion in chapter six, which ties together the thesis and includes final remarks and future work. Lastly, chapter seven and eight contain references and appendices, respectively.

2 METHODS AND MATERIALS

2.1 Microbiological methods

The work in this thesis primarily used *Escherichia coli* K-12 PHL644, an optimised biofilm-producing variety of the parental strain MC4100. PHL644 has a single point mutation at position 43 in the *ompR234* gene which replaced leucine with arginine and resulted in the constitutive expression of curli (Vidal *et al.*, 1998). The mutation also upregulates four genes not associated with curli, *gadE*, *yjbR*, *chbG*, and *recT*; only GadE may potentially influence biofilm formation via regulation of *rcsA* in the Rcs phosphorelay cascade, described in section 1.3.4 (Brombacher *et al.*, 2003; Wall, Majdalani and Gottesman, 2018). MC4100 is a derivative of another parental strain, MG1655, and both strains were also used in the following work. A summary of strains used in this study can be found in Table 2.1.

The reporter plasmid pJLC-T was also heavily used in this thesis as a *csgB::gfp* reporter (Leech, 2017). This was made by first constructing an insert consisting of a promoter, a ribosomal binding site, a degradation tag, and restriction enzyme sites to clone into pPROBE'-TT, a promoterless GFP reporter gene. The intergenic region between *E. coli* MC4100 CsgD and CsgB was cloned to act as the promoter in pPROBE'-TT. CsgBAC's ribosomal binding site was replaced with a more efficient binding site (AGGAAACAGCT) which was then fused with eGFP followed by the C-terminus and restriction enzyme sites. The C-terminus consisted of a degradation tag (AANDENYALVA), which reduces the GFP half-life from 24 hours to around 60 minutes (Miller, Leveau and Lindow, 2000). The whole *csgB::gfp*-TAG construct was cloned into pPROBE'-TT via the restriction enzyme EcoRI-HindIII sites which flanked the two ends of the construct (Andersen *et al.*, 1998). The pPROBE'-TT has a pBBR1 origin of replication and features a tetracycline resistance cassette as well as a *gfp* (half-life 24 hours). The promoterless pPROBE-TT' in PHL644 was used as a control.

Another plasmid used in this work, specifically in chapter 5, was pT7-CsgD. When transformed into cells, pT7-CsgD caused the expression of *csgD* under the T7 promoter along with an ampicillin resistance cassette. The empty vector pT-7 was used to make pT7-CsgD and thus was used as a control. A summary of plasmids used in this study can be found in Table 1.1. All plasmids were transformed using the heat-shock method and grown as described in the following sections.

Species/Strains	**Genotype**	**Reference or Source**
E. coli K-12 MG1655	F^- λ^- $ilvG^-$ rfb-50 rph-1	Reference strain
E. coli K-12 MC4100	*araD139*Δ(*argF-lac*)*U169 rpsL150 relA1 flbB5301 deoC1 ptsF25 rbsR*	Reference strain
E. coli K-12 PHL644	MC4100 malA-kan *ompR234*	Vidal *et al*., 1998
Plasmid	Description	Reference or Source
pJLC-T	*pcsgB::gfp*; pBBR1 ori; TetR	Leech, 2017
pT7-7	T7 RNA polymerase-dependent promoter; AmpR	Brombacher *et al*., 2006
pT7-CsgD	pT7-7 carrying *csgD* gene	Brombacher *et al*., 2006*

Table 2.1 Bacterial strains and plasmids used in this study.

*gift from Regina Hengge, Humboldt-Universität, Berlin.

2.2 Media

2.2.1 Luria-Bertani broth

Luria-Bertani (LB) broth (Miller formula: 10 g L^{-1} tryptone, 5 g L^{-1} yeast extract, 10 g L^{-1} NaCl) was purchased from Sigma-Aldrich and 25 g was dissolved into 1.0 L of deionised water and autoclaved before use. LB was used for overnight cultures exclusively as it is a rich medium that supports *E. coli* K-12 growth.

2.2.2 M63+ minimal media

M63+ media (100 mM KH_2PO_4 (Sigma-Aldrich), 15 mM $(NH_4)_2SO_4$ (Sigma-Aldrich), 1 mM $MgSO_4$ (ThermoFisher), 1.8 μM $FeSO_4$ (Sigma-Aldrich), 10 mM D-glucose (ThermoFisher), and 17 mM sodium succinate (ThermoFisher)) was prepared as follows to prevent interactions between components during autoclaving. First, 100 mM KH_2PO_4, 17 mM sodium succinate, 15 mM $(NH_4)_2SO_4$ was dissolved in deionised water and the pH was adjusted to 7.0 using potassium hydroxide (Sigma-Aldrich) before being autoclaved. The following components were prepared individually and either autoclaved or filter sterilised (as stated) in the following working stocks before being added to achieve previously stated final concentrations: $MgSO_4$ (100 mM) autoclaved, D-glucose (1 M) filter sterilised or autoclaved, and $FeSO_4$ (1.5 mM) filter sterilised. Once sterilised, the four components were combined for a final working concentration stated above. M63+ media was used for biofilm and pellicle growth exclusively as it is a minimal medium that supports *E. coli* K-12 biofilm and pellicle formation.

2.2.3 Nutrient agar plates

Nutrient agar (Oxoid) plates were prepared by dissolving 28 g of nutrient agar powder (Thermo Scientific) in 1.0 L of deionised water. The suspension was autoclaved and roughly 25 mL was sterilely poured into individual Petri dishes before solution cooled and solidified.

2.2.4 Luria-Bertani semi-solid agar plates

Luria-Bertani (LB) semi-solid agar plates were made for motility assays containing 0.3% agar. To make a 1.0 L stock, 25 g LB and 3.0 g of agar were dissolved in 1.0 L (1000 g) of deionised water. The suspension was autoclaved and roughly 25 mL was sterilely poured into individual Petri dishes before solution cooled and solidified.

2.3 Overnight cultures

Untransformed strains were grown on Nutrient Agar plates. As stated in the following section (section 2.3 Plasmid transformations), transformed bacterial strains were selected on Nutrient Agar supplemented with tetracycline (10 μg mL^{-1}) or ampicillin (100 μg mL^{-1}). Single colonies were used to inoculate 5.0 mL of LB broth in 25 mL sterile test tubes and grown overnight (22 – 28 hours) at 30 °C and 150 rpm shaking before being harvested by centrifugation (1122 g for 20 minutes) and resuspended in M63+ minimal media.

2.4 Plasmid transformations

2.4.1 Chemically-competent cell preparation

To prepare cells for heat-shock transformation, cells had to be made chemically-competent. A single colony of the desired strain was used to inoculate 5 mL of Luria-Bertani (LB) broth (10 g L^{-1} tryptone, 5 g L^{-1} yeast extract, 10 g L^{-1} NaCl) which was then grown overnight (21 – 28 hours) at 30 °C and 150 rpm shaking. Next, 400 µL of the overnight culture was used to inoculate 40 mL LB broth to make a 1.0% inoculum in a sterile Falcon tube or equivalent. The inoculum was grown for 2 – 4 hours at 30 °C with 150 rpm shaking until the optical density (OD_{600}) reached 0.3 – 0.5 before being placed on ice for 20 minutes to stop or slow growth. The Falcon tube was kept on ice for all subsequent steps. After 20 minutes, the culture was centrifuged at 1122 g at 4 °C for 15 minutes, and the supernatant was sterilely removed and discarded. The pellet was resuspended in 8 mL of chilled sterile 4 °C 100 mM calcium chloride to make the outside of cells positively-charged (allows for more efficient transformation with negatively-charged DNA). After incubating in calcium chloride on ice for 20 minutes, the solution was centrifuged as before, and the supernatant was removed and discarded. The pellet was resuspended in 2 mL of chilled sterile 4 °C 100 mM calcium chloride/15% glycerol solution. The solution (consisting of chemically-competent cells) was aliquoted as 200 µL volumes into sterile microcentrifuge tubes and kept at -80 °C for a maximum of 12 months.

2.4.2 Plasmid transformation protocol

To transform plasmids into cells, chemical-competent cells were made as described in the previous section 2.4.1 Chemically-competent cell preparation. First,

one microcentrifuge tube containing 200 µL chemically-competent cells was thawed on ice. Under sterile condition, 100 µL was pipetted to a new sterile microcentrifuge tube, and the two tubes were labelled for one positive and one negative transformation. Under sterile conditions, 1.0 µL of plasmid was pipetted into the positive transformation tube and gently mixed. The tubes were incubated on ice for 30 – 60 minutes to allow the negatively-charged plasmid DNA to arrange around the positively-charged (competent) cells. The cells were then heat shocked to allow the plasmid to enter the cells by placing the tubes in a heat block at 42 °C for 1 minute and 15 seconds. The tubes were placed on ice for 2 minutes and 700 µL of sterile LB broth was added to each positive and negative transformation tube and the tubes were gently mixed. The tubes were returned to the heat block at 37 °C for 1 – 2 hours to allow cells to grow. The tubes were then centrifuged (5000 g for 5 minutes) before all but around 50 µL of supernatant was discarded under sterile conditions. The positively- and negatively-transformed cells (pellet) were resuspended in the remaining ~ 50 µL supernatant before being sterilely pipetted and spread onto Nutrient Agar (Oxoid) plates supplemented with tetracycline (10 µg mL^{-1}) or ampicillin (100 µg mL^{-1}). Plates were incubated at 30 °C statically overnight (< 24 hours) and were then stored at 4 °C for up to two weeks. Negative transformants should have no colonies on the Nutrient Agar plates, while positive transformations should have roughly 100 colonies. Single colonies were selected sterilely using an inoculation loop and were grown for use in experiments as described in the previous section 2.3 Overnight cultures.

2.5 Preparation of solutions

2.5.1 Propidium iodide

Propidium Iodide (PI, Sigma-Aldrich) was used to detect DNA of dead cells in viability assays by flow cytometry as this dye cannot pass the membrane of intact (alive) cells. A 200 μg mL^{-1} working solution was made by dissolving of 4 mg of PI powder in 20 mL deionised water. The working solution was filter sterilised before being aliquoted and stored at 4 °C.

2.5.2 Bis-oxonol

Bis (1,3-dibutylbarbituric acid) trimethine oxonol also known as Bis-oxonol (BOX, Sigma-Aldrich) was used to stain depolarised membranes of injured or dead cells in viability assays by flow cytometry. A 200 μg mL^{-1} stock solution concentration was made by dissolving 5 mg BOX powder in 25 mL dimethyl sulfoxide (DMSO, Sigma-Aldrich). The working solution was not filter sterilised as DMSO is a solvent and the solution was aliquoted and stored at 4 °C.

2.5.3 Concanavalin A

Concanavalin A (ConA, ThermoFisher Scientific) conjugated to Alexa Fluor 488 was used to stain α-mannopyranosyl and α-glucopyranosyl residues of the extracellular polymeric substances (EPS) of the biofilm or pellicle, specifically termed colanic acid, for visualisation by confocal microscopy. ConA was received as a 5 mg powder and a stock solution of 5.0 mg mL^{-1} was made by dissolving 5 mg of ConA into

1.0 mL of 0.1 M Sodium Bicarbonate (Sigma-Aldrich) solution made with deionised water. A 200 μg mL^{-1} working solution was prepared by combining 40 μL of stock into 960 μL PBS. Working solutions were filter sterilised and stored in the refrigerator at 4 °C for a maximum of 6 months.

2.5.4 Wheat Germ agglutinin

Wheat Germ Agglutinin (WGA, ThermoFisher Scientific) conjugated to Fluorescein isothiocyanate (FITC) was used to stain sialic acid and N-acetylglucosaminyl residues of the extracellular polymeric substances (EPS) of the biofilm or pellicle, specifically termed poly-β(1-6)-N-acetylglucosamine (PNAG), for visualisation by confocal microscopy. WGA was received as a liquid (1.0 mg mL^{-1} in PBS). A working solution of 5 μg mL^{-1} was prepared by combining 5.0 μL of stock into 995.0 μL PBS. Working solutions were filter sterilised and stored in the refrigerator at 4 °C for a maximum of 6 months.

2.5.5 Phosphate Buffer Saline

Phosphate Buffered Saline (PBS) was used as a balanced salt solution for diluting cells for analysis on the flow cytometer or rinsing the biofilm to remove unattached cells. The PBS solution was prepared per manufacturer's instructions of dissolving 1 tablet (Oxoid) into 100 mL deionised water and then autoclaved. PBS was also used in osmolarity experiments and solutions of $1/10^{th}$ and $1/20^{th}$ strength PBS were made by diluting PBS into deionised water.

2.5.6 Aromatic amino acid solutions

Working solutions 56 mM tryptophan, 2.48 mM tyrosine, 179 mM L-phenylalanine, and 181.6 mM D-phenylalanine were made by dissolving 0.46 g into 40 mL, 0.23 g into 500 mL, 29.6 g into 40 mL, and 1.2 g into 40 mL, respectively, before being filter sterilised. These concentrations are the greatest possible based on each amino acid's solubility. In curli gene expression studies, a final concentration of 0.1 mM was reached by adding 0.39 mL tryptophan to 218.61 mL M63 medium; 8.83 mL tyrosine to 210.17 mL M63 medium; 0.12 mL L-phenylalanine to 218.88 mL M63 medium, respectively, in a 500 mL Erlenmeyer flask. A final concentration of 10 mM was reached by adding 12.23 mL L-phenylalanine to 206.77 mL M63 medium and 12.06 mL D-phenylalanine to 206.94 mL M63 medium, respectively, in a 500 mL conical flask. During biofilm generation studies, a final concentration of 10 mM was reached by adding 3.91 mL L-phenylalanine to 14 mL M63 stock and 52.19 mL sterile deionised water; 3.85 mL D-phenylalanine to 17 mL M63 stock and 52.15 mL sterile deionised water; or adding 3.91 mL L-phenylalanine and 3.85 mL D-phenylalanine to 14 mL M63 stock and 48.2 mL sterile deionised water, respectively, in a 100 mL Duran bottle.

2.6 Generation of biofilm and pellicles

2.6.1 Biofilm growth model

The Duran bottle method was developed in the Overton laboratory as a means of replicable biofilm generation (Leech, 2017). To set up the biofilm growth model as depicted in Fig. 3.1, termed the Duran Bottle method, 5.0 mL overnight cultures (section 2.3 Overnight cultures) were centrifuged (1122 g for 20 minutes) and

resuspended in 2.1 mL M63+ minimal media before 700 μL was inoculated into 100 mL Duran bottles containing 70 mL of M63+ minimal medium and a standard 76 mm x 26 mm microscope slide (VWR International) wrapped with 12 mm x 12 mm x 0.075 mm polytetrafluoroethylene thread seal tape (PTFE, RS Components). In previous work, the slides generated 7 times more biofilm when wrapped with PTFE (Leech, 2017). Bottles were incubated in an orbital shaker at 30 °C and 70 rpm shaking for a period of one to three days. Microscope slides carrying biofilm were removed with forceps and washed with PBS before analysis.

2.6.2 Pellicle growth model and photography

To set up the pellicle growth model, 5.0 mL of cultures grown overnight (section 2.3 Overnight cultures) were centrifuged (1122 g for 20 minutes) and resuspended in 2.1 mL M63+ minimal media before 20 μL was inoculated into test tubes (Fisher Scientific) containing 5.0 mL of M63+ minimal medium. Tubes were incubated in an orbital shaker at 30 °C and 70 rpm shaking for a period of one to six days. Pellicles were photographed with an Apple iPhone 5S as required.

2.7 Biofilm analytical techniques

2.7.1 Analysis of curli expression in the biofilm growth model

Biofilms were generated following practices detailed in section 2.6.1. Cells transformed with pJLC-T were harvested with a sterile inoculation loop or pipette from three distinct locations in the Duran bottle (planktonic, biofilm, and sediment) on day three. Samples were suspended in sterile PBS and vortexed before being analysed using

an BD Accuri C6 flow cytometer (BD, UK). Samples were excited using a 488 nm laser and fluorescence emission was detected using a 533/30 nm filter until 25,000 events were recorded. Samples were not stained because only GFP was measured. Forward scatter (FSC) was calculated based on the size of each event and an FSC threshold of 12,000 units was set to eliminate recordings from events smaller than the standard *E. coli* cell size and thus reduce large collections of background data, or "noise." Mean GFP fluorescence (FL1-A) was calculated using CFlow software (BD, UK). Cleaning procedures after experiments followed manufacturer's guidelines, and also included running 70% ethanol and filtered water for 1 – 5 minutes at fast settings between samples as needed.

2.7.2 Visualisation EPS components by confocal microscopy

Following biofilm generation as described in section 2.6.1, PTFE-wrapped microscope slides carrying biofilm were harvested at timepoints during maturation. Using forceps to remove the microscope slide from the Duran bottle, biofilms were washed with PBS to remove unadhered cells before being stained as necessary. Stains included either adding 20 μL of 200 μg mL^{-1} Concanavalin A Alexa Fluor 488 (ConA; Fisher Scientific) and incubation in darkness overnight at 4 °C or 20 μL of 5 μg mL^{-1} or Wheat Germ Agglutinin conjugated to FITC (WGA; Fisher Scientific) and incubation in darkness for two hours at 4 °C and/or 20 μL of 200 μM SYTO 62 (Fisher Scientific) and incubation in darkness for 15 minutes before visualisation. ConA and WGA bind to the biofilm components poly-β(1-6)-N-acetylglucosamine (PNAG) and colanic acid (ConA), respectively, while SYTO 62 binds to DNA of cells in the biofilm. After staining, a 22 mm x 32 mm coverslip (Thermo Scientific) was gently placed on the biofilm and immersion oil was gently dropped onto the coverslip. The microscope slide

carrying biofilm was placed on the microscope stage and examined on either a Leica TCS SPE Confocal Laser Scanning Microscope (Wetzlar, Germany) with a 40x oil immersion objective or a Lecia TCS SP8 confocal equipped with a Leica DM8 CS5 Microscope (Wetzlar, Germany) with a 63x oil immersion objective. A 635 nm laser was used for biofilms stained with SYTO 62 with an excitation/emission filter of 650/640-740; a 488 nm laser was used for biofilms stained with ConA with an excitation/emission filter of 500/480-580; a 488 nm laser was used for biofilms stained with WGA with an excitation/emission filter of 500/480-580; and a 488 nm laser was used for biofilms transformed with pJLC-T for curli expression analysis with an excitation/emission filter of 488/490-520. Optical section images and three-dimensional images were acquired by LasX software and subsequent image analysis was performed with Fiji or ImageJ software.

2.7.3 Crystal violet assay

The biofilm was quantified using the standard method of crystal violet assay following biofilm generation as described in section 2.6.1. First, microscope slides carrying biofilm were removed with forceps from the Duran bottle and gently rinsed with sterile PBS to remove unadhered cells from the biofilm. Before the microscope slide was replaced back in the Duran bottle, 70 μL of 1.0% Crystal Violet solution (Sigma-Aldrich) was added to the spent medium in the Duran bottle and swirled gently. The microscope slide carrying biofilm was then placed in the same Duran bottle with crystal violet solution and incubated at room temperature for 30 minutes. The crystal violet dye binds to DNA (cells) during this incubation. The microscope slides carrying biofilm were again removed with forceps from the Duran bottle and gently washed with sterile PBS to remove unbound crystal violet solution and unadhered cells from the

biofilm. The microscope slide carrying biofilm was then placed into a 50 mL Falcon tube (Fisher Scientific) containing 35 mL of 100% ethanol (Thermofisher) for at least 30 minutes to remove the crystal violet dye from the biofilm. The microscope slide carrying biofilm was then removed from the Falcon tube using forceps and discarded. The Falcon tube containing ethanol and crystal violet stain from the biofilm was vortexed and 1.0 mL was measured on an Evolution 300 spectrophotometer (Thermo Scientific, UK) at OD_{585}. The optical density of the crystal violet destained from the biofilm measured the relative biofilm biomass.

2.8 Pellicle analytical technique

2.8.1 Analysis of curli expression in the pellicle growth model

Pellicles were generated following practices detailed in section 2.6.2. Cells transformed with pJLC-T were harvested with a sterile inoculation loop or pipette from four distinct locations in the test tube method (air-liquid interface, pellicle, planktonic, and sediment) as depicted in Fig. 5.11 at days one, two, and three. Samples were suspended in sterile PBS and vortexed before being analysed using an BD Accuri C6 flow cytometer (BD, UK). Samples were excited using a 488 nm laser and fluorescence emission was detected using a 533/30 nm filter until 25,000 events were recorded. Samples were not stained because only GFP was measured. Forward scatter (FSC) was calculated based on the size of each event and an FSC threshold of 12,000 was set to eliminate recordings from events smaller than the standard *E. coli* cell size. Mean GFP fluorescence (FL1-A) was calculated using CFlow software (BD, UK).

2.8.2 Visualisation of EPS components by confocal microscopy

Following practices detailed in section 2.6.2, pellicles were harvested by using forceps to gently dip sterile PTFE tape (RCS Components) cut approximately into 6 mm x 6 mm sections into the surface of the medium allowing the pellicle to adhere to the PTFE. The pellicles were harvested at timepoints during maturation and mounted on standard 76 mm x 26 mm microscope slides (VWR International). Mounted pellicles were subsequently stained either 20 μL of 200 μg mL^{-1} Concanavalin A Alexa Fluor 488 (ConA; Fisher Scientific) and incubated in darkness overnight at 4 °C or 20 μL of 5 μg mL^{-1} or Wheat Germ Agglutanin conjugated to FITC (WGA; Fisher Scientific) incubated in darkness for two hours at 4 °C, and then stained with 20 μL of 200 μM SYTO 62 (Fisher Scientific) for 15 minutes at room temperature before visualisation. ConA and WGA bind to the matrix components poly-β(1-6)-N-acetylglucosamine (PNAG) and colanic acid (ConA), while SYTO 62 binds to DNA of cells of the pellicle. After staining, a 22 mm x 32 mm coverslip was gently placed on the pellicle and immersion oil was gently dropped onto the cover slip. In order to ensure pellicle integrity, adhesive PTFE spacers were placed on either side of the sample so the cover slip was propped above the pellicle and contact between cover slip and pellicle was minimised. The microscope slide carrying the pellicle was placed on the microscope stage and pellicles were examined on a Lecia TCS SP8 confocal equipped with a Leica DM8 CS5 Microscope (Wetzlar, Germany) with a 63x oil immersion objective. A 635 nm laser was used for pellicles stained with SYTO 62 with an excitation/emission filter of 650/640-740; a 488 nm laser was used for pellicles stained with ConA with an excitation/emission filter of 500/480-580; a 488 nm laser was used for pellicles stained with WGA with an excitation/emission filter of 500/480-580; and a 488 nm laser was used for pellicles transformed with pJLC-T for curli expression analysis with an

excitation/emission filter of 488/490-520. Optical section images and three-dimensional images were acquired by LasX software and subsequent image analysis was performed with Fiji or ImageJ software.

2.9 Additional assays

2.9.1 Optimisation of curli expression in conical flasks

In order to optimise curli expression in response to aromatic amino acids, cells transformed with pJLC-T were grown overnight (section 2.3 Overnight cultures) and centrifuged (1122 g for 20 minutes). Cells were then resuspended in 2.1 mL M63+ minimal media before 1.0 mL was inoculated into 500 mL conical flasks containing 219 mL M63+ minimal medium and supplemented with aromatic acids (2.5.6 aromatic amino acid solutions) as required. Flasks were incubated at 30 °C and 70 rpm unless otherwise stated. Samples were taken from the flask as different time points and were suspended in sterile PBS and vortexed before being analysed using an BD Accuri C6 flow cytometer (BD, UK). Samples were excited using a 488 nm laser and fluorescence emission was detected using a 533/30 nm filter until 25,000 events were recorded. Samples were not stained because only mean cellular GFP was measured. Forward scatter (FSC) was calculated based on the size of each event and an FSC threshold of 12,000 was set to eliminate recordings from events smaller than the standard *E. coli* cell size. Mean GFP fluorescence (FL1-A) was calculated using CFlow software (BD, UK).

2.9.2 Viability assay

To test the viability of cells in a biofilm, samples were scraped from the biofilm generated as described in section 2.6.1 and resuspended in roughly 1.0 mL PBS

in microcentrifuge tubes or flow cytometer tubes. Next, cells in suspension were treated with 10 µL of 200 µg mL^{-1} Bis-oxonol (BOX) to stain cells with depolarised membrane (injured or dead cells), and 20 µL of 200 µg mL^{-1} propidium iodide (PI) to stain DNA of dead cells, then were analysed by flow cytometry to determine the percentage of cells that were "injured" (BOX^+), "dead" (PI^+ and BOX^+), or "healthy" (PI^- and BOX^-). Live and dead controls were also employed and stained with PI and BOX in order to gate for *E. coli* cells and then categorise quadrant gating regions for "healthy," "injured," and "dead" cells. Cells for the "alive" control were untreated cells grown overnight in LB broth, which were then centrifuged (2800 g for 5 minutes) and resuspended in PBS. Cells for the "dead" control were grown as the alive control before being killed by either heat (95 °C for 5 minutes and cooled) or by resuspending cells in 100% ethanol (rather than PBS) for 10 minutes. All samples were analysed using an BD Accuri C6 flow cytometer (BD, UK) and excited using a 488 nm laser. Fluorescence emission was detected using a 530 nm +/- 15 nm (BOX) and > 670 nm (PI) filter until 25,000 events were recorded. Forward scatter (FSC) was calculated based on the size of each event and an FSC threshold of 12,000 was set to eliminate recordings from events smaller than the standard *E. coli* cell size. Mean BOX (FL1-A) and PI (FL3-A) fluorescence values were calculated using CFlow software (BD, UK).

2.9.3 Agglutination assay

To test agglutination, untransformed PHL644 was grown for 21 – 24 hours in 15 mL M63+ minimal medium in a 25 mL Falcon tubes (Fisher Scientific) with and without 10 mM L-phenylalanine at 30 °C and 70 rpm shaking. Cells were then centrifuged (3200 g for 10 minutes) and washed with 5 mL PBS. The pellet was resuspended in a 25 mL Falcon tube containing 15 mL PBS at a starting $OD_{600} \approx 0.8$

and incubated statically at 30 °C. Samples were taken from the top of the tube 0.5 cm beneath the surface of the liquid at specified timepoints and the optical density (OD_{600}) was measured. As the OD_{600} decreased over time, this indicated agglutination.

2.9.4 Motility assay

The OD_{600} of overnight cultures was measured and dilutions were calculated and prepared with PBS to make the biomass concentrations the same between each inoculum. The diluted culture was then point inoculated at the centre of 0.3% semisolid LB agar plates in duplicate and incubated statically for 24 hours at 30 °C. The zone of growth from the inoculation point was measured.

2.9.5 Analysis of curli expression in response to osmolarity

Cells transformed with pJLC-T were grown in test tubes containing 15 mL M63+ minimal medium overnight at 30 °C and 70 rpm shaking before 1.0 mL of sedimented cells (with low curli expression) were harvested by pipetting from the sediment at the bottom of the test tube. The sedimented cells were then centrifuged (3200 g for 10 minutes) and washed with 1.0 mL sterile PBS before being resuspended in either 1.0 mL sterile PBS, 1/5 strength PBS or 1/20 strength PBS at a final biomass concentration of either $OD_{600} \approx 0.07$ or OD_{600} between 0.7 – 1.2. Test tubes were incubated at 30 °C statically for 24 hours. After 24 hours, the suspensions were vortexed and used to measure the osmolarity, mean green fluorescence (indicating curli expression), cell concentration (OD_{600}), and pH. Osmolarity was measured according to the manufacturer's instructions of pipetting 20 μL onto a small disc of paper and placing the disc into a Vapor Pressure Osmometer 5500 (Utah, USA) for analysis. Curli expression was analysed by measuring roughly 50 μL diluted in 1.0 mL sterile PBS on

an Accuri C6 flow cytometer (BD, UK) excited using a 488 nm laser. Fluorescence emission was detected using a 533/30 nm filter until 25,000 events were recorded. Mean GFP fluorescence (FL1-A) was calculated using CFlow software (BD, UK). Cell concentration was measured by an Evolution 300 spectrophotometer (Thermo Scientific, UK) at OD_{600}, while pH was measured by an XL200 pH Benchtop Meter (Fisherbrand, UK).

2.9.6 Genome sequencing

PHL644 and a hypermotile variant, PHL644h, isolated from the motility assay were sequenced by microbesNG (https://microbesng.uk/). After being grown on nutrient agar, PHL644 and PHL644 were sent to microbesNG on beads. Three beads for each strain were first washed with extraction buffer and RNase A and incubated at 37 °C for 25 minutes. Next, Proteinase K and RNaseA were added and incubated at 65 °C for 5 minutes. Purified DNA from each bead was extracted in EB buffer. The Quantit dsDNA HS assay quantified the DNA in triplicate by use of an Ependorff AF2200 plate reader. A Nextera XT Library Prep Kit (Illumina, San Diego, USA) was used to prep the genomic DNA libraries of both strains using a modified version of the manufacturer's instructions (input DNA was increased from 1 ng to 2 ng, and PCR elongation time was increased from 30 seconds to 1 minute). The Hamilton Microlab STAR performed library preparation and quantified the DNA. The Kapa Biosystems Library Quantification Kit for Illumina on a Roche light cycler 96 qPCR machine quantified pooled libraries, while the libraries were sequenced on an Illumina HiSeq using a 250bp paired end protocol. Variant calling was performed using VarScan (Koboldt *et al*., 2009) using the following parameters: minimum coverage 3, minimum variant

frequency 10%, p-value 0.05. A summary table of all mutations and comments can be found in Appendix 1.

3 Optimisation of Biofilm Model: Curli Expression and Competition Sensing

3.1 Introduction

There is a growing industry which uses biofilm-based biotechnology in their applications; however, a great portion of this research is still in its infancy (Lee, Maeda, Hong and Wood, 2009; Muffler *et al.*, 2014). There are many complex signalling/sensing pathways, mechanisms and physical conditions that influence biofilm production and regulation that need to be understood in order to successfully harness the biocatalytic capabilities of biofilms (Stoodley *et al.*, 1997; Van Houdt and Michiels, 2005; Lee and Lee, 2010). Some of these sensing pathways include detecting contact with surfaces, changes in pH and osmolarity, and competition sensing. As discussed in 1.4.2, competition sensing is the cell's ability to sense molecules released from neighbouring bacteria (such as antibiotics, ethanol, or acids) and respond defensively by forming a biofilm (Whitman, Coleman and Wiebe, 1998; Jefferson, 2004). Unlike quorum sensing, competition sensing involves identifying any molecules produced by neighbouring bacteria that are not made for the purpose of communication, nor is this process quorum-dependent on reaching a specific density of molecules or cells. The following work delves into the intricacies of sensing pathways in relation to biofilm formation.

Generally, there are five steps necessary to form an *E. coli* K-12 biofilm: initial contact and reversible attachment; irreversible attachment; growth and production of PNAG and colanic acid (EPS matrix); maturation; and dispersion (Palmer, *et al.*, 2007; García-Contreras *et al.*, 2008). Irreversible attachment is one of the primary focuses of this work. As previously discussed in 1.2.2.1, initial attachment of *E. coli* K-12 in biofilm formation is primarily facilitated by curli, an extracellular amyloid fibre (Tuson and Weibel, 2013). The regulation of curli expression is multifaceted and greatly

influenced by the environment, making it a difficult but crucial process to interpret and illustrate.

The strain of *E. coli* K-12 used in the majority of this study, PHL644, is an optimised biofilm-producing strain because of a mutation in the *ompR* gene that causes cells to constitutively express curli (Vidal *et al.*, 1998). Additionally, biofilm formation by *E. coli* PHL644 has been previously measured and optimised by crystal violet analysis in the current growth model, termed "the Duran Bottle method" (Van Houdt and Michiels, 2005; Beloin, Roux and Ghigo, 2008; Leech, 2017). Given this and the importance of curli in biofilm formation, the first half of this chapter focuses on characterising and optimising curli expression in PHL644. Specifically, it assesses curli regulation in response to physical conditions such as osmolarity, growth medium, glucose concentration, secondary carbon sources, temperature, and physical aspects of the biofilm growth model.

The second half of this chapter focuses on competition sensing. While some physical conditions have been optimised for maximal biofilm accumulation, less is known about the effect of competition sensing on biofilm formation (Cornforth and Foster, 2013). One of the best and most well-studied examples of competition sensing is the defence response and induction of biofilm formation caused by sensing antibiotics in the environment (Kaplan, 2011). Much of the antibiotic-induced biofilm formation research supports the theory that bacteria use molecules released by neighbouring bacteria (nonpurposeful signals) as ways of sensing competitors (Nadell, Xavier and Foster, 2009). To study competition sensing, crystal violet analysis, live/dead staining, and confocal microscopy were employed on single species *E. coli* cultures. The aim was to determine the effect of spent media (waste) generated by bacteria and individual chemicals not generated by the bacteria, such as lactic acid, on biofilm formation.

3.2 General protocol

Previous work used crystal violet analysis and confocal microscopy to explore conditions that would maximise biofilm accumulation using the Duran Bottle method (Leech, 2017). In the following work, a *csgB::gfp* reporter was used to investigate the effect of physical conditions, such as glucose concentration, on curli formation using the Duran Bottle method. The Duran Bottle method is a biofilm growth model consisting of a 100 mL Duran® bottle containing 70 mL of M63+ medium and an inserted PTFE-wrapped microscope slide (Fig. 3.1). Biofilm generates on the PTFE.

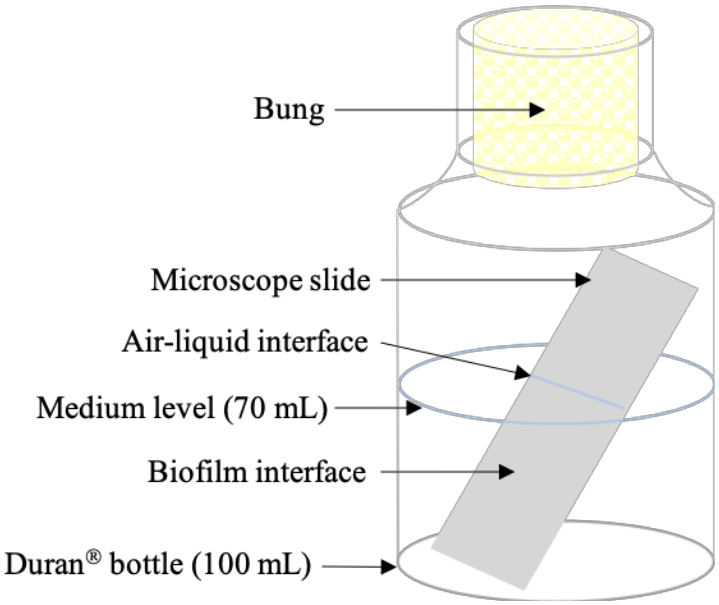

Figure 3.1: Duran Bottle model.

Diagram of Duran Bottle model for generation of biofilm. This model consists of a 100 mL Duran® bottle filled with 70 mL of medium. A PTFE-wrapped microscope slide is inserted and biofilm forms on the PTFE.

Mean cellular GFP fluorescence (representing *csgB* promoter activity) was measured by flow cytometry, while cell concentration was determined by measuring the optical density (OD_{600}) in order to observe differences in growth and cell concentration and understand their relationship to curli expression. All curli expression assays were performed for roughly 30 hours, unless otherwise stated. Competition sensing studies used crystal violet analysis, live/dead staining by flow cytometry, and confocal microscopy (section 3.3.6), among other assays, to study the effect of bacterial spent medium and individual chemical waste components not generated by bacteria on biofilm formation. Other procedures used in the following chapter include confocal microscopy and stains of individual EPS matrix components, where necessary.

3.3 Characterisation and optimisation of curli expression in biofilms

3.3.1 Curli expression: location, surface sensing, and osmolarity

It is known that curli expression is highly regulated, and important for initial attachment during *E. coli* K-12 biofilm formation (Kikuchi *et al.*, 2005). To investigate the factors that regulate curli expression, it was decided to first study how curli expression is regulated within three distinct locations in the biofilm growth model, termed the Duran Bottle method (Fig. 3.2a): the cells at the bottom of the bottle (sediment), the planktonic cells in the growth medium, and solid surface-attached cells on the inserted slide (biofilm). The *csgB::gfp* reporter (pJLC-T) was transformed into PHL644 and transformants were grown using the Duran Bottle method containing

M63+ minimal medium at 30 °C and 70 rpm shaking for three days. After three days, samples were taken from the biofilm, planktonic phase, and sediment and were analysed by flow cytometry. The mean cellular GFP fluorescence indicating curli expression (*csgB::gfp*) was measured by flow cytometry and compared for each location (Fig. 3.2b). The unattached planktonic cells had higher curli expression than the cells in the sediment and the biofilm, suggesting that cells that are attached to a solid surface downregulate curli expression. Furthermore, the biofilm had higher curli expression than the sediment. While it is not stated in the literature, it is possible that cells are able to differentiate adhering to an abiotic surface or biofilm opposed to another cell in the planktonic phase (which becomes sediment) and can regulate their curli expression accordingly (Tuson and Weibel, 2013; Nagy *et al.*, 2015). Additionally, there could be differences in osmolarity, nutrient availability, or other factors between the sediment and the biofilm which alter curli regulation or expression differently in these locations. Two explanations for curli downregulation of attached cells have been hypothesised: the cells "sense" attachment to abiotic or biotic surfaces and reduce curli expression and/or the cells respond to higher concentration of solutes (high osmolarity) in the sediment/biofilm by reducing curli expression (Zobell *et al.*, 1943; Wang *et al.*, 2012). The former hypothesis is investigated first, while latter hypothesis was tested later in this section.

(a)

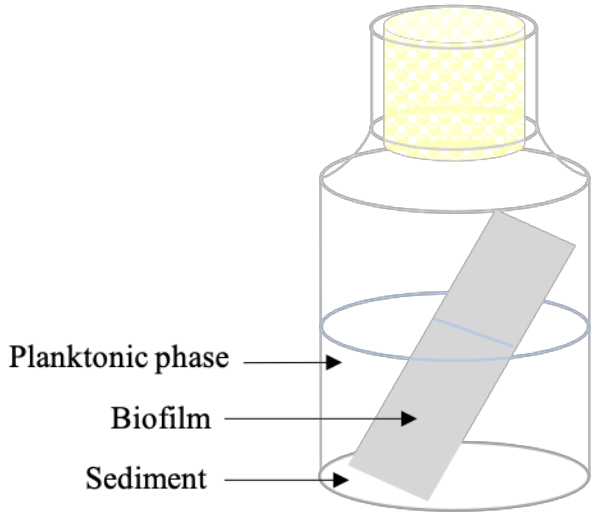

(b)

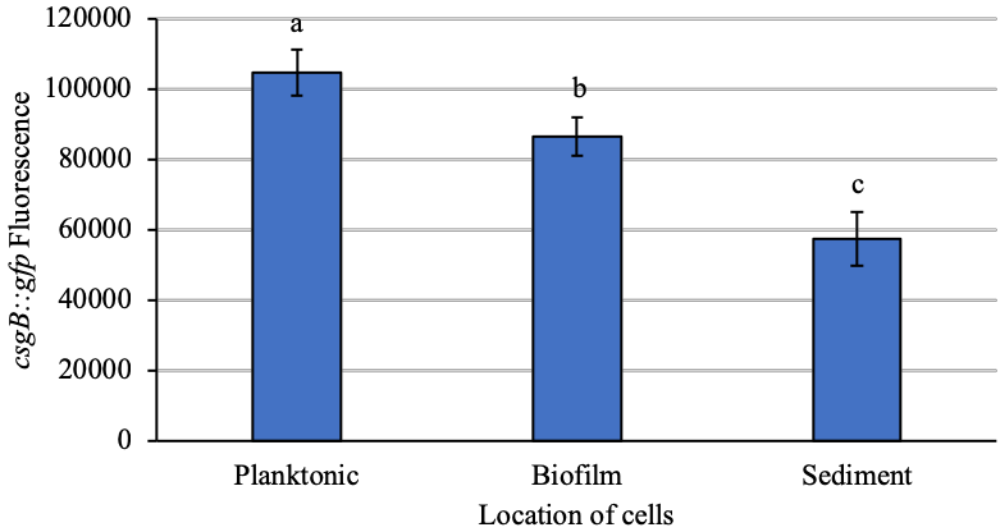

Figure 3.2: Measuring curli promoter activity at different locations in the system.

E. coli PHL644 transformed with a csgB::gfp fusion reporter (pJLC-T) was grown in triplicate using the Duran Bottle method containing M63+ minimal medium at 30 °C and 70 rpm shaking for three days. Samples were taken from three distinct locations, planktonic phase, biofilm, and sediment (a) and analysed by flow cytometry. Mean green fluorescence (*csgB* promoter activity) was measured (b). Bars representing ± standard deviation from the mean value of three independent cultures are shown. Statistics were performed using a two-tailed two-sample unequal variance t-test where $P < 0.05$ was significant. Mean values with different letters were significantly different.

Surface sensing pathways in *E. coli* are not completely known. Otto and coworker have proposed that curli expression in response to surface attachment is a three-component pathway (Otto and Silhavy, 2002). First, surface attachment is sensed by NIpE, an outer membrane lipoprotein, which then activates CpxAR, a two-component regulatory system. CpxAR represses *csgD* and *csgB*, which decreases curli formation (Prigent-Combaret *et al.*, 2001; Barnhart and Chapman, 2006). While this three-component system supports observations in this work, recently this pathway has been questioned and alternatively reported that the Rcs pathway is activated during surface contact which negatively regulates curli expression (Kimkes and Heinemann, 2018). Regardless, these data demonstrate a link between curli expression and surface sensing and the downregulation of curli caused by surface attachment would explain why cells in the sediment and the biofilm expressed less *csgB* than the planktonic cells. However, a difference in osmolarity in these locations may also play a role and is explored in this section. It was decided to test if the downregulation of curli in the sediment could be relieved by

To study the effect of osmolarity on curli expression, it was decided to select cells at sufficient concentrations and with low curli expression to see if curli downregulation could be relieved. PHL644 transformed with pJLC-T was grown in test tubes containing M63+ medium overnight at 30 °C and 70 rpm shaking before 1 mL of sedimented cells (with low curli expression) were harvested. The sedimented cells were then centrifuged and washed with PBS before being resuspended in either PBS, 1/5 strength PBS or 1/20 strength PBS at a final biomass concentration of $OD_{600} \approx 0.07$. Osmolarity, GFP fluorescence (indicating curli expression), cell concentration (OD_{600}), and pH were measured after 24 hours (Fig. 3.3). Although there was no significant difference in pH or cell concentration, curli expression and osmolarity were inversely

related. However, this trend was not observed at higher biomass concentrations (OD_{600} between 0.7 and 1.2) after 24 hours (Fig. 3.4).

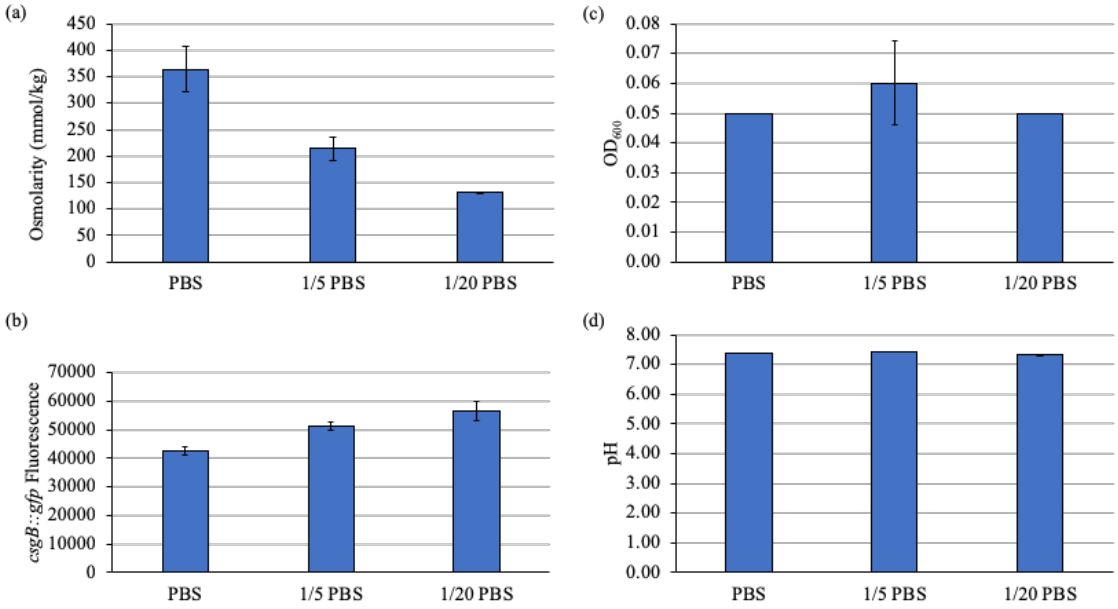

Figure 3.3: Relationship between osmolarity and *csgB* activity at $OD_{600} \approx 0.07$.

E. coli PHL644 transformed with a *csgB::gfp* fusion reporter (pJLC-T) was grown in duplicate in M63+ minimal medium at 30 °C and 70 rpm shaking overnight. Sedimented cells were washed and resuspended in either PBS, 1/5 PBS, or 1/20 PBS at final $OD_{600} \approx 0.07$. After 24 hours, osmolarity (a), mean green fluorescence representing *csgB* promoter activity (b), OD_{600} (c) and pH were measured (d). Bars representing ± standard deviation from the mean value of two independent cultures are shown. Despite no significant difference in cell concentration or pH between conditions, osmolarity and curli expression are inversely related.

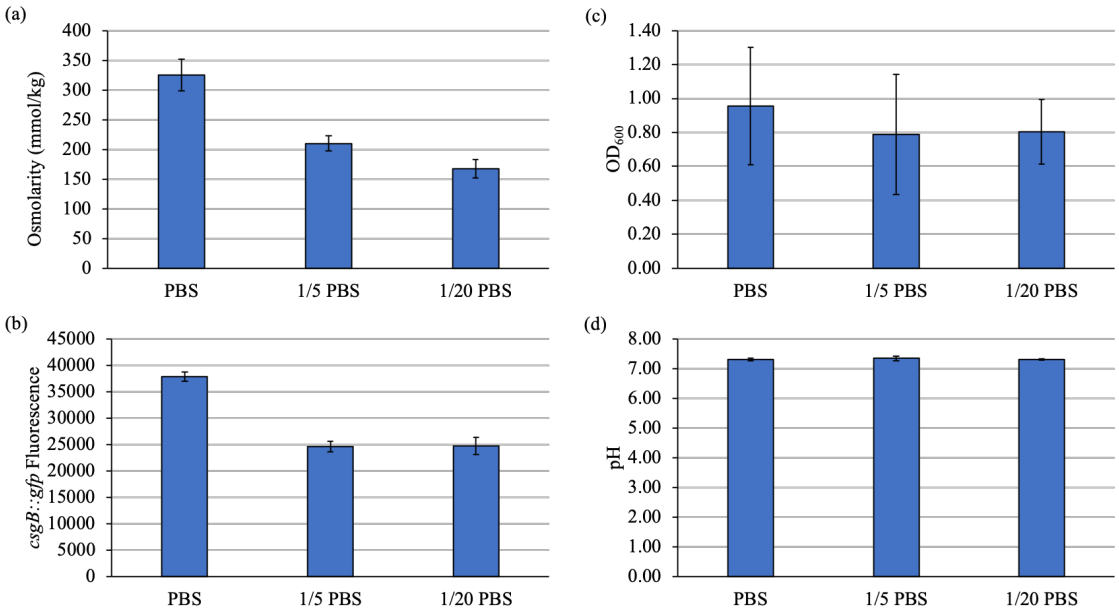

Figure 3.4: Relationship between osmolarity and *csgB* activity at $OD_{600} \approx 0.7 – 1.2$.

E. coli PHL644 transformed with a *csgB::gfp* fusion reporter (pJLC-T) was grown in duplicate in M63+ minimal medium at 30 °C and 70 rpm shaking overnight. Sedimented cells were washed in PBS and resuspended in either PBS, 1/5 PBS, or 1/20 PBS at an $OD_{600} = 0.7 – 1.2$. After 24 hours, osmolarity (a), mean green fluorescence (*csgB*) (b), OD_{600} (c) and pH were measured (d). Bars representing ± standard deviation from the mean value of two independent cultures are shown. Despite no change in cell concentration or pH, curli expression and osmolarity are proportionally related, to an extent.

At higher biomass concentrations, curli expression was, to an extent, related to osmolarity. When osmolarity was reduced from an average of 325 mmol/kg (PBS) to an average of 210 mmol/kg (1/5 strength PBS) curli expression was reduced. Curli expression was not further reduced when osmolarity was decreased to an average of 167 mmol/kg (1/20 strength PBS). Taken together, this suggests that potentially both osmolarity and biomass concentration (in terms of surface sensing, growth phase of the cells, or other mechanisms) play a role in the regulation of curli expression. It is possible that there is overlap in stimuli or the responding pathways which control curli expression that results in a link between osmolarity and cell concentration. Similarly, this could be a result of cells sensing the presence of neighbouring cells, which should be studied in future work. It was also noted in the low cell concentration experiment the osmolarity of 1/20 strength PBS was measured at 131 mmol/kg compared to 167 mmol/kg in the high cell concentration experiment, which could suggest that cell concentration affects osmometer readings, or the osmometer has limited sensitivity.

As previously mentioned, there are numerous complex curli regulatory pathways that respond to environmental stimulus, such as surface attachment, osmolarity, pH, and so forth. While the CpxAR pathway is the widely-accepted response system for surface sensing and envelope stress, a study by Kimkes and colleague on surface contact by *E. coli* found that instead of CpxAR activation, the Rcs pathway was activated and is responsible for downregulating curli expression (Kimkes and Heinemann, 2018). This supports other data that Rcs negatively regulates curli expression (Jubelin *et al.*, 2005). Like the CpxAR cascade, the Rcs pathway is also responsible for responding to envelope stress but instead of initiating during outer membrane disruptions, the Rcs pathway responds to peptidoglycan layer damage (Laubacher and Ades, 2008). Additionally, the Rcs pathway regulates EPS production of colanic acid (Majdalani and Gottesman, 2005).

The osmolarity of a growth system differs based on location, and changes near surfaces as cells adhere (Tuson and Weibel, 2013). Changes in osmolarity have been found to induce both the CpxAR pathway and the EnvZ/OmpR pathway, which regulate curli in different ways (Prigent-Combaret *et al.*, 2001). Additionally, in low osmolarity, the EnvZ (inner membrane lipoprotein and also a phosphatase) can remove the phosphoryl group from OmpR, which changes is conformation and allows it to bind to the *csgD* promoter and activate curli expression (Jubelin *et al.*, 2005). Alternatively, as previously described in this section, CpxAR is a stress response pathway that can sense high osmolarity (in addition to surface attachment, envelope stress, pH, high salt concentration, and so forth) and repress curli expression (Hunke, Keller and Müller, 2012; Weatherspoon-Griffin *et al.*, 2014). In addition to the CpxAR and the EnvZ/OmpR pathways, work with an *E. coli hns* mutant at low osmolarity showed reduced *csgD* expression, which indicates that H-NS, a global regulatory protein, will activate *csgD* in low osmolarity (Jubelin *et al.*, 2005). However, H-NS has no identifiable binding sequence and will reportedly activate or repress *csgD* based on bacterial strain, growth medium, or other factors (A Olsén *et al.*, 1993; Gerstel, Park and Römling, 2004). It is clear from the current research that there is an intricate, intertwining and sometimes contradictory network of environment-sensing pathways that can regulate curli expression, among many other genes, and should be studied further (Gerstel, Park and Römling, 2004; Ogasawara *et al.*, 2010; Ogasawara, Yamamoto and Ishihama, 2010).

While the crossover of closely-related stimuli and the complexity of the signalling pathways and gene regulation make some inferences indecipherable, there is a probable link between *E. coli* K-12 cell concentration, osmolarity, and curli expression. As the cells come into contact with abiotic or biotic surfaces, they adhere to the surface where osmolarity is potentially higher due to surface conditioning (Prigent-

Combaret *et al.*, 1999; Lejeune, 2003; Wong *et al.*, 2012). The osmolarity near surfaces increase as cells approach and attach and trap pools of molecules and ions near the surface (Heukelekian and Heller, 1940; Zobell *et al.*, 1943). It could be deduced that the floating cells in the planktonic phase have less surface interactions than cells in the sediment or biofilm. To theorise, the planktonic cells have higher curli expression because they have less surface interactions and experience relatively low osmolarity in the M63+ medium (compared to surfaces with nutrient deposits and trapped ions from cells). In the biofilm or sediment, the activation of surface attachment pathways and high osmolarity pathways would repress curli expression. On the other hand, it was shown in this work that high cell concentrations expressed more curli in high osmolarity conditions. Potentially, the high cell concentrations reach stationary phase more quickly and/or have factors which interfere with osmoregulatory pathways of curli. It has been reported that strains with an *ompR234* mutation (such as PHL644) which overexpress curli obtain greatest curli expression in stationary phase (A Olsén *et al.*, 1993). Additionally, work by Prigent-Combaret and colleagues showed that an *ompR234* mutation in *E. coli* K-12 in stationary phase can, to an extent, override negative regulation by CpxR in high osmolarity conditions (Prigent-Combaret *et al.*, 2001). This corresponds with findings in this work as it is possible that the higher cell concentrations achieved stationary phase more quickly, and thus were able to override repression of curli expression in high osmolarity conditions and continued to express curli.

Due to these findings and the difference between curli expression of the planktonic phase and sediment, subsequent experiments involving the study and optimisation of curli expression were performed on samples from both the planktonic and sedimented cells. Next, curli expression was optimised in terms of the growth model.

3.3.2 Optimisation of curli gene expression

3.3.2.1 Presence of a microscope slide does not hinder curli expression

The Duran Bottle method consists of a Duran® bottle containing 70 mL M63+ medium and an inserted PTFE-wrapped microscope slide on which biofilm can generate (Fig. 3.1). The slide can then be analysed by confocal microscopy to visualise biofilm structure and thickness or by crystal violet assay to measure relative biofilm accumulation. First in the process to optimise curli expression using the Duran Bottle method, curli expression in the presence and absence of the inserted microscope slide was analysed to ensure curli expression was not hindered. The *csgB::gfp* reporter (pJLC-T) was transformed into PHL644 and transformants were grown using the Duran Bottle method containing M63+ minimal medium either with (slide+) or without a microscope slide (slide-) at 30 °C and 70 rpm shaking. Samples from the top (planktonic phase) and the bottom (sediment) of the bottles were taken over time and analysed by flow cytometry. The mean green fluorescence (*csgB::gfp*) was measured and the OD_{600} was also measured to ensure any difference in GFP fluorescence between the slide+ and slide- bottles was not due to a difference in growth (Fig. 3.5). After 28 hours, there was no difference between the presence or absence of a microscope slide on curli expression or cell concentration (OD_{600}). At 30 hours, planktonic cells in the presence of the slide expressed slightly higher *csgB::gfp* fluorescence, despite similar cell concentrations. While the slide+ only conferred slightly higher curli expression after 30 hours, it was important to note that the slide did not hinder curli expression and it was decided to continue using the Duran Bottle method with a PTFE-wrapped microscope slide. It was also noted that the planktonic cells (top) in the system expressed significantly more curli than the cells in the sediment (bottom), as observed

previously. Next, curli expression was tested in response to minimal and rich growth media.

(a)

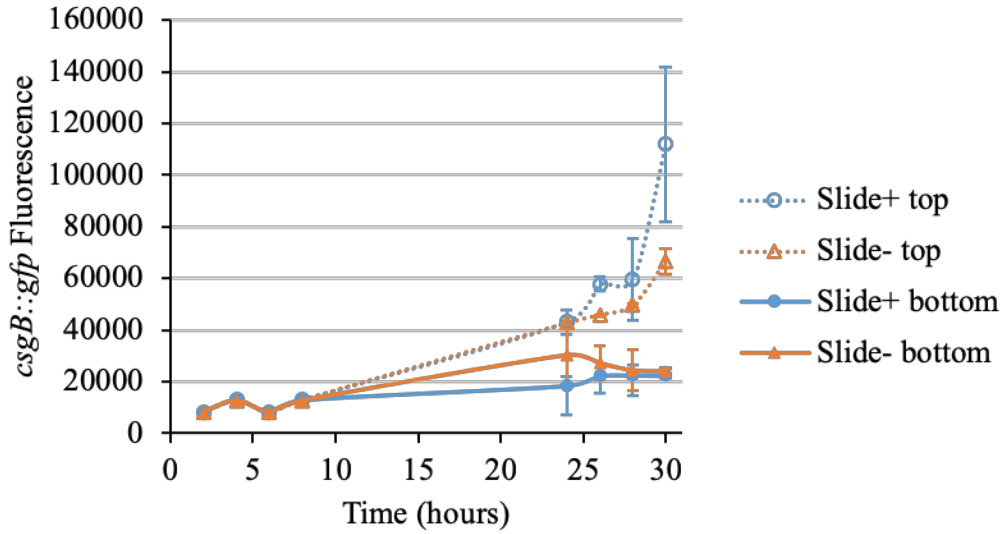

(b)

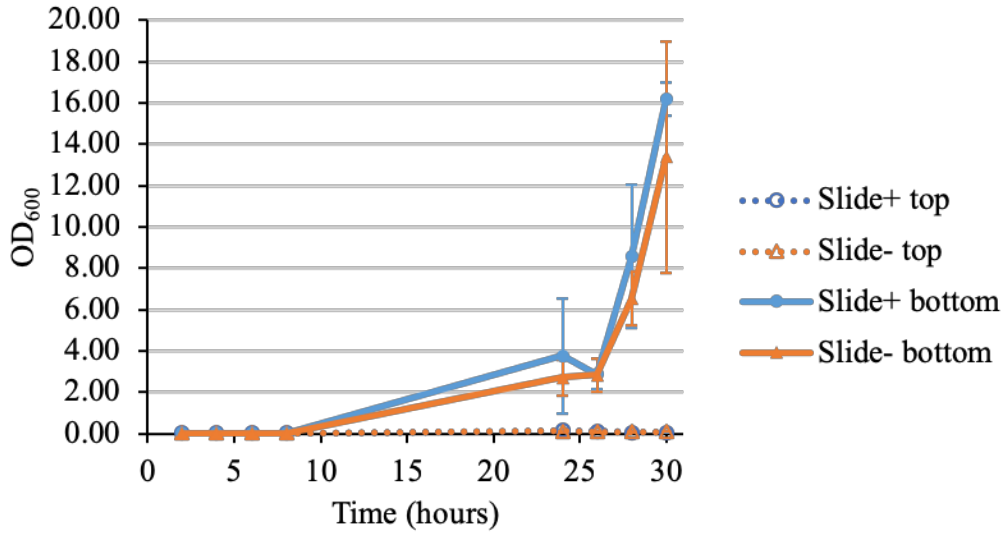

Figure 3.5: Presence of a slide does not hinder *csgB* activity.

E. coli PHL644 transformed with a *csgB::gfp* fusion reporter (pJLC-T) was grown in duplicate in either with (slide+) or without a microscope slide (slide-) in M63+ minimal medium at 30 °C and 70 rpm shaking. Samples were taken over 30 hours from planktonic phase (top) and sediment (bottom) and analysed by flow cytometry. Mean green fluorescence representing *csgB* promoter activity (a), and OD_{600} were measured (b). Bars representing ± standard deviation from the mean value of two independent cultures are shown. The presence of the microscope slide did not affect cell concentration nor hinder curli expression.

3.3.2.2 M63+ minimal medium increases curli expression

Previous work in the Overton laboratory with crystal violet analysis revealed that PHL644 grown in the Duran Bottle method with M63+ minimal medium accumulated more biofilm than with rich LB medium (Leech, 2017). To investigate the effect of minimal versus rich media on curli expression, the *csgB::gfp* reporter (pJLC-T) was transformed into PHL644 and transformants were grown using the Duran Bottle method containing either M63+ minimal medium or LB medium at 30 °C and 70 rpm shaking. Samples from the planktonic phase (top) and the sediment (bottom) of the bottles were taken over time and analysed by flow cytometry. The mean green fluorescence (*csgB::gfp*) and OD_{600} was measured for 30 hours (Fig. 3.6). Over the 30 hours, M63+ minimal medium had consistently higher curli expression in both the sediment and the planktonic phase than rich LB medium. Although cells grew faster in the rich LB medium in the first 8 hours, curli expression in the M63+ minimal media was significantly higher than the LB, which corresponds to crystal violet data in a prior study (Leech, 2017). After 8 hours, OD_{600} sampling error increased due to greater cell concentrations and it was difficult to differentiate true values.

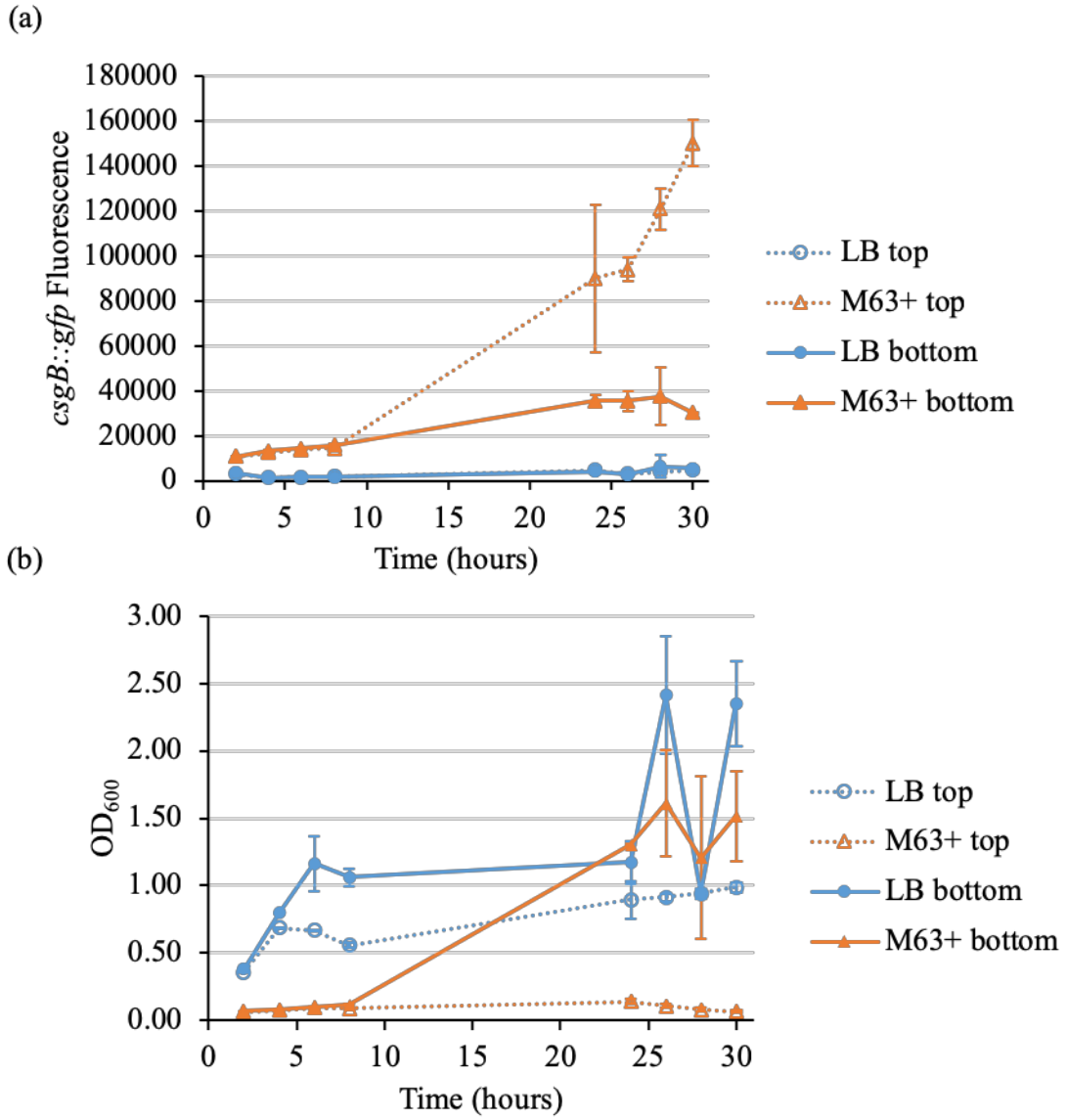

Figure 3.6: Expression of *csgB* in minimal media.

E. coli PHL644 transformed with a *csgB::gfp* fusion reporter (pJLC-T) was grown in duplicate in either M63+ minimal medium or rich LB medium at 30 °C and 70 rpm shaking. Samples were taken over 30 hours from planktonic phase (top) and sediment (bottom) and analysed by flow cytometry. Mean green fluorescence representing *csgB* promoter activity (a), and OD_{600} were measured (b). Bars representing ± standard deviation from the mean value of two independent cultures are shown. Despite differences in growth, curli expression was highest in M63+ minimal medium in both the planktonic phase and sediment.

The curli expression data corresponds to a reporter gene study by Brombacher and colleagues which showed an *E. coli* strain overproducing CsgD had higher curli expression in minimal media, and could suggest that more biofilm was detected by crystal violet assay in minimal media due to increased curli expression (Brombacher *et al.*, 2006). Additionally, it was noted that planktonic cells (top) expressed more curli than the cells in the sedimented (bottom) in M63+ medium, but not in LB medium. This observation could support earlier hypotheses that curli expression is regulated by both osmolarity and cell concentration; the LB media has a higher osmolarity (Fig. 3.7) and produces higher cell concentrations which may induce curli repression via high osmolarity and surface sensing pathways. Similarly to osmolarity, it has also been reported that cells grown in LB media have less curli expression because the high salt concentrations present in LB media reduce curli formation (Smith *et al.*, 2017). Next, curli expression was optimised for glucose concentration.

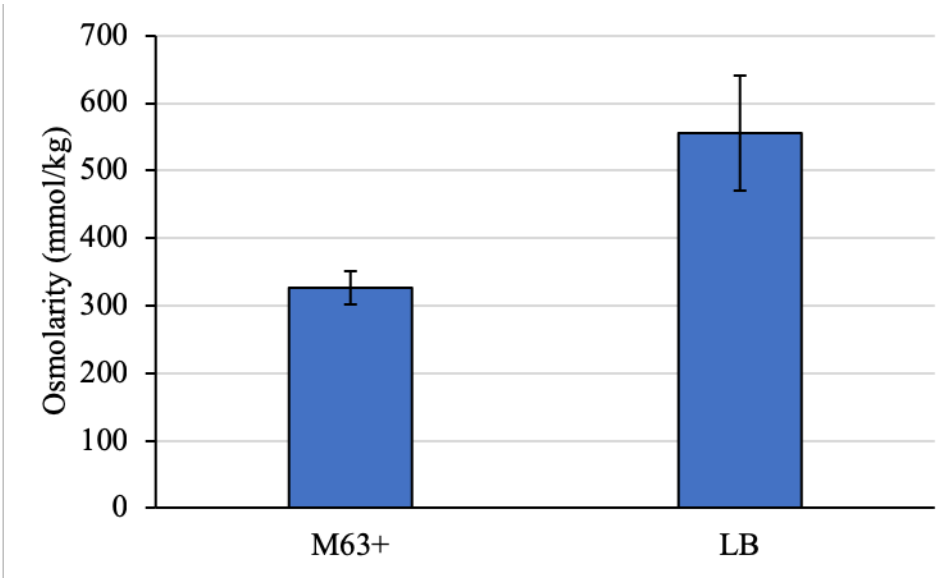

Figure 3.7: Osmolarity of M63+ versus LB.

The osmolarity of sterile M63+ minimal media and LB rich media were measured three times at standard conditions. Bars representing ± standard deviation from the mean value of three independent replicates are shown. Statistics were performed using a two-tailed two-sample unequal variance t-test where $P < 0.05$ was significant. Mean values with different letters were significantly different.

3.3.2.3 Curli expression is regulated by catabolite repression

Carbon catabolite repression (CCR) is a system which upregulates genes for the metabolism of preferential carbon sources (glucose), while repressing unnecessary metabolism genes (Kremling *et al.*, 2015). In low glucose concentrations, adenylate cyclase (CyaA) is able to synthesise cyclic AMP (cAMP) which forms a complex with the cAMP receptor protein (CRP). The cAMP-CRP complex can then bind and upregulate genes necessary for metabolism of alternative sugars and biofilm formation (Zheng *et al.*, 2004; Fic *et al.*, 2009). When glucose is present, it inhibits CyaA activity so that it cannot synthesise cAMP; subsequently, the low concentration of the cAMP-

CRP complex will not upregulate genes for alternative sugar metabolism or biofilm formation (Ishizuka *et al.*, 1993; Jackson, Simecka and Romeo, 2002).

Previous work showed that supplementing M63+ medium with 10 mM glucose (standard for M63 medium) resulted in the greatest biofilm accumulation by crystal violet assay (Leech, 2017). It was inferred that less glucose hindered overall cell growth, while more glucose potentially activated the catabolite repression pathway and resulted in reduced biofilm formation. The absence of glucose did not produce a biofilm, even though succinate was supplemented as a secondary carbon source. To investigate the effect of glucose concentration on curli expression, PHL644 transformed with pJLC-T was grown using the Duran Bottle method containing M63+ minimal medium with either 0 mM, 1 mM, 10 mM (generated the most biofilm) or 100 mM glucose at 30 °C and 70 rpm shaking. Samples from the top (planktonic phase) and the bottom (sediment) of the bottles were taken over time and analysed by flow cytometry. The mean green fluorescence (*csgB::gfp*) and OD_{600} were measured for 30 hours (Fig. 3.8), but it was decided that in order to accurately see trends and significance in curli expression (particularly the upward trend in curli expression of 10 mM planktonic phase), this experiment was repeated and sampling was extended to 56 hours (Fig. 3.9).

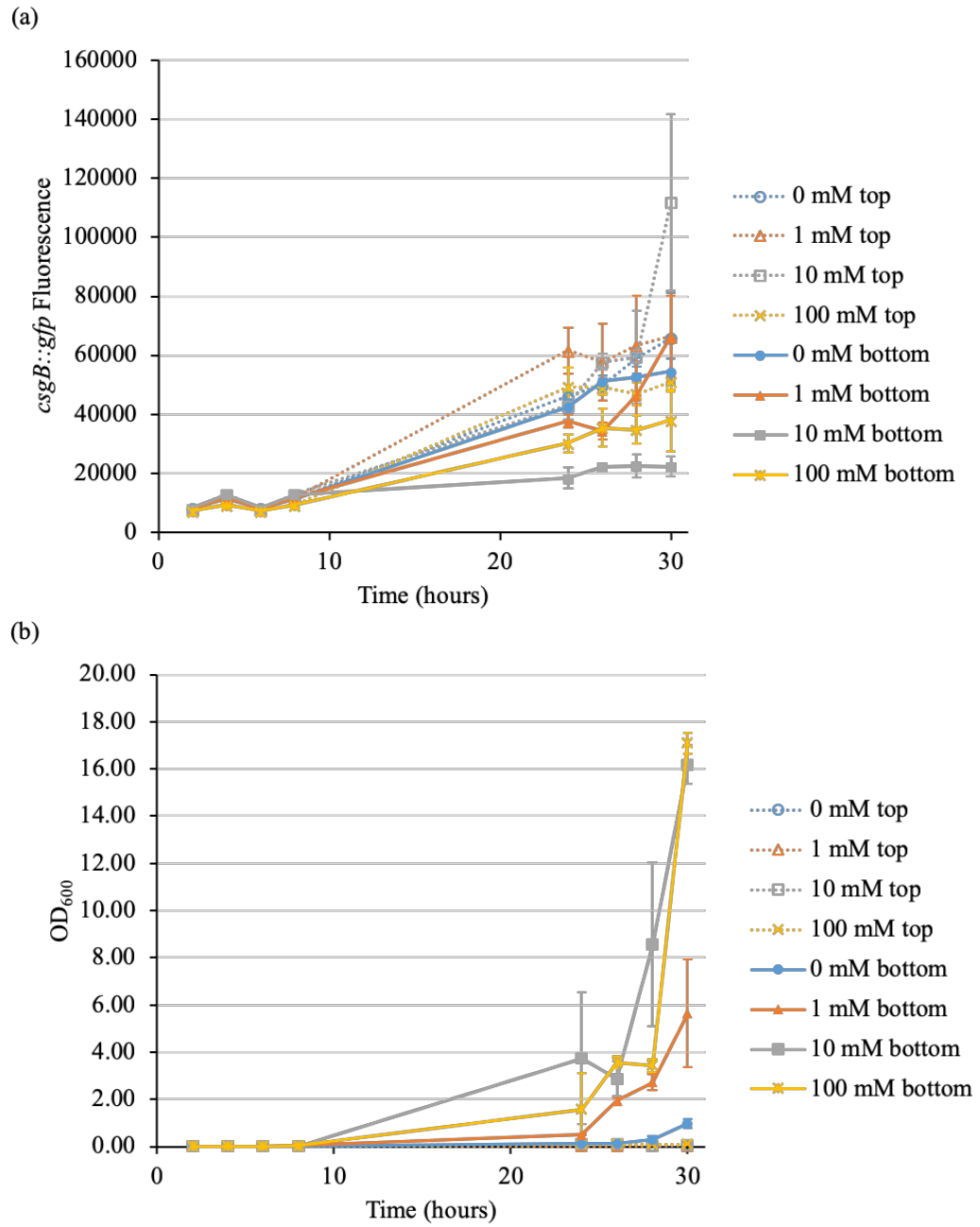

Figure 3.8: Expression of *csgB* in differing glucose concentrations over 30 hours.

E. coli PHL644 transformed with a *csgB::gfp* fusion reporter (pJLC-T) was grown in duplicate in M63+ medium with either 0 mM, 1 mM, 10 mM (standard), or 100 mM glucose at 30 °C and 70 rpm shaking. Samples were taken over 30 hours from planktonic phase (top) and sediment (bottom) and analysed by flow cytometry. Mean green fluorescence representing *csgB* promoter activity (a), and OD_{600} were measured (b). Bars representing ± standard deviation from the mean value of two independent cultures are shown. Despite differences in growth after 30 hours, 10 mM glucose in the planktonic phase had the highest curli expression. As observed previously, it was noted that the sediment cells had low curli expression, possibly due to downregulation of curli by increased surface sensing or osmolarity. To better visualise this trend, the experiment was repeated and sampling was extended to 56 hours (Fig. 3.9).

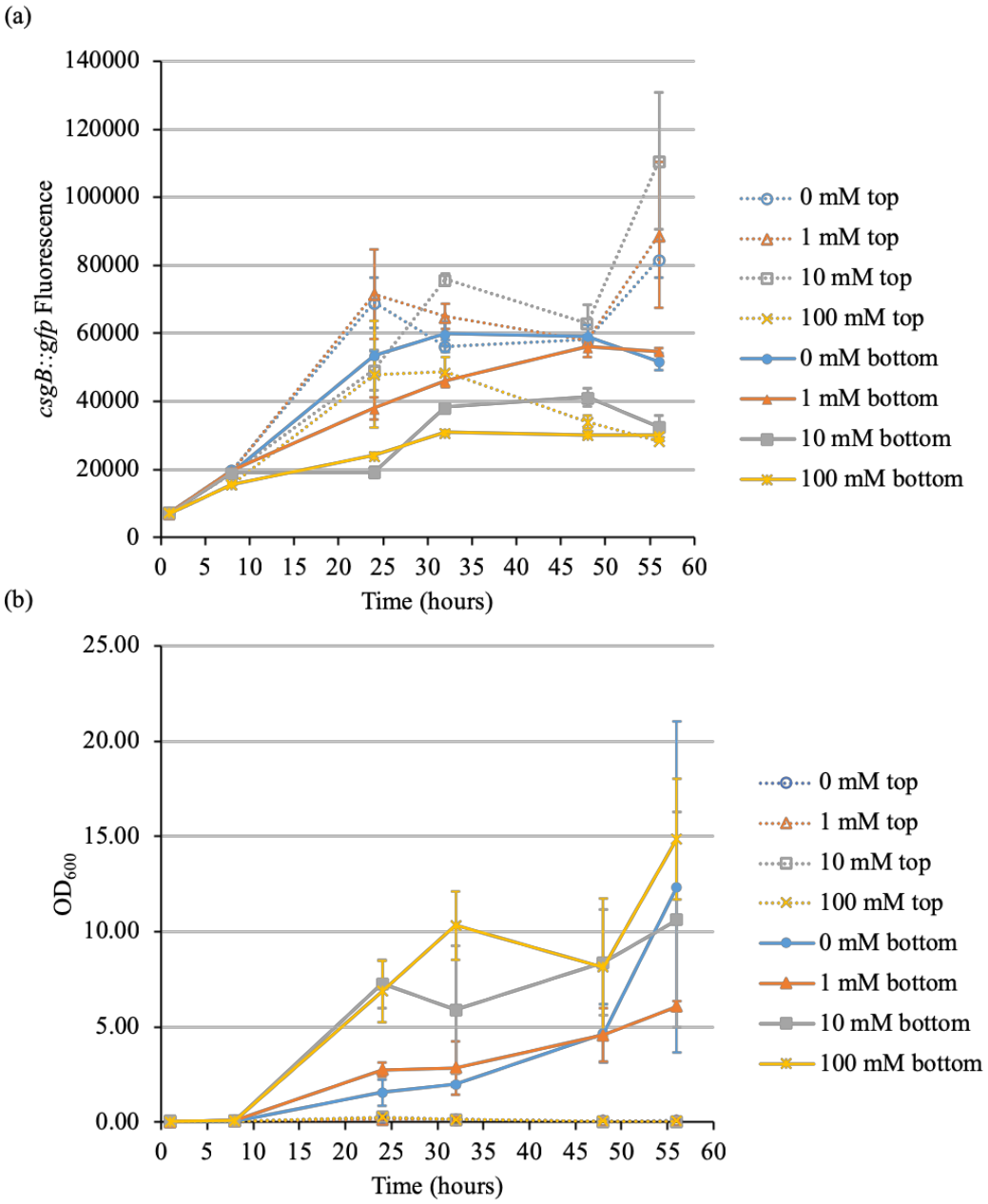

Figure 3.9: Expression of *csgB* in differing glucose concentrations over 56 hours.

E. coli PHL644 transformed with a *csgB::gfp* fusion reporter (pJLC-T) was grown in duplicate in M63+ medium with either 0 mM, 1 mM, 10 mM (standard), or 100 mM glucose at 30 °C and 70 rpm shaking. Samples were taken over 56 hours from planktonic phase (top) and sediment (bottom) and analysed by flow cytometry. Mean green fluorescence representing *csgB* promoter activity (a), and OD_{600} were measured (b). Bars representing ± standard deviation from the mean value of two independent cultures are shown. Despite differences in growth after 30 hours, 10 mM glucose in the planktonic phase had the highest curli expression, which agrees with Fig. 3.7. Additionally, it was noted that growth and curli expression were inversely related.

Both figures were compared and used to verify results between 0 — 30 hours. At 30 hours, the sediment of 10 mM and 100 mM glucose concentrations had similarly high cell concentrations while 1 mM and 0 mM had the lowest cell concentrations. However between 30 — 56 hours, OD_{600} sampling error increased due to greater cell concentrations and clumps forming at the bottom of the flasks and it was difficult to differentiate true values after 30 hours. The planktonic cell concentrations were low for all conditions. While large error bars made the curli expression of some conditions indistinguishable, both experiments in Fig. 3.8 and Fig. 3.9 at hour 30 showed the planktonic phase of the condition with 10 mM glucose had the highest curli expression. While the upward trend of 10 mM glucose of the planktonic phase did not continue after 30 hours, this condition consistently induced the highest curli expression, rivalled by only 1 mM glucose in the planktonic phase and 0 mM glucose in the planktonic phase at hour 56. Both the planktonic cells and cells in the sediment grown with 100 mM glucose had consistently middle-to-low range values around 30 hours, which decreased between hours 30 and 56. Previous crystal violet analysis of biofilm accumulation corresponded with these observations, which concluded conditions with 0 mM/1 mM, and 100 mM glucose to be a poor biofilm producers, possibly due to poor growth conditions and decreased curli expression, respectively (Leech, 2017). Knowing *E. coli* biofilm accumulation is reduced with the addition of 0 mM and 1 mM glucose (poor growth conditions) and 100 mM glucose does not increase curli expression, 10 mM glucose is considered the best concentration for M63+ medium in terms of both the cell's curli expression and growth. It was noted that the planktonic cells tended to have higher curli expression than the cells in the sediment as observed previously. It was also noted that curli expression was inversely related to glucose concentration, possibly due to catabolite repression. In conditions with low glucose concentrations, cAMP is produced by CyaA which then binds CRP and activates *csgD* (curli expression)

(Hufnagel *et al.*, 2016). In order to increase curli and improve surface attachment, conditions must limit glucose concentrations while also allowing for adequate *E. coli* growth. It was concluded that 10 mM would fulfil both of these needs. It was decided to next optimise the effect of temperature on curli formation.

3.3.2.4 Curli expression is regulated by temperature in planktonic cells

Previous crystal violet analysis showed that more biofilm accumulated in the Duran Bottle method at 30 °C, rather than 25 °C or 37 °C (Leech, 2017). However, studies have shown that maximal curli expression occurs at temperatures below 30 °C (Barnhart and Chapman, 2006). Consequently, a preliminary experiment was performed which compared curli expression at 28 °C and 30 °C for 24 hours. PHL644 transformed with pJLC-T was grown using the Duran Bottle method containing M63+ minimal medium and 70 rpm shaking at either 28 °C and 30 °C. The preliminary experiment sampled the centre of the bottle over time which were then analysed by flow cytometry. The mean green fluorescence (*csgB::gfp*) and OD_{600} were measured for 24 hours (Fig. 3.10). Curli expression was reasonably similar between the two temperatures except for hours 2 and 6 when 28 °C had higher curli expression. This suggests that 28 °C may be the optimal temperature for curli formation; however, the difference was minimal, and cells grown at 28 °C did not grow as well as those grown at 30 °C. It was then decided to test a larger range of temperatures for a longer period of time. PHL644 pJLC-T transformed cells were grown at 25 °C, 28 °C, 30 °C or 37 °C in the Duran Bottle method containing M63+ minimal medium and 70 rpm shaking. Samples were taken over 56 hours from the top (planktonic phase) and the bottom (sediment) and analysed by flow cytometry. The mean green fluorescence (*csgB::gfp*) and cell concentration (OD_{600}) were measured (Fig. 3.11).

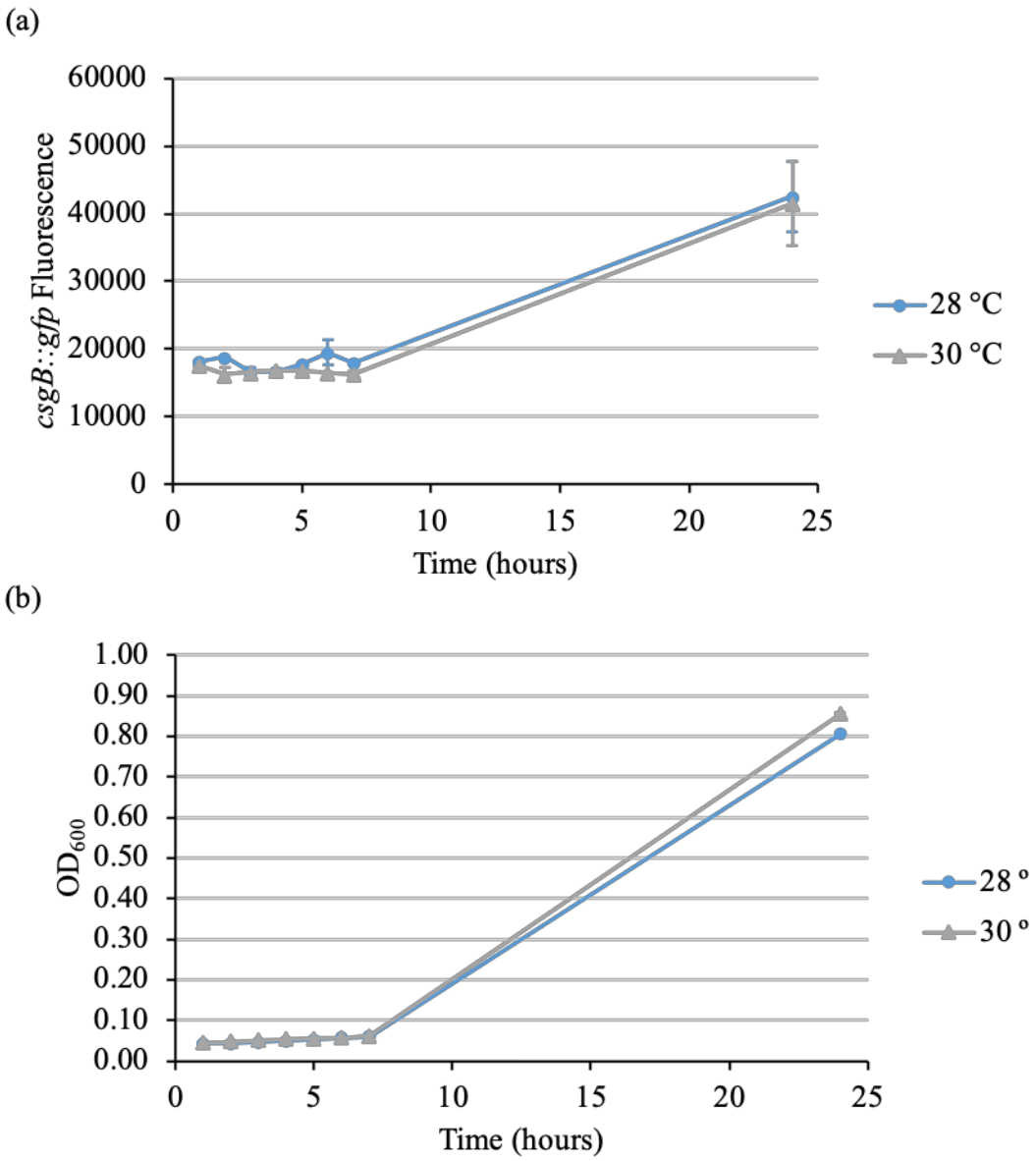

Figure 3.10: The effect of 28 °C and 30 °C on curli expression and cell concentration.

E. coli PHL644 transformed with a *csgB::gfp* fusion reporter (pJLC-T) was grown in duplicate in M63+ medium either 28 °C or 30 °C and 70 rpm shaking. Samples from the centre of the bottle were taken over 24 hours and analysed by flow cytometry. Mean green fluorescence representing *csgB* promoter activity (a), and OD_{600} were measured (b). Bars representing ± standard deviation from the mean value of two independent cultures are shown. Despite slightly better growth at 30 °C, there was no difference in curli expression, except for hours 2 and 6 where 28 °C had higher curli expression.

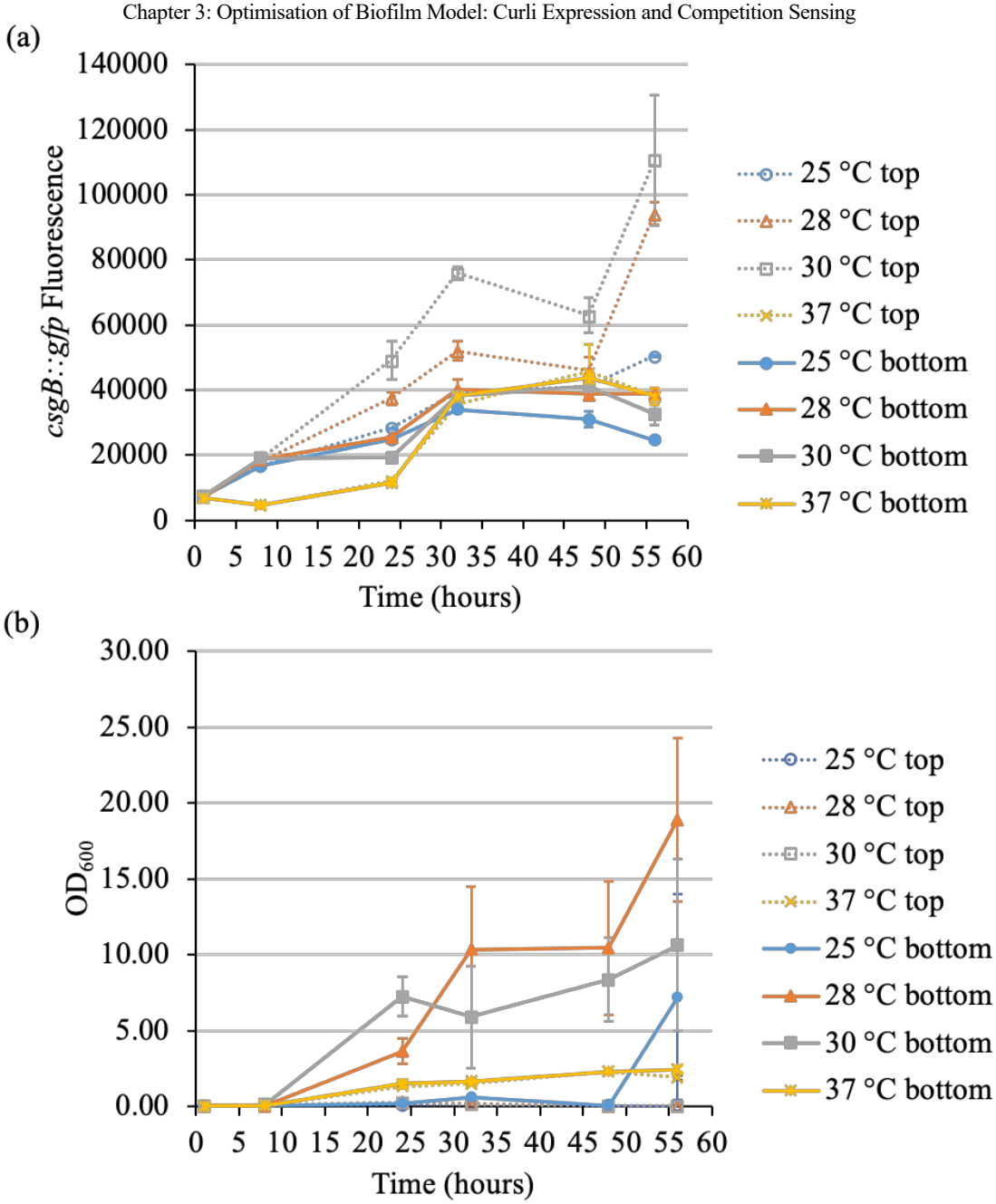

Figure 3.11: The effect of varying temperature on curli expression and cell concentration.

E. coli PHL644 transformed with a *csgB::gfp* fusion reporter (pJLC-T) was grown in duplicate in M63+ medium either 25 °C, 28 °C, 30 °C or 37 °C and 70 rpm shaking. Samples were taken over 56 hours from planktonic phase (top) and sediment (bottom) and analysed by flow cytometry. Mean GFP representing *csgB* promoter activity (a), and OD_{600} were measured (b). Bars representing ± standard deviation from the mean value of two independent cultures are shown. Growth and curli expression in the first 48 hours was highest at 28 °C and 30 °C. The planktonic phase tended to have the highest curli expression, while cell concentration was higher in the sediment, as observed previously. Curli expression at 25 °C and 37 °C planktonic and sediment had similarly low curli expression.

Over 48 hours, planktonic curli expression was consistently highest at 30 °C, supporting crystal violet data in a previous study (Leech, 2017). The largest difference in curli expression between 28 °C and 30 °C was at hour 32; however, at hour 56 there was not a significant difference between planktonic curli expression at 28 °C or 30 °C. The lowest curli expression of the planktonic phase was at 25 °C and 37 °C, except at hour 48 when 25 °C, 28 °C, and 37 °C were similarly low. Comparable reporter studies found that *E. coli* K-12 grown at 25 °C and 37 °C did not have a significant difference in curli expression, which was also observed in this study (Brombacher *et al.*, 2006; Perrin *et al.*, 2009). Cell concentrations were similar between the top and the bottom of the bottles incubated at 25 °C and 37 °C, despite cultures incubated at 25 °C not growing as well as those at 37 °C. This possibly indicates that the low curli expression at these two temperatures prevented cells from clumping and adhering to each other and sedimenting to the bottom.

While there are other surface proteins and factors which can cause agglutination of *E. coli* K-12 it is unlikely that factors such as Ag43 are responsible for the different optical densities of the sediment because the regulation of this aggregative surface protein is generally stable over time and is not thermoregulated (van der Woude and Henderson, 2008). On the other hand, cultures incubated at 28 °C and 30 °C had higher cell concentrations at the bottom (sediment) than in the top (planktonic). This may indicate that the high curli expression of the planktonic phase at these temperatures resulted in cells adhering, clumping, and sedimenting to the bottom of the bottle which increased cell concentration at bottom of the bottle. Furthermore, as the cells sedimented at 28 °C and 30 °C, surface sensing pathways were potentially activated and started downregulating curli expression, which is why curli expression in the sediment is lower than the planktonic cells at these temperatures. It was noted that bottles

incubated at 25 °C had very low cell concentrations both in the planktonic phase and in the sediment, and is most likely due to poor *E. coli* growth at this temperature.

Overall, sedimented cells had similarly low curli expression despite being grown at different temperatures. Cultures grown at 37 °C had lower curli expression than other temperatures between hours 0 and 24, and cultures grown at 25 °C had the lowest curli expression between hours 32 and 56. Alternatively, planktonic curli expression appeared to be highly thermoregulated and changes as little as 2 °C affected curli expression. Possibly, planktonic cells are either more susceptible to thermoregulation, or the activation of regulatory pathways that decrease curli (such as surface attachment and high osmolarity) override thermoregulation in the sediment.

Despite reports which claim temperatures below 30 °C elicit maximal curli expression in *E. coli* laboratory strains, studies by Brombacher and coworkers and Bougdour and colleagues found that the *csgBA* can be upregulated at 30 °C when Crl binds and enhances RpoS, a general stress sigma factor, which then binds and activates the *csgBA* promoter (Bougdour, Lelong and Geiselmann, 2004; Barnhart and Chapman, 2006; Brombacher *et al.*, 2006). The binding of the RpoS-Crl complex to the *csgBA* promoter relieves repression of *csgA* by H-NS, but is influenced by other factors such as osmolarity and the master regulator CsgD (Arnqvist *et al.*, 1992; Arne Olsén *et al.*, 1993). It is likely that because the thermoregulatory Crl protein is not expressed at 37 °C, curli are not as highly expressed in either the planktonic phase or in the sediment at this temperature, which supports the *csgB::gfp* data (Arnqvist *et al.*, 1992). Furthermore, Gualdi and colleagues purported that more curli is expressed in *E. coli* K-12 at temperatures less than 32 °C when compared to 37 °C (Gualdi *et al.*, 2008). Due to these reports and the *csgB::gfp* reporter data, experiments will continue to be performed at 30 °C due to greater curli expression elicited at this temperature, and the

greater cell concentrations at this temperature at hour 24 and similarly high cell concentrations as cultures grown at 26 °C between hours 24 — 56.

3.3.2.5 Curli expression and PNAG production may be regulated by succinate

In earlier work with M63 medium, Tsoligkas and coworkers supplemented M63 medium with potassium succinate (Tsoligkas *et al*., 2012). It was postulated that adding potassium succinate would add a secondary carbon source that would be metabolised once glucose is depleted; however, unlike glucose, succinate could enter the tricarboxylic acid (TCA) cycle directly and therefore avoid catabolite repression and the inhibitory effects of glucose on biofilm formation (Wolfe, 2005; Hufnagel *et al.*, 2016). Previous work by crystal violet analysis investigating other potential succinate sources revealed that the addition of 17 mM sodium succinate to cultures grown in the Duran Bottle method resulted in more biofilm accumulation compared to the addition of succinic acid, potassium succinate, or no succinate (Leech, 2017). Sodium ions activate NhaR, the transcriptional regulator of the *pgaABCD* operon, which encodes synthesis of the EPS component, PNAG (Goller *et al.*, 2006; Itoh *et al.*, 2008) It was hypothesised in the study that the addition of sodium ions would increase secretion of PNAG, thus potentially increasing biofilm accumulation. Both the effect of succinate on curli expression and PNAG formation in the biofilm was tested in this section.

First, to test the effect of succinate on curli expression, PHL644 transformed with pJLC-T was grown using the Duran Bottle method containing M63+ minimal medium at 30 °C and 70 rpm shaking with either no succinate, 17 mM succinic acid, 17 mM sodium succinate (best by crystal violet analysis), or 17 mM potassium succinate. Samples from the top (planktonic phase) and the bottom (sediment) of the bottles were

taken for 30 hours and analysed by flow cytometry. The mean green fluorescence (*csgB::gfp*) and cell concentration (OD_{600}) were measured (Fig. 3.12).

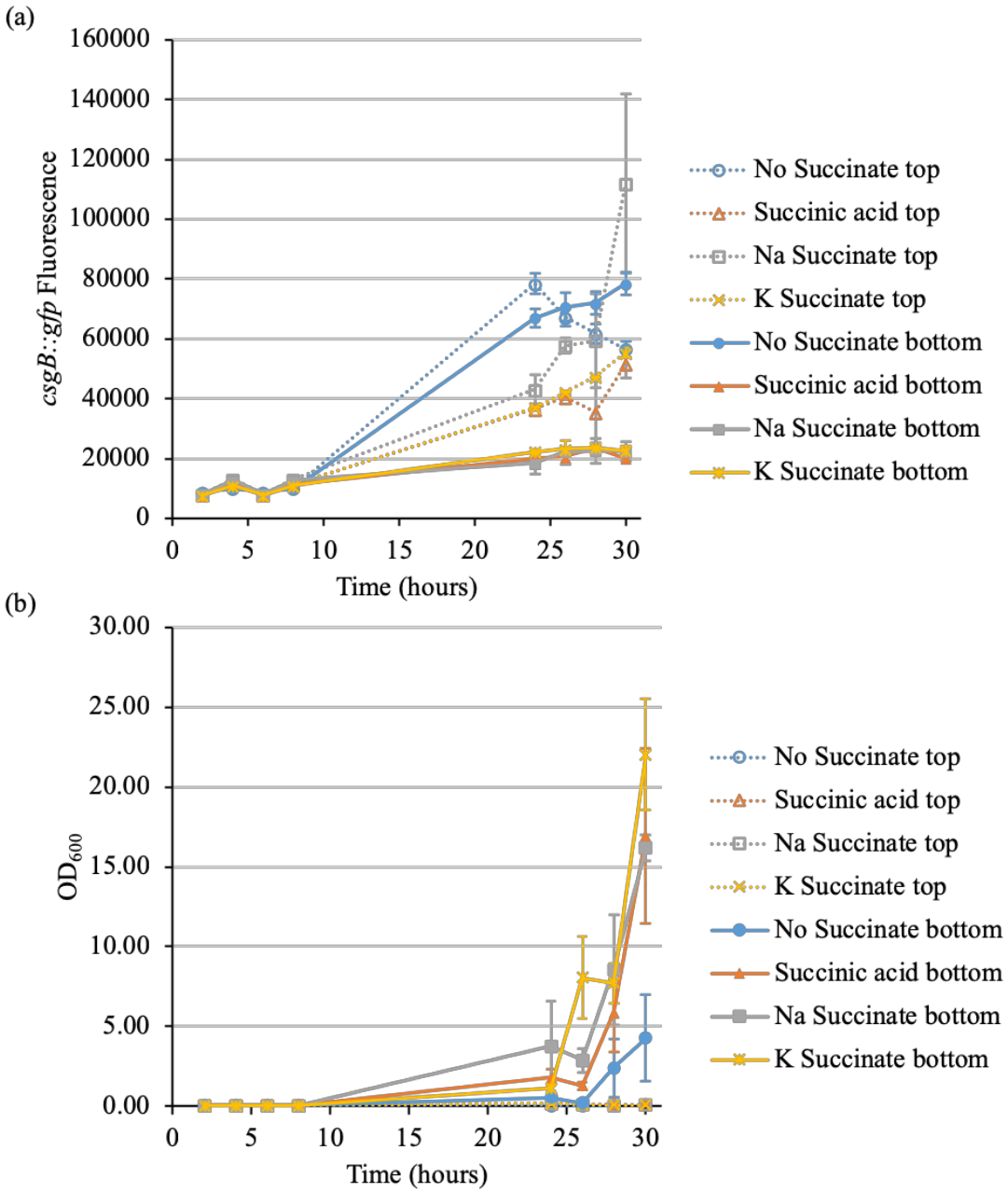

Figure 3.12: The effect of succinate on curli expression and cell concentration.

E. coli PHL644 transformed with a *csgB::gfp* fusion reporter (pJLC-T) was grown in duplicate in M63+ medium either with no additional carbon source (no succinate), 17 mM succinic acid, 17 mM sodium succinate, or 17 mM potassium succinate at 30 °C and 70 rpm shaking. Samples were taken over 30 hours from planktonic phase (top) and sediment (bottom) and analysed by flow cytometry. Mean green fluorescence representing *csgB* promoter activity (a), and OD_{600} were measured (b). Bars representing ± standard deviation from the mean value of two independent cultures are shown. The lack of a secondary carbon source produced the highest curli expression in both the planktonic phase and the sediment, however curli expression was much lower in the sediment than in the planktonic phase. At 30 hours, curli expression of the planktonic phase was highest in the presence of sodium succinate.

In the first 24 hours, the culture without succinate had the highest fluorescence in both the sediment and planktonic phase. Cell concentration (OD_{600}) was the lowest in this condition as curli expression is known to be maximally produced during nutrient deprivation (A Olsén *et al.*, 1993). However between hours 24 — 30 in the condition without succinate, the planktonic phase decreased curli expression, while the curli expression of the sediment remained roughly the same. Concurrently, planktonic cells grown in sodium succinate had begun to increase curli expression until values were similar to those of the planktonic and sediment cells in cultures grown without succinate. The data supports findings that curli expression is produced maximally in nutrient-limiting conditions, as the condition without a secondary carbon source had the highest or second highest curli expression over 30 hours (Brombacher *et al.*, 2006). An RNA sequencing profile of an *E. coli* O157:H7 curli-producing variant revealed when grown to stationary phase in nutrient-limiting conditions, genes for curli expression, among other biofilm-promoting genes, were upregulated while genes responsible for some metabolic functions, such as use of succinate in the TCA cycle, were downregulated (Sharma 2017). These reports and the data indicate there may be a link between metabolism and curli expression/genes for biofilm formation which should be explored in future work.

As observed previously, cell concentrations over the 30 hours tended to be greater in the sediment than the planktonic phase and cell concentrations of cultures containing succinate were significantly greater than without. Although, at 30 hours there was no significant difference in cell concentration between any cultures containing succinate. In order to retain both high curli expression and cell concentration, the addition of sodium succinate was selected as a suitable secondary carbon source as it fulfils both of these needs. While 17 mM sodium succinate had the highest curli

expression after 30 hours, the potential that sodium ions could increase PNAG production needs to be explored.

To investigate the effect of succinate on PNAG production, PHL644 was grown using the Duran Bottle method containing M63+ minimal medium with either no succinate, 17 mM succinic acid, 17 mM sodium succinate (best crystal violet analysis and *csgB::gfp* expression), or 17 mM potassium succinate at 30 °C and 70 rpm shaking for three days. PTFE-wrapped microscope slides carrying biofilm were then washed with PBS, stained with SYTO 62 (stains DNA, shown in magenta) and WGA (stains PNAG, shown in green) and visualised by confocal microscopy (Fig. 3.13a). By use of ImageJ, green fluorescence representing PNAG was measured for each biofilm sample and then divided by the total biofilm area which gave the relative amount of PNAG in each condition (Fig. 3.13b). Overall, biofilms grown with sodium succinate grew slightly thicker than other succinate sources and biofilm formation was severely hindered without the addition of succinate. This data supports previous work with crystal violet data (Leech, 2017).

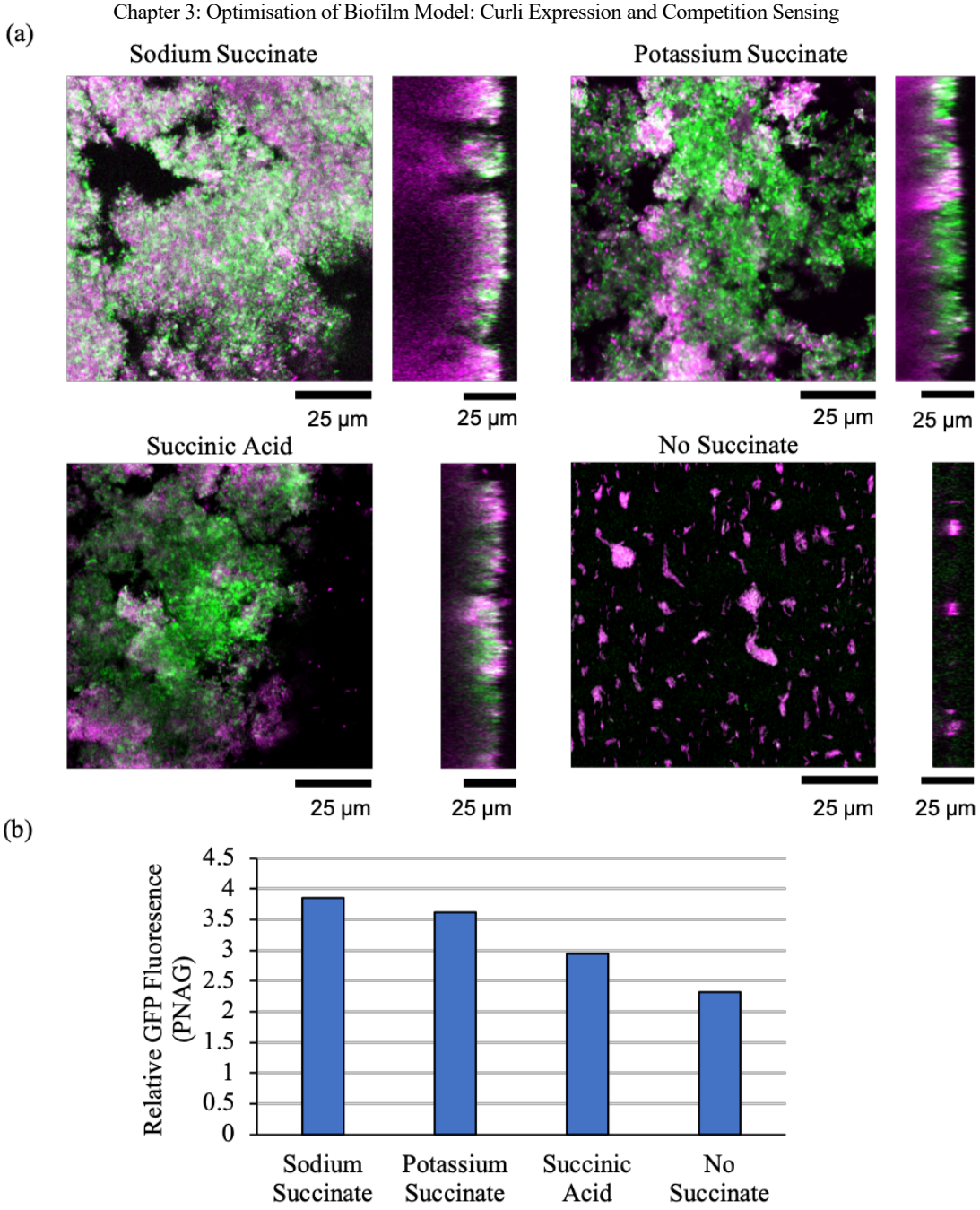

Figure 3.13: The effect of succinate on production of the matrix component PNAG.

E. coli PHL644 was grown in the Duran Bottle method with M63+ medium and either with no succinate, 17 mM succinic acid, 17 mM sodium succinate, or 17 mM potassium succinate at 30 °C and 70 rpm shaking for three days. Biofilms were stained with SYTO 62 (DNA, magenta) and WGA (PNAG, green) and visualised by confocal microscopy. Representative single-plane images of biofilm as well as side-views are shown (a). The side-views are shown left (top) to right (bottom). Images include 25 µm scale bars. By use of ImageJ software, mean GFP representing PNAG was measured for the entire sample and divided by the total area, which gave the relative amounts of PNAG for each sample (b). Biofilms grown with sodium succinate and potassium succinate grew thicker than succinic acid, and possibly produced more PNAG.

Matrix component PNAG was produced similarly in all conditions except when no succinate is added; however, sodium succinate and potassium succinate produced slightly more PNAG than succinic acid. PNAG was stained throughout the biofilm and tended to be present more heavily at the base of the biofilm. This suggest the first cells in the microcolony (which becomes the biofilm) initiate PNAG production because it helps anchor the initial cells to the surface and to each other (Beloin, Roux and Ghigo, 2008). Furthermore, there is evidence that PNAG production is required for irreversible attachment and the resulting biofilm architecture (Agladze, Wang and Romeo, 2005). Perhaps it is the attachment to an abiotic surface which stimulates PNAG production in the first cells, and cells that attach to the biofilm later produce different matrix components.

While sodium succinate appears to be the best supplement for M63+ minimal medium, the notion that sodium ions stimulate more PNAG production than potassium ions was inconclusive. Sodium succinate may stimulate more PNAG production or curli expression, and could be used to produce a thicker, more robust biofilm, and would continue to be used in subsequent experiments. Next, the effect of rotational speed on curli expression was tested

3.3.2.6 The effect of rotational speed and oxygen availability on curli expression

The last physical condition of the Duran Bottle method to be tested for the effect on curli expression was rotational speed. Work by Thomen and colleagues with flow channels revealed two important features of movement and shear force on *E. coli* biofilm formation; first, it allows for initial attachment and colonisation to the surface, and secondly, it allows for the availability of oxygen (Thomen *et al.*, 2017). Previous work investigating the effect of shaking at 0 rpm, 35 rpm, 70 rpm (standard), and 150

rpm on biofilm formation by crystal violet analysis revealed 70 rpm accumulated the most biofilm (Leech, 2017). The study went on to postulate that shear force (above 35 rpm) is necessary for biofilm formation but too of high shear force (150 rpm) will damage the biofilm. To dissect and study this further, the effect of the "optimal" shaking (70 rpm) and faster shaking (150 rpm) on curli expression was investigated. PHL644 transformed with pJLC-T was grown using the Duran Bottle method containing M63+ minimal medium at 30 °C and either 70 rpm or 150 rpm shaking. Due to the vigorous mixing of the sediment and planktonic phase occurring at 150 rpm, samples were only taken from the planktonic phase (centre of the bottle) and analysed by flow cytometry. The mean green fluorescence (*csgB::gfp*) and cell concentration (OD_{600}) were measured (Fig. 3.14). After 25 hours, cell concentration was higher when shaken at 150 rpm, likely due to the increased aeration improving cell growth (McDaniel, Bailey and Zimmerli, 1965). However, curli expression was marginally higher in 70 rpm rotational speed, which could support observations that this rotational speed increased biofilm accumulation in previous crystal violet work.

Reports that microaerophilic environments maximise curli expression in rich medium and aerobic environments maximise curli expression in minimal medium indicate that oxygen tension plays a role on curli expression (Gerstel, Park and Römling, 2004). Western blot analysis showed that AgfD activity, which stimulates biofilm formation in *S. typhimurium* by production of fimbriae, is highest in minimal medium with aeration (Römling *et al.*, 1998; Gerstel and Römling, 2001). Furthermore, shear force has been shown to be important in the production of strong bacterial surface adhesins (Liu and Tay, 2002; Thomas *et al.*, 2002; Park *et al.*, 2011). Taken together, this suggests that nutrient limitation, shear force and oxygen availability all influence the production of adhesins. While there is no velocity gradient in the flasks it is thus unlikely that shear is different between 70 rpm and 150 rpm; it is possible that shaking

at 70 rpm provides optimal oxygen levels to stimulate curli production. The effect of oxygen on curli expression was then studied.

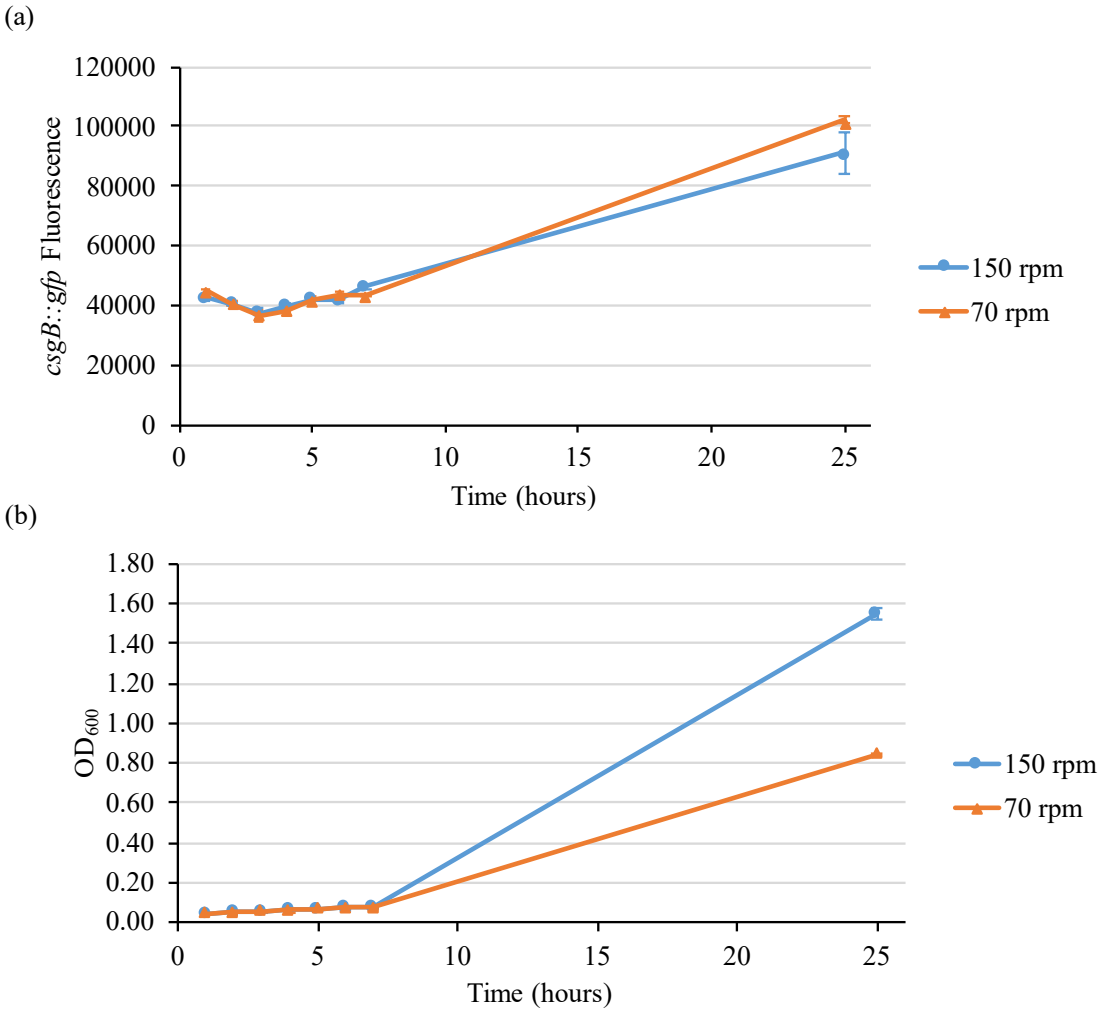

Figure 3.14: The effect of rotational speed on curli expression.

E. coli PHL644 transformed with a *csgB::gfp* fusion reporter (pJLC-T) was grown in duplicate in M63+ medium at 30 °C and either 70 rpm or 150 rpm shaking. Samples were taken over 25 hours and analysed by flow cytometry. Mean green fluorescence representing *csgB* promoter activity (a), and OD_{600} were measured (b). Bars representing ± standard deviation from the mean value of two independent cultures are shown. Despite 150 rpm conferring better planktonic cell concentrations at 25 hours, 70 rpm had slightly higher curli expression, which may result in more biofilm formation as observed in previous studies.

Cells encounter different levels of oxygen in the medium and in the biofilm, which then regulates curli expression, and other genes, differently (Costerton *et al.*, 1995; Prigent-Combaret *et al.*, 1999). It has been established that while *E. coli* K-12 biofilms cannot form in anaerobic conditions, microaerophilic conditions in rich medium and aerobic conditions in minimal medium produce maximal curli expression, which is important in biofilm formation (Gerstel and Römling, 2001; Colón-González, Méndez-Ortiz and Membrillo-Hernández, 2004; Barnhart and Chapman, 2006). When grown to stationary phase aerobically, ArcZ (Anoxic Redox Control) stimulates RpoS which in turn stimulates *csgD* and curli expression increases (Mika and Hengge, 2014). Alternatively in anaerobic environments, the two component system ArcBA represses ArcZ activity which ultimately reduces curli expression. ArcB, a sensor kinase, first autophosphorylates which begins a cascade where ArcA a response regulator, along with the transcription factor FNR, modulate a multitude of genes in *E. coli* K-12 (Kwon *et al.*, 2000; Salmon *et al.*, 2005; Tseng, 2006). Additionally, cultures grown anaerobically have elevated H-NS, which also interferes with RpoS and curli expression is repressed (Landini and Zehnder, 2002; Zhou and Gottesman, 2006). Integration host factor (IHF) is reportedly required to the increase *csgD* promoter expression in microaerophilic environments, which shows the intricate regulation of curli expression by IHF, H-NS, and OmpR in response to oxygen levels (Gerstel, Park and Römling, 2004). A study investigating the effect of rich and minimal medium and oxygen levels on *S. typhimurium* revealed that curli expression is highest in rich medium grown with less oxygen, or in minimal medium grown aerobically (Gerstel and Römling, 2001).

To examine the effect of oxygen on *E. coli* K-12 curli expression, PHL644 transformed with pJLC-T was grown in 100 mL conical flasks containing either 60 mL (full) or 20 mL (less full) M63+ minimal medium at 30 °C. Flasks were incubated at either static conditions or 70 rpm shaking. It was proposed that the flasks with less

medium would have more dissolved oxygen available, while the flasks that were shaken at 70 rpm would be more highly aerated than those at static conditions. Samples from the flasks were taken over time and analysed by flow cytometry, but it was decided that due to the different amounts of medium in the flasks, cell concentration (OD_{600}) would not be measured. Mean green fluorescence (*csgB::gfp*) was measured over 70 hours (Fig. 3.15).

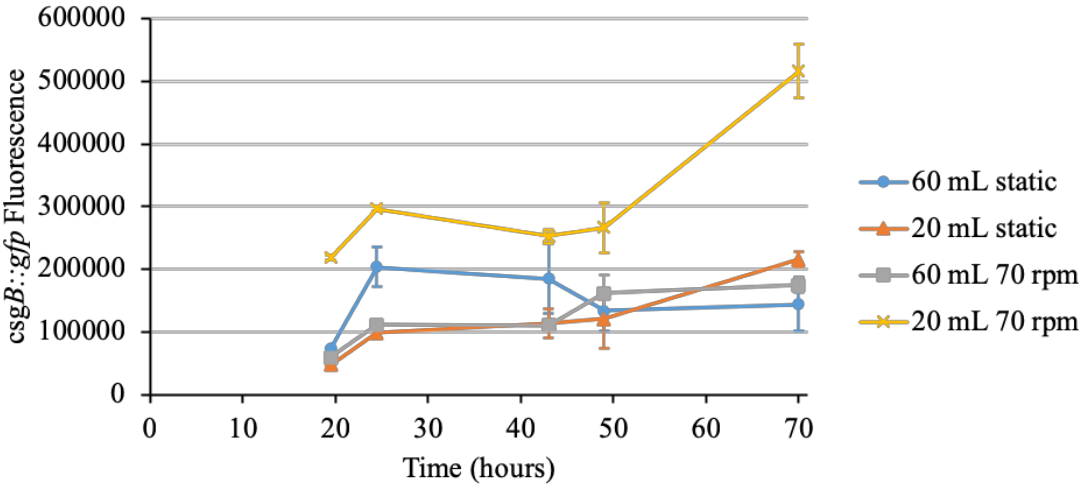

Figure 3.15: The effect of aeration on curli expression.

E. coli PHL644 transformed with a *csgB::gfp* fusion reporter (pJLC-T) was grown in 100 mL flasks in duplicate containing either 60 mL (full) or 20 mL (less full) M63+ medium at 30 °C and either 70 rpm shaking or static conditions. Samples were taken over 70 hours and analysed by flow cytometry. Mean green fluorescence representing *csgB* promoter activity was measured (a). Bars representing ± standard deviation from the mean value of two independent cultures are shown. Curli expression was highest in 20 mL (less full, more oxygen) and 70 rpm shaking.

The flask shaking at 70 rpm with less medium (most dissolved oxygen) had the highest curli expression over time, especially at 70 hours which had the largest difference in curli expression from the other conditions. Curli expression between the 60 mL (full) flask at static conditions, the 60 mL (full) flask at 70 rpm shaking, and the 20 mL (less full) flask at static conditions were similar except between the hours of 24 – 43 where the 60 mL (full) flask at static conditions had the highest curli expression and at hour 70 where the 20 mL (less full) flask at static conditions had slightly higher curli expression.

Aerobic environments in minimal medium are reportedly best for curli expression, but there is also literature that reveals the importance of shear force and other environmental conditions on curli expression and biofilm formation (Gerstel and Römling, 2001; Liu and Tay, 2002; Barnhart and Chapman, 2006; Park *et al.*, 2011). While the 20 mL culture shaken at 70 rpm was the most aerated, it is possible that this condition provided optimal shear force on the cells which stimulated curli expression the most over 70 hours. Alternatively, flasks with the least oxygen available (60 mL medium, full, at static conditions) were the second highest curli-expressing condition between hours 20 – 43. These results may indicate that both shear force and oxygen tension are important in curli expression grown in minimal medium. Additionally, there have been reports that oxygen depletion affects other factors of biofilm formation. For instance, Acetyl phosphate (AcP) has been shown as a link between oxygen depletion and *E. coli* biofilm formation; as local oxygen levels decrease so do intracellular AcP levels, which results in the upregulation of genes associated with biofilm formation, such as colanic acid production (Wolfe *et al.*, 2003). These reports indicate that oxygen tension can affect *E. coli* K-12 biofilm formation in terms of curli and EPS secretion differently, and should be studied further. Once the physical conditions of the Duran

Bottle method had been optimised for curli expression, it was decided to understand the effect of competition sensing on biofilm formation.

3.3.3 Competition sensing in response to individual chemicals

Once the biofilm model had been characterised and optimised for curli expression, other methods of stimulating biofilm formation were investigated. Competition sensing is a theory which states that bacteria are able to respond competitively after sensing molecules produced by the neighbouring bacteria (Cornforth and Foster, 2013). Research by Chen *et al.* reported *Bacillus subtilis* produced acetic acid which induced biofilm formation in neighbouring, but separated *B. subtilis* cells (Chen *et al.*, 2015). In a study by Tashiro and colleagues, it was found that the addition of low amounts of ethanol (1 – 2%) could increase biofilm formation in the Gram negative bacterium *Pseudomonas aeruginosa* (Tashiro *et al.*, 2014). In another study, the addition of ethanol was recognised as a stress signal which induced biofilm formation in *S. typhimurium* (Gerstel and Romling, 2001). Since *E. coli* K-12 can produce one mole of ethanol from one mole of glucose in anaerobic conditions, it was decided to test the competition sensing theory by treating *E. coli* K-12 with varying concentrations of ethanol and measuring the accumulation of biofilm (Clark, 1989; Koppolu and Vasigala, 2016). Additionally, it was decided to include other treatment conditions: lactic acid (an organic acid produced by *E. coli*) and hydrochloric acid (an inorganic acid not produced by *E. coli*). PHL644 was grown using the Duran Bottle method containing M63+ minimal medium with either 0 mM, 1 mM, 5 mM, or 10 mM of ethanol, lactic acid, or hydrochloric acid at 30 °C and 70 rpm shaking for three days. The biofilm accumulation was measured by crystal violet assay (Fig. 3.16).

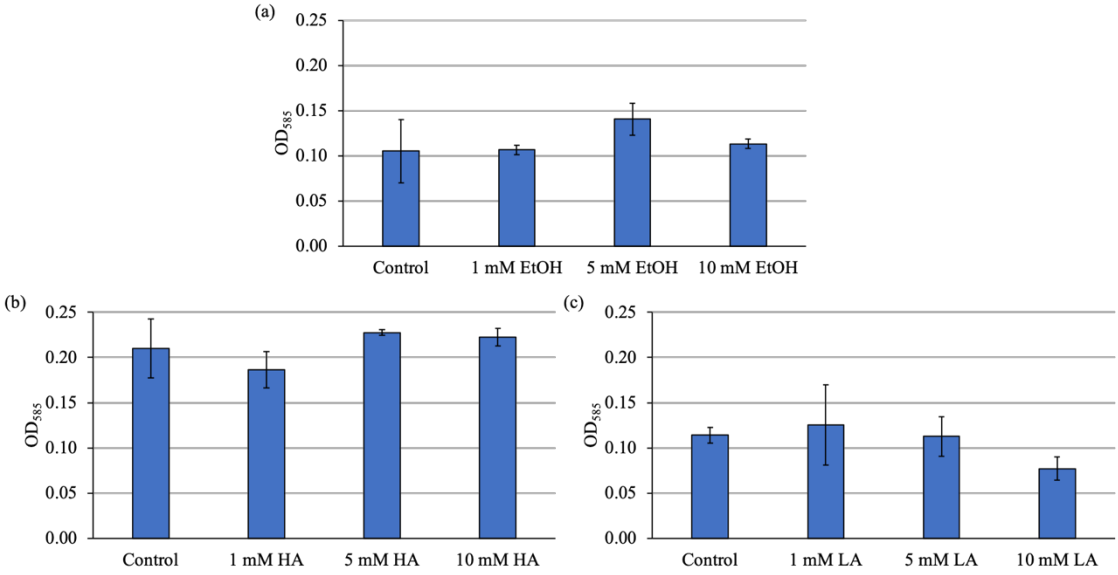

Figure 3.16: Biofilm accumulation when treated with ethanol, hydrochloric acid, and lactic acid.

E. coli PHL644 was grown using the Duran Bottle method in triplicate in M63+ medium either with no additive, 1 mM, 5 mM, or 10 mM of ethanol (EtOH), hydrochloric acid (HA), or lactic acid (LA) at 30 °C and 70 rpm shaking for three days. EtOH (a), HA (b), and LA (c) biofilm samples were washed with PBS and analysed by crystal violet assay (OD_{585}). Bars representing ± standard deviation from the mean value of a minimum of three independent replicates are shown. No additive significantly improved biofilm accumulation.

No additive significantly improved biofilm accumulation, however the sensitivity of crystal violet analysis is limited. While there was no increase of biofilm accumulation, it was hypothesised that these chemicals may affect the planktonic cells before they attach and form a biofilm, and as such may change the viability of the biofilm. To observe trends in the viability, PHL644 was grown using the Duran Bottle method containing M63+ minimal medium with either 0 mM, 1 mM, or 10 mM of ethanol, lactic acid, or hydrochloric acid at 30 °C and 70 rpm shaking for three days. Samples were scraped from the biofilm and resuspended in PBS before being treated with Bis-oxonol (BOX) to stain cells with depolarised membrane (injured or dead cells), and propidium iodide (PI) to stain DNA of dead cells. Cells were then analysed by flow cytometry to determine the percentage of cells that were "injured" (BOX+), "dead" (PI+ and BOX+), or "healthy" (PI- and BOX-) (Fig. 3.17). Ethanol did not significantly change the percentage of healthy, dead, or injured cells, whereas the addition of hydrochloric acid caused more cell injury and death. The addition of 1 mM and 10 mM lactic acid caused a larger percentage of cells in the biofilm to be healthy than cells grown without lactic acid. This corresponds with a study which reported that organic acids, specifically lactic acid, increased gene expression of genes that encode acid resistance in *E. coli*, which resulted in a protective effect and the bacteria survived (Bjornsdottir *et al.*, 2006). This may suggest that treating the biofilm with lactic acid increased acid resistance gene expression, among other gene regulation, and the resulting biofilm may be more viable. Next, it was decided to see if the addition of lactic acid changed the biofilm structure, physiology, or thickness.

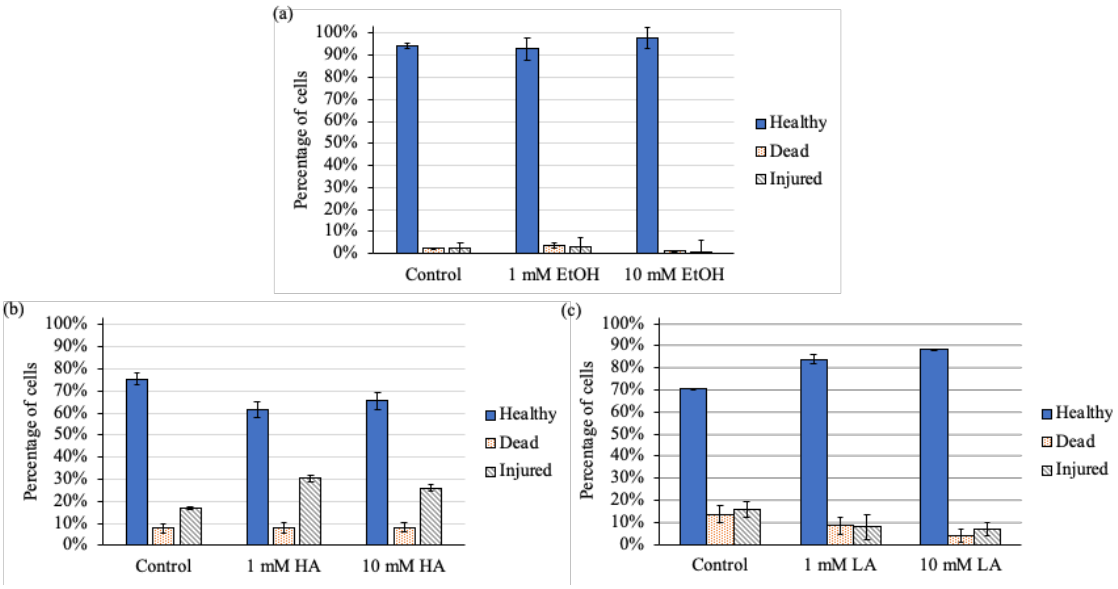

Figure 3.17: Viability of biofilms when treated with ethanol, hydrochloric acid, and lactic acid.

E. coli PHL644 was grown in triplicate in M63+ medium either with no additive, 1 mM, or 10 mM of ethanol (EtOH), hydrochloric acid (HA), or lactic acid (LA) at 30 °C and 70 rpm shaking for three days. EtOH (a), HA (b), and LA (c) biofilm samples were treated with either Bis-oxonol (BOX) to stain cells with depolarised membrane (injured or dead cells) and propidium iodide (PI) to stain DNA of dead cells and were then analysed by flow cytometry to determine the percentage of cells that were "injured" (BOX+), "dead" (PI+ and BOX+), or "healthy" (PI- and BOX-). Bars representing ± standard deviation from the mean value of a minimum of three independent replicates are shown. The addition of ethanol and hydrochloric acid did not increase the percentage of healthy cells. The addition of either 1 mM or 10 mM lactic acid gave rise to more healthy cells than no addition.

To better understand the effect of lactic acid on the biofilm physiology, PHL644 was grown using the Duran Bottle method containing M63+ minimal medium with either 0 mM, 1 mM, 5 mM, or 10 mM of lactic acid at 30 °C and 70 rpm shaking for three days. The microscope slide carrying biofilm was then washed with PBS and the biofilm was treated with SYTO 62 (stains DNA of cells, shown in red) and visualised by confocal microscopy. Representative single-plane images of the biofilm cross section and side-views with scale bars were shown (Fig. 3.18). Biofilm grown in 1 mM lactic acid formed a thicker biofilm (side-view) than biofilms grown in either 10 mM lactic acid or no lactic acid. While crystal violet analysis did not indicate a difference in biofilm accumulation when treated with lactic acid, there are sensitivity limitations to the assay and it may not be able to indicate small differences in biofilm accumulation. In addition to thickness, visualisation by confocal microscopy revealed that treatment with 1 mM lactic acid resulted in biofilms with larger mushroom structures (single-plane images) and more confluent growth that had less gaps in the morphology.

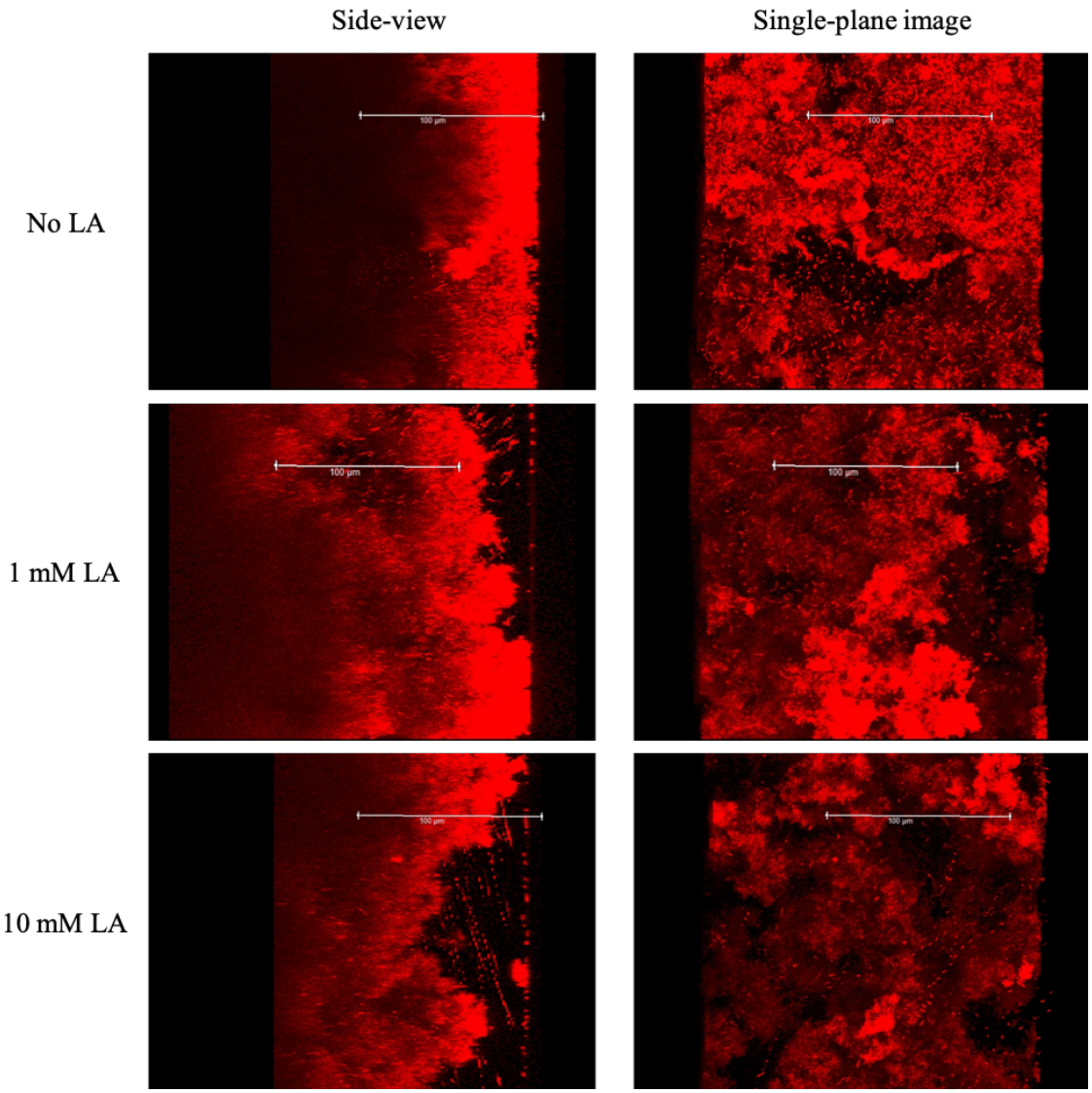

Figure 3.18: Visualisation by confocal microscopy of biofilms treated with lactic acid.

E. coli PHL644 was grown in duplicate using the Duran Bottle method containing M63+ medium with either with no lactic acid, 1 mM, or 10 mM of lactic acid at 30 °C and 70 rpm shaking for three days. Biofilm samples were treated with SYTO 62 to stain DNA (red) and then analysed by confocal microscopy. Representative single-plane images of biofilm as well as side-views are shown. Side-view is oriented left (top) to right (bottom). Images include 100 µm scale bars (white). Treatment with 1 mM produced a thicker biofilm than 10 mM treatment or no treatment. The addition of 1 mM lactic acid produced larger mushroom structures and more confluent growth than the addition of 10 mM lactic acid.

Studies of biofilm physiology and morphology have indicated themes within *E. coli* K-12 biofilms. Biofilms consisting of curli, PNAG, and colanic acid result in protective tree-like structures capable of withstanding stress with organised channels that allow for transport/exchange of waste and nutrients (Picioreanu, Van Loosdrecht and Heijnen, 2000; Agladze, Wang and Romeo, 2005; Hobley *et al.*, 2015). Knowing this, it is possible that the larger mushroom structures and confluent growth caused by 1 mM lactic acid may be indicative of a physically robust and thriving biofilm. If so, this would support earlier viability assays on the flow cytometry. One study of global stress responses in *E. coli* biofilm formation found that a *ycfR* mutant had increased biofilm accumulation but was more sensitive to acid, indicating acid stress may be linked to biofilm formation (Zhang, García-Contreras and Wood, 2007). To continue testing the effect of competition sensing on biofilm formation, it was hypothesised that spiking cell cultures with spent medium (bacterial waste) may affect biofilm formation.

3.3.4 Competition sensing in response to spent media

A study by Cabellos-Avelar and colleagues reported that supplementing with spent medium of cultures grown aerobically allowed *E. coli* K-12 to produce biofilms anaerobically, even though normally it cannot (Cabellos-Avelar, Souza and Membrillo-Hernández, 2006). The group postulated that oxygen tension is important in biofilm formation as the bacteria require oxygen to produce molecules necessary for cooperative biofilm formation and the addition of spent medium from *E. coli* K-12 grown aerobically to bacteria grown anaerobically would include these molecules and could induce biofilm formation.

To further test if competition sensing can result in the generation of a more robust *E. coli* biofilm, it was decided to treat *E. coli* with filtered spent media produced from the same strain and a different strain. PHL644 and MG1655 (which does not overproduce curli) were grown to stationary phase in LB medium and cells were filtered to isolate sterile spent medium. PHL644 and MG1655 were each grown using the Duran Bottle method containing M63+ minimal medium and 500 µl of either unspent (fresh) LB medium, MG1655 spent medium or PHL644 spent medium at 30 °C and 70 rpm shaking for three days. Biofilm accumulation was measured by crystal violet analysis (Fig. 3.19).

While neither spent media significantly increased PHL644 biofilm accumulation, the addition of either spent media doubled MG1655 biofilm accumulation. It is possible that the PHL644 strain mutation that causes *csgD* to overproduce curli overrides competition sensing pathways, or because PHL644 is able to produce so much more biofilm small changes in biofilm formation in response to spent media is negligible or beyond the sensitivity of the crystal violet assay. It is unlikely that AHL quorum sensing molecules in the spent medium caused the increase in MG1655 biofilm formation, as neither MG1655 nor PHL644 makes these molecules (as previously described in section 1.4.1); however, this does not rule out the possibility of the presence of other signalling molecules such as AI-2 (universal communication) or other communication factors (Ahmer, 2004; Lee, Jayaraman and Wood, 2007; Beloin, Roux and Ghigo, 2008). It was noted that PHL644 produced seven times more biofilm than MG1655, corresponding to earlier reports (Vidal *et al.*, 1998). While competition sensing is still newly researched, it is clear that the addition of bacterially-produced chemicals can induce biofilm formation. The most well-studied and best examples of this being antibiotic-induced biofilm formation (Kaplan, 2011).

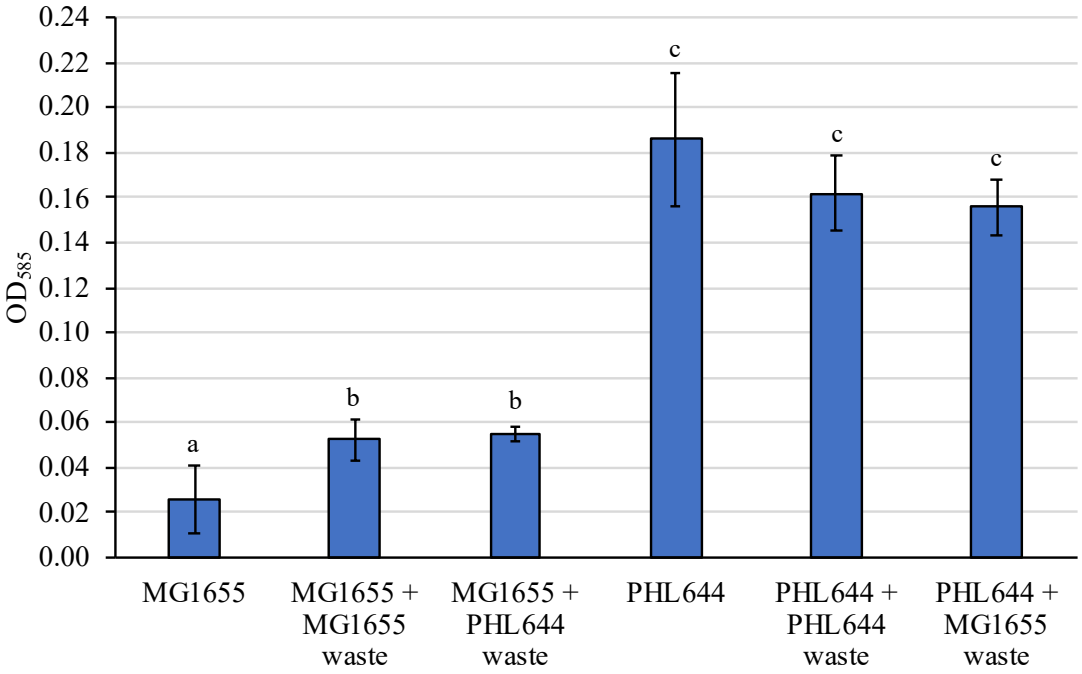

Figure 3.19: Biofilm accumulation when treated with *E. coli* spent medium.

Two *E. coli* strains, MG1655 and PHL644, were grown in quadruplicate in the Duran Bottle method containing M63+ medium with either no treatment, or dosing with either MG1655 or PHL644 spent medium at 30 °C and 70 rpm shaking for three days. Biofilms were then washed with PBS and biofilm accumulation was determined by crystal violet assay (OD_{585}). Bars representing ± standard deviation from the mean value of at least four independent replicates are shown. Dosing with both MG1655 and PHL644 spent medium resulted in more MG1655 biofilm accumulation, but did not significantly change the PHL644 biofilm accumulation. Statistics were performed using a two-tailed two-sample unequal variance t-test where $P < 0.05$ was significant. Mean values with different letters were significantly different.

3.4 Conclusions

Taken together, this data shows that curli expression is highly regulated by many environmental stimuli and sensing pathways, which is summarised in Table 3.1. These pathways are connected in an intricate web of sensitive regulatory steps that can efficiently fine-tune curli formation as needed; many of these pathways still need to be studied and further elucidated (Renner and Weibel, 2011). Additionally, the data shows curli expression is an important step in *E. coli* K-12 biofilm formation and can be optimised in the biofilm model. Osmolarity, cell density, among other factors, influence curli formation of a PHL644 biofilm grown using the Duran Bottle method. Low osmolarity in low cell concentrations, and high osmolarity in high cell concentrations resulted in more curli expression. Possibly the *ompR234* mutation in PHL644 grown to stationary phase overrides osmoregulatory pathways, to an extent, and retains elevated curli expression in high osmolarity.

Additionally, PHL644 grown using the Duran Bottle method produced more curli in the planktonic phase in minimal medium (M63+) supplemented with 10 mM glucose, at temperatures ~ 30 °C and 70 rpm shaking and access to oxygen. Many of these conditions also supported cell growth, which is required for biofilm formation. Future work should include a method of measuring and optimising shear force to elucidate the effects of oxygen availability and shear force at different rpms. The results did not show that the presence of a microscope slide or adding sodium succinate negatively affected curli expression. However, while unclear, the addition of sodium succinate may stimulate curli expression and PNAG production, which may result in more biofilm accumulation.

Parameter Tested	Condition with maximal curli expression	Parameter Tested	Condition with maximal curli expression
Planktonic versus sediment cells	Planktonic cells	Glucose concentration	10 mM
Osmolarity starting OD_{600} ≈ 0.07	Low osmolarity	Temperature	30 °C
Osmolarity starting OD_{600} ≈ 0.7 – 1.2	High osmolarity	Addition of succinate	Possibly sodium succinate
Presence of microscope slide in Duran bottle	Equal	150 rpm versus 70 rpm	70 rpm
Minimal versus rich media	Minimal media	Aeration	Possibly more aeration

Table 3.1 Summary of curli optimisation.

The second half of this chapter's data shows competition sensing may be important in biofilm formation. PHL644 can grow a more viable, slightly thicker biofilm with larger mushroom cloud structures and confluent cell growth when grown in the presence of 1 mM lactic acid. The biofilm formed in the presence of 1 mM lactic acid may be more robust as the cells are more viable, and have grown larger mushroom structures typical of *E. coli* K-12. The biofilm morphology was not significantly affected by the addition or ethanol or hydrochloric acid. Additionally, treating cells with bacterial spent medium may contribute to more biofilm accumulation in strains that do not overproduce curli, such as MG1655. It is possible that the increase in biofilm accumulation is due to AI-2 or other signalling molecules in the spent medium (quorum

sensing), the presence of acids or other chemicals (competition sensing) in the bacterial waste/spent medium. Future work should continue to investigate other acids and compounds that may induce competition sensing responses and to perform microarray experiments to better understand the change is gene expression within the cell when exposed to these compounds, such as 1 mM lactic acid. It may also be useful to continue waste dosing experiments with other strains of *E. coli*, such as *P. fluorescens*, which produce AHL's. Purified AHL and AI-2 molecules can also be supplemented to cultures to understand the relationship between competition sensing and quorum sensing.

4 Aromatic Amino Acids and Biofilm Formation

4.1 Introduction

There is a body of research which aims to exploit the robust nature of biofilms to protect the biocatalytic enzymes necessary for synthesis of a wide-range of products such as chemicals and pharmaceuticals. By using bacteria in a biofilm, manufacturers could reduce costs, wastes and energy needs associated with other more expensive means of production (Rosche *et al.*, 2009; Winn *et al.*, 2012). Some of this work uses single-species biofilms to catalyse the biotransformation of a range of products, such as 5-halo-tryptophan, a chemical precursor, by *E. coli* K-12 (Li, Hauer and Rosche, 2007; Tsoligkas *et al.*, 2011). This is achieved by insertion of a plasmid (pSTB7) into *E. coli* K-12 that results in the constitutive expression of recombinant tryptophan synthase, *trpBA* (Tong *et al.*, 2016). However, previous work by Perni and coworkers to optimise the process of 5-halo-tryptophan production found strains which overproduce curli (PHL628, derived from MG1655) have reduced biofilm accumulation when transformed with pSTB7 which was later confirmed in other work (Perni *et al.*, 2013; Leech, 2017). As previous described in section 1.4.3, *E. coli* K-12 is able to produce tryptophan from indole and L-serine by tryptophan synthase (Henning *et al.*, 1962; Lane and Kirschner, 1983; Li and Young, 2013). Due to previous reports that intracellular tryptophan disrupts biofilm formation, it was hypothesised that when *E. coli* K-12 overproduces tryptophan this decreases biofilm accumulation (Shimazaki *et al.*, 2012).

Previous unpublished work from the Overton laboratory investigated the importers and exporters of tryptophan, tyrosine, and phenylalanine with an aim to decrease intracellular tryptophan concentrations and therefore increase biofilm accumulation while not affecting overall tryptophan levels in the system. A marked increase in biofilm accumulation was measured by crystal violet analysis when phenylalanine was added to PHL644 transformed with pSTB7. It was hypothesised that

the addition of phenylalanine may increase expression of genes responsible for tryptophan export and/or decrease expression of genes that are responsible for the reuptake of tryptophan outside the cell; however, this had not been confirmed. There is very little research detailing the effect of phenylalanine on *E. coli* K-12 biofilm formation and research into the structure and function of aromatic amino acids revealed phenylalanine has been shown to form amyloid-like fibrils which can aggregate (Adler-Abramovich *et al.*, 2012). It was decided that further investigation and characterisation of the effect of tryptophan, tyrosine, and phenylalanine on *E. coli* K-12 biofilm formation is required.

Work in the following chapter explored the effect of phenylalanine, tyrosine, and tryptophan on biofilm formation by measuring curli expression and agglutination, among other assays. The effect of phenylalanine on curli expression was characterised, and conditions were optimised to maximise curli expression and cell concentration with the objective to maximise biofilm accumulation. A hypothesis explaining the increase of biofilm accumulation was proposed and tested.

4.2 General protocol

Previous unpublished work in the Overton laboratory used crystal violet analysis and confocal microscopy to explore how the addition of phenylalanine, tyrosine, and tryptophan affected biofilm accumulation using the Duran Bottle method. In the following work, a *csgB::gfp* reporter was used to investigate the effect of these amino acids on curli formation in 500 mL conical flasks. The flasks did not contain PTFE-wrapped microscope slides thus no biofilm was formed and the mean cellular GFP fluorescence (representing *csgB* promoter activity) of the planktonic phase was measured. GFP fluorescence was measured by flow cytometry, while biomass concentration was determined by measuring the optical density (OD_{600}) in order to observe differences in growth/biomass concentration and understand the relationship to curli expression. All curli expression assays were performed for roughly 24 hours in duplicate, unless otherwise stated. In addition to measuring curli expression, an agglutination assay was developed to measure the rate at which cells aggregated to the bottom of a static container, which could indicate the relative amount of curli or other adhesins in each condition. Other procedures used in the following chapter included crystal violet analysis to measure biofilm accumulation, and confocal microscopy to visualise biofilm morphology and thickness. All additional tests were performed in duplicate unless otherwise stated.

4.3 Understanding the effect of aromatic amino acids on curli expression

4.3.1 The addition of phenylalanine increases curli expression

Previous unpublished work by Robert Millar in the Overton laboratory investigated ways to more efficiently export tryptophan from the *E. coli* K-12 biofilm constitutively expressing tryptophan synthase without altering overall tryptophan levels in the system. The objective was to decrease intercellular halotryptophan concentrations which have been shown to decrease biofilm formation; thus increasing the biomass of a biofilm constitutively expressing tryptophan synthase and hopefully increase halotryptophan yields (Shimazaki *et al.*, 2012). During this work, it was found the addition of phenylalanine may increase biofilm accumulation. In order to study this further, the effect of these amino acids on curli expression was investigated.

Due to the relative insolubility of tyrosine and tryptophan in water, concentrations greater than 0.1 mM could not be obtained. The *csgB::gfp* reporter (pJLC-T) was transformed into PHL644 and transformants were grown in 500 mL conical flasks containing M63+ minimal medium either with no supplement, or supplemented with either 10 mM L-phenylalanine, 0.1 mM L-tyrosine, or 0.1 mM L-tryptophan at 30 °C and 70 rpm shaking. Samples were taken from the centre of the medium in the conical flasks over 6 hours and again at 24 hours and analysed by flow cytometry and spectrophotometry. The mean green fluorescence (*csgB*) and the cell concentration (OD_{600}) were measured (Fig. 4.1). Between hours 3 – 6, the addition of phenylalanine caused an increase in both optical density and curli expression. Cultures containing tryptophan or tyrosine displayed no increase in optical density or curli

expression. By hour 24, there was no significant difference in optical density or curli expression between all conditions.

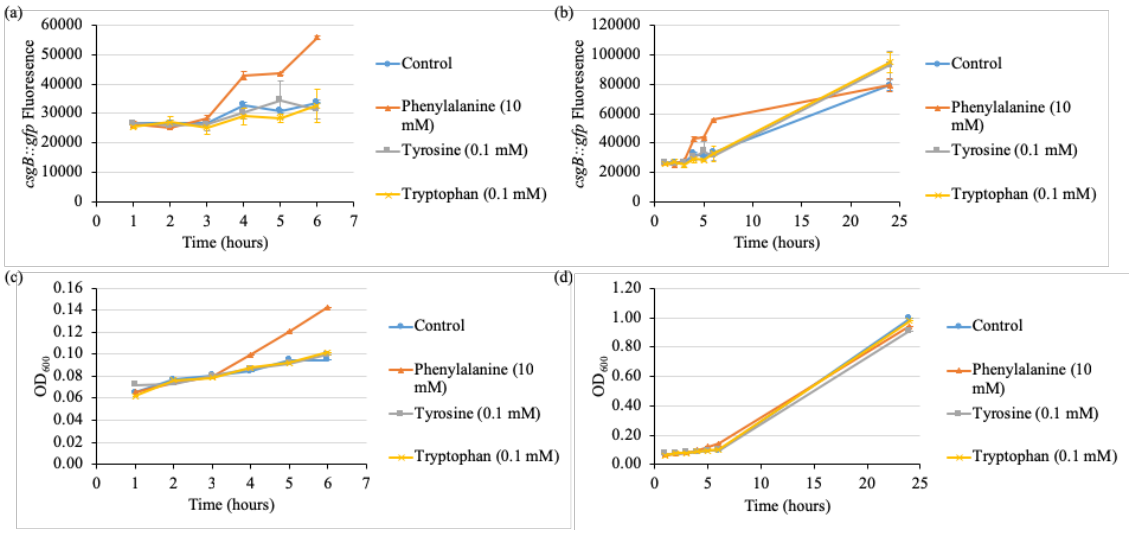

Figure 4.1: The effect of aromatic amino acids on curli expression.

E. coli PHL644 transformed with a *csgB::gfp* fusion reporter (pJLC-T) was grown in flasks containing M63+ minimal medium with no supplement or either 10 mM L-phenylalanine, 0.1 mM L-tyrosine, or 0.1 mM L-tryptophan at 30 °C and 70 rpm shaking. All conditions were performed in duplicate. Samples were taken over hours 1 – 6 and hour 24 and analysed by flow cytometry and spectrophotometry. Mean green fluorescence representing *csgB* promoter activity hours 1 – 6 (a), hours 1 – 24 (b), and OD_{600} hours 1 – 6 (c) and hours 1 – 24 (d) were measured. The addition of 10 mM phenylalanine significantly increased both curli expression and cell concentration (OD_{600}) hours 3 – 6, but all conditions were similar for curli expression and cell concentration by hour 24.

To test if the greater concentration of phenylalanine was the cause of this increase in both curli expression and optical density, 0.1 mM (the concentration of tyrosine and tryptophan in the previous experiment) L-phenylalanine was tested and compared to 10 mM L-phenylalanine. Again, reporter *csgB::gfp* (pJLC-T) was transformed into PHL644 and transformants were grown in 500 mL conical flasks containing M63+ minimal medium either with no supplement, or with either 0.1 mM or 10 mM L-phenylalanine at 30 °C and 70 rpm shaking. Samples were taken from the centre of the medium in the conical flask over 7 hours and again at 24 hours and analysed by flow cytometry and spectrophotometry. The mean green fluorescence (*csgB*) and the cell concentration (OD_{600}) were measured (Fig. 4.2).

The addition of 0.1 mM phenylalanine did not significantly increase curli expression or optical density, however 10 mM phenylalanine still increased curli expression and optical density between hours 3 – 7. After 24 hours, the control had slightly higher curli expression than 10 mM phenylalanine conditions, and 10 mM phenylalanine had slightly greater optical density. It was first assumed that the increase in optical density in cultures containing 10 mM phenylalanine was a result of *E. coli* K-12 metabolising phenylalanine preferentially over glucose, but this would not necessarily explain the increase in *csgB* expression. While there is very little literature regarding the effect of phenylalanine on *E. coli* K-12 curli expression, there are reports that MG1655, an archetypal *E. coli* K-12 strain, can degrade some amino acids for use as nitrogen or carbon sources (Yang *et al.*, 2015). However, the study used 1.0 mM, not 10 mM, concentrations of amino acids and did not report an increase in growth when supplementing with phenylalanine. It was decided to investigate this effect further, and supplement MG1655 with 10 mM phenylalanine and measure the effect on optical density and curli expression.

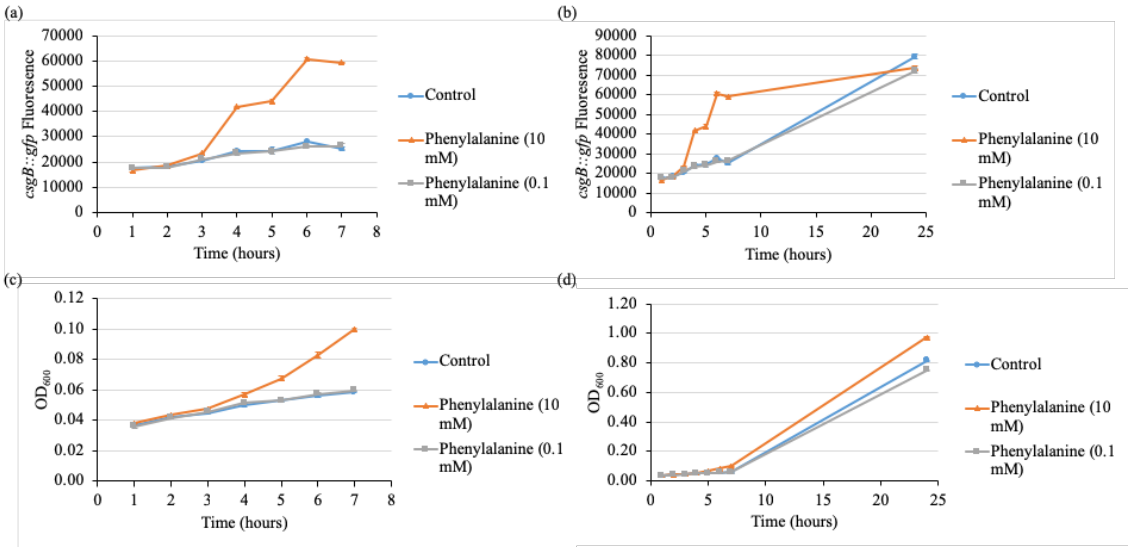

Figure 4.2: The effect of high and low phenylalanine concentration on curli expression.

E. coli PHL644 transformed with a *csgB::gfp* fusion reporter (pJLC-T) was grown in flasks containing M63+ minimal medium with no supplement or either 10 mM or 0.1 mM phenylalanine at 30 °C and 70 rpm shaking. All conditions were performed in duplicate. Samples were taken over hours 1 – 7 and 24 and analysed by flow cytometry and spectrophotometry. Mean green fluorescence representing *csgB* promoter activity hours 1 – 7 (a), hours 1 – 24 (b), and OD_{600} hours 1 – 7 (c) and hours 1 – 24 (d) were measured. The addition of 0.1 mM phenylalanine did not significantly increase curli expression or OD_{600}.

4.3.2 Phenylalanine does not affect MG1655 curli expression

PHL644, a mutant which overexpresses curli, was developed from MC4100, a MG1655 derivative (Vidal *et al.*, 1998). While previous reports concluded that MG1655 was not able to use 1.0 mM phenylalanine as a carbon or nitrogen source, this effect has not been tested for 10 mM phenylalanine nor has the effect on curli expression been examined (Yang *et al.*, 2015). In order to investigate the effect of phenylalanine on curli expression in MG1655 and compare to the effect on PHL644 between hours 1 – 6, the *csgB::gfp* reporter (pJLC-T) was transformed into MG1655 and transformants were grown in 500 mL conical flasks containing M63+ minimal medium either with no supplement or supplemented with 10 mM L-phenylalanine at 30 °C and 70 rpm shaking. Samples were taken over 6 hours and analysed by flow cytometry and spectrophotometry. The mean green fluorescence (*csgB*) and the cell concentration (OD_{600}) were measured (Fig. 4.3).

Like PHL644, the addition of phenylalanine increases OD_{600} of MG1655 cultures, but unlike PHL644 the addition of phenylalanine did not affect curli expression. This suggests that the OD_{600} increases in the presence of phenylalanine regardless of the strain, while only strains overexpressing curli (PHL644) have an increase in curli expression in the presence of phenylalanine. PHL644 contains a mutation in the *ompR* gene, which allows for more efficient binding of OmpR to the *csgDEFG* promoter and increased activation of the gene resulting in increased curli expression (Prigent-Combaret *et al.*, 2001). MG1655, a wild-type K-12 strain, does not have this *ompR* mutation and does not constitutively express curli. Although *E. coli* K-12 cannot reportedly use phenylalanine as a carbon or nitrogen source, it is important to test this with the PHL644 strain used in this study, and show that the increase in OD in

cultures containing phenylalanine is not a result of PHL644 using phenylalanine as an energy source (Yang *et al.*, 2015).

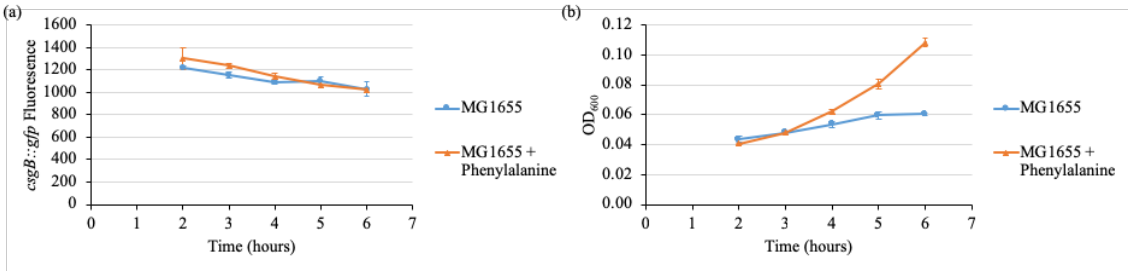

Figure 4.3: The effect of phenylalanine on MG1655.

E. coli MG1655 transformed with a *csgB::gfp* fusion reporter (pJLC-T) was grown in flasks containing M63+ minimal medium with no supplement or with 10 mM phenylalanine at 30 °C and 70 rpm shaking. All conditions were performed in duplicate. Samples were taken over 6 hours and analysed by flow cytometry and spectrophotometry. Mean green fluorescence representing *csgB* promoter activity (a) and OD_{600} (b) were measured. Like PHL644 (curli overexpressed), the addition of phenylalanine caused an increase in OD_{600}, but unlike PHL644 the addition of phenylalanine did not increase curli expression.

4.3.3 Phenylalanine is not used as a carbon source

While it has been shown that some microorganisms can use phenylalanine as a carbon and/or nitrogen source, *E. coli* K-12 has not been shown to do so (Ogata, Uchiyama and Yamada, 1967; Halvorson, 1972). However, a report studying the biodegradation of aromatic compounds, such as products of phenylalanine, by various *E. coli* strains suggested that due to intraspecies variation and genetic adaptation in nutrient-poor conditions, some *E. coli* species have adapted to metabolise these products (Díaz *et al.*, 2001). When confronted with multiple carbon sources, *E. coli* K-12 will induce carbon catabolite repression (CCR) to preferentially metabolise one preferred carbon source (glucose), while repressing the expression and activities needed for metabolism of other carbon sources (Görke and Stülke, 2008). As discussed previously (section 1.3.3), low levels of glucose cannot repress cAMP production and so cAMP levels increase which allow for binding to CRP (cAMP Receptor Protein). Bound CRP activates *csgD* (curli expression) and a multitude of other operons, including genes that allow the cell to metabolise alternative sugars (Hufnagel *et al.*, 2016). Alternatively, high levels of glucose will inhibit curli expression by repressing cAMP, decreasing bound CRP and decreasing gene activation.

While glucose is the preferred carbon source of *E. coli* K-12 in most conditions and is the standard additive in our M63+ minimal medium, glycerol can also be metabolised without the same inhibitory effects of curli expression caused by glucose (Lin, 1976; Kopp *et al.*, 2017). It is possible that an alternative carbon source, such a glycerol, could be employed to increase curli expression. In order to understand the relationship between curli expression and alternative carbon metabolism in strains overexpressing curli, glycerol was supplemented instead of glucose and optical density and curli expression were measured.

The *csgB::gfp* reporter (pJLC-T) was transformed into PHL644 and transformants were grown in 500 mL conical flasks containing M63+ minimal medium with 10 mM glucose (standard), 10 mM L-phenylalanine and 10 mM glucose, or 10 mM glycerol at 30 °C and 70 rpm shaking. Samples were taken over 6 hours and again at 24 hours and analysed by flow cytometry and spectrophotometry. The mean green fluorescence (*csgB*) and the cell concentration (OD_{600}) were measured (Fig. 4.4). PHL644 grown with glucose (control) had a similar optical density to glycerol over 6 hours (c), but after 24 hours the glucose condition had a higher OD_{600} than glycerol (d). This corresponds with reports that *E. coli* K-12 grows preferentially on glucose in most conditions and the yield on glucose is higher than the yield on glycerol (Bren *et al.*, 2016). Cultures with glucose and phenylalanine had the greatest optical density over 6 hours but had similar OD values to glucose after 24 hours. Curli expression over hours 3 – 6 was highest in conditions with phenylalanine, and glycerol had higher curli expression than glucose between hours 3 – 6. This indicates that glycerol does not have the same inhibitory effects on curli expression as glucose, however the addition of phenylalanine still produced the highest curli expression. All conditions had similar curli expression after 24 hours.

Agreeing with earlier reports, *E. coli* K-12 was able to grow using glycerol which did not negatively affect curli expression; although glucose is the preferred carbon source in nitrogen-rich environments and resulted in a greater optical density after 24 hours (Bren *et al.*, 2016). Regardless, phenylalanine with glucose still had the highest optical density and greatest curli expression between hours 3 – 6 and had similar growth to the control after 24 hours which is still preferred over the glycerol condition. To test if phenylalanine is somehow being utilised instead of glucose, resulting in a higher optical density in hours 3 – 6, PHL644 was grown with phenylalanine with and without glucose.

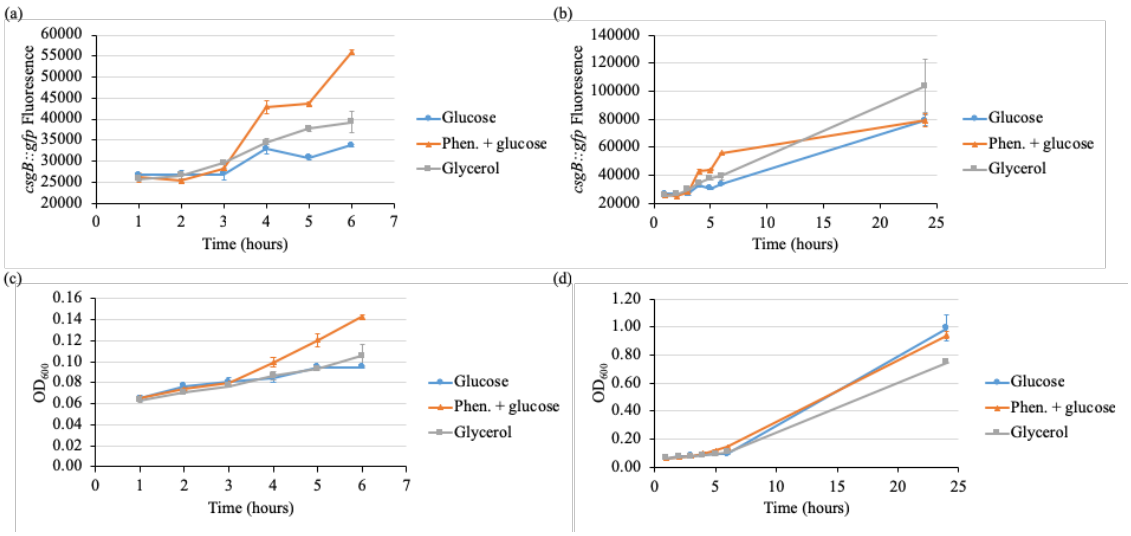

Figure 4.4: The effect of glycerol on curli expression.

E. coli PHL644 transformed with a *csgB::gfp* fusion reporter (pJLC-T) was grown in flasks containing M63+ minimal medium with either glucose (standard), 10 mM phenylalanine and glucose, or 10 mM glycerol at 30 °C and 70 rpm shaking. All conditions were performed in duplicate. Samples were taken over 6 hours and again at 24 hours and analysed by flow cytometry and spectrophotometry. Mean green fluorescence representing *csgB* promoter activity hours 1 – 6 (a), hours 1 – 24 (b), and OD_{600} hours 1 – 6 (c) and hours 1 – 24 (d) were measured. While glycerol is not a preferred carbon source, it does not have the same inhibitory effects as glucose. However, the addition of phenylalanine caused the most curli expression.

The *csgB::gfp* reporter (pJLC-T) was transformed into PHL644 and transformants were grown in 500 mL conical flasks containing M63+ minimal medium supplemented with 10 mM phenylalanine with or without glucose at 30 °C and 70 rpm shaking. Samples were taken over 7 hours and again at 24 hours and analysed by flow cytometry and spectrophotometry. The mean green fluorescence (*csgB*) and the optical density (OD_{600}) were measured (Fig. 4.5). The addition of phenylalanine to glucose again increased the OD_{600} and curli expression. Alternatively, when phenylalanine is added to cultures without glucose, PHL644 does not grow and nor has an increase in the expression of curli. This suggests that phenylalanine is not being used preferentially as a carbon source. Global gene expression analysis of the wild-type *E. coli* strain LJ110 by Polen and coworkers in response to the addition of phenylalanine to growth medium showed that phenylalanine concentration did not decrease during their work (Polen *et al.*, 2005). This supports other studies that *E. coli* K-12 cannot metabolise phenylalanine for use as a carbon or nitrogen source (Ogata, Uchiyama and Yamada, 1967). While it is evident that phenylalanine is not being used as a nutrient source, there is another reason for the increase in optical density and curli expression. Potentially, phenylalanine is activating curli expression via one of the many regulatory pathways, but this would not explain the increase in optical density. Before investigating the effect of phenylalanine further, it was decided to confirm if phenylalanine truly causes an increase in *csgB* expression which results in a measurable effect of the cell's ability to agglutinate.

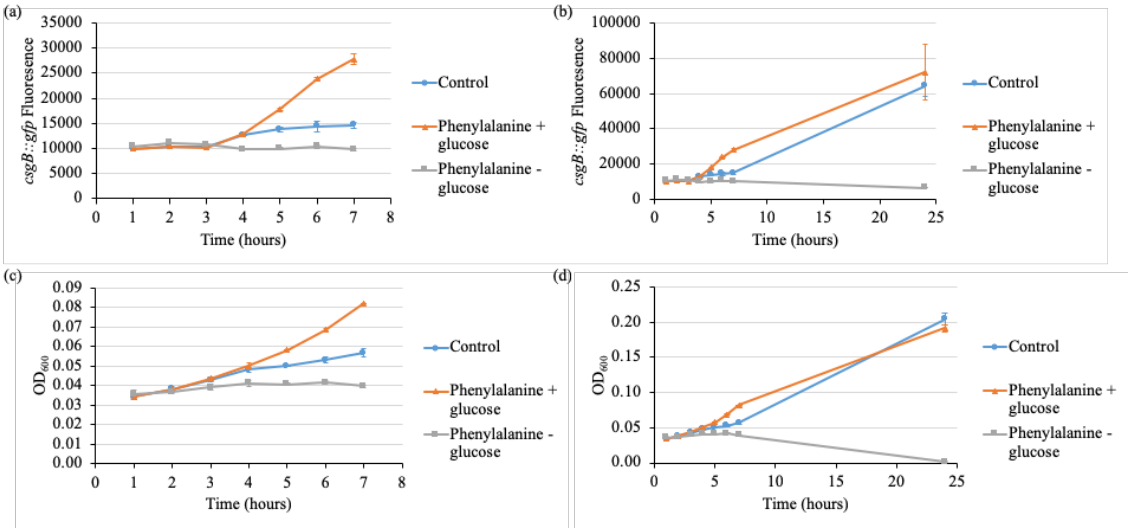

Figure 4.5: The effect of phenylalanine with and without glucose on curli expression**.**

E. coli PHL644 transformed with a *csgB::gfp* fusion reporter (pJLC-T) was grown in flasks containing M63+ minimal medium with glucose (control), or either 10 mM phenylalanine with glucose, or 10 mM phenylalanine without glucose at 30 °C and 70 rpm shaking. All conditions were performed in duplicate. Samples were taken over 24 hours and analysed by flow cytometry. Mean green fluorescence representing *csgB* promoter activity hours 1 – 7 (a), hours 1 – 24 (b), and OD_{600} hours 1 – 7 (c) and hours 1 – 24 (d) were measured. Without glucose, cells grown in 10 mM phenylalanine do not grow nor produce curli, indicating that phenylalanine is not being used a preferential carbon source.

4.3.4 The addition of phenylalanine aggregates cells

In order to determine if the increase in *csgB* expression in cultures with phenylalanine result in increased adherence, an agglutination test was developed and employed. PHL644 was grown for 21 – 24 hours in 25 mL Falcon tubes containing 15 mL M63+ minimal medium at 30 °C and 70 rpm shaking. Cells were then centrifuged, washed with PBS, and resuspended in 25 mL Falcon tubes containing 15 mL PBS at an $OD_{600} \approx 0.8$ at 30 °C statically. Samples were taken from the top 0.5 cm beneath the surface of the liquid at hours 1 and 24 and the optical density (OD_{600}) was measured. Agglutination of cells led to a decrease in OD_{600} over time (Fig. 4.6a). After 24 hours, cultures with phenylalanine had a lower OD_{600}, meaning more cells had agglutinated to the bottom than the control. This suggests the addition of phenylalanine to cultures causes cells to agglutinate faster, possibly by increasing factors, such as curli, that increase cell-cell attachment. This supports the *csgB* reporter data which indicated that the addition of phenylalanine increased curli expression in hours 3 – 7. It is possible this resulted in more curli formation and increased agglutination after 24 hours. It is important to note that at 24 hours GFP (curli) expression was the same between cultures with and without phenylalanine.

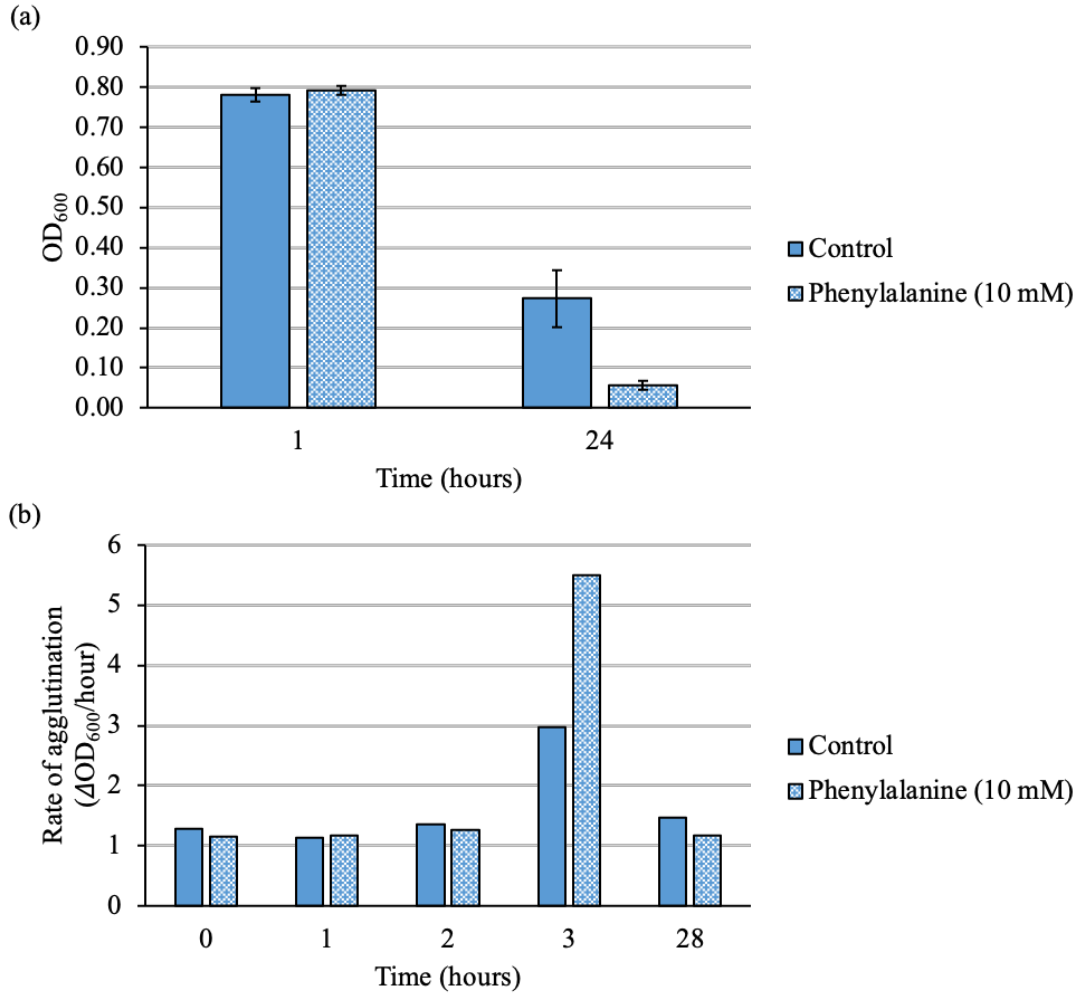

Figure 4.6: The effect of phenylalanine addition on agglutination.

E. coli PHL644 was grown for 24 hours in M63+ minimal medium with either no supplement or 10 mM phenylalanine at 30 °C and 70 rpm shaking. Cells were then centrifuged, washed with PBS, and resuspended in 15 mL PBS to reach an $OD_{600} \approx 0.8$ and were incubated at 30 °C statically. All conditions were performed in duplicate. Samples were taken 0.5 cm from the top of the liquid after 1 hour and 24 hours and the OD_{600} was measured to show the cell concentration at the top of the liquid (a). After 24 hours, cells with phenylalanine had agglutinated to the bottom more than the control. This indicates the addition of phenylalanine increased factors which caused cells to agglutinate, such as curli, and supports reporter data which showed that the addition of phenylalanine increases curli expression. A repeat experiment was performed and samples were taken from the top of the tube at 0, 1, 2, 3, 28, and 29 hours and the OD_{600} was measured. The difference in OD_{600} between hours 0 – 1, 1 – 2, 2 – 3, 3 – 28, and 28 – 29, was calculated and then divided by the time to generate the rate of agglutination between these hours (b). This shows cells agglutinate the most between hours 3 and 28 (shown at hour 3), and agglutinate the fastest when phenylalanine is supplemented.

The experiment was repeated, and samples were taken from the top of the tube after 0, 1, 2, 3, 28, and 29 hours and the OD_{600} was measured. The rate of agglutination (ΔOD_{600}/hour) between specific time points (hours 0 – 1, 1 – 2, 2 – 3, 3 – 28, and 28 – 29) was calculated by taking the difference in OD_{600} between each time point and then dividing by the time between each time point (Fig. 4.6b). This indicated that cells agglutinate the most between hours 3 and 28 because the OD_{600} of the top of the tubes decreased the most between these hours. Furthermore, the data indicated conditions with phenylalanine agglutinate at a faster rate than the control. It was then decided to test if the addition of phenylalanine would increase biofilm accumulation, but first the effect of shaking in phenylalanine conditions would be optimised for curli expression and OD.

4.3.5 Optimising shear force and phenylalanine on curli expression

In order to understand the effect phenylalanine has on curli expression and optical density and how this affects biofilm accumulation, it was decided to first optimise the physical conditions, such as shaking and temperature, before testing biofilm accumulation by crystal violet assay. The *csgB::gfp* reporter (pJLC-T) was transformed into PHL644 and transformants were grown in 500 mL conical flasks containing M63+ minimal medium with and without 10 mM phenylalanine at 30 °C and either 70 or 150 rpm shaking. Samples were taken over 7 hours and again at 25 hours and analysed by flow cytometry and spectrophotometry. The mean green fluorescence (*csgB*) and the optical density (OD_{600}) were measured (Fig. 4.7).

As before, conditions containing phenylalanine had the greatest optical density between hours 4 – 7; additionally, there was no difference in optical density between 150 or 70 rpm shaking in hours 1 – 7. However, after 25 hours conditions with phenylalanine at 150 rpm had the greatest optical density with the control at 150 rpm being second greatest. The lowest optical densities were 70 rpm control and 70 rpm phenylalanine. The increase in oxygenation at 150 rpm may confer better growth conditions for *E. coli* thus resulting in a greater optical density, as observed previously. Between hours 3 – 7, phenylalanine conditions had the greatest curli expression with conditions at 70 rpm shaking having higher expression than 150 rpm. After 25 hours, curli expression was similar amongst conditions, with 70 rpm control having the greatest value and 70 rpm phenylalanine having the lowest. The effect of different rpms on *E. coli* PHL644 follows other experiments in chapter 3; curli expression was highest at 70 rpm but 150 rpm confers greater optical densities. Due to the importance of curli formation in the initial adhesion of biofilm formation, it was proposed that the condition with greatest curli expression would allow for increased attachment to the surface, and a

thicker, more robust biofilm (Barnhart and Chapman, 2006). Thus, supplementing with phenylalanine and incubating with 70 rpm shaking was selected as it had the highest curli expression in hours 5 – 7, had only marginally lower curli expression than 150 rpm at hour 25. Next, temperature and phenylalanine conditions were optimised.

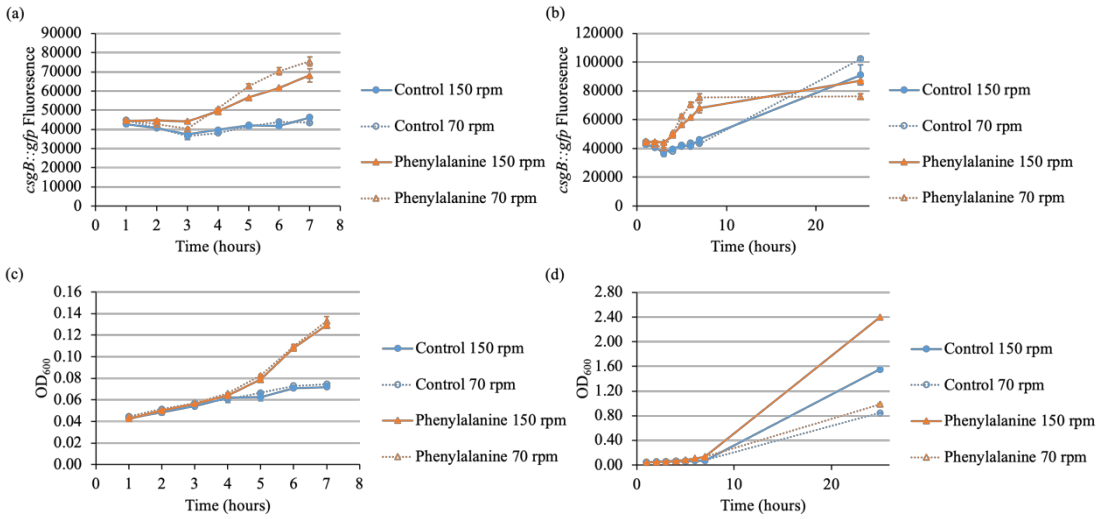

Figure 4.7: The effect shaking and phenylalanine on curli expression.

E. coli PHL644 transformed with a *csgB::gfp* fusion reporter (pJLC-T) was grown in flasks containing M63+ minimal medium with no supplement or 10 mM phenylalanine at 30 °C and either 70 or 150 rpm shaking. All conditions were tested in duplicate. Samples were taken over 24 hours and analysed by flow cytometry and spectrophotometry. Mean green fluorescence representing *csgB* promoter activity hours 1 – 7 (a), hours 1 – 25 (b), and OD_{600} hours 1 – 7 (c) and hours 1 – 25 (d) were measured. Optical density between hours 4 – 7 was highest in conditions with phenylalanine. There was no difference between 150 or 70 rpm on optical density until hour 25, where phenylalanine 150 rpm was highest, followed by the control at 150 rpm. The lowest optical densities were at 70 rpm at hour 25. Between hours 3 – 7, phenylalanine conditions had the greatest curli expression with 70 rpm having greater values than 150 rpm. After 25 hours, curli expression was similar amongst conditions, with 70 rpm control having the greatest value and 70 rpm phenylalanine having the lowest.

4.3.6 Optimising temperature and phenylalanine on curli expression

Before testing the effect of phenylalanine on biofilm accumulation by crystal violet assay, temperature and phenylalanine conditions needed to be optimised. Considering work in the previous chapter (section 3.3.2.4) that found 30 °C to be optimal for curli expression, and other reports that *E. coli* K-12 curli expression is produced maximally at temperatures below 30 °C, a preliminary comparison of 30 °C and < 30 °C was tested with phenylalanine for the effect on curli expression. The *csgB::gfp* reporter (pJLC-T) was transformed into PHL644 and transformants were grown in 500 mL conical flasks containing M63+ minimal medium with or without 10 mM phenylalanine at 26 °C or 30 °C and 70 rpm shaking. Samples were taken over 24 hours and analysed by flow cytometry and spectrophotometry. The mean green fluorescence (*csgB*) and the optical density (OD_{600}) were measured (Fig. 4.8).

While the stark increase in optical density for phenylalanine conditions was not measured between hours 3 – 7 as before, these conditions were still greater than the controls at hours 5 – 7 and were somewhat greater than the controls at hour 24. This could be because PHL644 transformed with the *csgB::gfp* reporter was near the end of the recommended 14-day period in which experiments can be performed and thus GFP was not fluorescing as efficiently. Or it could be due to improper sampling technique as the cells in the medium tend to agglutinate to the bottom of the flask making the solution heterogenous and need to be thoroughly mixed before sampling. As before, conditions with phenylalanine increased curli expression hours 4 – 7. At hour 4 conditions with phenylalanine incubated at 30 °C had a higher curli expression than phenylalanine at 26 °C, but by hour 5 the two temperatures with phenylalanine were similar. Between hours 6 and 7, conditions with phenylalanine at 26 °C had greater curli expression until hour 24 when there was no difference between any of the conditions.

While adhesion is an important step in biofilm formation and is primarily mediated by curli fibre formation, it is unknown at what hour the greatest curli expression would result in the most biofilm accumulation. In order to continue investigating the increase in optical density and curli expression by the addition of phenylalanine to PHL644, it was decided to test a similar amino acid at the same concentration. Since curli expression was greatest at 26 °C by hour 7, this was selected as the temperature for testing the alternative amino acid to compare to phenylalanine.

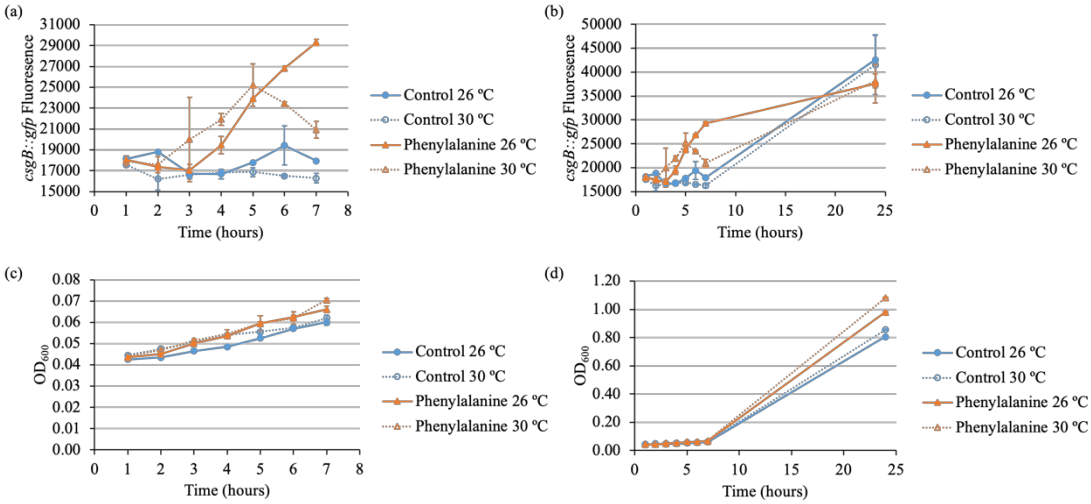

Figure 4.8: The effect of phenylalanine and temperature on curli expression.

E. coli PHL644 transformed with a *csgB::gfp* fusion reporter (pJLC-T) was grown in flasks containing M63+ minimal medium with no supplement or 10 mM phenylalanine at 26 °C or 30 °C and 70 rpm shaking. All conditions were tested in duplicate. Samples were taken over 24 hours and analysed by flow cytometry and spectrophotometry. Mean green fluorescence representing *csgB* promoter activity hours 1 – 7 (a), hours 1-25 (b), and OD_{600} hours 1 – 7 (c) and hours 1 – 25 (d) were measured. Although the increase in optical density in the first 7 hours was not as stark as previous experiments, the addition of phenylalanine at both temperatures produced the highest optical densities, including at hour 25. Similarly, the addition of phenylalanine at both temperatures resulted in the greatest curli expression between hours 3 and 7, but were similar to the controls after 24 hours. Curli expression was greatest at 26 °C with 10 mM phenylalanine in hours 6 and 7, but was similar to all other conditions after 24 hours.

4.3.7 PHL644 curli expression is not affected by the addition of alanine

As previously discussed, tyrosine and tryptophan cannot reach concentrations of 10 mM due to their relative insolubility in water. Alanine was selected as an alternative amino acid for comparison to phenylalanine because it is similar to phenylalanine in structure and because a concentration of 10 mM could be achieved (Fig. 4.9). Alanine, like tyrosine and tryptophan, are similar to phenylalanine due to their nonpolar, hydrophobic and neutral side chains which make them insoluble or only slightly soluble in water (Lodish *et al.*, 2000). However, alanine is smaller and more flexible than phenylalanine because it does not have a large, rigid aromatic group on the side chain. Unlike phenylalanine, *E. coli* K-12 can reportedly utilise alanine as a carbon source upon entry into stationary phase (Yang *et al.*, 2015).

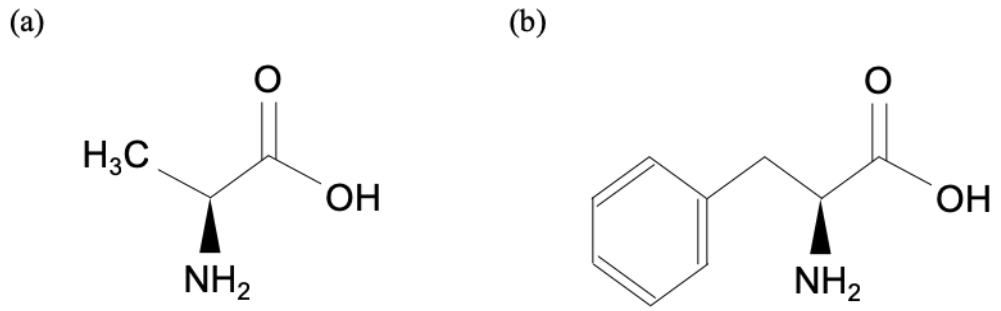

Figure 4.9: The structure of L-alanine and L-phenylalanine.

Alanine (a) and phenylalanine (b) are similarly characterised by nonpolar, hydrophobic, and neutral side chains, which make them insoluble or slightly soluble in water (Lodish *et al*., 2000). Alanine is smaller and more flexible than phenylalanine because it does not have a large, rigid aromatic side chain.

In order to determine if the effect on PHL644 is specific to phenylalanine, alanine was supplemented and optical density and curli expression were measured over time. The *csgB::gfp* reporter (pJLC-T) was transformed into PHL644 and transformants were grown in 500 mL conical flasks containing M63+ minimal medium with either no supplement, 10 mM L-phenylalanine, or 10 mM L-alanine at 26 °C and 70 rpm shaking. Samples were taken over 7 hours and again at 24 hours and analysed by flow cytometry and spectrophotometry. The mean green fluorescence (*csgB*) and the optical density (OD_{600}) were measured (Fig. 4.10).

The addition of alanine did not affect curli expression, while as before the addition of phenylalanine increased curli expression between hours 5 and 7. After 24 hours, curli expression was similar amongst all conditions. Conditions with alanine had the highest optical density at hour 3, but values were similar to conditions with phenylalanine. Between hours 4 – 7 phenylalanine had the greatest optical density and alanine had second greatest. After 24 hours, phenylalanine had the greatest optical density while flasks supplemented with alanine were similar to the control. It is known that *E. coli* will preferentially metabolise glucose over alanine, and it can be presumed based on previous experiments that the cells would not consume all of the glucose between 4 – 7 hours. Thus, it is likely that between hours 4 – 7 alanine was not metabolised by the cells and did not stimulate any growth advantages. These results indicate that potentially the addition of alanine and phenylalanine cause an increase in optical density, but only specific properties of phenylalanine increase curli expression in PHL644 (section 4.3.9). It was then decided that before investigating and testing the properties of these amino acids to first test the effect of phenylalanine on biofilm accumulation.

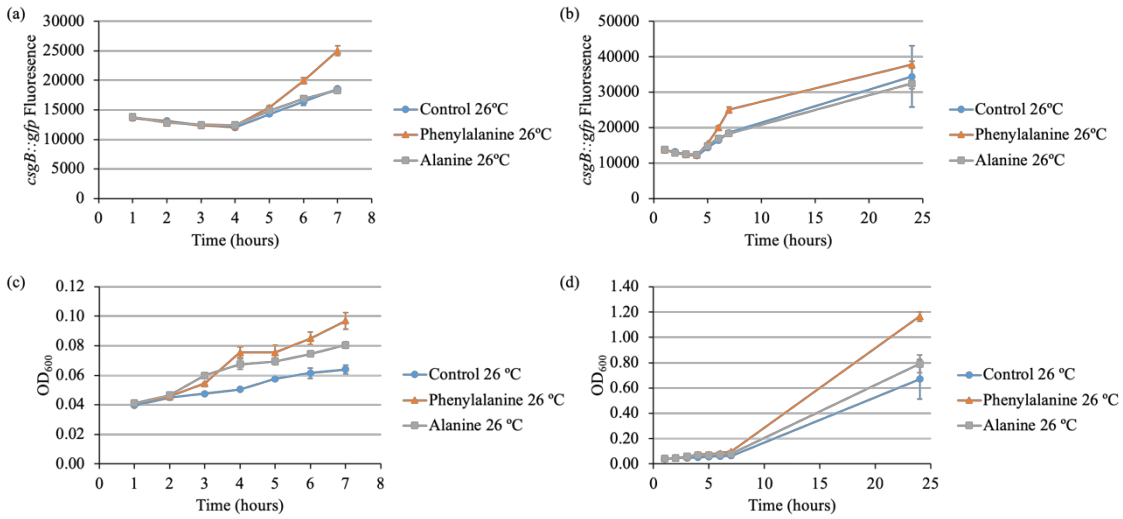

Figure 4.10: The effect of phenylalanine and alanine on curli expression.

E. coli PHL644 transformed with a *csgB::gfp* fusion reporter (pJLC-T) was grown in flasks containing M63+ minimal medium with no supplement or either 10 mM phenylalanine or 10 mM alanine at 26 °C and 70 rpm shaking. All conditions were tested in duplicate. Samples were taken over 24 hours and analysed by flow cytometry and spectrophotometry. Mean green fluorescence representing *csgB* promoter activity hours 1 – 7 (a), hours 1 – 25 (b), and OD_{600} hours 1 – 7 (c) and hours 1 – 24 (d) were measured. The addition of phenylalanine caused in increase in optical density from hours 3 – 24 greater than both alanine or the control, although curli expression was higher than other conditions hours 6 and 7 and were similar to other conditions by hour 24.

4.3.8 The addition of phenylalanine at 30 °C increases biofilm accumulation

Previous crystal violet analysis of biofilm accumulation by Leech asserted that both an optimal temperature adequately supporting bacterial growth as well as curli formation is necessary for maximal biofilm accumulation (Leech, 2017). Knowing this, cultures supplemented with phenylalanine were tested at both 26 °C and 30 °C for their effect on biofilm accumulation because both temperatures increased curli expression at different time points between hours 4 – 7. It's also important to note that flasks supplemented with phenylalanine grown at 30 °C had the greatest optical density. *E. coli* PHL644 was grown in the Duran Bottle method containing M63+ minimal medium with or without 10 mM phenylalanine at either 26 °C or 30 °C and 70 rpm shaking. Samples were grown for 3 days before microscope slides with attached biofilm were washed with PBS and analysed by crystal violet assay. Optical density (OD_{585}) of the crystal violet dye representing biofilm accumulation was measured (Fig. 4.11).

The addition of phenylalanine grown at 30 °C resulted in more biofilm biomass than any other conditions, while the biofilm biomass of cultures with phenylalanine grown at 26 °C were similar to controls. This possibly indicates that both the increase of curli formation caused by the addition of phenylalanine and the increase of optical density caused by incubation at 30 °C are important in biofilm formation. It is important to note that the sensitivity of the crystal violet assay is limited, and minute differences between biofilm accumulation may not be detected. Knowing that the addition of phenylalanine increases optical density and curli expression which increases biofilm accumulation, it was decided to investigate properties of phenylalanine and how those properties may increase curli expression and/or optical density.

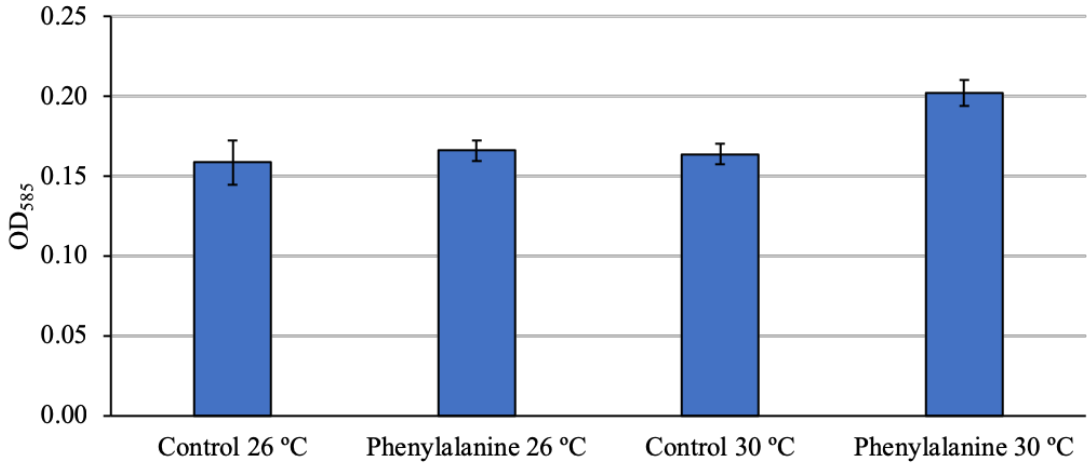

Figure 4.11: The effect of phenylalanine and temperature on biofilm accumulation.

E. coli PHL644 was grown in the Duran Bottle method containing M63+ minimal medium with no supplement or 10 mM phenylalanine at either 26 °C or 30 °C and 70 rpm shaking. All conditions were tested in duplicate. Samples were grown for 3 days before microscope slides comprising biofilm were washed with PBS and analysed by crystal violet assay. Optical density of the crystal violet dye representing biofilm accumulation was measured (OD_{585}). The addition of phenylalanine at 30 °C had more biofilm biomass than any other conditions, possibly indicating that this temperature is optimal for curli expression and cell concentration which may both be important in biofilm formation. However, crystal violet analysis is relatively insensitive and results should be confirmed by confocal microscopy, which was performed in section 4.3.9.

4.3.9 L-phenylalanine may form amyloid fibrils

As previously discussed in section 1.2.2.1, amyloids, such as curli, are a type of protein that can aggregate and have been linked to neurodegenerative diseases, such as Alzheimer's disease (Chapman *et al.*, 2002; Chiti and Dobson, 2006; Eisenberg and Jucker, 2012). Furthermore, amyloid proteins are characterised by their ability to self-assemble into β-sheet-rich fibres which can be measured by polymerised Thioflavin T (ThT), an amyloid-binding dye (Sleutel *et al.*, 2017). Research of neurological diseases such as phenylketonuria caused by phenylalanine accumulation, revealed phenylalanine self-assembles into similar amyloid-like fibrils which aggregate (Adler-Abramovich *et al.*, 2012). However, investigations into the effect of amino acids on biofilm formation revealed that the addition of D-amino acids reduced biofilm formation in some bacteria (Kolodkin-Gal *et al.*, 2010; Hochbaum *et al.*, 2011; Xing *et al.*, 2015).

Further work with phenylalanine by Singh *et al.* revealed that L-phenylalanine self-assembles into amyloid fibres which is measurable by light scatter and ThT polymerisation, but an D/L-phenylalanine mixture formed flakes that solidified from the solution (Singh *et al.*, 2015a). Additionally, it was revealed that preformed aggregates of L-phenylalanine are able to "seed" other L-phenylalanine solutions which then aggregate more quickly. The observation of a seeding effect by amyloid protein has been reported in other research (Hu *et al.*, 2009; Burwinkel *et al.*, 2018). Recall from section 1.3.4 that the CpxAR pathway consists of an inner membrane protein CpxA, which is stimulated by envelope stress and high osmolarity conditions (Dong *et al.*, 1993; Jubelin *et al.*, 2005). It has been hypothesised that proteins are susceptible to denaturing during envelope stress and high osmolarity and thus these denatured proteins also stimulate CpxA so the cascade will repress production and export of proteins like CsgA (Raivio and Silhavy, 1997). Furthermore, Prigent-Combaret *et al*. purported that

CpxA can be stimulated by curlin accumulation, which would induce the CpxAR cascade and repress curli expression (Prigent-Combaret *et al.*, 2001). Once stimulated, CpxA phosphorylates CpxR which then binds upstream of CsgBA and blocks expression of *csgBA* and the binding of positive regulators, like CsgD. It could be theorised that because pre-assembled CsgA can seed curli formation, L-phenylalanine fibres may be able to seed CsgA assembly into curli faster in PHL644 producing a gradient of CsgA exiting the cell (Wang *et al.*, 2006; Wang, Hammer and Chapman, 2008). The lack of CsgA in the envelope would not be able to stimulate the CpxAR pathway; subsequently, *csgBA* would no longer be negatively affected and more *csgB* expression could occur (Fig. 4.12) (Prigent-Combaret *et al.*, 2001). It could also be

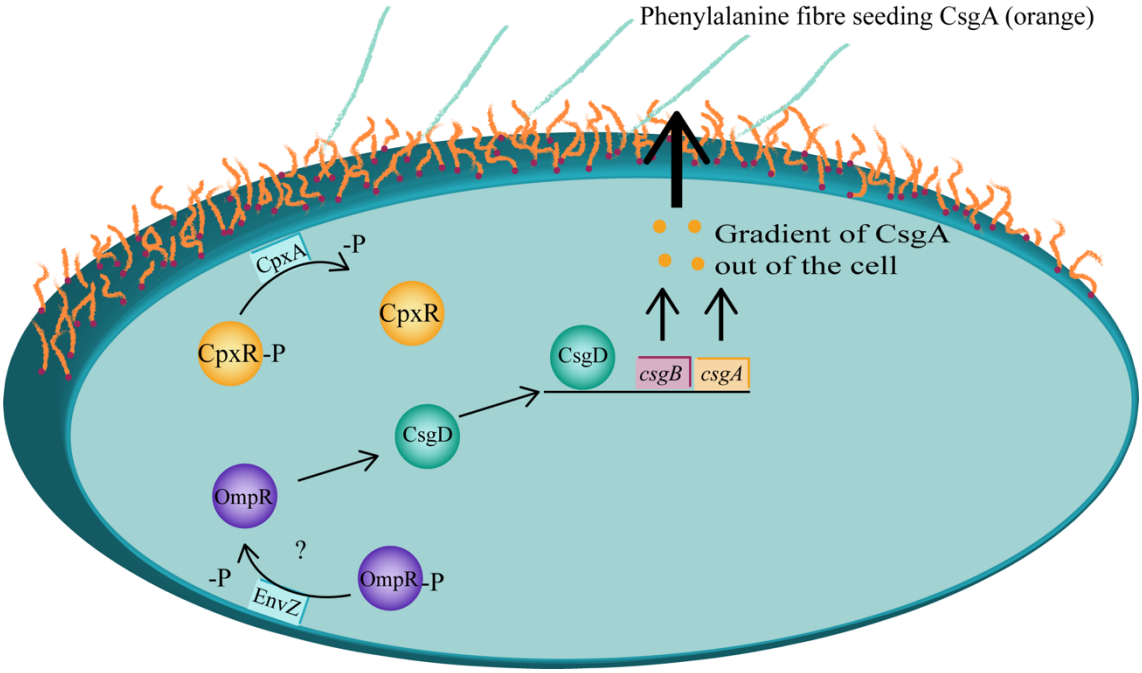

Figure 4.12: A figure theorising L-phenylalanine seeding CsgA thus increasing curli expression.

It is theorised that because L-phenylalanine has amyloid-like characteristics and form fibres (blue lines) they are able to "seed" curli formation (orange). A gradient of CsgA leaving the cell means curlin is not able to induce the CpxAR pathway. CpxA switches to phosphatase activity and dephosphorylates CpxR which can no longer repress *csgBA*. It is unknown if EnvZ/OmpR is also stimulated by curlin as is the CpxAR pathway.

hypothesised that phenylalanine may induce other stress factors, such as the global stress response RpoS, which would increase CsgD and thus *csgBA* expression. Additionally, it was hypothesised that similar to light scattering assays at 450 nm by Singh *et el.*, L-phenylalanine could be self-assembling in the medium like a scaffold and seeding curli formation which scatters light and causes in increase in optical density (OD_{600}) in both *E. coli* K-12 strains PHL644 and MG1655 (Singh *et al.*, 2015a). Thus, the amyloid fibre self-assembly and seeding effect by L-phenylalanine may causing an increase in optical density (OD_{600}), increased agglutination and increased *csgB* expression observed previously. It was decided to test this hypothesis by studying the effect of D/L-phenylalanine on curli expression in *E. coli* K-12.

In order to determine if L-phenylalanine is "seeding" curli fibres in *E. coli* K-12, it was decided to test if a mixture of D/L-phenylalanine (which reportedly does not produce fibres) would attenuate the increase of curli expression observed when supplementing with L-phenylalanine. While Singh *et al*. showed by SEM that D-phenylalanine can form fibres, there is data that D-amino acids can become incorporated in the cell membrane and disrupt surface proteins, like amyloid, in biofilms and thus result in dispersal and reduced biofilm formation (Kolodkin-Gal *et al.*, 2010; Hochbaum *et al.*, 2011; Singh *et al.*, 2015a). Additionally, it was shown by Xing *et al*. that *E. coli* grown in mineral medium with D-tyrosine had less surface proteins, likely because D-tyrosine decreased protein secretion in the cell, which reduced the cell's ability to adhere to surfaces (Xing *et al.*, 2015). The *csgB::gfp* reporter (pJLC-T) was transformed into PHL644 and transformants were grown in 500 mL conical flasks containing M63+ minimal medium with either 10 mM D-phenylalanine, 10 mM L-phenylalanine, or an equal parts mixture of 10 mM D-phenylalanine and 10 mM L-phenylalanine at 30 °C and 70 rpm shaking. Samples were taken over 8 hours and again at 24 hours and

analysed by flow cytometry and spectrophotometry. The mean green fluorescence (*csgB*) and the optical density (OD_{600}) were measured (Fig. 4.13).

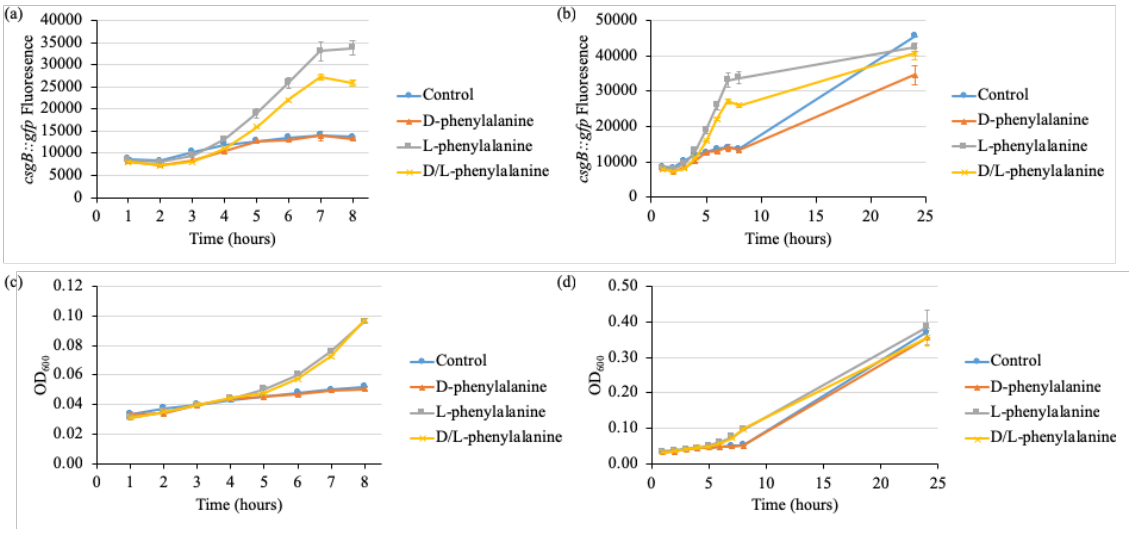

Figure 4.13: The effect D-phenylalanine, L-phenylalanine and D/L-phenylalanine on curli expression.

E. coli PHL644 transformed with a *csgB::gfp* fusion reporter (pJLC-T) was grown in flasks containing M63+ minimal medium with no supplement or either 10 mM L-phenylalanine, 10 mM D-phenylalanine or 10 mM L-phenylalanine and 10 mM D-phenylalanine at 30 °C and 70 rpm shaking. All conditions were tested in duplicate. Samples were taken over 8 hours and again at 24 hours and analysed by flow cytometry and spectrophotometry. Mean green fluorescence representing *csgB* promoter activity hours 1 – 8 (a), hours 1 – 24 (b), and OD_{600} hours 1 – 8 (c) and hours 1 – 24 (d) were measured. The addition of L-phenylalanine increased curli expression and optical density, while D-phenylalanine did not affect curli expression or optical density. The addition of D/L-phenylalanine had an attenuated effect on curli expression compared to L-phenylalanine, but increased the optical density similarly to L-phenylalanine.

As observed previously between hours 1 – 4, all conditions expressed curli similarly. At hour 4, conditions supplemented with L-phenylalanine started to increase curli expression. It was observed between hours 4 – 8 that conditions with L-phenylalanine had the greatest curli expression, while conditions with D/L-phenylalanine also increased curli expression but not as much as the conditions with L-phenylalanine. Despite reports that D-phenylalanine forms fibres, D-phenylalanine did not increase curli expression (Singh *et al.*, 2015a). This could be due to enantiomeric differences between D- and L-phenylalanine fibres, which may prevent D-phenylalanine from seeding CsgA or influencing response or regulatory pathways that induce RpoS or CsgD and increase *csgBA*. After 24 hours, conditions without phenylalanine had the greatest curli expression, followed by conditions with L-phenylalanine and then D/L-phenylalanine. D-phenylalanine had the lowest curli expression. As before, the addition of L-phenylalanine increased the optical density (OD_{600}) at hour 5. The addition of D/L-phenylalanine also increased the optical density (OD_{600}), but not as much as L-phenylalanine. After 24 hours all conditions had similar optical densities (OD_{600}).

From this data, it's possible that D/L-phenylalanine produced flakes as previously reported by Singh *et al*. and had reduced amyloid fibre formation which reduced the hypothesised seeding effect on PHL644 curli (Singh *et al.*, 2015a). While an equal ratio of 10 mM concentrations of L- and D-phenylalanine were supplemented, perhaps future experiments could titrate the addition of D-phenylalanine to test the attenuation effect on curli expression and optical density. While there was a greater attenuation of curli expression, it's possible that fibre formation (OD_{600}) was also similarly attenuated but the formation of flakes was measured by the spectrophotometer at 600 nm or the presence of bacterial cells reduced the sensitivity of detecting flake formation. It was decided to visualise the effect of D/L-amino acids on PHL644 biofilm formation by confocal microscopy.

4.3.10 Visualisation of the effects D/L-phenylalanine on biofilm formation

Previously, the addition of L-phenylalanine increased both curli expression and optical density between hours 4 – 7 and had similar values to the control after 24 hours. Work by Singh *et al.* indicated that L-phenylalanine can self-assemble into amyloid fibres while D/L-phenylalanine produces flakes instead (Singh *et al.*, 2015a). Other reports have shown that D-amino acids reduce biofilm formation by interfering with amyloid fibres during adhesion (Kolodkin-Gal *et al.*, 2010; Hochbaum *et al.*, 2011; Xing *et al.*, 2015). The addition of D/L-phenylalanine mixture to PHL644 potentially indicated an attenuation effect on curli expression compared to L-phenylalanine, while D-phenylalanine did not increase optical density or curli expression compared to the control. It was decided to supplement again with either 10 mM D-phenylalanine, 10 mM L-phenylalanine, or an equal parts mixture of 10 mM D-phenylalanine and 10 mM L-phenylalanine and then visualise the biofilm and curli expression by confocal microscopy after 21 hours because biofilms could not be sufficiently visualised before 21 hours. The *csgB::gfp* reporter (pJLC-T) was transformed into PHL644 and transformants were grown using the Duran Bottle method containing M63+ minimal medium with either no supplement, 10 mM D-phenylalanine, 10 mM L-phenylalanine, or equal parts 10 mM D-phenylalanine and 10 mM L-phenylalanine at 30 °C and 70 rpm shaking. After 21 hours, microscope slides with attached biofilm were washed with PBS and *csgB* activity (curli expression, shown in green) was visualised by confocal microscopy. Representative single-plane images of the biofilm as well as the side-view images are shown with scale bars (Fig. 4.13).

The addition of D-phenylalanine reduced the thickness of the biofilm to ~15 μm, which had flatter morphology and less mushroom structures compared to the control (~29 μm). The biofilm thickness of the control was similar to L-phenylalanine

(~27 μm) which also had similar mushroom cloud morphology to one another. Biofilms generated in the presence of D/L-phenylalanine had similar thickness (~28 μm) compared to L-phenylalanine and the control, but had less defined morphology and reduced *csgB* fluorescence. The results align with previous reports that the addition of D-amino acids interfere with amyloid protein and biofilm formation, as the addition of D-phenylalanine reduced biofilm thickness (Kolodkin-Gal *et al.*, 2010; Hochbaum *et al.*, 2011; Xing *et al.*, 2015). While the biofilms of the control, L-phenylalanine and D/L-phenylalanine had similar biofilm thickness (~27 – 29 μm), only the addition of L-phenylalanine had the typical structures and mushroom-cloud morphology of *E. coli* K-12 biofilms. Future work may include titrating the addition of D-phenylalanine to L-phenylalanine for visualisation by confocal microscopy. It's possible the flake-formation of D/L-phenylalanine is tuneable and can attenuate both curli expression and biofilm formation. While L-phenylalanine produced a similar biofilm to the control, the data supports that this amino acid is potentially able to increase curli expression, increase agglutination, and increase biofilm biomass which may be important in future *E. coli* K-12 work. There are also implications that the amyloid characteristics of L-phenylalanine allows for seeding of bacterial amyloid, which has yet to be published in research.

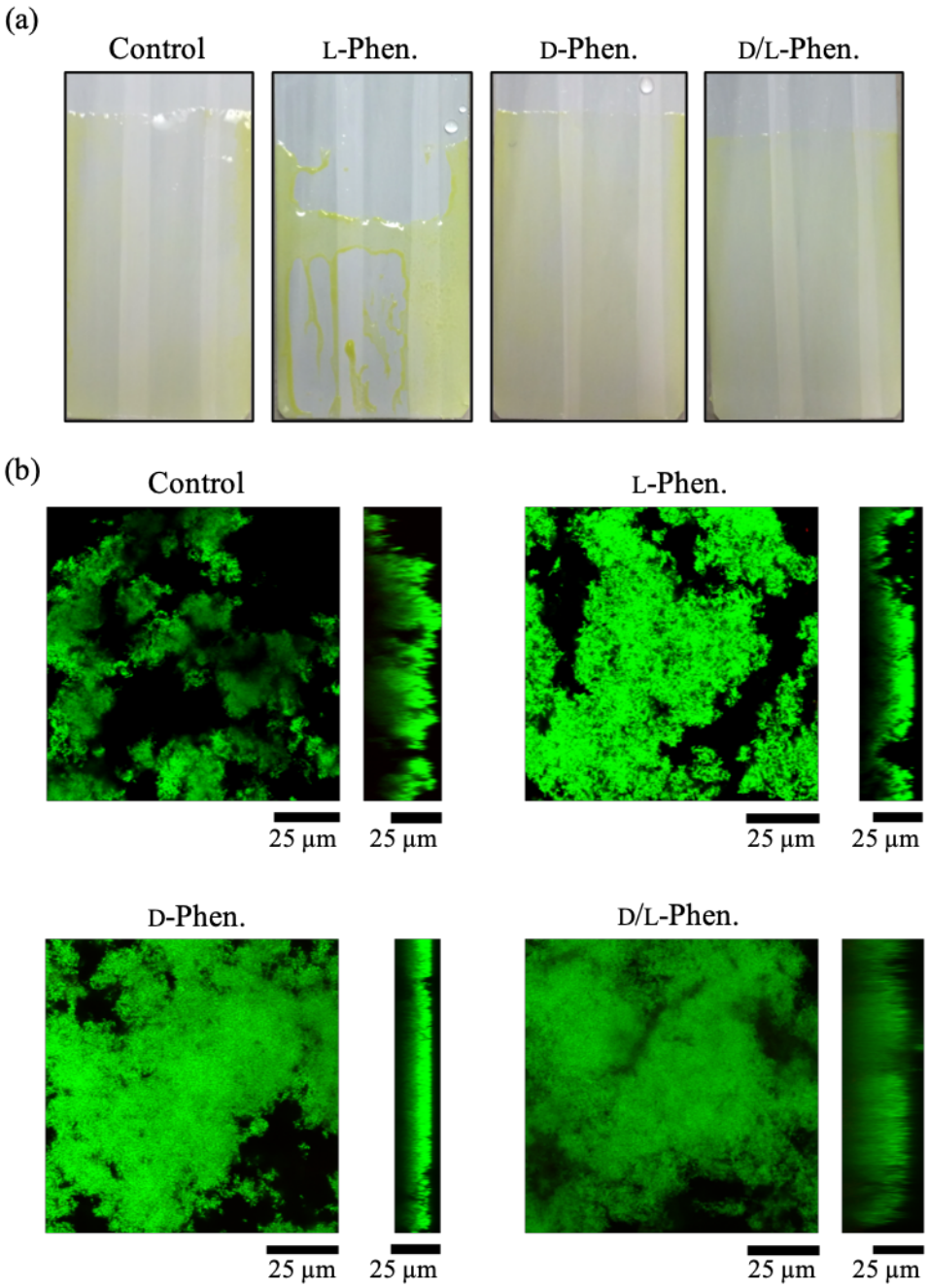

Figure 4.14: Visualisation of the effect of D/L-phenylalanine on curli expression and biofilm formation by confocal microscopy.

E. coli PHL644 transformed with a *csgB::gfp* fusion reporter (pJLC-T) was grown using the Duran Bottle method containing M63+ minimal medium with either 10 mM L-phenylalanine, 10 mM D-phenylalanine or 10 mM L-phenylalanine and 10 mM D-phenylalanine at 30 °C and 70 rpm shaking for 21 hours. All conditions were tested in duplicate. Microscope slides containing biofilm were washed with PBS (a) before being visualised by confocal microscopy for *csgB* activity (curli expression, shown in green). Representative single-plane images from each biofilm as well as the side-view are shown with scale bars (b). Side-view is oriented left (top) to right (bottom).

4.4 Conclusions

Previous unpublished work from the Overton laboratory investigated ways to decrease intracellular tryptophan in *E. coli* K-12 biofilms constitutively producing tryptophan (pSTB7 plasmid) so biofilm accumulation could increase and protect the biocatalytic properties while not affecting overall tryptophan levels in the system (Tsoligkas *et al.*, 2011; Shimazaki *et al.*, 2012; Tong *et al.*, 2016). A marked increase in biofilm accumulation was measured by crystal violet assay in previous unpublished work in the Overton laboratory when phenylalanine was supplemented to growth medium containing PHL644 transformed with pSTB7. This phenomenon was further investigated in this chapter.

By use of a *csgB::gfp* reporter in this work, it was revealed that 10 mM phenylalanine increased curli expression and optical density (OD_{600}) of PHL644 (overexpresses curli) between the hours 4 – 7. This was not observed when supplementing with 0.1 mM phenylalanine, 0.1 mM tryptophan, or 0.1 mM tyrosine; although due to their relative insolubility greater concentrations of tryptophan and tyrosine could not be tested. The increase in optical density (OD_{600}) was also observed when MG1655, an *E. coli* K-12 strain not overexpressing curli, was supplemented with 10 mM phenylalanine, but no increase in curli expression was observed. Upon investigating glycerol as a potential carbon source in PHL644, which does not have the same curli expression inhibition from cAMP-CRP regulation as glucose, it was noted that conditions with phenylalanine with glucose had better curli expression than glycerol without phenylalanine between hour 3 – 6 and had similar curli expression after 24 hours. Phenylalanine with glucose also produced higher optical densities than conditions with glycerol without phenylalanine after hour 4 and at hour 24. Regardless of the addition of phenylalanine, PHL644 did not grow and did not increase the

expression of curli if glucose was not present, indicating that phenylalanine was not being used as a carbon source. This supported other studies that *E. coli* K-12 cannot metabolise phenylalanine for use as a carbon or nitrogen source (Ogata, Uchiyama and Yamada, 1967). Future work should measure the concentration of phenylalanine in the growth medium before and after experiments to observe if the increase in curli expression or optical density is a result of phenylalanine being degraded into proteins that are incorporated into the cell.

After confirming that phenylalanine was not being used as a carbon source, the effect on agglutination was tested. The addition of phenylalanine caused cells to agglutinate faster, indicating phenylalanine not only increased curli expression (*csgB*) but it also increased factors that cause agglutination, such as functional curli. Although it's important to note there are other surface adhesins that cause agglutination, such as Ag43, which also may play a role. Before testing the effect of curli on biofilm accumulation by crystal violet assay, shaking and temperature with phenylalanine addition were optimised and alternative amino acids needed to be tested. It was decided the addition of 10 mM phenylalanine and 70 rpm shaking at either 26 °C or 30 °C was optimal for curli expression. The addition of alanine was tested on PHL644 because it is in the same class of hydrophobic amino acids as phenylalanine and concentrations of 10 mM could be supplemented for accurate comparison to phenylalanine. While alanine increased the optical density between hours 4 – 7, phenylalanine had a greater optical density between hours 4 – 7 and at hour 24. Curli expression increased in the conditions with phenylalanine between hours 5 – 7, but alanine did not illicit a change in curli expression. Upon testing the effect of phenylalanine at either 26 °C or 30 °C on biofilm accumulation by crystal violet assay, it was determined that adding phenylalanine at 30 °C produced the most biofilm biomass.

Investigations into the structure of phenylalanine revealed a report that L-phenylalanine can self-assemble in amyloid fibres measurable by both light scattering and ThT binding assays which are capable of seeding unassembled L-phenylalanine (Singh *et al.*, 2015a). The report also concluded that the fibre formation of L-phenylalanine can be arrested by the addition of D-phenylalanine, and this D/L-phenylalanine mixture formed flakes instead of fibres. According to research, D-amino acids disrupt biofilm formation and it was hypothesised that D-phenylalanine would not increase curli expression even though it forms fibres like L-phenylalanine on the SEM (Kolodkin-Gal *et al.*, 2010; Hochbaum *et al.*, 2011; Xing *et al.*, 2015). It was further hypothesised that the increase in optical density and curli expression was a direct result of L-phenylalanine's ability to self-assemble and seed CsgA during *E. coli* K-12 curli formation. This seeding effect could reduce the amount of CsgA available in the cell, which would be unable to then stimulate the CpxAR pathway. The CpxAR pathway negatively regulates *csgBA*, so reducing the induction of this pathway would increase curli expression. In this same vein, phenylalanine may be increasing global stress responses, such as RpoS, or other regulatory networks, such as CsgD, which increase *csgBA*.

Upon testing these theories with the *csgB::gfp* reporter, D-phenylalanine did not increase curli expression and equal parts D/L-phenylalanine showed attenuated curli expression in comparison to L-phenylalanine. The addition of D/L-phenylalanine increased optical density similarly to L-phenylalanine, but it's possible the purported flake formation by D/L-phenylalanine was also measured on the spectrophotometer at OD_{600} and skewed the results. Future work should titrate the addition of D-phenylalanine to L-phenylalanine and test the tuneable nature of D/L-phenylalanine on curli expression. Future work should also include measuring the cultures by dynamic light scattering instead of spectrophotometer which would elucidate information about

the size of the particles or polymers in the medium and help understand if flakes or fibres are being formed, or by a scanning electron microscope to visualise fibre formation. Finally, this effect was also visualised by confocal microscopy. Supporting previous data that D-amino acids reduce biofilm formation, *E. coli* K-12 biofilms grown with D-phenylalanine were less thick (15 μm) and had flatter, less defined structures and altered morphology compared to the control (Kolodkin-Gal *et al.*, 2010; Hochbaum *et al.*, 2011; Xing *et al.*, 2015). The addition L-phenylalanine had similar thickness (~28 μm) and mushroom cloud morphology as the control. The biofilm grown with D/L-phenylalanine did not have reduced thickness but did have reduced *csgB* fluorescence and less-defined morphology. Future work should also include titrating the addition of D-phenylalanine to L-phenylalanine in the Duran Bottle model and potentially optimising a tuneable system that can increase or decrease curli expression and biofilm formation measurable by the confocal microscope or other sensitive methods.

While L-phenylalanine produced a similar biofilm to the control, the data supports that this amino acid is potentially able to increase curli expression, agglutination, and biofilm biomass which may be important in future *E. coli* K-12 biofilm work. There are also implications that the amyloid characteristics of L-phenylalanine allows for seeding of bacterial amyloid. This is an exciting discovery of amyloid cross-seeding function, which has potential to be an innovative and novel approach to tuneable curli expression and biofilm accumulation in *E. coli* K-12.

5 CHARACTERISATION AND OPTIMISATION OF PELLICLE FORMATION

5.1 Introduction

In order to investigate biofilms for biocatalytic applications, a biofilm generation model needed to be developed, optimised, and tested for its reproducibility. During initial work to generate physically robust *Escherichia coli* K-12 biofilms in a new biofilm growth model, a biofilm was observed floating at the air-liquid interface, commonly referred to as a pellicle. While solid surface-attached *E. coli* K-12 biofilms are fairly well-studied, less is known about the *E. coli* K-12 pellicles, because unlike other species where pellicle formation is well-characterised, such as *Bacillus subtilis*, there are few reports of *E. coli* K-12 pellicles in the literature. Pellicle formation has been proposed by Armitano *et al*. to occur in one of two ways after the cells localise to the air-liquid interface by motility or passive movement: the bacteria either form floating aggregates on the air-liquid interface (like rafts) and grow together, or the bacteria forms on the solid surface of the growth vessel wall and then grows across the air-liquid interface (Armitano, Méjean and Jourlin-Castelli, 2014). Confluent growth across the entire air-liquid interface occurs as cells continue to replicate and the pellicle matures by secreting EPS and increasing in thickness (Fig.1.2).

The few reports of *E. coli* pellicle formation focus mainly on uropathogenic *E. coli* (UPEC) and enteropathogenic *E. coli* (EPEC) and there are significant differences between the two (Lim, May and Cegelski, 2012; Wu *et al.*, 2012, 2013). While not all pellicle-forming EPEC strains produce curli, curli are a required component of UPEC pellicles. It has been proposed that the mat-like network of curli in pellicles may confer greater support and structural strength (Hung *et al.*, 2013; Wu *et al.*, 2013; Eberly *et al.*, 2017). Additionally, unlike *E. coli* K-12, UPEC produce cellulose as an extracellular polymeric substance (EPS) in the matrix which strengthens the pellicle (Hung *et al.*, 2013). It has also been reported that a number of other EPEC strains produce cellulose

which makes the pellicle matrix more elastic, rather than the rigid structure curli without cellulose provides (Weiss-Muszkat *et al.*, 2010; DePas *et al.*, 2014). The transcription factor CsgD is a master regulator responsible for both curli and cellulose production in UPEC and EPEC strains (Hammar *et al.*, 1995; Zogaj *et al.*, 2001; DePas *et al.*, 2014; Hufnagel *et al.*, 2016). The composition of *E. coli* pellicle matrices is not abundant in literature; however, it is proposed that they are similar to solid surface-attached biofilms and are comprised of curli, PNAG and colanic acid (Hung *et al.*, 2013). Other strains, such as *P. aeruginosa*, have been shown to form pellicles comprised of adhesions and various polysaccharides (Laverty, Gorman and Gilmore, 2014; Limoli, Jones and Wozniak, 2015).

Curli expression of *E. coli* in terms of location within the growth vessel and within the pellicle matrix was investigated as well as the individual EPS components poly-N-acetyl glucosamine (PNAG) and colanic acid. The results were compared to *E. coli* K-12 biofilms and pellicles formed by other bacterial species and discussed in terms of the current knowledge.

5.2 General protocol

The beginning of this study details the development of a new *E. coli* K-12 biofilm growth model capable of generating replicable biofilm and it was during this work an *E. coli* K-12 pellicle was observed. In order to characterise *E. coli* pellicles and how they are formed, a pellicle growth model was developed and pellicle formation was photographed over time using an Apple iPhone 5S. PHL644 (overexpresses curli) and MC4100 (parental strain of PHL644 which does not overexpress curli) are two bacterial strains used in the majority of this work. A motility assay was developed using 0.3% semi-solid LB agar plates to determine motility of different strains. From the motility assay, a hypermotile variant of PHL644 (termed PHL644h) was isolated and used in the following work as well. The genome of PHL644h was sequenced and discussed (full summary of results in Appendix 1). Mechanical forces (orbital shaking and motility) were investigated for their effect on pellicle formation. Additionally, curli expression was studied by use of a *csgB::gfp* reporter on both the flow cytometer and the confocal microscope. Curli expression was analysed in terms of location of the cells within the pellicle growth vessel and within the pellicle matrix. The pellicle matrix was also examined for the presence and location of the EPS components poly-N-acetyl glucosamine (PNAG) and colanic acid by the use of stains that were analysed on the confocal microscope. The thickness and morphology of the pellicle was also revealed and discussed.

5.3 Characterisation of visualisation of pellicles

5.3.1 Initial work: optimisation and design of a biofilm model

While the Duran Bottle method (Fig. 3.1) is a sufficient technique for generating replicable biofilms, it has many limitations. Biofilm studies must be executed for each condition a minimum of two replicates. Screening multiple biofilm replicates by use of bulky 100 mL Duran bottles is difficult due to space limitations. Furthermore, post-handling in the Duran Bottle method is time-consuming as each bottle contains only one biofilm for analysis by a single technique. However, a benefit of this model is that the microscope slide carrying biofilm can be used for a number of analytical techniques, including microscopy. In order to circumvent the space and time limitations of the Duran Bottle method, while keeping the benefit of using a wide variety of analytical procedures, it was proposed to optimise the current model or design a new method to generate biofilms.

The first route to optimise the Duran Bottle method was to make the set-up process more efficient and less wasteful. All aspects of the physical model, such as the glass Duran bottle and bung can be re-used and re-autoclaved for multiple experiments, although re-using bungs more than two or three events is not encouraged as the bung tends to change shape once autoclaved. The PTFE-wrapped microscope slides comprising biofilm, however, are not reusable and wrapping the slides with PTFE tape is time-consuming. It was proposed to instead use PTFE board cut to the same dimensions as the microscope slides which can be re-used in each experiment, thus removing waste and laborious preparation. In order to test the new method, biofilm accumulation on both PTFE-wrapped microscope slides and 4 mm thick PTFE boards (cut to the same dimensions as the 76 mm x 26 mm microscope slides) were measured

by crystal violet analysis and compared. *E. coli* K-12 PHL644 was grown in quadruplicate using the Duran Bottle method containing M63+ minimal medium with either PTFE-wrapped microscope slides or PTFE board at 30 °C and 70 rpm shaking for three days. The relative accumulation of biofilm was measured by crystal violet analysis and the OD_{585} was measured (Fig 5.1). The PTFE-wrapped slides had accumulated on average 2.7 times more biofilm than the PTFE board. Although the surface topography was not measured by scanning electron microscopy or other methods, it was hypothesised that the PTFE tape produced a rougher surface than the PTFE board, and thus biofilm grew better on the PTFE-wrapped slides. It was decided to continue to use the PTFE-wrapped slides for biofilm generation using the Duran Bottle method, while new designs for a model that reproducibly formed biofilms were developed.

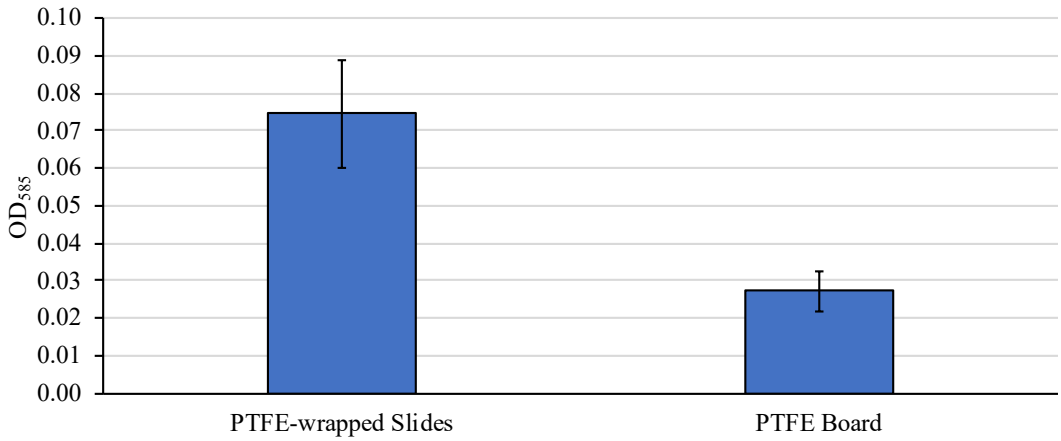

Figure 5.1: Biofilm accumulation on PTFE-wrapped slides versus PTFE board.

Work to optimise the Duran Bottle method first attempted to remove time-consuming preparation and the consumables (microscope and PTFE tape) by replacing these items with 4 mm thick PTFE board cut to the same dimensions as the slide which could be re-used in experiments. *E. coli* K-12 PHL644 was grown using the Duran Bottle method in quadruplicate with either a PTFE-wrapped slide or PTFE board on which biofilm could grow at 30 °C and 70 rpm shaking for three days. After three days, crystal violet analysis was performed and measured relative biofilm accumulation (OD_{585}). Bars representing ± standard deviation from the mean value of four independent cultures are shown. The PTFE-wrapped slides grew more biofilm than the PTFE board.

The new biofilm generation design consisted of a 500 mL conical flask with a biofilm-generation insert. The insert consisted of a sterile 20 mL Falcon tube with three PTFE-wrapped microscope slides affixed to the outside on which biofilm could grow (Fig. 5.2a). The top of the tube was inserted into and attached to a bung so the entire biofilm-generation insert functioned as a single piece and could be placed into the 500 mL conical flask (not shown) before sterilisation. After initial experiments, the 20 mL Falcon tube was changed to an inverted 25 mL glass test tube with PTFE-wrapped microscope slides affixed to the outside, as this could be sterilised and reused thus reducing unnecessary plastic waste. During trial experiments with the inverted glass test tube, biofilm was observed growing on the outside and inside of the glass test tube (Fig. 5.2b and Fig. 5.2c).

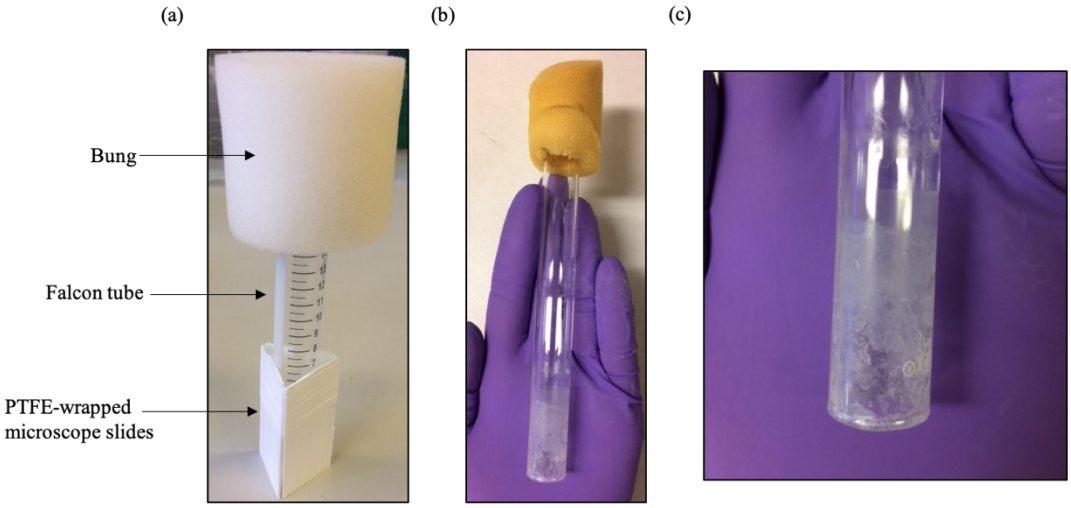

Figure 5.2: Biofilm generation flask insert and biofilm accumulation on test tube.

Work to develop a new biofilm-generation model first consisted of a 20 mL plastic Falcon tube. The top of the tube was inserted into a bung, while the bottom had three PTFE-wrapped microscope slides affixed to the outside (a). Later versions used an inverted 25 mL glass test tube with PTFE-wrapped slides affixed to the outside (not shown). The entire insert was placed into a 500 mL conical flask containing media and then autoclaved before testing. During work to develop a new biofilm generation model, biofilm was observed on the glass test tube of the flask insert once PTFE-wrapped microscope slides were removed (b). An enlarged photograph of the biofilm on the test tube is shown (c).

While work by Vidal and colleagues showed that PHL644 will grow on glass, previous work in the Overton laboratory showed that PTFE-wrapped glass accumulated 7 times more biofilm than glass (Vidal *et al.*, 1998; Leech, 2017). Furthermore, biofilms grown on glass in previous work were roughly 25 μm thick and were not observable to the naked eye. Upon further visual inspection of the test tube in Fig. 5.2, it appeared more biofilm formed on the inside of the inverted glass test tube than the outside of the test tube. It was then decided to measure the accumulation of biofilm on the inside versus the outside of the inverted test tube by crystal violet assay. It was speculated that conditions inside the inverted test tube, such as specific oxygen limitations, could be altering biofilm formation. A glass tube with the same internal diameter as the 25 mL glass test tube was employed, except the tube was bunged on the top to allow normal oxygen flow compared to the limited oxygen found inside the inverted test tube. The effect of the "closed" test tube (oxygen limiting) versus the "open" tube (oxygen is similar to the rest of the flask) was tested on biofilm accumulation on the inside and outside of the tubes.

In order to test the accumulation of biofilm formed on the inside versus the outside of an inverted test tube and in different oxygen environments, PHL644 was grown in 500 mL conical flasks in duplicate containing M63+ medium at 30 °C and 70 rpm shaking for three days with either an "open" tube in the flask or a "closed" inverted test tube. Crystal violet analysis was performed first on the inside and then the outside of the test tube and OD_{585} was measured (Fig. 5.3).

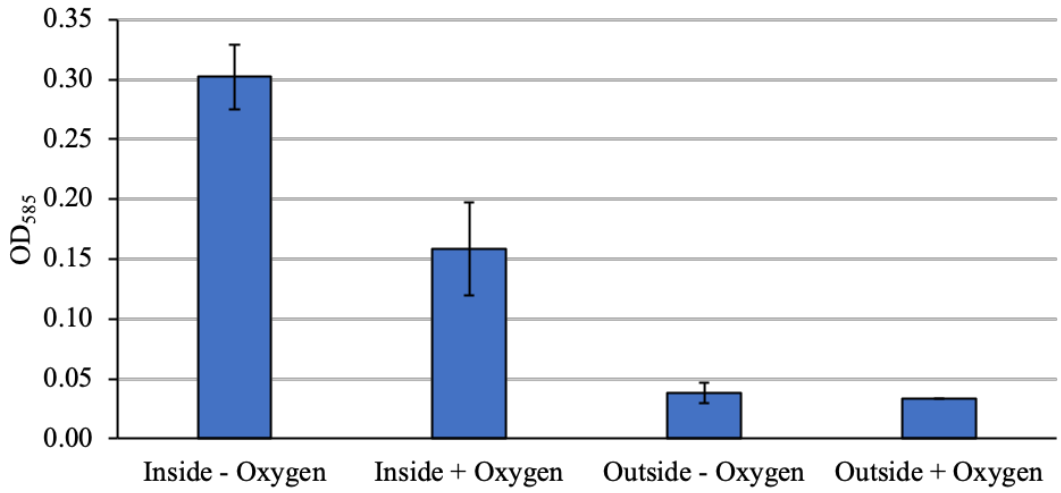

Figure 5.3: Biofilm accumulation inside and outside the inverted glass test tube.

E. coli K-12 PHL644 was grown in 500 mL flasks in duplicate containing M63+ minimal medium at 30° C and 70 rpm shaking for three days with either an (a) "open" tube in the flask (+oxygen) or a "closed" inverted test tube (-oxygen). Crystal violet analysis was performed on both the inside and outside of both "open" (+oxygen) and "closed" tubes (-oxygen), and OD_{585} was measured. Bars representing ± standard deviation from the mean value of two independent cultures are shown. The inside of the tube had more biofilm accumulation than the outside, and the "closed" inverted test tube which limited oxygen (-oxygen) had more biofilm accumulation than the tube that was "open" and had similar access to oxygen (+oxygen) as the rest of the tube. Bars representing ± standard deviation from the mean value of two independent cultures are shown.

The inside of the tube had more biofilm accumulation than the outside, and the ”closed” inverted test tube which limited oxygen (-oxygen) had more biofilm accumulation than the tube that was ”open” and had similar access to oxygen (+oxygen) as the rest of the 500 mL conical flask. Potentially, both the physical conditions of the inside of the tube (such as the tube curvature and/or the increased surface interaction of the cells in a confined space) and the oxygen limitation of the inverted test tube provided an environment which induced biofilm formation. It was during this work that a floating biofilm, also known as a pellicle, was observed (Fig. 5.4). The rest of the chapter focused on elucidating pellicle formation of *E. coli* K-12. The role of curli and motility, the structure of the pellicle and presence of extracellular polymeric substances (EPS) was investigated.

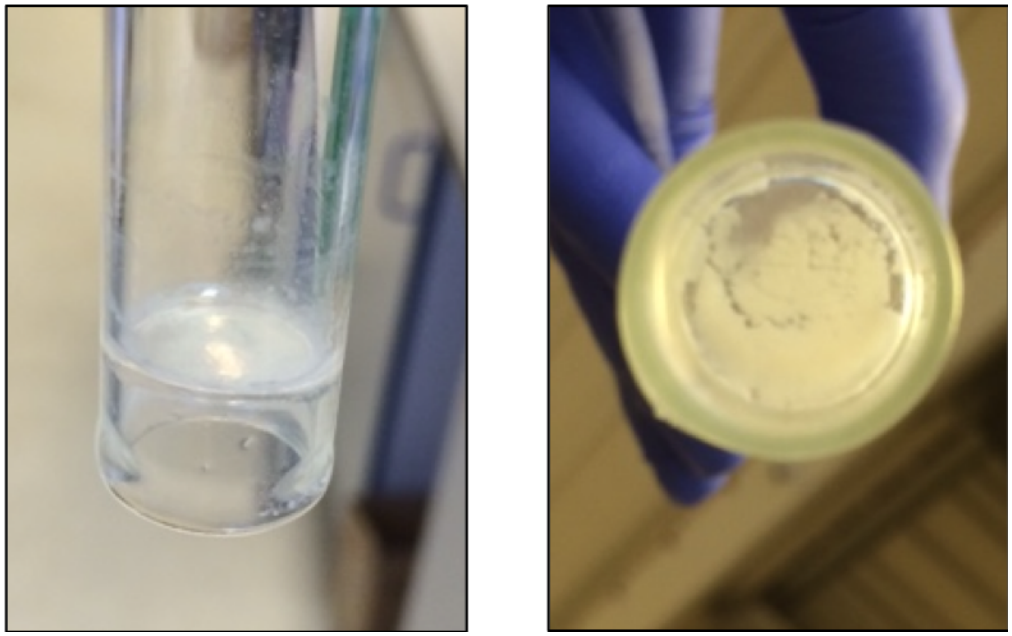

Figure 5.4: Initial observation of a pellicle.

Above is a photograph of a floating biofilm, also known as a pellicle.

5.3.2 *E. coli* K-12 form pellicles over time

During work exploring biofilm growth in test tubes, biofilms were observed floating at the air-liquid interface, also referred to as a pellicle (Fig. 5.4). Macroscopic observation revealed that the floating *E. coli* K-12 pellicle was heterogeneous and appeared to vary in thickness, morphology, and structure (Fig. 5.5a). In order to understand a timescale of how *E. coli* K-12 forms a pellicle, PHL644 was grown in upright test tubes containing M63+ minimal medium at 30 °C with 70 rpm shaking over six days and pellicle formation was photographed over time (Fig. 5.5b). The test tubes were bunged to maintain sterility and medium was not replenished. Variability in morphology was observed as the pellicles formed over time from small floating aggregates to confluent layers of growth at the air-liquid interface. After two days of growth, cells had begun to aggregate into "raft-like" formations at the air-liquid interface. After four days of growth, aggregates had begun to grow together into a thin pellicle. By day six, confluent pellicle growth was observed. It was also noted that cells formed solid surface-attached biofilms on the test tube walls at the air-liquid interface, and some cells settled to the bottom of the tube forming a sediment. Next, MC4100, the parental strain of PHL644 which does not overproduce curli, was tested for its ability to form a pellicle.

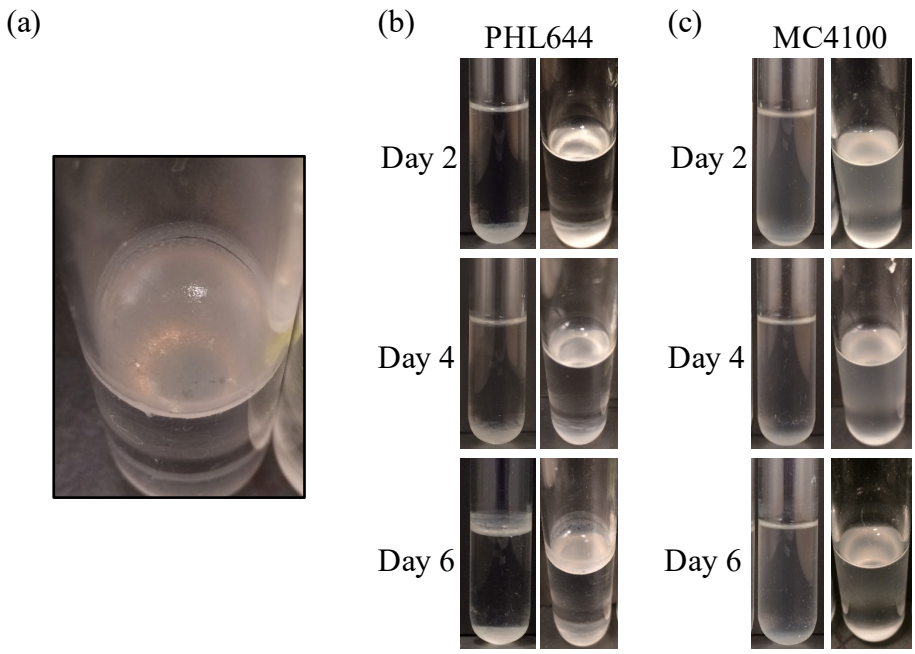

Figure 5.5: Timescale of *E. coli* K-12 pellicle formation.

E. coli K-12 PHL644 and MC4100 were grown in test tubes containing M63+ minimal medium at 30 °C for six days with shaking at 70 rpm. A pellicle was observed at the surface of the medium which reveals macroscopically that a pellicle has varying morphology and thickness (a). Timescale of *E. coli* PHL644 pellicle formation (b). After two days growth, aggregates, or "rafts" formed at the surface of the medium. After four days, aggregates had grown together. At day six confluent pellicle growth was observed. Timescale of *E. coli* MC4100 pellicle formation (c). After six days, *E. coli* MC4100 (which does not overexpress curli) was not able to form a pellicle.

5.3.3 Pellicle formation requires curli

In order to understand the role of curli in pellicle formation, the parental strain of PHL644, MC4100 (which does not overproduce curli), was tested in the test tube model. MC4100 was grown in test tubes containing M63+ minimal medium at 30 °C and 70 rpm shaking over six days and pellicle formation was photographed (Fig. 5.5c). While PHL644, which overproduces curli, was able to generate a pellicle, its parental strain MC4100 (synthesising less curli) was not. This suggests that curli are important for pellicle formation in *E. coli* K-12. The significance of curli in *E. coli* K-12 pellicle formation is supported by UPEC pellicle research. Andersson *et al*. identified chemical inhibitors of curli fibre assembly *in vitro* which also prevented pellicle formation in the UPEC strain UTI89; a similar effect was observed in the same study with purified *E. coli* CsgE protein, a chaperone which inhibits curli fibre assembly (Andersson *et al.*, 2013). Another study showed the deletion of *csgA* (encoding a curlin subunit) prevented UTI89 pellicle formation altogether (Hung *et al.*, 2013). Wu and coworkers used varying concentrations of DMSO and ethanol to optimise curli production and thus optimised UTI89 pellicle formation (Wu *et al.*, 2012). They also used a surfactant, Tween20, to interfere with curli interactions at the air-liquid interface and found curli and their strong entanglements were essential for pellicle formation in UTI89 (Wu *et al.*, 2013). Similarly to UPEC, pellicle formation requires curli in the atypical EPEC strain DMS9 (Weiss-Muszkat *et al.*, 2010).

In addition to curli, other surface organelles are important for pellicle formation. Work with Gram negative pellicles indicated that motility and the presence of flagella play an important role in initiating pellicle formation (Armitano, Méjean and Jourlin-Castelli, 2014). Next, the role of motility on pellicle formation was investigated.

5.3.4 Pellicle formation is partially driven by motility

To investigate the role of motility in pellicle formation, first a motility assay was developed on semi-solid LB agar plates which was used to measure motility of *E. coli* K-12 strains. It was through the motility assay that a hypermotile variant of PHL644 was isolated from semi-solid LB agar plates (referred to from now as PHL644h). The motility of PHL644, PHL644h, and MC4100 (parental strain) was measured by use of the motility assay, and the strains were motile, hypermotile, and non-motile, respectively (Fig. 5.6).

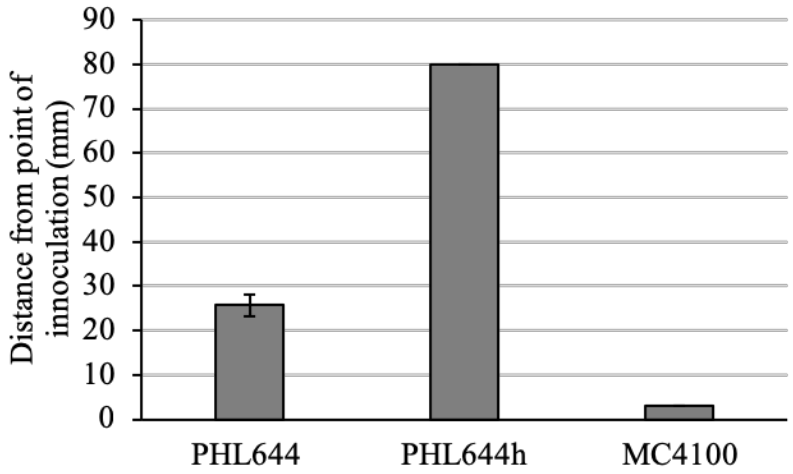

Figure 5.6: Motility of PHL644, PHL644h, and MC4100.

A motility assay was developed on semi-solid LB agar plates. From the motility assay, a hypermotile variant of PHL644 (referred to as PHL644h) was isolated. *E. coli* strains PHL644, PHL644h, and MC4100 were grown in LB at 30 °C for 24 hours with shaking at 150 rpm, then point inoculated on semisolid agar in duplicate and grown for 24 hours at 30 °C. The diameter of the zone of growth was measured. They were motile, hypermotile, and nonmotile, respectively. Bars representing ± standard deviation from the mean value of two independent measurements are shown.

To observe the effect of motility on pellicle formation, test tubes containing M63+ minimal medium and either PHL644 or PHL644h were grown at 30 °C and 70 rpm and pellicle formation was photographed and compared (Fig. 5.7). After two days, PHL644h had formed a thin pellicle and distinct solid surface-attached biofilm on the test tube at the air-liquid interface, while PHL644 had simply formed aggregate "rafts." After four days, PHL644h had grown into a fully confluent pellicle of visibly greater thickness than PHL644. At day six, PHL644 had formed a fully confluent pellicle, while the PHL644h pellicle had continued to grow thicker. By day eight, both PHL644 and PHL644h had grown pellicles of substantial bulk.

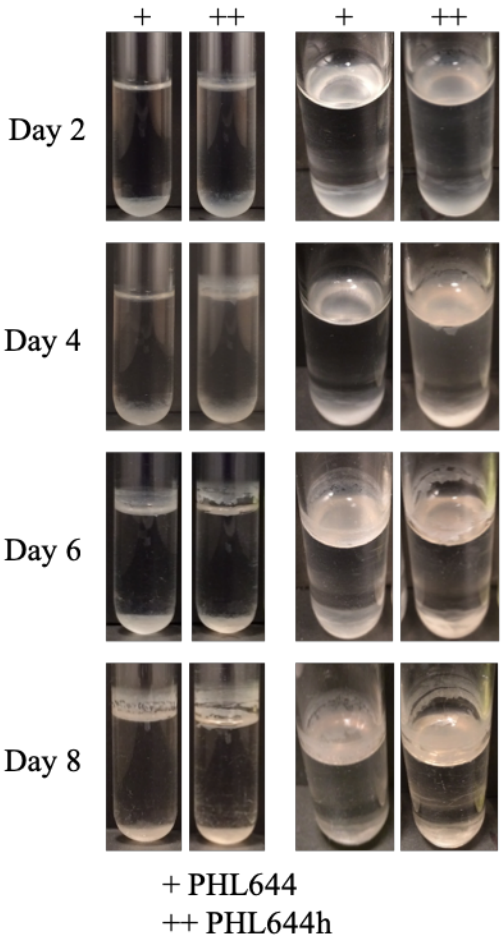

Figure 5.7: Hypermotile PHL644 forms a pellicle faster.

PHL644 and PHL644h were grown in test tubes containing M63+ minimal medium at 30 °C and 70 rpm shaking and pellicle formation was photographed and compared. The hypermotile PHL644 variant (PHL644h) formed a pellicle faster and the pellicle was thicker.

It was proposed that the mutation that allowed for hypermotility of PHL644h may also confer a difference in growth which enhanced PHL644h pellicle formation. In order to ensure the difference between PHL644 and PHL644h is not associated with a difference in growth, the growth rates of PHL644 and PHL644h were measured. PHL644 and PHL644h were grown in 500 mL conical flasks containing LB medium and the OD_{600} was measured over 1 – 8 hours and again at hour 24 (Fig. 5.8). The growth rates of PHL644 and PHL644h were similar over 24 hours, suggesting that PHL644h's enhanced pellicle formation was not an effect of a growth benefit or defect. Although motility and biofilm formation are interlinked, it was important to understand the mutation in PHL644h that allowed for enhanced pellicle formation (Pesavento *et al.*, 2008). Therefore, the PHL644 and PHL644h genomes were sequenced and compared (Appendix 1). Notably, a number of mutations were located in the Ras prophage and DLP12 prophage, which have been linked to motility and biofilm formation (Liu *et al.*, 2015). To further understand the role of motility and mobility on pellicle formation, the role of shaking was tested.

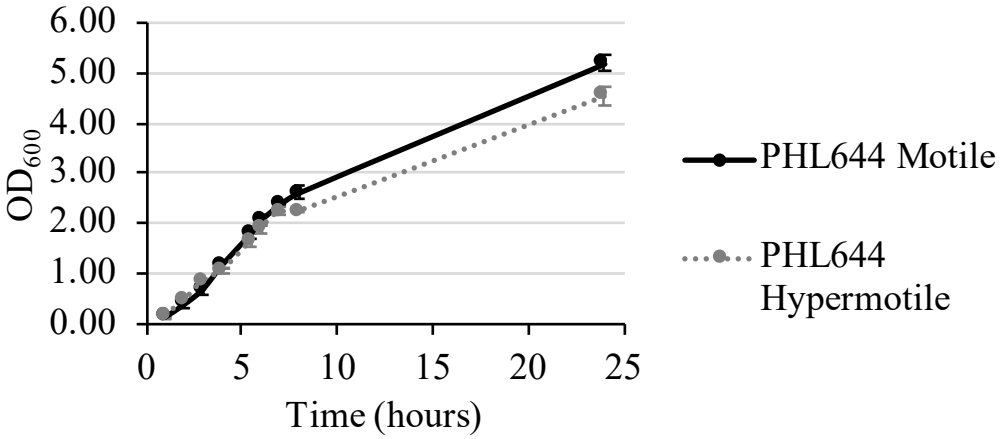

Figure 5.8: Growth curve of PHL644 and PHL644h in LB medium over 24 hours.

PHL644 and PHL644h were grown in duplicate in 500 mL flasks containing LB medium at 30 °C and 70 rpm shaking for 24 hours. The OD_{600} was measured hours 1 – 8 and again at hour 24 and compared. The growth rates of both PHL644 and PHL644h were similar and the mutation that allowed for hypermotility of PHL644h did not cause a change in growth rate.

5.3.5 Shaking contributes to pellicle formation

Localisation of bacteria to the air-liquid interface during the initial stage of pellicle formation has been shown to be influenced by both motility and passive movement, for example by shaking or Brownian motion (Frymier *et al.*, 1995; Hölscher *et al.*, 2015). To further investigate the role of active motility and passive movement in *E. coli* K-12 pellicle formation, the ability of PHL644 and PHL644h to form pellicles without shaking was assessed. PHL644 and PHL644h were grown in test tubes containing M63+ minimal medium at 30 °C statically for eight days to see if a pellicle was formed (Fig. 5.9a). After eight days, PHL644 was not able to form a pellicle, while PHL644h was able to form a pellicle. To understand the effect of shaking on pellicle formation, PHL644 was grown in test tubes containing M63+ minimal medium at 30 °C and was either incubated statically for eight days, shaken at 70 rpm for one day and then kept static for seven days, or shaken at 70 rpm for eight days (Fig. 5.9b). PHL644 was not able to form a mature pellicle in static conditions after eight days: even though the typical "raft" colonies were observed at the air-liquid interface after 24 hours, pellicle maturation did not proceed. However, PHL644 tubes shaken at 70 rpm for 24 hours and then placed at static conditions for another 7 days were able to form a pellicle, albeit one less substantial than tubes shaken for eight days. This suggests that shaking enables cells to move to the air-liquid interface, "seeding" pellicle formation.

Motility is a significant part of biofilm formation and it is clear that motility and passive movement play important roles in *E. coli* K-12 pellicle formation (Pratt and Kolter, 1998). Hypermotility reduces the need for passive movement by shaking, and also confers a greater ability to form an *E. coli* K-12 pellicle in less time**.** In other species, motility is not always required to form a pellicle: by mutating different motility genes in *B. subtilis*, Kobayashi revealed that a lack of motility significantly delayed

pellicle formation, but did not prevent it altogether as some cells were able to use other means of passive mobility or Brownian motion to eventually reach the air-liquid interface (Kobayashi, 2007). This evidence suggests that while motility is important and perhaps the simplest and fastest route for the cell to overcome counteractive forces, such as gravity, to reach the air-liquid interface, other forms of movement can localise cells to the interface where they can form a pellicle. To understand the interplay of motility and curli production, it was decided to further investigate the effect of curli overproduction on pellicle formation in the nonmotile strain MC4100.

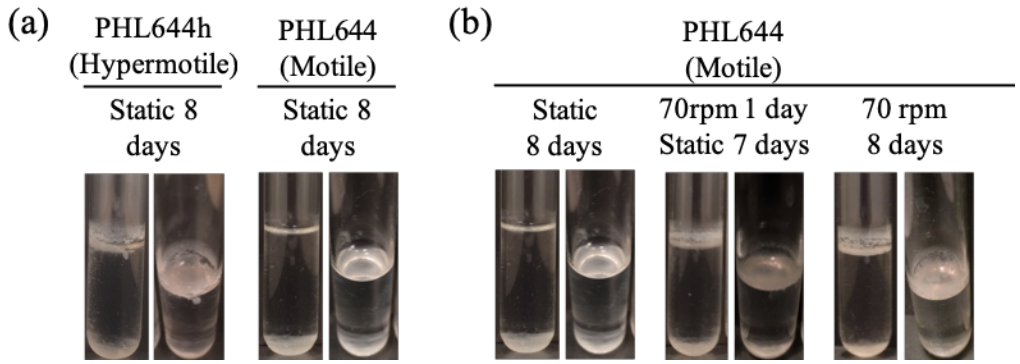

Figure 5.9: Role shaking on pellicle formation.

To test the necessity of shaking on pellicle formation, *E. coli* strains PHL644 and PHL644h were grown in test tubes containing M63+ medium at 30 °C statically for eight days (a). Only PHL644h was able to form a pellicle statically. Next, it was investigated if shaking is necessary for the entire growth period in order to form the pellicle. PHL644 was grown in test tubes containing M63+ minimal medium at 30 °C either: statically; with 70 rpm agitation for one day and then statically for seven days; or with 70 rpm agitation for eight days (b). Shaking is only required for the first 24 hours in order for a pellicle to form.

5.3.6 Curli overproduction in nonmotile MC4100

It is important to note that MC4100 (non-motile and not overproducing curli) cannot form a pellicle even when shaken (Fig. 5.5c), but it is unclear if lack of motility or lack of curli overproduction is the cause. Therefore, a plasmid was used to increase curli expression in MC4100 to dissect this phenomenon. Plasmid pT7-CsgD, which overexpresses the curli master regulator CsgD, was transformed into MC4100; previous work showed that the effect of CsgD overexpression from this plasmid on biofilm formation was comparable to that of the *ompR234* mutation carried in PHL644 in this study (Brombacher *et al.*, 2006). PHL644 is derived from MC4100 and only differs because of the *ompR234* mutation and a *malA* knockout, which does not reportedly affect biofilm formation (Boos and Shuman, 1998). An empty vector, pT7-7, was transformed into MC4100 as a control. A motility assay revealed that MC4100 remained non-motile when transformed with either pT7-CsgD or pT7-7 (data not shown). MC4100 transformed with either pT7-CsgD or pT7-7 were grown in test tubes containing M63+ minimal medium and incubated at 30 °C with 70 rpm shaking and were monitored and photographed over eight days (Fig. 5.10a). MC4100 transformed with the pT7-7 control did not grow a pellicle nor formed aggregates over the eight days. Pellicle growth in cells transformed with pT7-CsgD was not observed until day four, where a thin pellicle could be seen near the rear wall of the test tube (Fig. 5.10b). Aggregate “rafts” were visualised by day six. At day eight a thin pellicle was observed.

Overexpression of curli in MC4100 permitted pellicle formation in shaking conditions despite lack of motility; although, pellicle formation was severely hindered when compared to PHL644 (motile) and PHL644h (hypermotile) pellicle formation. Therefore, to produce a thick, mature pellicle a combination of curli expression, mobility (shaking), and motility are required. Overexpression of curli is required to

form a pellicle and partially reduces the need for motility but not the need for mobility (shaking); shaking is required unless cells are hypermotile.

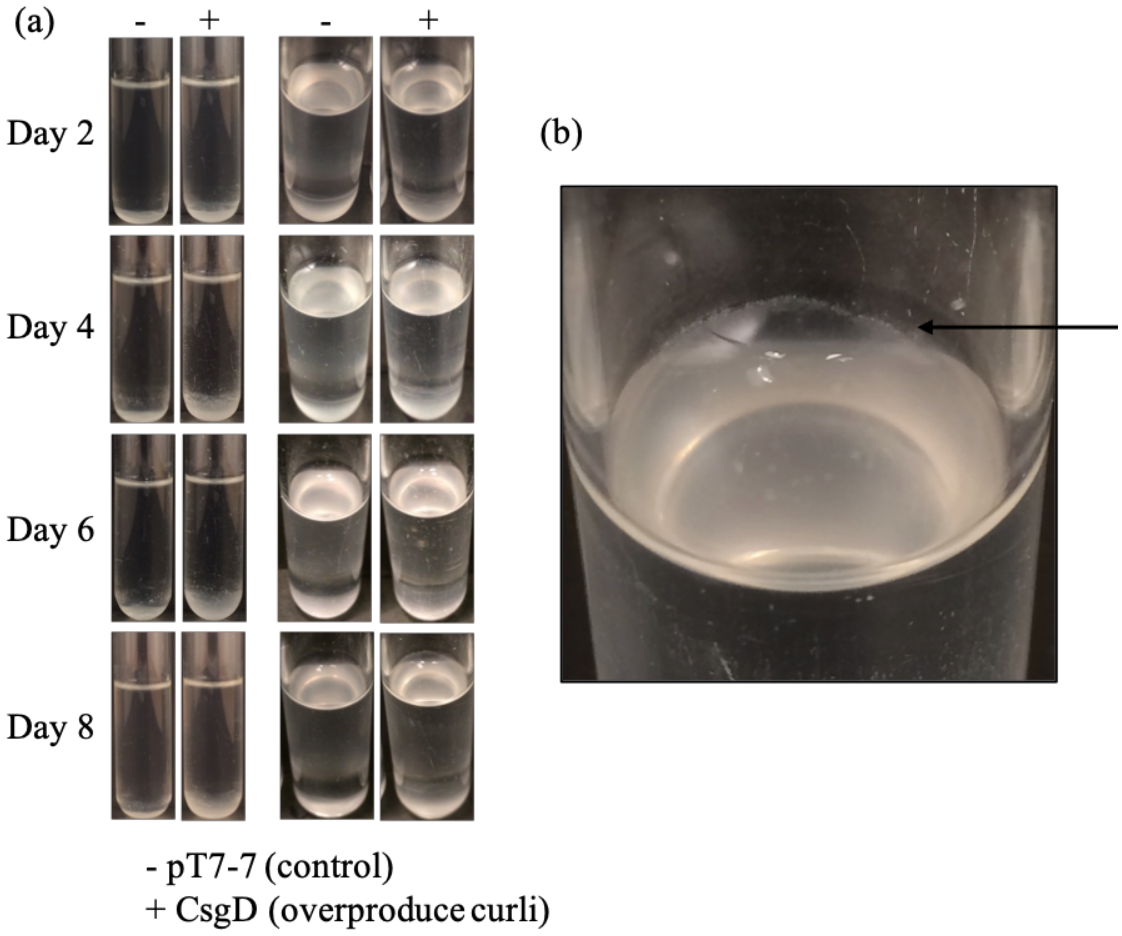

Figure 5.10: The effect of curli overproduction in non-motile MC4100 on pellicle formation.

To test the effect of curli overproduction in MC4100, a nonmotile *E. coli* K-12 strain, MC4100 was transformed with either PT7-CsgD (curli overproduction) or pT7-7 (an empty vector). Transformants were grown in test tubes containing M63+ medium at 30 °C with 70 rpm agitation for eight days. (a) Overexpression of curli produces a thin pellicle. Photograph of day eight pellicle enlarged for detail (b).

5.3.7 Curli formation is regulated based on location in the pellicle growth model

It has been shown previously in this chapter that curli are necessary to form a pellicle in *E. coli* K-12. It is also known that curli expression is regulated by numerous environmental stimuli (Smith *et al.*, 2017). To explore the regulation of curli during pellicle formation, a *csgB::gfp* reporter (pJLC-T) was transformed into PHL644. Transformants were grown in test tubes containing M63+ minimal medium at 30 °C and 70 rpm for one, two or three days. Cells were then extracted from four distinct locations within the tube and analysed by flow cytometry (Fig. 5.11a): air-liquid interface on the tube wall; pellicle; planktonic; and sediment. The mean GFP fluorescence which signifies the expression of *csgB* was evaluated for each location (Fig. 5.11b). After one day, the pellicle and planktonic cells had high levels of *csgB* expression, while the cells at the solid surface of the air-liquid interface and the sediment at the bottom of the tube had lower expression. The sediment cells and cells attached to the tube at the air-liquid interface increased curli expression over three days, while expression in the planktonic and pellicle cells remained consistently high.

(a)

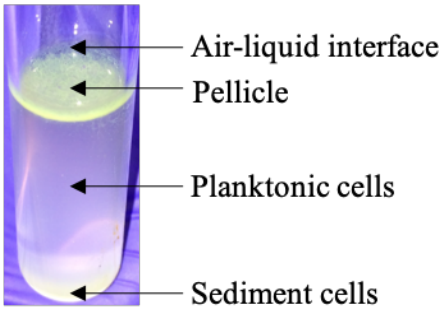

(b)

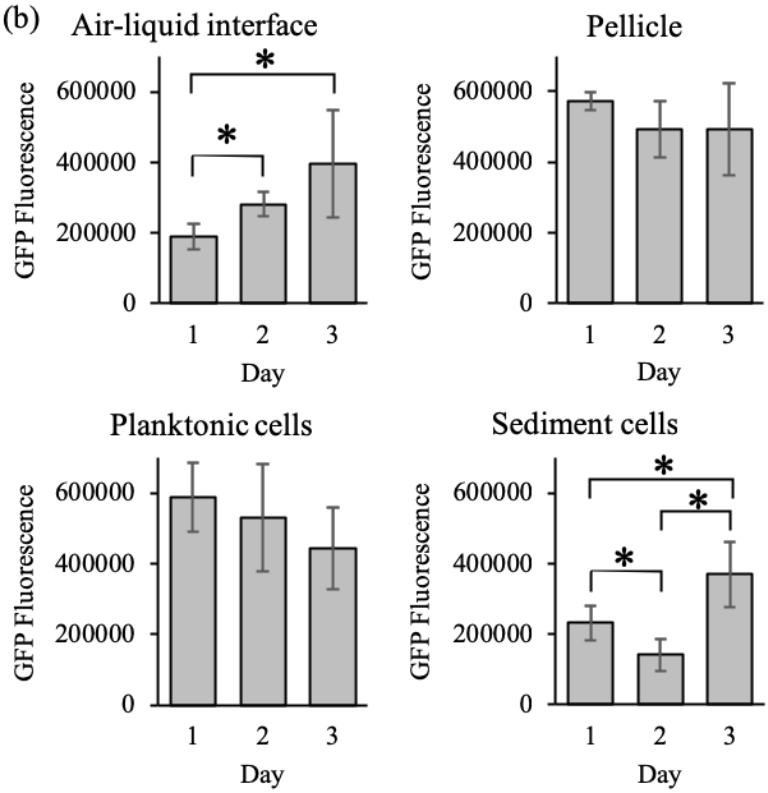

(c)

Comparison	Day 1	Day 2	Day 3
Pellicle to AL	*	*	NS
Pellicle to Planktonic	NS	NS	NS
Pellicle to Sediment	*	*	NS
AL to Planktonic	*	*	NS
AL to Sediment	NS	*	NS
Planktonic to Sediment	*	*	NS

Figure 5.11: Measurement of curli promoter activity in pellicles and other cells.

In order to measure curli promoter activity in four distinct locations in the system, *E. coli* PHL644 pJLC-T (carrying a *csgB::gfp* fusion) was grown in triplicate in M63+ medium at 30 °C with 70 rpm shaking for three days. Samples were taken from four locations (a) and analysed by flow cytometry; mean green fluorescence was measured representing *csgB* promoter activity (b). Bars representing ± standard deviation from the mean value of three independent cultures are shown. Statistical analysis for the comparison of the same location over three days was performed by a paired t test, which is shown as bars on the charts. Statistical analysis for the comparison of different locations for the same day was performed by an unpaired t test of unequal variances, which is shown in the table (c). For all statistics * = $p < 0.05$ while NS = $p > 0.05$.

Curli formation is a highly regulated process in response to a variety of environmental and chemical factors (Evans and Chapman, 2014). Curli expression in response to surface attachment is suggested to be regulated by a three-component pathway: surface attachment is sensed first by outer membrane lipoprotein NIpE, which then activates a two-component regulatory system CpxAR, which represses *csgD* and *csgB* expression and thus reduces curli formation (Prigent-Combaret *et al.*, 2001; Otto and Silhavy, 2002; Barnhart and Chapman, 2006).

This downregulation of curli expression when in contact with a surface is consistent with the *csgB* expression of the cells within the tube after 24 hours; cells attached to the tube wall at the air-liquid interface and in the sediment at the bottom of the tube downregulated their curli expression once attached and had lower expression than planktonic or pellicle cells. However, an increase in *csgB* expression in the surface-attached cells was measured over time, which could be due to the expansion of the biofilm and growth of cells along the surfaces over time (observed in Fig. 5.5b). The expansion of biofilm and sediment would likely require more curli. The lack of solid surface contact in the pellicle and planktonic cells results in relatively high *csgB* expression over the three days as they possibly keep producing curli while awaiting solid-surface attachment. To understand curli expression within the pellicle, it was decided to visualise the cells by confocal microscopy.

5.3.8 Visualisation of pellicle morphology and curli at microscopic levels

To visualise curli production within the pellicle, PHL644 and PHL644h transformed with the pJLC-T (*csgB::gfp* reporter) were grown in test tubes containing M63+ minimal medium at 30 °C and 70 rpm for one to six days. PHL644 pellicles were harvested and mounted onto microscope slides on days two, three, four, and six, while

PHL644h was harvested on days two, three, and four as they grew more quickly than PHL644. Day one was not harvested because pellicle formation was not mature enough. Once mounted on the microscope slide, transformed cells were stained with SYTO 62 (a DNA stain). Pellicles were then analysed by confocal microscopy for the presence of GFP (curli), shown in green, and SYTO 62 (cells), shown in magenta (Fig. 5.12 and Fig. 5.13). Areas of white consist of both GFP and SYTO 62 fluorescence.

For PHL644 and PHL644h, the top, air-facing side of the pellicle tended to be flatter and confluent, while the bottom, medium-facing side was more irregular and formed droplet-like structures. After two days, PHL644 pellicles were thin (ranging from 20 µm – 25 µm in thickness) with thicker regions that resembled early aggregate "raft" that were visually observed during previous experiments. These aggregates tended to have higher curli expression (shown as green), although other areas also expressed curli. At day three, the PHL644 pellicle had become thicker (25 µm – 35 µm in thickness) and more uniform in thickness. Curli were expressed throughout the PHL644 pellicle, although the remnants of areas of high curli expression were still observed. After four days, the PHL644 pellicle had continued growing thicker (ranging from 30 µm – 40 µm in thickness) and was more homogenous in structure. Curli expression at day four was observed throughout the pellicle with patches of higher expression. By day six, pellicles ranged from 40 µm – 50 µm in thickness and curli expression was limited to specific regions within the pellicle, which spanned the thickness of the pellicle top to bottom.

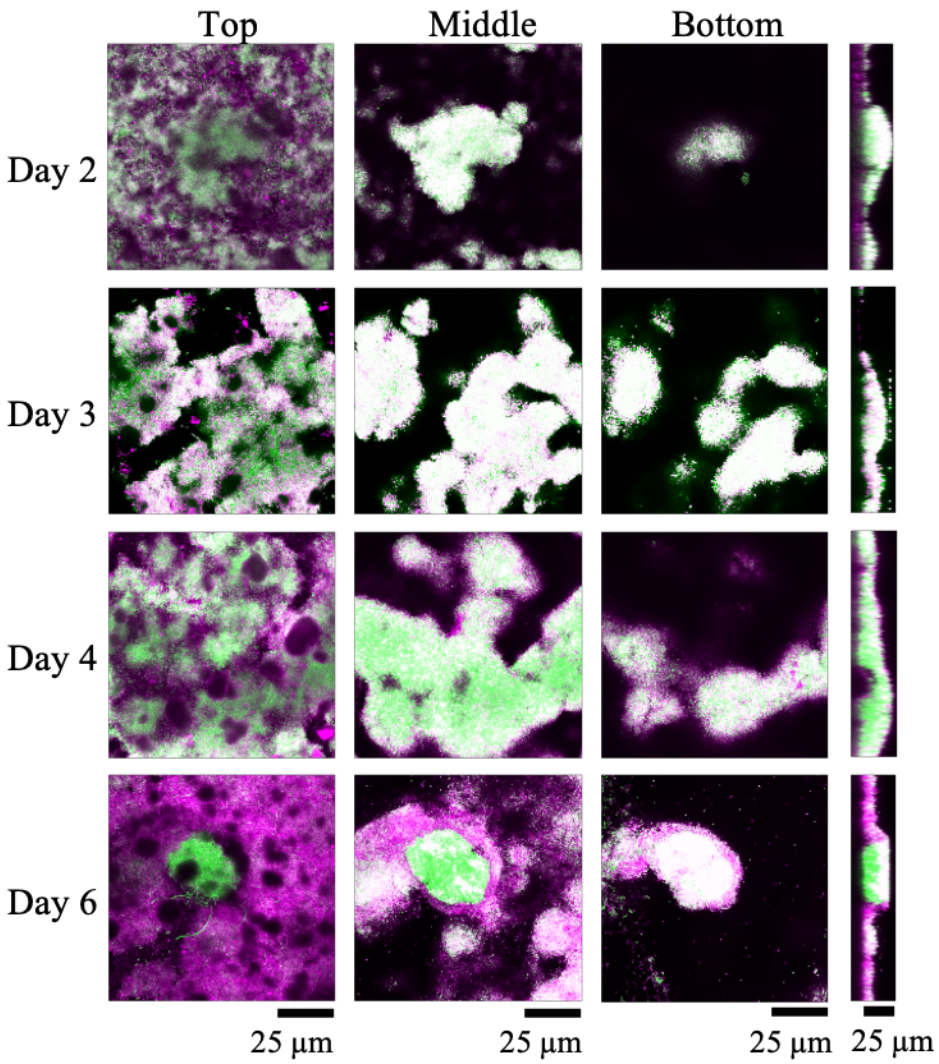

Figure 5.12: Visualisation of PHL644 curli production by confocal microscopy.

E. coli PHL644 pJLC-T was grown in M63+ medium at 30 °C and 70 rpm for six days and pellicles were harvested and stained with SYTO 62 (stains cellular material, shown as magenta). Cells stained with SYTO 62 and GFP-expressing (curli, shown as green) cells were visualised by confocal microscopy on days 2, 3, 4 and 6. Representative single plane images from the top (air-facing), middle, and bottom (media-facing) of each pellicle are shown. Side-view images traversing top (left) to bottom (right) are shown. Scale bars representing 25 µm are shown.

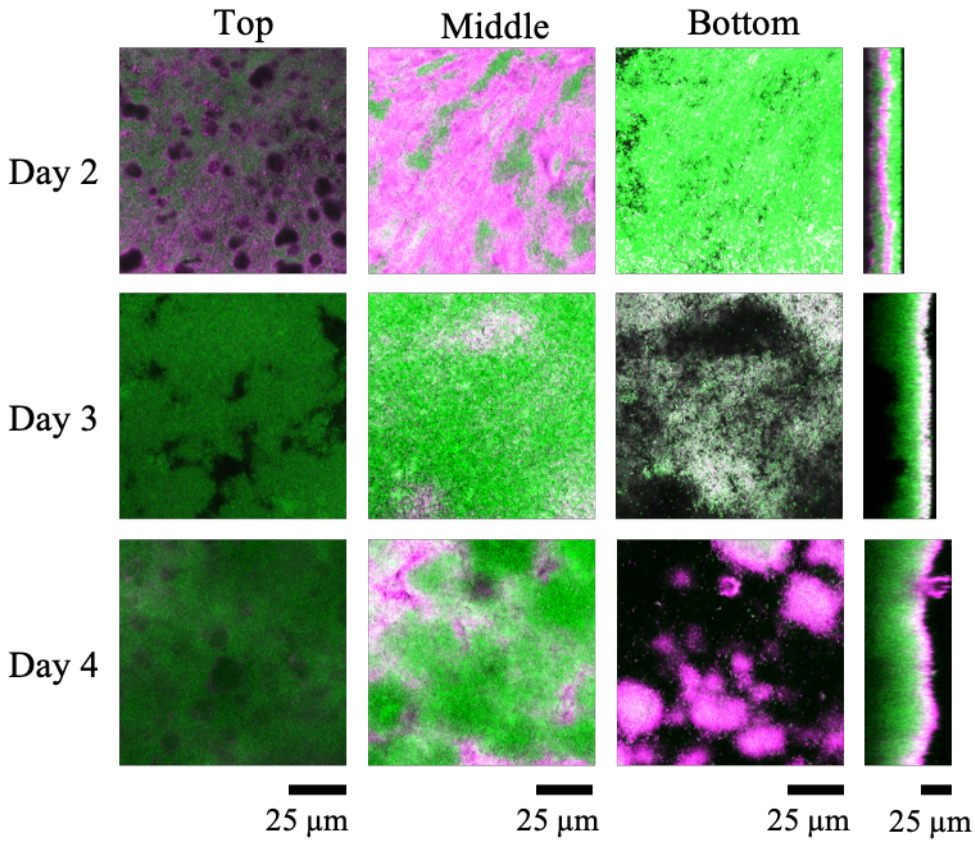

Figure 5.13: Visualisation of PHL644h curli production by confocal microscopy.

E. coli PHL644h pJLC-T was grown in M63+ medium at 30 °C and 70 rpm for six days and pellicles were harvested and stained with SYTO 62 (stains cellular material, shown as magenta). Cells stained with SYTO 62 and GFP-expressing (curli, shown as green) cells were visualised by confocal microscopy on days 2, 3, and 4. Representative single plane images from the top (air-facing), middle, and bottom (media-facing) of each pellicle are shown. Side-view images traversing top (left) to bottom (right) are shown. Scale bars representing 25 µm are shown.

Taken together, curli expression is highly heterogenous within PHL644 pellicles, and changes as the pellicle develops. The PHL644 pellicle thickness is comparable to that of *E. coli* O55 pellicles (Weiss-Muszkat *et al.*, 2010). Additionally, the morphological characteristics of *E. coli* K-12 pellicles observed were also similar to those of UTEC pellicles in a study by Hung *et al*., who observed that three day old pellicles had air-facing sides that were smoother and flatter and liquid-facing sides that were more irregular (Hung *et al.*, 2013). However, the morphology of the top, air-facing side of *E. coli* K-12 pellicles is more complex and not as flat as that observed in UTEC. Unlike UTEC pellicles observed by Hung *et al*., *E. coli* K-12 *csgB::gfp* activity was not reduced on the liquid-facing side, rather curli expression traversed the pellicle from top to bottom. As measured by flow cytometry previously in this chapter (Fig. 5.11), PHL644 curli expression was high during pellicle maturation; although confocal microscopy revealed that high *csgB* expression is confined to patches within the pellicle at early and late stages of development. Amyloid-rich regions within pellicles have been associated with resistance to mechanical stress and it could be postulated that persistent curli production is needed to maintain pellicle form and structure (Wu *et al.*, 2012).

Pellicles formed by PHL644h on day two were thicker (ranging from 30 µm – 40 µm in thickness) and more homogeneous in structure than those of PHL644 at four days of growth (Fig. 5.13); in addition, they did not display the same regulation of curli as PHL644. While PHL644 had specific areas of high curli expression that traversed the pellicle top to bottom much like a column, curli in PHL644h was evenly expressed and tended to be highest at the media-facing side on day two and highest at the air-facing side on day four. By day three, the PHL644h pellicle had a thickness ranging from 35 µm – 50 µm, which grew to roughly 40 µm – 65 µm in thickness by day four. It is possible that because PHL644h pellicles are thicker, they require more curli present

throughout to increase cohesion. Now that curli expression with in the pellicle had been observed, it was decided to investigate other components of the pellicle matrix.

5.3.9 Investigations of pellicle matrix components

To investigate the distribution of the polysaccharide components of poly-β-1,6-N-Acetylglucosamine (PNAG) and colanic acid in the matrix, untransformed PHL644 and PHL644h were grown in test tubes containing M63+ minimal medium at 30 °C with 70 rpm shaking for one to six days. PHL644 pellicles were harvested and mounted onto microscope slides at day two, three, four, and six, while PHL644h pellicles were harvested on days two, three, and four as they grew more quickly than PHL644. Day one was not harvested because pellicle formation was not mature enough. The harvested pellicles were stained with either WGA-FITC, which binds to N-acetylglucosamine thereby staining PNAG, or ConA-Alexa Fluor 488, which binds to mannose and glucose and thus stains colanic acid. Pellicles were counterstained with SYTO 62 as a DNA stain (shown in magenta versus green for the lectins) and visualised by confocal microscopy (Fig. 5.14 and Fig. 5.15). Areas of white consist of both GFP and SYTO 62 fluorescence. It was observed that the presence of both colanic acid and PNAG increased over time as both the PHL644 and PHL644h pellicles matured.

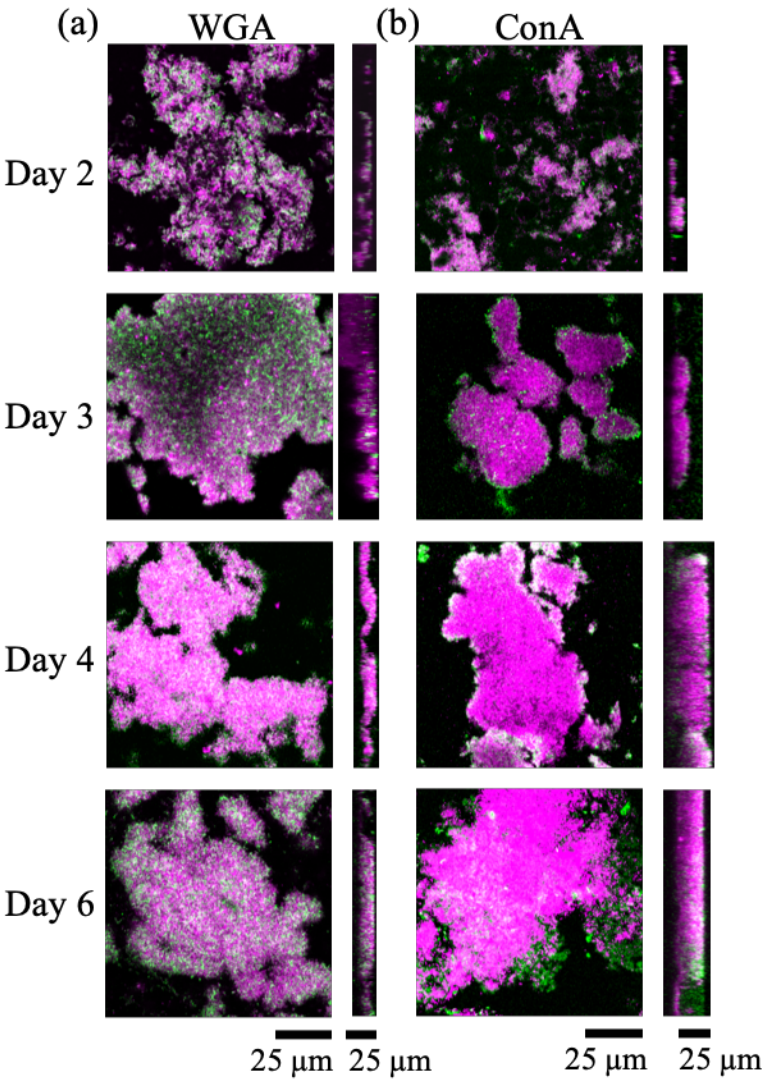

Figure 5.14: Visualisation of PHL644 EPS production by confocal microscopy.

E. coli PHL644 was grown in M63+ medium at 30 °C and 70 rpm for six days and pellicles were harvested and stained with SYTO 62 (stains cellular material, shown as magenta), and either ConA (stains colonic acid, shown as green), or WGA (stains PNAG, shown as green). Cells with respective cellular and EPS stains were visualised by confocal microscopy on days 2, 3, 4 and 6. Representative single plane images from the top (air-facing), middle, and bottom (media-facing) of each pellicle are shown. Side-view images traversing top (left) to bottom (right) are shown. Scale bars representing 25 µm are shown.

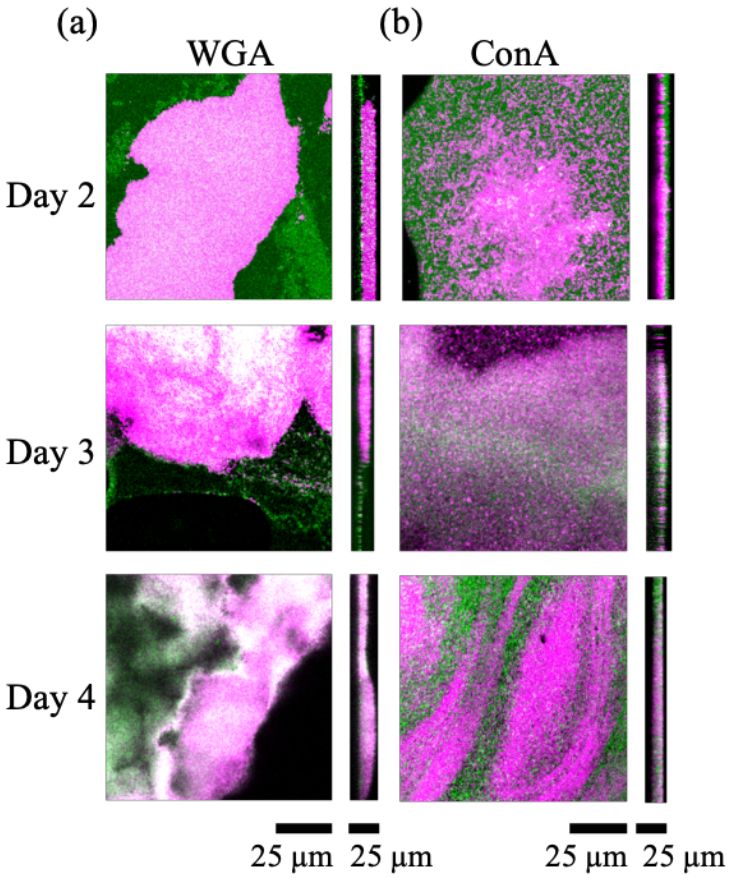

Figure 5.15: Visualisation of PHL644h EPS production by confocal microscopy.

E. coli PHL644h was grown in M63+ medium at 30 °C and 70 rpm for four days and pellicles were harvested and stained with SYTO 62 (stains cellular material, shown as magenta), and either ConA (stains colonic acid, shown as green), or WGA (stains PNAG, shown as green). Cells with respective cellular and EPS stains were visualised by confocal microscopy on days 2, 3, and 4. Representative single plane images from the top (air-facing), middle, and bottom (media-facing) of each pellicle are shown. Side-view images traversing top (left) to bottom (right) are shown. Scale bars representing 25 µm are shown.

In both PHL644 and PHL644h pellicles, WGA stained throughout the pellicle while ConA tended to stain more of the periphery of the pellicle. Colanic acid has previously been identified as being dispensable for adhesion, but can form a protective capsule around *E. coli* biofilms. It could be proposed that similarly to biofilms, colanic acid may also be capsular-like in pellicles, which would explain why ConA tends to stain the periphery of the pellicle instead of throughout (Beloin, Roux and Ghigo, 2008). Conversely, PNAG is proposed to function as a cell-cell and cell-surface adhesin and stabilise *E. coli* biofilms and therefore is more likely to be present throughout pellicles (Wang, Preston and Romeo, 2004; Agladze, Wang and Romeo, 2005).

It was concluded that more EPS was produced, and earlier in pellicle development, in PHL644h than PHL644. After two days, PHL644h had produced thick pellicles with large areas stained with both ConA and WGA, while PHL644 had only formed small aggregates. Similarly to PHL644, WGA stained PHL644h throughout the pellicle, while ConA stained the periphery of the PHL644h pellicle. It was noted that the thickness of the pellicles had inherent variability, possibly due to pellicle harvesting techniques, stain incubation times, or the heterogeneous nature of pellicles. Furthermore, it was noted that ConA is a tetramer of 28 kDa subunits while WGA is a dimer of 17 kDa subunits. This could explain why ConA tended to stain the outside edges of the pellicle growth in PHL644. However, we observed ConA staining in thick regions of EPS in PHL644h which may show that the larger size of ConA is not a factor in its different staining pattern.

5.4 Conclusions

Initial work for this chapter included optimising conditions to form a robust *E. coli* K-12 biofilm. Glass microscope slides wrapped in PTFE grew more biofilm than PTFE board of the same dimensions. During work to optimise a biofilm generation

model, biofilm was observed growing on test tubes inserted into the medium; subsequent crystal violet analysis revealed more biofilm accumulated on the inside of the test tubes than the outside. It was also shown that more biofilm accumulated inside the glass test tube with limited oxygen. It was proposed that the smaller environment inside the tube provided more opportunity for cell-surface interactions and optimal oxygen tension, or both, resulting in more biofilm formation. During this work to optimise *E. coli* K-12 biofilm formation in test tubes, a pellicle was observed at the air-liquid interface. *E. coli* K-12 pellicle formation was then characterised.

Pellicle formation in *E. coli* K-12 was shown to be dependent upon the adhesin curli as strains not constitutively expressing curli (MC4100) could not form a pellicle. When transformed with the plasmid pT7-CsgD (overexpresses *csgD* and has similar effects on biofilm formation as the *ompR234* mutation carried in PHL644), MC4100 was able to form a thin pellicle (Brombacher *et al.*, 2006).

Cellular movement, provided by flagellar motility, shaking of the growth vessel, or both, was also important in pellicle formation. Hypermotility was shown to eliminate the need for shaking so it was theorised that hypermotile cells are able to reach to the air-liquid interface more efficiently thus reducing the requirement for other forms of mobility (shaking). Hypermotile cells also formed thicker pellicles in less time despite having similar growth rates, which may also indicate that motility is an important method of allowing cells to overcome counteractive forces and localise to the air-liquid interface in order to initiate pellicle formation. This is further supported by observations that motile PHL644 incubated without shaking formed thin “raft-like” aggregates at the air-liquid interface but was unable to form a mature pellicle. In this same vein, the observation that PHL644 required shaking only during early stages of pellicle formation (24 hours) to form a confluent pellicle may suggest that pellicle formation is ‘seeded’ from cells that later develop into a mature pellicle. It is likely a

combination of curli, motility, and mobility are important in *E. coli* K-12 pellicle formation.

Curli expression varied in the growth vessel between cells located in the pellicle, planktonic phase, the air-liquid interface on the vessel wall, and the sediment over time. Curli expression in the pellicle and the planktonic phase was high and remained consistently high over three days. Alternatively, curli expression of solid surface-attached cells at the air-liquid interface and the sediment were lower after 24 hours. It was theorised that higher curli expression in pellicles is needed to maintain cell-cell attachment during pellicle development, whereas curli in biofilms can be downregulated once attached to a solid surface. It was also proposed that unattached planktonic cells will continue to produce curli until solid surface-attached. Additionally, it was observed that the solid surface-attached cells increased curli expression over three days, which could be due to growth of the biofilm in the sediment and along the surface of the vessel at the air-liquid interface which may require the cells produce more curli.

Confocal microscopy of *E. coli* K-12 pellicles revealed hypermotile cells formed thicker pellicles in less time compared to motile cells, which supports earlier visual observations. Visualisation of GFP in cells transformed with pJLC-T showed curli expression changes spatially within the pellicle and over time as they develop. There were also significant differences in curli expression between PHL644 and PHL644h pellicles which suggest motility may be linked to curli formation and the pellicle architecture. It was hypothesised that because hypermotile cells form pellicles faster, more curli expression is required throughout the pellicle for structural strength rather than in localised areas like in the PHL644 pellicles. The matrix components of *E. coli* K-12 pellicles appear to contain both PNAG (located throughout the pellicle) and colanic acid (located mainly on the periphery of the pellicle). Taken together, *E. coli* K-

12 pellicles appear to share structural characteristics of both *B. subtilis* and UPEC pellicles and *E. coli* solid surface-attached biofilms.

6 CONCLUSIONS AND FUTURE WORK

In summary, the three results chapters highlighted the regulation of curli expression from various stimuli and how this can be optimised. The use of plasmid reporters to this end are extremely useful when examining and optimising different aspects of biofilm formation. Individual stains for the matrix components PNAG and colanic acid also useful in visualising the EPS in solid surface-attached biofilms and pellicles.

Curli expression was optimised in the Duran Bottle method. PHL644, an engineered biofilm-producing strain, increased curli expression when grown in minimal media with 10 mM glucose and 17 mM sodium succinate at temperatures around 30 °C and 70 rpm shaking. Sodium succinate provides sodium ions which may increase PNAG production. Osmolarity, surface sensing, and cell concentration may also play a role on curli expression and should be studied further. Potentially constructing a fluorophore bound to the membrane kinase of osmolarity or surface sensing pathways that could fluorescence when the kinase undergoes a conformational change (to induce their respective pathways) would give insight to conditions that stimulate these cascades and how they affect biofilm or pellicle formation. Oxygen tension may also affect curli expression, but the crossover of stimuli with shear force and rpm shaking make it difficult to test. The conditions with the greatest curli expression often correlated with conditions that accumulated the most biofilm by previous crystal violet data. This supports data showing that curli formation is important in *E. coli* K-12 biofilm formation. Future work may include the construction of new reporter plasmids for other genes important during biofilm formation, such as PNAG or colanic acid production. Understanding the expression of genes required for matrix synthesis would give insight into the functions of individual matrix components.

Competition sensing may play a part in biofilm formation. The data suggests that addition of 1 mM lactic acid to cultures may produce a thicker, more viable biofilm.

The data also suggests that the addition of MG1655 or PHL644 spent medium to MG1655 cultures increases biofilm accumulation. This is potentially a result of AI-2 or other signalling molecules in the spent medium (quorum sensing), or the presence acids (competition sensing) in the bacterial waste/spent medium. A reporter plasmid for AI-2 quorum sensing signalling pathways would indicate if communication molecules are present in the spent medium and this would help clarify if quorum sensing molecules are causing the increase in biofilm accumulation. The effects of competition sensing are still relatively unknown in *E. coli* K-12 and this should be studied further.

In order to increase biocatalytic yield and retain robust biofilm formation of *E. coli* K-12 constitutively producing halotryptophan, amino acids were investigated for their effect on tryptophan export from the cell (Tsoligkas *et al.*, 2011; Perni *et al.*, 2013). It was revealed that the addition of 10 mM phenylalanine increased curli expression, optical density, and rate of agglutination in PHL644. It was also shown that the increase in curli expression of PHL644 supplemented with 10 mM phenylalanine at 30 °C resulted in more biofilm accumulation. When investigating the potential of fibre formation in L-phenylalanine from reports by Singh *et al.* it was shown that D/L-phenylalanine reduced curli expression by flow cytometry and confocal microscopy, while D-phenylalanine did not increase curli expression (Singh *et al.*, 2015). A hypothesis has been developed to describe these phenomena.

Potentially, if L-phenylalanine is able to form fibres which seed CsgA so quickly that it forms a gradient out of the cell, it is possible that CpxA (which can be stimulated by curlin subunits), switches to maximal phosphatase activity and removes phosphoryl groups from CpxR. The dephosphorylated CpxR will no longer repress *csgBA* and thus curli expression will increase. This may also have the same effect on the EnvZ/OmpR pathway, which would result in PHL644 (which has more OmpR present) having maximal dephosphorylated OmpR to activate curli expression. However, it is

unknown if EnvZ is stimulated by curlin. It has been further hypothesised that if phenylalanine is able to form fibres in the medium that this would increase the optical density of the cultures, which corresponds with the data. Measuring the optical density of the cultures with phenylalanine but without cells would be able to show if the optical density increases due to fibre formation; however, phenylalanine may need bacterial amyloid or other factors provided by the cells in order to form fibres ("cross-seeding") thus if the optical density does not increase in the phenylalanine test without cells this would not disprove the fibre-formation theory. Further testing, such as visualisation with a Scanning Electron Microscope (SEM) for phenylalanine fibre formation may be required. Additionally, future work should include investigating the potential for amyloid cross-seeding between aromatic amino acids and bacterial amyloid. Titrations of D-phenylalanine to L-phenylalanine should be performed for the effect on curli expression by flow cytometry and confocal microscopy. The potential of a tuneable system by cross-seeding amyloid would be of great importance to biofilm research.

Lastly, pellicle formation of *E. coli* K-12 was characterised in terms of curli formation and motility and the components and structure of the pellicle matrix was described. Curli are important for pellicle formation in *E. coli* K-12. The data suggests a combination of curli, active motility, and passive movement by shaking are important in *E. coli* K-12 pellicle formation. Hypermotility was shown to eliminate the need for shaking so it was theorised that hypermotile cells are able to reach to the air-liquid interface more efficiently thus reducing the requirement for other forms of mobility (shaking). PHL644 required shaking only during early stages of pellicle formation (24 hours) to form a confluent pellicle which may suggest that pellicle formation is 'seeded' from cells that later develop into a mature pellicle. Confocal microscopy of *E. coli* K-12 pellicles revealed hypermotile cells grew thicker in less time compared to motile cells, which supports earlier visual observations. *E. coli* K-12 pellicles appear to contain both

PNAG (located throughout the pellicle) and colanic acid (located mainly on the periphery of the pellicle) in the matrix. Future work should continue to study and characterise *E. coli* K-12 pellicles as there is little regarding this in the literature. Specifically, it would be interesting to study the effect of chemotaxis on *E. coli* K-12 pellicle formation. Additionally, it would be beneficial to test if *E. coli* pellicles are capable of biocatalysis and if they are useful in industrial applications due to their proximity to the air-liquid interface.

7 REFERENCES

Adler-Abramovich, L. *et al.* (2012) 'Phenylalanine assembly into toxic fibrils suggests amyloid etiology in phenylketonuria', *Nature Chemical Biology*. Nature Publishing Group, 8(8), pp. 701–706. doi: 10.1038/nchembio.1002.

Adler, J. and Templeton, B. (1967) 'The Effect of Environmental Conditions on the Motility of *Escherichia coli*', *Journal of General Microbiology*. Microbiology Society, 46(2), pp. 175–184. doi: 10.1099/00221287-46-2-175.

Agladze, K., Wang, X. and Romeo, T. (2005) 'Spatial Periodicity of *Escherichia coli* K-12 Biofilm Microstructure Initiates during a Reversible, Polar Attachment Phase of Development and Requires the Polysaccharide Adhesin PGA', *Journal of Bacteriology*, 187(24), pp. 8237–8246. doi: 10.1128/JB.187.24.8237-8246.2005.

Ahmer, B. M. M. (2004) 'Cell-to-cell signalling in *Escherichia coli* and *Salmonella enterica*', *Molecular Microbiology*, 52(4), pp. 933–945. doi: 10.1111/j.1365-2958.2004.04054.x.

Amit, R., Oppenheim, A. B. and Stavans, J. (2003) 'Increased Bending Rigidity of Single DNA Molecules by H-NS, a Temperature and Osmolarity Sensor', *Biophysical Journal*. Cell Press, 84(4), pp. 2467–2473. doi: 10.1016/S0006-3495(03)75051-6.

Andersen, J. B. *et al.* (1998) 'New unstable variants of green fluorescent protein for studies of transient gene expression in bacteria.', *Applied and environmental microbiology*. American Society for Microbiology (ASM), 64(6), pp. 2240–6. Available at: http://www.ncbi.nlm.nih.gov/pubmed/9603842 (Accessed: 8 May 2019).

Andersson, E. K. *et al.* (2013) 'Modulation of curli assembly and pellicle biofilm formation by chemical and protein chaperones.', *Chemistry & biology*. NIH Public Access, 20(10), pp. 1245–54. doi: 10.1016/j.chembiol.2013.07.017.

Armitano, J., Méjean, V. and Jourlin-Castelli, C. (2014) 'Gram-negative bacteria can also form pellicles', *Environmental Microbiology Reports*. John Wiley & Sons, Ltd (10.1111), 6(6), pp. 534–544. doi: 10.1111/1758-2229.12171.

Arnqvist, A. *et al.* (1992) 'The Crl protein activates cryptic genes for curli formation and fibronectin binding in *Escherichia coli* HB101.', *Molecular microbiology*, 6(17), pp. 2443–52. Available at: http://www.ncbi.nlm.nih.gov/pubmed/1357528 (Accessed: 16 April 2019).

Atlung, T. and Ingmer, H. (1997) ‘H-NS: a modulator of environmentally regulated gene expression.’, *Molecular microbiology*, 24(1), pp. 7–17. Available at: http://www.ncbi.nlm.nih.gov/pubmed/9140961 (Accessed: 16 June 2019).

Bachmann, B. J., Low, K. B. and Taylor, A. L. (1976) 'Recalibrated Linkage Map of *Escherichia coli* K-121'. Available at: https://www.ncbi.nlm.nih.gov/pmc/articles/PMC413944/pdf/bactrev00051-0122.pdf (Accessed: 11 June 2019).

Bansal, T. *et al.* (2007) ‘Differential Effects of Epinephrine, Norepinephrine, and Indole on *Escherichia coli* O157:H7 Chemotaxis, Colonization, and Gene Expression’, *Infection and Immunity*, 75(9), pp. 4597–4607. doi: 10.1128/IAI.00630-07.

Barnhart, M. M. and Chapman, M. R. (2006) ‘Curli Biogenesis and Function’, *Annual Review of Microbiology*. Annual Reviews, 60(1), pp. 131–147. doi: 10.1146/annurev.micro.60.080805.142106.

Barth, M. *et al.* (1995) ‘Role for the histone-like protein H-NS in growth phase-dependent and osmotic regulation of sigma S and many sigma S-dependent genes in *Escherichia coli*.’, *Journal of bacteriology*. American Society for Microbiology (ASM), 177(12), pp. 3455–64. Available at: http://www.ncbi.nlm.nih.gov/pubmed/7768855 (Accessed: 23 April 2019).

Belas, R. (2014) ‘Biofilms, flagella, and mechanosensing of surfaces by bacteria.’, *Trends in microbiology*. Elsevier, 22(9), pp. 517–27. doi: 10.1016/j.tim.2014.05.002.

Beloin, C., Roux, A. and Ghigo, J. M. (2008) *Escherichia coli biofilms*, *Current Topics in Microbiology and Immunology*. Inserm. doi: 10.1007/978-3-540-75418-3_12.

Bernal-Bayard, J. *et al.* (2018) ‘Short genome report of cellulose-producing commensal *Escherichia coli* 1094.’, *Standards in genomic sciences*. BioMed Central, 13, p. 13. doi: 10.1186/s40793-018-0316-0.

Birch, L. C. (2002) ‘The Meanings of Competition’, *The American Naturalist*. doi: 10.1086/281957.

Bjornsdottir, K. *et al.* (2006) ‘Protective effects of organic acids on survival of *Escherichia coli* O157:H7 in acidic environments.’, *Applied and environmental microbiology*. American Society for Microbiology (ASM), 72(1), pp. 660–4. doi: 10.1128/AEM.72.1.660-664.2006.

Blattner, F. R. *et al.* (1997) 'The complete genome sequence of *Escherichia coli* K-12.', *Science (New York, N.Y.)*, 277(5331), pp. 1453–62. Available at: http://www.ncbi.nlm.nih.gov/pubmed/9278503 (Accessed: 30 April 2019).

Blumer, C. *et al.* (2005) 'Regulation of type 1 fimbriae synthesis and biofilm formation by the transcriptional regulator LrhA of *Escherichia coli*', *Microbiology*. Microbiology Society, 151(10), pp. 3287–3298. doi: 10.1099/mic.0.28098-0.

von Bodman, S. B., Willey, J. M. and Diggle, S. P. (2008) 'Cell-cell communication in bacteria: united we stand.', *Journal of bacteriology*. American Society for Microbiology Journals, 190(13), pp. 4377–91. doi: 10.1128/JB.00486-08.

Boehm, A. *et al.* (2010) 'Second Messenger-Mediated Adjustment of Bacterial Swimming Velocity', *Cell*, 141(1), pp. 107–116. doi: 10.1016/j.cell.2010.01.018.

Boos, W. and Shuman, H. (1998) 'Maltose/maltodextrin system of *Escherichia coli*: transport, metabolism, and regulation.', *Microbiology and molecular biology reviews : MMBR*, 62(1), pp. 204–29. Available at: http://www.ncbi.nlm.nih.gov/pubmed/9529892 (Accessed: 10 May 2019).

Botsford, J. L. and Harman, J. G. (1992) 'Cyclic AMP in prokaryotes.', *Microbiological reviews*, 56(1), pp. 100–22. Available at: http://www.ncbi.nlm.nih.gov/pubmed/1315922 (Accessed: 20 June 2019).

Bougdour, A., Lelong, C. and Geiselmann, J. (2004) 'Crl, a low temperature-induced protein in *Escherichia coli* that binds directly to the stationary phase sigma subunit of RNA polymerase.', *The Journal of biological chemistry*. American Society for Biochemistry and Molecular Biology, 279(19), pp. 19540–50. doi: 10.1074/jbc.M314145200.

Branda, S. S. *et al.* (2005) 'Biofilms: the matrix revisited.', *Trends in microbiology*. Elsevier, 13(1), pp. 20–6. doi: 10.1016/j.tim.2004.11.006.

Bren, A. *et al.* (2016) 'Glucose becomes one of the worst carbon sources for *E. coli* on poor nitrogen sources due to suboptimal levels of cAMP.', *Scientific reports*. Nature Publishing Group, 6, p. 24834. doi: 10.1038/srep24834.

Brombacher, E. *et al.* (2003) 'The curli biosynthesis regulator CsgD co-ordinates the expression of both positive and negative determinants for biofilm formation in *Eschericia coli*', *Microbiology*. doi: 10.1099/mic.0.26306-0.

Brombacher, E. *et al.* (2006) ‘Gene expression regulation by the curli activator CsgD protein: Modulation of cellulose biosynthesis and control of negative determinants for microbial adhesion’, *Journal of Bacteriology*. doi: 10.1128/JB.188.6.2027-2037.2006.

Brown, P. K. *et al.* (2001) ‘MlrA, a novel regulator of curli (AgF) and extracellular matrix synthesis by *Escherichia coli* and *Salmonella enterica* serovar Typhimurium’, *Molecular Microbiology*. John Wiley & Sons, Ltd (10.1111), 41(2), pp. 349–363. doi: 10.1046/j.1365-2958.2001.02529.x.

Burwinkel, M. *et al.* (2018) ‘Intravenous injection of beta-amyloid seeds promotes cerebral amyloid angiopathy (CAA).’, *Acta neuropathologica communications*. BioMed Central, 6(1), p. 23. doi: 10.1186/s40478-018-0511-7.

Cabellos-Avelar, T., Souza, V. and Membrillo-Hernández, J. (2006) ‘Spent media from cultures of environmental isolates of *Escherichia coli* can suppress the deficiency of biofilm formation under anoxic conditions of laboratory *E. coli* strains’, *FEMS Microbiology Ecology*. John Wiley & Sons, Ltd (10.1111), 58(3), pp. 414–424. doi: 10.1111/j.1574-6941.2006.00186.x.

Cerca, N. *et al.* (2007) ‘Protection against *Escherichia coli* infection by antibody to the *Staphylococcus aureus* poly-N-acetylglucosamine surface polysaccharide.’, *Proceedings of the National Academy of Sciences of the United States of America*. National Academy of Sciences, 104(18), pp. 7528–33. doi: 10.1073/pnas.0700630104.

Cerca, N. and Jefferson, K. K. (2008) ‘Effect of growth conditions on poly-N-acetylglucosamine expression and biofilm formation in *Escherichia coli*’, *FEMS Microbiology Letters*, 283(1), pp. 36–41. doi: 10.1111/j.1574-6968.2008.01142.x.

Chang, M. C. Y. and Keasling, J. D. (2006) ‘Production of isoprenoid pharmaceuticals by engineered microbes’, *Nature Chemical Biology*. Nature Publishing Group, 2(12), pp. 674–681. doi: 10.1038/nchembio836.

Chapman, M. R. *et al.* (2002) ‘Role of *Escherichia coli* curli operons in directing amyloid fiber formation.’, *Science (New York, N.Y.)*. American Association for the Advancement of Science, 295(5556), pp. 851–5. doi: 10.1126/science.1067484.

Chauhan, A. *et al.* (2013) ‘Did I Pick the Right Colony? Pitfalls in the Study of Regulation of the Phase Variable Antigen 43 Adhesin’, *PLoS ONE*. Edited by S. Semsey, 8(9), p. e73568. doi: 10.1371/journal.pone.0073568.

Chen, Y. *et al.* (2012) 'Evidence for cyclic Di-GMP-mediated signaling in *Bacillus subtilis*.', *Journal of bacteriology*. American Society for Microbiology Journals, 194(18), pp. 5080–90. doi: 10.1128/JB.01092-12.

Chen, Y. *et al.* (2015) 'Acetic Acid Acts as a Volatile Signal To Stimulate Bacterial Biofilm Formation.', *mBio*. American Society for Microbiology (ASM), 6(3), p. e00392. doi: 10.1128/mBio.00392-15.

Chilcott, G. S. and Hughes, K. T. (2000) 'Coupling of flagellar gene expression to flagellar assembly in *Salmonella enterica* serovar typhimurium and *Escherichia coli*.', *Microbiology and molecular biology reviews : MMBR*, 64(4), pp. 694–708. doi: 10.1128/mmbr.64.4.694-708.2000.

Chiti, F. and Dobson, C. M. (2006) 'Protein Misfolding, Functional Amyloid, and Human Disease', *Annual Review of Biochemistry*. Annual Reviews , 75(1), pp. 333–366. doi: 10.1146/annurev.biochem.75.101304.123901.

Clark, D. P. (1989) 'The fermentation pathways of *Escherichia coli*', *FEMS Microbiology Letters*. Narnia, 63(3), pp. 223–234. doi: 10.1111/j.1574-6968.1989.tb03398.x.

Coenye, T. and Nelis, H. J. (2010) 'In vitro and in vivo model systems to study microbial biofilm formation', *Journal of Microbiological Methods*, 83(2), pp. 89–105. doi: 10.1016/j.mimet.2010.08.018.

Colón-González, M., Méndez-Ortiz, M. M. and Membrillo-Hernández, J. (2004) 'Anaerobic growth does not support biofilm formation in *Escherichia coli* K-12', *Research in Microbiology*, 155(7), pp. 514–521. doi: 10.1016/j.resmic.2004.03.004.

Conway, T. and Cohen, P. S. (2015) 'Commensal and Pathogenic *Escherichia coli* Metabolism in the Gut.', *Microbiology spectrum*. NIH Public Access, 3(3). doi: 10.1128/microbiolspec.MBP-0006-2014.

Cornforth, D. M. and Foster, K. R. (2013) 'Competition sensing: The social side of bacterial stress responses', *Nature Reviews Microbiology*. doi: 10.1038/nrmicro2977.

Correnti, J. *et al.* (2002) 'Dam-dependent phase variation of Ag43 in *Escherichia coli* is altered in a seqA mutant', *Molecular Microbiology*. John Wiley & Sons, Ltd (10.1111), 44(2), pp. 521–532. doi: 10.1046/j.1365-2958.2002.02918.x.

Costerton, J. W. *et al.* (1994) 'Biofilms, the customized microniche.', *Journal of Bacteriology*. American Society for Microbiology (ASM), 176(8), p. 2137. Available at: https://www.ncbi.nlm.nih.gov/pmc/articles/PMC205331/ (Accessed: 28 June 2019).

Costerton, J. W. *et al.* (1995) 'Microbial Biofilms', *Annual Review of Microbiology*, 49(1), pp. 711–745. doi: 10.1146/annurev.mi.49.100195.003431.

Culler, H. F. *et al.* (2018) 'Role of SdiA on Biofilm Formation by Atypical Enteropathogenic *Escherichia coli*.', *Genes*. Multidisciplinary Digital Publishing Institute (MDPI), 9(5). doi: 10.3390/genes9050253.

D'Argenio, D. A. and Miller, S. I. (2004) 'Cyclic di-GMP as a bacterial second messenger', *Microbiology*, 150(8), pp. 2497–2502. doi: 10.1099/mic.0.27099-0.

Danese, P. N. *et al.* (2000) 'The outer membrane protein, Antigen 43, mediates cell-to-cell interactions within *Escherichia coli* biofilms', *Molecular Microbiology*. John Wiley & Sons, Ltd (10.1111), 37(2), pp. 424–432. doi: 10.1046/j.1365-2958.2000.02008.x.

Danese, P. N., Pratt, L. A. and Kolter, R. (2000) 'Exopolysaccharide production is required for development of *Escherichia coli* K-12 biofilm architecture.', *Journal of bacteriology*. American Society for Microbiology Journals, 182(12), pp. 3593–6. doi: 10.1128/jb.182.12.3593-3596.2000.

Davey, M. E. and O'toole, G. A. (2000) 'Microbial Biofilms: from Ecology to Molecular Genetics', *Microbiology and Molecular Biology Reviews*. American Society for Microbiology, 64(4), pp. 847–867. doi: 10.1128/MMBR.64.4.847-867.2000.

Davis, S. J., Peters, G. P. and Caldeira, K. (2011) 'The supply chain of CO2 emissions.', *Proceedings of the National Academy of Sciences of the United States of America*. National Academy of Sciences, 108(45), pp. 18554–9. doi: 10.1073/pnas.1107409108.

DeLisa, M. P. *et al.* (2001) 'DNA microarray-based identification of genes controlled by autoinducer 2-stimulated quorum sensing in *Escherichia coli*.', *Journal of bacteriology*. American Society for Microbiology (ASM), 183(18), pp. 5239–47. doi: 10.1128/jb.183.18.5239-5247.2001.

DePas, W. H. *et al.* (2014) 'Biofilm formation protects *Escherichia coli* against killing by *Caenorhabditis elegans* and *Myxococcus xanthus*.', *Applied and environmental microbiology*. American Society for Microbiology, 80(22), pp. 7079–87. doi: 10.1128/AEM.02464-14.

Dewasthale, S., Mani, I. and Vasdev, K. (2018) 'Microbial biofilm: current challenges in health care industry'. doi: 10.15406/jabb.2018.05.00132.

Díaz, E. *et al.* (2001) 'Biodegradation of aromatic compounds by *Escherichia coli*.', *Microbiology and molecular biology reviews : MMBR*. American Society for Microbiology (ASM), 65(4), pp. 523–69, table of contents. doi: 10.1128/MMBR.65.4.523-569.2001.

Domka, J. *et al.* (2007) 'Temporal gene-expression in *Escherichia coli* K-12 biofilms', *Environmental Microbiology*. John Wiley & Sons, Ltd (10.1111), 9(2), pp. 332–346. doi: 10.1111/j.1462-2920.2006.01143.x.

Domka, J., Lee, J. and Wood, T. K. (2006) 'YliH (BssR) and YceP (BssS) regulate *Escherichia coli* K-12 biofilm formation by influencing cell signaling.', *Applied and environmental microbiology*. American Society for Microbiology, 72(4), pp. 2449–59. doi: 10.1128/AEM.72.4.2449-2459.2006.

Dong, J. *et al.* (1993) 'The deduced amino-acid sequence of the cloned cpxR gene suggests the protein is the cognate regulator for the membrane sensor, CpxA, in a two-component signal transduction system of *Escherichia coli*.', *Gene*, 136(1–2), pp. 227–30. Available at: http://www.ncbi.nlm.nih.gov/pubmed/8294007 (Accessed: 16 June 2019).

Donlan, R. M. (2002) 'Biofilms: microbial life on surfaces.', *Emerging infectious diseases*. Centers for Disease Control and Prevention, 8(9), pp. 881–90. doi: 10.3201/eid0809.020063.

Dorel, C. *et al.* (1999) 'Involvement of the Cpx signal transduction pathway of *E. coli* in biofilm formation', *FEMS Microbiology Letters*, 178(1), pp. 169–175. doi: 10.1111/j.1574-6968.1999.tb13774.x.

Doroshenko, V. *et al.* (2007) 'YddG from *Escherichia coli* promotes export of aromatic amino acids', *FEMS Microbiology Letters*, 275(2), pp. 312–318. doi: 10.1111/j.1574-6968.2007.00894.x.

Dressaire, C. *et al.* (2015) 'BolA is a transcriptional switch that turns off motility and turns on biofilm development.', *mBio*. American Society for Microbiology (ASM), 6(1), pp. e02352-14. doi: 10.1128/mBio.02352-14.

Dudin, O. *et al.* (2014) ‘Repression of Flagellar Genes in Exponential Phase by CsgD and CpxR, Two Crucial Modulators of *Escherichia coli* Biofilm Formation’, *Journal of Bacteriology*, 196(3), pp. 707–715. doi: 10.1128/JB.00938-13.

Duncan, M. J. *et al.* (2005) ‘The Distinct Binding Specificities Exhibited by Enterobacterial Type 1 Fimbriae Are Determined by Their Fimbrial Shafts’, *Journal of Biological Chemistry*, 280(45), pp. 37707–37716. doi: 10.1074/jbc.M501249200.

Eberly, A. R. *et al.* (2017) ‘Biofilm Formation by Uropathogenic *Escherichia coli* Is Favored under Oxygen Conditions That Mimic the Bladder Environment.’, *International journal of molecular sciences*. Multidisciplinary Digital Publishing Institute (MDPI), 18(10). doi: 10.3390/ijms18102077.

Eboigbodin, K. E. and Biggs, C. A. (2008) ‘Characterization of the Extracellular Polymeric Substances Produced by *Escherichia coli* Using Infrared Spectroscopic, Proteomic, and Aggregation Studies’, *Biomacromolecules*, 9(2), pp. 686–695. doi: 10.1021/bm701043c.

Edwards, S. J. and Kjellerup, B. V. (2013) ‘Applications of biofilms in bioremediation and biotransformation of persistent organic pollutants, pharmaceuticals/personal care products, and heavy metals’, *Applied Microbiology and Biotechnology*, 97(23), pp. 9909–9921. doi: 10.1007/s00253-013-5216-z.

Egger, L. A., Park, H. and Inouye, M. (1997) ‘Signal transduction via the histidyl-aspartyl phosphorelay.’, *Genes to cells : devoted to molecular & cellular mechanisms*, 2(3), pp. 167–84. Available at: http://www.ncbi.nlm.nih.gov/pubmed/9189755 (Accessed: 22 March 2019).

Eisenberg, D. and Jucker, M. (2012) ‘The amyloid state of proteins in human diseases.’, *Cell*. Elsevier, 148(6), pp. 1188–203. doi: 10.1016/j.cell.2012.02.022.

Ercan, D. and Demirci, A. (2015) ‘Current and future trends for biofilm reactors for fermentation processes’, *Critical Reviews in Biotechnology*. Informa Healthcare, 35(1), pp. 1–14. doi: 10.3109/07388551.2013.793170.

Evans, M. L. *et al.* (2015) ‘The bacterial curli system possesses a potent and selective inhibitor of amyloid formation.’, *Molecular cell*. NIH Public Access, 57(3), pp. 445–55. doi: 10.1016/j.molcel.2014.12.025.

Evans, M. L. and Chapman, M. R. (2014) 'Curli biogenesis: order out of disorder.', *Biochimica et biophysica acta*. NIH Public Access, 1843(8), pp. 1551–8. doi: 10.1016/j.bbamcr.2013.09.010.

Fang, X. *et al.* (2014) 'GIL, a new c-di-GMP-binding protein domain involved in regulation of cellulose synthesis in enterobacteria'. doi: 10.1111/mmi.12672.

Federle, M. J. and Bassler, B. L. (2003) 'Interspecies communication in bacteria.', *The Journal of clinical investigation*. American Society for Clinical Investigation, 112(9), pp. 1291–9. doi: 10.1172/JCI20195.

Ferrières, L. and Clarke, D. J. (2003) 'The RcsC sensor kinase is required for normal biofilm formation in *Escherichia coli* K-12 and controls the expression of a regulon in response to growth on a solid surface', *Molecular Microbiology*. John Wiley & Sons, Ltd (10.1111), 50(5), pp. 1665–1682. doi: 10.1046/j.1365-2958.2003.03815.x.

Fic, E. *et al.* (2009) 'cAMP Receptor Protein from *Escherichia coli* as a Model of Signal Transduction in Proteins-A Review', *J Mol Microbiol Biotechnol*, 17, pp. 1–11. doi: 10.1159/000178014.

Forsman, K. *et al.* (1992) 'Antirepression function in *Escherichia coli* for the cAMP-cAMP receptor protein transcriptional activator.', *Proceedings of the National Academy of Sciences of the United States of America*. National Academy of Sciences, 89(20), pp. 9880–4. doi: 10.1073/pnas.89.20.9880.

Fowler, D. M. *et al.* (2007) 'Functional amyloid – from bacteria to humans', *Trends in Biochemical Sciences*, 32(5), pp. 217–224. doi: 10.1016/j.tibs.2007.03.003.

Friedlander, R. S. *et al.* (2013) 'Bacterial flagella explore microscale hummocks and hollows to increase adhesion', *Proceedings of the National Academy of Sciences*. National Academy of Sciences, p. 201219662. doi: 10.1073/PNAS.1219662110.

Friedlander, R. S., Vogel, N. and Aizenberg, J. (2015) 'Role of Flagella in Adhesion of *Escherichia coli* to Abiotic Surfaces'. doi: 10.1021/acs.langmuir.5b00815.

Frymier, P. D. *et al.* (1995) 'Three-dimensional tracking of motile bacteria near a solid planar surface.', *Proceedings of the National Academy of Sciences of the United States of America*. National Academy of Sciences, 92(13), pp. 6195–9. doi: 10.1073/pnas.92.13.6195.

García-Contreras, R. *et al.* (2008) 'Protein translation and cell death: The role of rare tRNAs in biofilm formation and in activating dormant phage killer genes', *PLoS ONE*. doi: 10.1371/journal.pone.0002394.

Gerstel, U., Park, C. and Römling, U. (2004) 'Complex regulation of csgD promoter activity by global regulatory proteins', *Molecular Microbiology*. John Wiley & Sons, Ltd (10.1111), 49(3), pp. 639–654. doi: 10.1046/j.1365-2958.2003.03594.x.

Gerstel, U. and Romling, U. (2001) 'Oxygen tension and nutrient starvation are major signals that regulate agfD promoter activity and expression of the multicellular morphotype in *Salmonella typhimurium*', *Environmental Microbiology*. John Wiley & Sons, Ltd (10.1111), 3(10), pp. 638–648. doi: 10.1046/j.1462-2920.2001.00235.x.

Ghigo, J.-M. (2001) 'Natural conjugative plasmids induce bacterial biofilm development', *Nature*. Nature Publishing Group, 412(6845), pp. 442–445. doi: 10.1038/35086581.

Goller, C. *et al.* (2006) 'The Cation-Responsive Protein NhaR of *Escherichia coli* Activates pgaABCD Transcription, Required for Production of the Biofilm Adhesin Poly-β-1,6-N-Acetyl-d-Glucosamine', *Journal of Bacteriology*. American Society for Microbiology Journals, 188(23), pp. 8022–8032. doi: 10.1128/JB.01106-06.

Görke, B. and Stülke, J. (2008) 'Carbon catabolite repression in bacteria: many ways to make the most out of nutrients', *Nature Reviews Microbiology*. Nature Publishing Group, 6(8), pp. 613–624. doi: 10.1038/nrmicro1932.

Grantcharova, N. *et al.* (2010) 'Bistable expression of CsgD in biofilm development of *Salmonella enterica* serovar typhimurium.', *Journal of bacteriology*. American Society for Microbiology Journals, 192(2), pp. 456–66. doi: 10.1128/JB.01826-08.

Gualdi, L. *et al.* (2008) 'Cellulose modulates biofilm formation by counteracting curli-mediated colonization of solid surfaces in *Escherichia coli*', *Microbiology*, 154(7), pp. 2017–2024. doi: 10.1099/mic.0.2008/018093-0.

Guttenplan, S. B. and Kearns, D. B. (2013) 'Regulation of flagellar motility during biofilm formation.', *FEMS microbiology reviews*. NIH Public Access, 37(6), pp. 849–71. doi: 10.1111/1574-6976.12018.

Haddadin, R. N. S. *et al.* (2010) 'The effect of subminimal inhibitory concentrations of antibiotics on virulence factors expressed by *Staphylococcus aureus* biofilms', *Journal of Applied Microbiology*. doi: 10.1111/j.1365-2672.2009.04529.x.

Haiko, J. and Westerlund-Wikström, B. (2013) 'The role of the bacterial flagellum in adhesion and virulence.', *Biology*. Multidisciplinary Digital Publishing Institute (MDPI), 2(4), pp. 1242–67. doi: 10.3390/biology2041242.

Hall-Stoodley, L., Costerton, J. W. and Stoodley, P. (2004) 'Bacterial biofilms: from the Natural environment to infectious diseases', *Nature Reviews Microbiology*. Nature Publishing Group, 2(2), pp. 95–108. doi: 10.1038/nrmicro821.

Halvorson, H. (1972) 'Utilization of single L -amino acids as sole source of carbon and nitrogen by bacteria', *Canadian Journal of Microbiology*, 18(11), pp. 1647–1650. doi: 10.1139/m72-255.

Hammar, M. *et al.* (1995) 'Expression of two csg operons is required for production of fibronectin- and congo red-binding curli polymers in *Escherichia coli* K-12.', *Molecular microbiology*, 18(4), pp. 661–70. Available at: http://www.ncbi.nlm.nih.gov/pubmed/8817489 (Accessed: 14 May 2019).

Hammar, M., Bian, Z. and Normark, S. (1996) 'Nucleator-dependent intercellular assembly of adhesive curli organelles in *Escherichia coli*.', *Proceedings of the National Academy of Sciences*, 93(13), pp. 6562–6566. doi: 10.1073/pnas.93.13.6562.

Hanna, A. *et al.* (2003) 'Role of capsular colanic acid in adhesion of uropathogenic *Escherichia coli*.', *Applied and environmental microbiology*, 69(8), pp. 4474–81. doi: 10.1128/aem.69.8.4474-4481.2003.

Harper, J. D. and Lansbury, P. T. (1997) 'Models of Amyloid Seeding in Alzheimer's Disease and Scrapie: Mechanistic Truths and Physiological Consequences of the Time-Dependent Solubility of Amyloid Proteins', *Annual Review of Biochemistry*, 66(1), pp. 385–407. doi: 10.1146/annurev.biochem.66.1.385.

Hasman, H., Schembri, M. A. and Klemm, P. (2000) 'Antigen 43 and type 1 fimbriae determine colony morphology of *Escherichia coli* K-12.', *Journal of bacteriology*. American Society for Microbiology Journals, 182(4), pp. 1089–95. doi: 10.1128/jb.182.4.1089-1095.2000.

Head, C. G., Tardy, A. and Kenney, L. J. (1998) 'Relative binding affinities of OmpR and OmpR-phosphate at the ompF and ompC regulatory sites', *Journal of Molecular Biology*. Academic Press, 281(5), pp. 857–870. doi: 10.1006/JMBI.1998.1985.

Heatwole, V. M. and Somerville, R. L. (1991) 'Cloning, nucleotide sequence, and characterization of mtr, the structural gene for a tryptophan-specific permease of

Escherichia coli K-12.', *Journal of bacteriology*. American Society for Microbiology Journals, 173(1), pp. 108–15. doi: 10.1128/jb.173.1.108-115.1991.

Hegde, M. *et al.* (2011) 'Chemotaxis to the Quorum-Sensing Signal AI-2 Requires the Tsr Chemoreceptor and the Periplasmic LsrB AI-2-Binding Protein', *Journal of Bacteriology*, 193(3), pp. 768–773. doi: 10.1128/JB.01196-10.

Henikoff, S., Wallace, J. C. and Brown, J. P. (1990) 'Finding protein similarities with nucleotide sequence databases.', *Methods in enzymology*, 183, pp. 111–32. Available at: http://www.ncbi.nlm.nih.gov/pubmed/2314271 (Accessed: 6 July 2019).

Henning, U. *et al.* (1962) 'The A protein of the tryptophan synthetase of *Escherichia coli*. Purification, crystallization, and composition studies.', *The Journal of biological chemistry*, 237, pp. 1523–30. Available at: http://www.ncbi.nlm.nih.gov/pubmed/13906502 (Accessed: 15 April 2019).

Heras, B. *et al.* (2014) 'The antigen 43 structure reveals a molecular Velcro-like mechanism of autotransporter-mediated bacterial clumping.', *Proceedings of the National Academy of Sciences of the United States of America*. National Academy of Sciences, 111(1), pp. 457–62. doi: 10.1073/pnas.1311592111.

Herzberg, M. *et al.* (2006) 'YdgG (TqsA) Controls Biofilm Formation in *Escherichia coli* K-12 through Autoinducer 2 Transport', *Journal of Bacteriology*, 188(2), pp. 587–598. doi: 10.1128/JB.188.2.587-598.2006.

Heukelekian, H. and Heller, A. (1940) 'Relation between Food Concentration and Surface for Bacterial Growth.', *Journal of bacteriology*. American Society for Microbiology (ASM), 40(4), pp. 547–58. Available at: http://www.ncbi.nlm.nih.gov/pubmed/16560368 (Accessed: 4 April 2019).

Hobley, L. *et al.* (2015) 'Giving structure to the biofilm matrix: an overview of individual strategies and emerging common themes.', *FEMS microbiology reviews*. Oxford University Press, 39(5), pp. 649–69. doi: 10.1093/femsre/fuv015.

Hochbaum, A. I. *et al.* (2011) 'Inhibitory effects of D-amino acids on *Staphylococcus aureus* biofilm development.', *Journal of bacteriology*. American Society for Microbiology (ASM), 193(20), pp. 5616–22. doi: 10.1128/JB.05534-11.

Hoffman, L. R. *et al.* (2005) 'Aminoglycoside antibiotics induce bacterial biofilm formation', *Nature*. doi: 10.1038/nature03912.

Hogema, B. M. *et al.* (1997) 'Catabolite repression by glucose 6-phosphate, gluconate and lactose in *Escherichia coli*.', *Molecular microbiology*, 24(4), pp. 857–67. Available at: http://www.ncbi.nlm.nih.gov/pubmed/9194712 (Accessed: 20 June 2019).

Hölscher, T. *et al.* (2015) 'Motility, Chemotaxis and Aerotaxis Contribute to Competitiveness during Bacterial Pellicle Biofilm Development.', *Journal of molecular biology*. NIH Public Access, 427(23), pp. 3695–3708. doi: 10.1016/j.jmb.2015.06.014.

Honoré, N. and Cole, S. T. (1990) 'Nucleotide sequence of the *aroP* gene encoding the general aromatic amino acid transport protein of *Escherichia coli* K-12: homology with yeast transport proteins', *Nucleic Acids Research*. Narnia, 18(3), pp. 653–653. doi: 10.1093/nar/18.3.653.

Van Houdt, R. and Michiels, C. W. (2005) 'Role of bacterial cell surface structures in *Escherichia coli* biofilm formation', *Research in Microbiology*. doi: 10.1016/j.resmic.2005.02.005.

Hu, X. *et al.* (2009) 'Amyloid seeds formed by cellular uptake, concentration, and aggregation of the amyloid-beta peptide', *Proceedings of the National Academy of Sciences*, 106(48), pp. 20324–20329. doi: 10.1073/pnas.0911281106.

Huang, K.-J., Lan, C.-Y. and Igo, M. M. (1997) 'Phosphorylation stimulates the cooperative DNA-binding properties of the transcription factor OmpR', *Proceedings of the National Academy of Sciences*, 94(7), pp. 2828–2832. doi: 10.1073/pnas.94.7.2828.

Huang, Y.-H., Ferrières, L. and Clarke, D. J. (2006) 'The role of the Rcs phosphorelay in Enterobacteriaceae', *Research in Microbiology*. Elsevier Masson, 157(3), pp. 206–212. doi: 10.1016/J.RESMIC.2005.11.005.

Hufnagel, D. A. *et al.* (2016) 'The Catabolite Repressor Protein-Cyclic AMP Complex Regulates csgD and Biofilm Formation in Uropathogenic *Escherichia coli*.', *Journal of bacteriology*. American Society for Microbiology Journals, 198(24), pp. 3329–3334. doi: 10.1128/JB.00652-16.

Hufnagel, D. A., Depas, W. H. and Chapman, M. R. (2015) 'The Biology of the *Escherichia coli* Extracellular Matrix', *Microbiology Spectrum*, 3(3). doi: 10.1128/microbiolspec.MB-0014-2014.

Hung, C. *et al.* (2013) '*Escherichia coli* Biofilms Have an Organized and Complex Extracellular Matrix Structure', *mBio*. American Society for Microbiology, 4(5), pp. e00645-13. doi: 10.1128/MBIO.00645-13.

Hunke, S., Keller, R. and Müller, V. S. (2012) ‘Signal integration by the Cpx-envelope stress system’, *FEMS Microbiology Letters*, 326(1), pp. 12–22. doi: 10.1111/j.1574-6968.2011.02436.x.

Ishizuka, H. *et al.* (1993) ‘A lowered concentration of cAMP receptor protein caused by glucose is an important determinant for catabolite repression in *Escherichia coli*’, *Molecular Microbiology*, 10(2), pp. 341–350. doi: 10.1111/j.1365-2958.1993.tb01960.x.

Itoh, Y. *et al.* (2008) ‘Roles of pgaABCD Genes in Synthesis, Modification, and Export of the *Escherichia coli* Biofilm Adhesin Poly-β-1,6-N-Acetyl-d-Glucosamine’, *Journal of Bacteriology*. American Society for Microbiology Journals, 190(10), pp. 3670–3680. doi: 10.1128/JB.01920-07.

Jackson, D. W. *et al.* (2002) ‘Biofilm formation and dispersal under the influence of the global regulator CsrA of *Escherichia coli*.’, *Journal of bacteriology*, 184(1), pp. 290–301. doi: 10.1128/jb.184.1.290-301.2002.

Jackson, D. W., Simecka, J. W. and Romeo, T. (2002) ‘Catabolite repression of *Escherichia coli* biofilm formation.’, *Journal of bacteriology*. American Society for Microbiology Journals, 184(12), pp. 3406–10. doi: 10.1128/JB.184.12.3406-3410.2002.

Jefferson, K. K. (2004) ‘What drives bacteria to produce a biofilm?’, *FEMS Microbiology Letters*. doi: 10.1016/j.femsle.2004.06.005.

Jenal, U. and Malone, J. (2006) ‘Mechanisms of Cyclic-di-GMP Signaling in Bacteria’, *Annual Review of Genetics*, 40(1), pp. 385–407. doi: 10.1146/annurev.genet.40.110405.090423.

Jo, B. H. *et al.* (2013) ‘Engineered Escherichia coli with periplasmic carbonic anhydrase as a biocatalyst for CO2 sequestration.’, *Applied and environmental microbiology*. American Society for Microbiology (ASM), 79(21), pp. 6697–705. doi: 10.1128/AEM.02400-13.

Jonas, K. *et al.* (2008) ‘The RNA binding protein CsrA controls cyclic di-GMP metabolism by directly regulating the expression of GGDEF proteins’, *Molecular Microbiology*, 70(1), pp. 236–257. doi: 10.1111/j.1365-2958.2008.06411.x.

Jones, C. H. *et al.* (1995) 'FimH adhesin of type 1 pili is assembled into a fibrillar tip structure in the Enterobacteriaceae', *Biochemistry*. Available at:

https://www.ncbi.nlm.nih.gov/pmc/articles/PMC42427/pdf/pnas01484-0297.pdf (Accessed: 11 June 2019).

Jubelin, G. *et al.* (2005) 'CpxR/OmpR interplay regulates curli gene expression in response to osmolarity in *Escherichia coli*.', *Journal of bacteriology*. American Society for Microbiology Journals, 187(6), pp. 2038–49. doi: 10.1128/JB.187.6.2038-2049.2005.

Kamaraju, K. *et al.* (2011) 'Effects on Membrane Lateral Pressure Suggest Permeation Mechanisms for Bacterial Quorum Signaling Molecules', *Biochemistry*, 50(32), pp. 6983–6993. doi: 10.1021/bi200684z.

Kanamaru, Kyoko *et al.* (2000) 'SdiA, an *Escherichia coli* homologue of quorum-sensing regulators, controls the expression of virulence factors in enterohaemorrhagic *Escherichia coli* O157:H7', *Molecular Microbiology*. John Wiley & Sons, Ltd (10.1111), 38(4), pp. 805–816. doi: 10.1046/j.1365-2958.2000.02171.x.

Kaplan, J. B. (2010) 'Biofilm dispersal: mechanisms, clinical implications, and potential therapeutic uses.', *Journal of dental research*. International Association for Dental Research, 89(3), pp. 205–18. doi: 10.1177/0022034509359403.

Kaplan, J. B. (2011) 'Antibiotic-induced biofilm formation', *International Journal of Artificial Organs*. doi: 10.5301/ijao.5000027.

Karunakaran, E. *et al.* (2011) '"Biofilmology": a multidisciplinary review of the study of microbial biofilms', *Applied Microbiology and Biotechnology*, 90(6), pp. 1869–1881. doi: 10.1007/s00253-011-3293-4.

Katouli, M. (2010) 'Population structure of gut *Escherichia coli* and its role in development of extra-intestinal infections.', *Iranian journal of microbiology*. Tehran University of Medical Sciences, 2(2), pp. 59–72. Available at: http://www.ncbi.nlm.nih.gov/pubmed/22347551 (Accessed: 4 June 2019).

Kendall, M. M. and Sperandio, V. (2014) 'Cell-to-Cell Signaling in *Escherichia coli* and Salmonella.', *EcoSal Plus*. NIH Public Access, 6(1). doi: 10.1128/ecosalplus.ESP-0002-2013.

Kikuchi, T. *et al.* (2005) 'Curli fibers are required for development of biofilm architecture in *Escherichia coli* K-12 and enhance bacterial adherence to human uroepithelial cells', *Microbiology and Immunology*. doi: 10.1111/j.1348-0421.2005.tb03678.x.

Kimkes, T. E. P. and Heinemann, M. (2018) 'Reassessing the role of the *Escherichia coli* CpxAR system in sensing surface contact', *PLOS ONE*. Edited by C. Beloin. Public Library of Science, 13(11), p. e0207181. doi: 10.1371/journal.pone.0207181.

Kjargaard, K. *et al.* (2000) 'Antigen 43 from *Escherichia coli* Induces Inter- and Intraspecies Cell Aggregation and Changes in Colony Morphology of *Pseudomonas fluorescens*', *Journal of Bacteriology*, 182(17), pp. 4789–4796. doi: 10.1128/JB.182.17.4789-4796.2000.

Klauck, G. *et al.* (2018) 'Spatial organization of different sigma factor activities and c-di-GMP signalling within the three-dimensional landscape of a bacterial biofilm.', *Open biology*. The Royal Society, 8(8). doi: 10.1098/rsob.180066.

Klemm, P. (1986) 'Two regulatory fim genes, fimB and fimE, control the phase variation of type 1 fimbriae in *Escherichia coli*.', *The EMBO journal*, 5(6), pp. 1389–93. Available at: http://www.ncbi.nlm.nih.gov/pubmed/2874022 (Accessed: 11 June 2019).

Kobayashi, K. (2007) '*Bacillus subtilis* Pellicle Formation Proceeds through Genetically Defined Morphological Changes', *Journal of Bacteriology*, 189(13), pp. 4920–4931. doi: 10.1128/JB.00157-07.

Kolenbrander, P. E. *et al.* (2002) 'Communication among oral bacteria.', *Microbiology and molecular biology reviews : MMBR*, 66(3), pp. 486–505, table of contents. doi: 10.1128/mmbr.66.3.486-505.2002.

Kolodkin-Gal, I. *et al.* (2010) 'D-amino acids trigger biofilm disassembly.', *Science (New York, N.Y.)*. NIH Public Access, 328(5978), pp. 627–9. doi: 10.1126/science.1188628.

Kopp, J. *et al.* (2017) 'Impact of Glycerol as Carbon Source onto Specific Sugar and Inducer Uptake Rates and Inclusion Body Productivity in *E. coli* BL21(DE3)', *Bioengineering*, 5(1), p. 1. doi: 10.3390/bioengineering5010001.

Koppolu, V. and Vasigala, V. K. (2016) 'Role of *Escherichia coli* in Biofuel Production.', *Microbiology insights*. SAGE Publications, 9, pp. 29–35. doi: 10.4137/MBI.S10878.

Krasowska, A. and Sigler, K. (2014) 'How microorganisms use hydrophobicity and what does this mean for human needs?', *Frontiers in cellular and infection microbiology*. Frontiers Media SA, 4, p. 112. doi: 10.3389/fcimb.2014.00112.

Kremling, A. *et al.* (2015) 'Understanding carbon catabolite repression in *Escherichia coli* using quantitative models', *Trends in Microbiology*, 23(2), pp. 99–109. doi: 10.1016/j.tim.2014.11.002.

Kwon, O. *et al.* (2000) 'The ArcB sensor kinase of *Escherichia coli*: genetic exploration of the transmembrane region.', *Journal of bacteriology*. American Society for Microbiology Journals, 182(10), pp. 2960–6. doi: 10.1128/JB.182.10.2960-2966.2000.

Laganenka, L., Colin, R. and Sourjik, V. (2016) 'Chemotaxis towards autoinducer 2 mediates autoaggregation in *Escherichia coli*', *Nature Communications*. Nature Publishing Group, 7(1), p. 12984. doi: 10.1038/ncomms12984.

De Lamo Marin, S. *et al.* (2007) 'Antibody catalyzed hydrolysis of a quorum sensing signal found in Gram-negative bacteria', *Bioorganic and Medicinal Chemistry Letters*. doi: 10.1016/j.bmcl.2006.12.118.

Landini, P. and Zehnder, A. J. B. (2002) 'The global regulatory hns gene negatively affects adhesion to solid surfaces by anaerobically grown *Escherichia coli* by modulating expression of flagellar genes and lipopolysaccharide production.', *Journal of bacteriology*. American Society for Microbiology Journals, 184(6), pp. 1522–9. doi: 10.1128/JB.184.6.1522-1529.2002.

Lane, A. N. and Kirschner, K. (1983) 'The catalytic mechanism of tryptophan synthase from *Escherichia coli*. Kinetics of the reaction of indole with the enzyme--L-serine complexes.', *European journal of biochemistry*, 129(3), pp. 571–82. Available at: http://www.ncbi.nlm.nih.gov/pubmed/6402362 (Accessed: 9 April 2019).

Latasa, C. *et al.* (2012) 'Salmonella biofilm development depends on the phosphorylation status of RcsB.', *Journal of bacteriology*. American Society for Microbiology Journals, 194(14), pp. 3708–22. doi: 10.1128/JB.00361-12.

Laubacher, M. E. and Ades, S. E. (2008) 'The Rcs phosphorelay is a cell envelope stress response activated by peptidoglycan stress and contributes to intrinsic antibiotic resistance.', *Journal of bacteriology*. American Society for Microbiology Journals, 190(6), pp. 2065–74. doi: 10.1128/JB.01740-07.

Laverty, G., Gorman, S. P. and Gilmore, B. F. (2014) 'Biomolecular Mechanisms of *Pseudomonas aeruginosa* and *Escherichia coli* Biofilm Formation.', *Pathogens (Basel, Switzerland)*. Multidisciplinary Digital Publishing Institute (MDPI), 3(3), pp. 596–632. doi: 10.3390/pathogens3030596.

Lécuyer, F. *et al.* (2018) ‘Biofilm Formation Drives Transfer of the Conjugative Element ICEBs1 in *Bacillus subtilis*’, *mSphere*. American Society for Microbiology Journals, 3(5), pp. e00473-18. doi: 10.1128/MSPHERE.00473-18.

Lee, J.-H. *et al.* (2012) ‘Indole-3-acetaldehyde from Rhodococcus sp. BFI 332 inhibits *Escherichia coli* O157:H7 biofilm formation’, *Applied Microbiology and Biotechnology*, 96(4), pp. 1071–1078. doi: 10.1007/s00253-012-3881-y.

Lee, J., Maeda, T., Hong, S. H. and Wood, T. K. (2009) ‘Reconfiguring the quorum-sensing regulator SdiA of *Escherichia coli* to control biofilm formation via indole and N-acylhomoserine lactones.’, *Applied and Environmental Microbiology*. American Society for Microbiology, 75(6), pp. 1703–16. doi: 10.1128/AEM.02081-08.

Lee, J. H. and Lee, J. (2010) ‘Indole as an intercellular signal in microbial communities’, *FEMS Microbiology Reviews*. doi: 10.1111/j.1574-6976.2009.00204.x.

Lee, J., Jayaraman, A. and Wood, Thomas K. (2007) ‘Indole is an inter-species biofilm signal mediated by SdiA’, *BMC Microbiology*. doi: 10.1186/1471-2180-7-42.

Leech, J. T. (2017) 'Development of an *Escherichia coli* Biofilm Platform for use in Biocatalysis', *University of Birmingham*. University of Birmingham.

Lehnen, D. *et al.* (2002) ‘LrhA as a new transcriptional key regulator of flagella, motility and chemotaxis genes in *Escherichia coli*’, *Molecular Microbiology*. John Wiley & Sons, Ltd (10.1111), 45(2), pp. 521–532. doi: 10.1046/j.1365-2958.2002.03032.x.

Lejeune, P. (2003) ‘Contamination of abiotic surfaces: what a colonizing bacterium sees and how to blur it.’, *Trends in microbiology*. Elsevier, 11(4), pp. 179–84. doi: 10.1016/S0966-842X(03)00047-7.

Lelong, C. *et al.* (2007) ‘The Crl-RpoS Regulon of *Escherichia coli*’, *Molecular & Cellular Proteomics*, 6(4), pp. 648–659. doi: 10.1074/mcp.M600191-MCP200.

Li, C. *et al.* (1993) ‘Adverse conditions which cause lack of flagella in *Escherichia coli*.’, *Journal of bacteriology*. American Society for Microbiology (ASM), 175(8), pp. 2229–35. doi: 10.1128/jb.175.8.2229-2235.1993.

Li, G., Tam, L.-K. and Tang, J. X. (2008) ‘Amplified effect of Brownian motion in bacterial near-surface swimming.’, *Proceedings of the National Academy of Sciences of the United States of America*. National Academy of Sciences, 105(47), pp. 18355–9. doi: 10.1073/pnas.0807305105.

Li, G. and Young, K. D. (2013) 'Indole production by the tryptophanase TnaA in *Escherichia coli* is determined by the amount of exogenous tryptophan', *Microbiology*, 159(Pt_2), pp. 402–410. doi: 10.1099/mic.0.064139-0.

Li, J. *et al.* (2007) 'Quorum sensing in *Escherichia coli* is signaled by AI-2/LsrR: effects on small RNA and biofilm architecture.', *Journal of bacteriology*. American Society for Microbiology Journals, 189(16), pp. 6011–20. doi: 10.1128/JB.00014-07.

Li, X. Z., Hauer, B. and Rosche, B. (2007) 'Single-species microbial biofilm screening for industrial applications', *Applied Microbiology and Biotechnology*, 76(6), pp. 1255–1262. doi: 10.1007/s00253-007-1108-4.

Li, Y. H. and Tian, X. (2012) 'Quorum sensing and bacterial social interactions in biofilms', *Sensors*. doi: 10.3390/s120302519.

Li, Z. *et al.* (2012) 'Structures of the PelD Cyclic Diguanylate Effector Involved in Pellicle Formation in *Pseudomonas aeruginosa* PAO1', *Journal of Biological Chemistry*, 287(36), pp. 30191–30204. doi: 10.1074/jbc.M112.378273.

Lim, J. Y., May, J. M. and Cegelski, L. (2012) 'Dimethyl sulfoxide and ethanol elicit increased amyloid biogenesis and amyloid-integrated biofilm formation in *Escherichia coli*.', *Applied and environmental microbiology*. American Society for Microbiology (ASM), 78(9), pp. 3369–78. doi: 10.1128/AEM.07743-11.

Limoli, D. H., Jones, C. J. and Wozniak, D. J. (2015) 'Bacterial Extracellular Polysaccharides in Biofilm Formation and Function.', *Microbiology spectrum*. NIH Public Access, 3(3). doi: 10.1128/microbiolspec.MB-0011-2014.

Lin, E. (1976) 'Glycerol Dissimilation and its Regulation in Bacteria', *Annual Review of Microbiology*, 30(1), pp. 535–578. doi: 10.1146/annurev.mi.30.100176.002535.

Liu, X. *et al.* (2015) 'Physiological Function of Rac Prophage During Biofilm Formation and Regulation of Rac Excision in *Escherichia coli* K-12', *Scientific Reports*. Nature Publishing Group, 5(1), p. 16074. doi: 10.1038/srep16074.

Liu, Y. and Tay, J.-H. (2002) 'The essential role of hydrodynamic shear force in the formation of biofilm and granular sludge', *Water Research*. Pergamon, 36(7), pp. 1653–1665. doi: 10.1016/S0043-1354(01)00379-7.

Lodish, H. *et al.* (2000) 'Hierarchical Structure of Proteins'. W. H. Freeman. Available at: https://www.ncbi.nlm.nih.gov/books/NBK21581/ (Accessed: 26 March 2019).

Lüdecke, C. *et al.* (2014) 'Reproducible Biofilm Cultivation of Chemostat-Grown *Escherichia coli* and Investigation of Bacterial Adhesion on Biomaterials Using a Non-Constant-Depth Film Fermenter', *PLoS ONE*. Public Library of Science, 9(1). doi: 10.1371/JOURNAL.PONE.0084837.

Macnab, R. M. (2003) 'How Bacteria Assemble Flagella', *Annual Review of Microbiology*. Annual Reviews 4139 El Camino Way, P.O. Box 10139, Palo Alto, CA 94303-0139, USA , 57(1), pp. 77–100. doi: 10.1146/annurev.micro.57.030502.090832.

Majdalani, N. and Gottesman, S. (2005) 'THE RCS PHOSPHORELAY: A Complex Signal Transduction System', *Annual Review of Microbiology*, 59(1), pp. 379–405. doi: 10.1146/annurev.micro.59.050405.101230.

Maksimova, Y. G. (2014) 'Microbial biofilms in biotechnological processes', *Applied Biochemistry and Microbiology*. Pleiades Publishing, 50(8), pp. 750–760. doi: 10.1134/S0003683814080043.

Di Martino, P. *et al.* (2003) 'Indole can act as an extracellular signal to regulate biofilm formation of *Escherichia coli* and other indole-producing bacteria', *Canadian Journal of Microbiology*, 49(7), pp. 443–449. doi: 10.1139/w03-056.

May, T. and Okabe, S. (2008) '*Escherichia coli* harboring a natural IncF conjugative F plasmid develops complex mature biofilms by stimulating synthesis of colanic acid and curli.', *Journal of bacteriology*. American Society for Microbiology (ASM), 190(22), pp. 7479–90. doi: 10.1128/JB.00823-08.

McDaniel, L. E., Bailey, E. G. and Zimmerli, A. (1965) 'Effect of Oxygen-Supply Rates on Growth of *Escherichia coli*', *Applied microbiology*. American Society for Microbiology (ASM), 13(1), pp. 109–14. Available at: http://www.ncbi.nlm.nih.gov/pubmed/14264837 (Accessed: 12 March 2019).

Mika, F. and Hengge, R. (2014) 'Small RNAs in the control of RpoS, CsgD, and biofilm architecture of *Escherichia coli*.', *RNA biology*. Taylor & Francis, 11(5), pp. 494–507. doi: 10.4161/rna.28867.

Miller, M. B. and Bassler, B. L. (2001) 'Quorum Sensing in Bacteria', *Annual Review of Microbiology*, 55(1), pp. 165–199. doi: 10.1146/annurev.micro.55.1.165.

Miller, W. G., Leveau, J. H. J. and Lindow, S. E. (2000) 'Improved gfp and inaZ Broad-Host-Range Promoter-Probe Vectors', *Molecular Plant-Microbe Interactions*. The

American Phytopathological Society, 13(11), pp. 1243–1250. doi: 10.1094/MPMI.2000.13.11.1243.

Molin, S. and Tolker-Nielsen, T. (2003) 'Gene transfer occurs with enhanced efficiency in biofilms and induces enhanced stabilisation of the biofilm structure.', *Current opinion in biotechnology*, 14(3), pp. 255–61. Available at: http://www.ncbi.nlm.nih.gov/pubmed/12849777 (Accessed: 11 June 2019).

Moreira, R. N. *et al.* (2017) 'BolA Is Required for the Accurate Regulation of c-di-GMP, a Central Player in Biofilm Formation', *mBio*. American Society for Microbiology, 8(5), pp. e00443-17. doi: 10.1128/MBIO.00443-17.

Muffler, K. *et al.* (2014) 'Application of biofilm bioreactors in white biotechnology', *Advances in Biochemical Engineering/Biotechnology*. doi: 10.1007/10_2013_267.

Müller, C. M. *et al.* (2009) 'Type 1 fimbriae, a colonization factor of uropathogenic *Escherichia coli*, are controlled by the metabolic sensor CRP-cAMP.', *PLoS pathogens*. Public Library of Science, 5(2), p. e1000303. doi: 10.1371/journal.ppat.1000303.

Nadell, C. D., Xavier, J. B. and Foster, K. R. (2009) 'The sociobiology of biofilms', *FEMS Microbiology Reviews*, 33(1), pp. 206–224. doi: 10.1111/j.1574-6976.2008.00150.x.

Nagy, A. *et al.* (2015) 'Role of Extracellular Structures of *Escherichia coli* O157:H7 in Initial Attachment to Biotic and Abiotic Surfaces.', *Applied and environmental microbiology*. American Society for Microbiology, 81(14), pp. 4720–7. doi: 10.1128/AEM.00215-15.

Nait Chabane, Y. *et al.* (2014) 'Characterisation of Pellicles Formed by *Acinetobacter baumannii* at the Air-Liquid Interface', *PLoS ONE*. Edited by A. Driks, 9(10), p. e111660. doi: 10.1371/journal.pone.0111660.

Narang, A. (2009) 'Quantitative effect and regulatory function of cyclic adenosine 5'-phosphate in *Escherichia coli*.', *Journal of biosciences*, 34(3), pp. 445–63. Available at: http://www.ncbi.nlm.nih.gov/pubmed/19805906 (Accessed: 19 June 2019).

Nenninger, A. A., Robinson, L. S. and Hultgren, S. J. (2009) 'Localized and efficient curli nucleation requires the chaperone-like amyloid assembly protein CsgF.', *Proceedings of the National Academy of Sciences of the United States of America*. National Academy of Sciences, 106(3), pp. 900–5. doi: 10.1073/pnas.0812143106.

Ogasawara, H. *et al.* (2010) 'Regulation of the *Escherichia coli* csgD promoter: interplay between five transcription factors', *Microbiology*, 156(8), pp. 2470–2483. doi: 10.1099/mic.0.039131-0.

Ogasawara, H., Yamamoto, K. and Ishihama, A. (2010) 'Regulatory role of MlrA in transcription activation of csgD, the master regulator of biofilm formation in *Escherichia coli*', *FEMS Microbiology Letters*. John Wiley & Sons, Ltd (10.1111), 312(2), pp. 160–168. doi: 10.1111/j.1574-6968.2010.02112.x.

Ogasawara, H., Yamamoto, K. and Ishihama, A. (2011) 'Role of the biofilm master regulator CsgD in cross-regulation between biofilm formation and flagellar synthesis.', *Journal of bacteriology*. American Society for Microbiology Journals, 193(10), pp. 2587–97. doi: 10.1128/JB.01468-10.

Ogata, K., Uchiyama, K. and Yamada, H. (1967) 'Metabolism of Aromatic Amino Acid in Microorganisms', *Agricultural and Biological Chemistry*, 31(2), pp. 200–206. doi: 10.1080/00021369.1967.10858795.

Oh, Y. J. *et al.* (2007) 'Biofilm formation and local electrostatic force characteristics of *Escherichia coli* O157:H7 observed by electrostatic force microscopy', *Applied Physics Letters*. American Institute of Physics, 90(14), p. 143901. doi: 10.1063/1.2719030.

Old, D. C. and Duguid, J. P. (1970) 'Selective outgrowth of fimbriate bacteria in static liquid medium.', *Journal of bacteriology*. American Society for Microbiology Journals, 103(2), pp. 447–56. Available at: http://www.ncbi.nlm.nih.gov/pubmed/4914569 (Accessed: 11 July 2019).

Olsén, A *et al.* (1993) 'The RpoS Sigma factor relieves H-NS-mediated transcriptional repression of csgA, the subunit gene of fibronectin-binding curli in *Escherichia coli*', *Molecular Microbiology*. John Wiley & Sons, Ltd (10.1111), 7(4), pp. 523–536. doi: 10.1111/j.1365-2958.1993.tb01143.x.

Olsen, P. B. *et al.* (1998) 'Differential temperature modulation by H-NS of the *fimB* and *fimE* recombinase genes which control the orientation of the type 1 fimbrial phase switch', *FEMS Microbiology Letters*, 162(1), pp. 17–23. doi: 10.1111/j.1574-6968.1998.tb12973.x.

Ong, Y.-L. *et al.* (1999) 'Adhesion Forces between *E. coli* Bacteria and Biomaterial Surfaces', *Langmuir*, 15(8), pp. 2719–2725. doi: 10.1021/la981104e.

Ono, S. *et al.* (2005) 'H-NS is a part of a thermally controlled mechanism for bacterial gene regulation.', *The Biochemical journal*. Portland Press Ltd, 391(Pt 2), pp. 203–13. doi: 10.1042/BJ20050453.

Ophir, T. and Gutnick, D. L. (1994) 'A role for exopolysaccharides in the protection of microorganisms from desiccation.', *Applied and environmental microbiology*. American Society for Microbiology, 60(2), pp. 740–5. Available at: http://www.ncbi.nlm.nih.gov/pubmed/16349202 (Accessed: 7 June 2019).

Orndorff, P. E. *et al.* (2004) 'Immunoglobulin-mediated agglutination of and biofilm formation by *Escherichia coli* K-12 require the type 1 pilus fiber.', *Infection and immunity*, 72(4), pp. 1929–38. doi: 10.1128/iai.72.4.1929-1938.2004.

Oshima, T. *et al.* (2002) 'Transcriptome analysis of all two-component regulatory system mutants of *Escherichia coli* K-12', *Molecular Microbiology*. John Wiley & Sons, Ltd (10.1111), 46(1), pp. 281–291. doi: 10.1046/j.1365-2958.2002.03170.x.

Otto, K. and Silhavy, T. J. (2002) 'Surface sensing and adhesion of *Escherichia coli* controlled by the Cpx-signaling pathway', *Proceedings of the National Academy of Sciences*. doi: 10.1073/pnas.042521699.

Palmer, J., Flint, S. and Brooks, J. (2007) 'Bacterial cell attachment, the beginning of a biofilm', *Journal of Industrial Microbiology and Biotechnology*. doi: 10.1007/s10295-007-0234-4.

Park, A. *et al.* (2011) 'Effect of shear stress on the formation of bacterial biofilm in a microfluidic channel', *BioChip Journal*. The Korean BioChip Society (KBCS), 5(3), pp. 236–241. doi: 10.1007/s13206-011-5307-9.

Paul, K. *et al.* (2010) 'The c-di-GMP Binding Protein YcgR Controls Flagellar Motor Direction and Speed to Affect Chemotaxis by a "Backstop Brake" Mechanism', *Molecular Cell*, 38(1), pp. 128–139. doi: 10.1016/j.molcel.2010.03.001.

Paytubi, S. *et al.* (2017) 'Nutrient Composition Promotes Switching between Pellicle and Bottom Biofilm in Salmonella', *Frontiers in Microbiology*. Frontiers, 8, p. 2160. doi: 10.3389/fmicb.2017.02160.

Pereira, C. S., Thompson, J. A. and Xavier, K. B. (2013) 'AI-2-mediated signalling in bacteria', *FEMS Microbiology Reviews*. Narnia, 37(2), pp. 156–181. doi: 10.1111/j.1574-6976.2012.00345.x.

Perni, S. *et al.* (2013) 'Optimisation of engineered *Escherichia coli* biofilms for enzymatic biosynthesis of l-halotryptophans.', *AMB Express*. Springer, 3(1), p. 66. doi: 10.1186/2191-0855-3-66.

Perrin, C. *et al.* (2009) 'Nickel promotes biofilm formation by *Escherichia coli* K-12 strains that produce curli.', *Applied and environmental microbiology*. American Society for Microbiology, 75(6), pp. 1723–33. doi: 10.1128/AEM.02171-08.

Pesavento, C. *et al.* (2008) 'Inverse regulatory coordination of motility and curli-mediated adhesion in *Escherichia coli*.', *Genes & development*. Cold Spring Harbor Laboratory Press, 22(17), pp. 2434–46. doi: 10.1101/gad.475808.

Pi, J., Wookey, P. J. and Pittard, A. J. (1991) 'Cloning and sequencing of the pheP gene, which encodes the phenylalanine-specific transport system of *Escherichia coli*.', *Journal of bacteriology*. American Society for Microbiology Journals, 173(12), pp. 3622–9. doi: 10.1128/jb.173.12.3622-3629.1991.

Picioreanu, C., Van Loosdrecht, M. C. and Heijnen, J. J. (2000) 'Effect of diffusive and convective substrate transport on biofilm structure formation: a two-dimensional modeling study.', *Biotechnology and bioengineering*, 69(5), pp. 504–15. Available at: http://www.ncbi.nlm.nih.gov/pubmed/10898860 (Accessed: 23 April 2019).

Pletnev, P. *et al.* (2015) 'Survival guide: *Escherichia coli* in the stationary phase.', *Acta naturae*. National Research University Higher School of Economics, 7(4), pp. 22–33. Available at: http://www.ncbi.nlm.nih.gov/pubmed/26798489 (Accessed: 21 June 2019).

Polen, T. *et al.* (2005) 'The global gene expression response of *Escherichia coli* to l-phenylalanine', *Journal of Biotechnology*. Elsevier, 115(3), pp. 221–237. doi: 10.1016/J.JBIOTEC.2004.08.017.

Povolotsky, T. L. and Hengge, R. (2012) '"Life-style" control networks in *Escherichia coli*: Signaling by the second messenger c-di-GMP', *Journal of Biotechnology*, 160(1–2), pp. 10–16. doi: 10.1016/j.jbiotec.2011.12.024.

Pratt, L. A. and Kolter, R. (1998) 'Genetic analysis of *Escherichia coli* biofilm formation: roles of flagella, motility, chemotaxis and type I pili.', *Molecular microbiology*, 30(2), pp. 285–93. Available at: http://www.ncbi.nlm.nih.gov/pubmed/9791174 (Accessed: 10 May 2019).

Prigent-Combaret, C. *et al.* (1999) 'Abiotic surface sensing and biofilm-dependent regulation of gene expression in *Escherichia coli*.', *Journal of bacteriology*, 181(19), pp. 5993–6002. Available at: http://www.ncbi.nlm.nih.gov/pubmed/10498711 (Accessed: 6 March 2019).

Prigent-Combaret, C. *et al.* (2000) 'Developmental pathway for biofilm formation in curli-producing *Escherichia coli* strains: role of flagella, curli and colanic acid.', *Environmental microbiology*, 2(4), pp. 450–64. Available at: http://www.ncbi.nlm.nih.gov/pubmed/11234933 (Accessed: 11 June 2019).

Prigent-Combaret, C. *et al.* (2001) 'Complex regulatory network controls initial adhesion and biofilm formation in *Escherichia coli* via regulation of the csgD gene.', *Journal of bacteriology*. American Society for Microbiology Journals, 183(24), pp. 7213–23. doi: 10.1128/JB.183.24.7213-7223.2001.

Raivio, T. L. and Silhavy, T. J. (1997) 'Transduction of envelope stress in *Escherichia coli* by the Cpx two-component system.', *Journal of bacteriology*. American Society for Microbiology (ASM), 179(24), pp. 7724–33. doi: 10.1128/jb.179.24.7724-7733.1997.

Rampersaud, A., Harlocker, S. L. and Inouye, M. (1994) 'The OmpR protein of *Escherichia coli* binds to sites in the ompF promoter region in a hierarchical manner determined by its degree of phosphorylation.', *The Journal of biological chemistry*, 269(17), pp. 12559–66. Available at: http://www.ncbi.nlm.nih.gov/pubmed/8175665 (Accessed: 16 June 2019).

Reisner, A. *et al.* (2003) 'Development and maturation of *Escherichia coli* K-12 biofilms.', *Molecular microbiology*, 48(4), pp. 933–46. Available at: http://www.ncbi.nlm.nih.gov/pubmed/12753187 (Accessed: 4 June 2019).

Ren, G. *et al.* (2016) 'Effects of Lipopolysaccharide Core Sugar Deficiency on Colanic Acid Biosynthesis in *Escherichia coli*.', *Journal of bacteriology*. American Society for Microbiology Journals, 198(11), pp. 1576–1584. doi: 10.1128/JB.00094-16.

Renner, L. D. and Weibel, D. B. (2011) 'Physicochemical regulation of biofilm formation', *MRS bulletin / Materials Research Society*. NIH Public Access, 36(5), p. 347. doi: 10.1557/MRS.2011.65.

Rodrigues, D. F. and Elimelech, M. (2009) 'Role of type 1 fimbriae and mannose in the development of *Escherichia coli* K12 biofilm: from initial cell adhesion to biofilm formation', *Biofouling*, 25(5), pp. 401–411. doi: 10.1080/08927010902833443.

Rodriguez, A. *et al.* (2014) 'Engineering *Escherichia coli* to overproduce aromatic amino acids and derived compounds.', *Microbial cell factories*. BioMed Central, 13(1), p. 126. doi: 10.1186/s12934-014-0126-z.

Römling, U. *et al.* (1998) 'Curli fibers are highly conserved between *Salmonella typhimurium* and *Escherichia coli* with respect to operon structure and regulation.', *Journal of bacteriology*, 180(3), pp. 722–31. Available at: http://www.ncbi.nlm.nih.gov/pubmed/9457880 (Accessed: 6 March 2019).

Römling, U. and Balsalobre, C. (2012) 'Biofilm infections, their resilience to therapy and innovative treatment strategies', *Journal of Internal Medicine*, 272(6), pp. 541–561. doi: 10.1111/joim.12004.

Römling, U. and Galperin, M. Y. (2015) 'Bacterial cellulose biosynthesis: diversity of operons, subunits, products, and functions.', *Trends in microbiology*. NIH Public Access, 23(9), pp. 545–57. doi: 10.1016/j.tim.2015.05.005.

Römling, U., Galperin, M. Y. and Gomelsky, M. (2013) 'Cyclic di-GMP: the first 25 years of a universal bacterial second messenger.', *Microbiology and molecular biology reviews : MMBR*. American Society for Microbiology (ASM), 77(1), pp. 1–52. doi: 10.1128/MMBR.00043-12.

Rosche, B. *et al.* (2009) 'Microbial biofilms: a concept for industrial catalysis?', *Trends in biotechnology*. Elsevier, 27(11), pp. 636–43. doi: 10.1016/j.tibtech.2009.08.001.

Ross, P., Mayer, R. and Benziman, M. (1991) 'Cellulose biosynthesis and function in bacteria.', *Microbiological reviews*. American Society for Microbiology (ASM), 55(1), pp. 35–58. Available at: http://www.ncbi.nlm.nih.gov/pubmed/2030672 (Accessed: 14 June 2019).

Roux, D. *et al.* (2015) 'Identification of Poly- *N*- acetylglucosamine as a Major Polysaccharide Component of the *Bacillus subtilis* Biofilm Matrix', *Journal of Biological Chemistry*, 290(31), pp. 19261–19272. doi: 10.1074/jbc.M115.648709.

Rusconi, R. *et al.* (2010) 'Laminar flow around corners triggers the formation of biofilm streamers', *Journal of The Royal Society Interface*, 7(50), pp. 1293–1299. doi: 10.1098/rsif.2010.0096.

Russo, F. D. and Silhavy, T. J. (1991) 'EnvZ controls the concentration of phosphorylated OmpR to mediate osmoregulation of the porin genes.', *Journal of*

molecular biology, 222(3), pp. 567–80. Available at: http://www.ncbi.nlm.nih.gov/pubmed/1660927 (Accessed: 16 June 2019).

Rutherford, S. T. and Bassler, B. L. (2012) 'Bacterial quorum sensing: Its role in virulence and possibilities for its control', *Cold Spring Harbor Perspectives in Medicine*. doi: 10.1101/cshperspect.a012427.

Ryjenkov, D. A. *et al.* (2006) 'The PilZ Domain Is a Receptor for the Second Messenger c-di-GMP', *Journal of Biological Chemistry*, 281(41), pp. 30310–30314. doi: 10.1074/jbc.C600179200.

Sabag-Daigle, A. *et al.* (2012) 'The acyl homoserine lactone receptor, SdiA, of *Escherichia coli* and *Salmonella enterica* serovar Typhimurium does not respond to indole.', *Applied and environmental microbiology*. American Society for Microbiology (ASM), 78(15), pp. 5424–31. doi: 10.1128/AEM.00046-12.

Salmon, K. A. *et al.* (2005) 'Global gene expression profiling in *Escherichia coli* K12: effects of oxygen availability and ArcA.', *The Journal of biological chemistry*. American Society for Biochemistry and Molecular Biology, 280(15), pp. 15084–96. doi: 10.1074/jbc.M414030200.

Schaefer, A. L. *et al.* (1996) 'Generation of cell-to-cell signals in quorum sensing: acyl homoserine lactone synthase activity of a purified *Vibrio fischeri* LuxI protein.', *Proceedings of the National Academy of Sciences of the United States of America*. National Academy of Sciences, 93(18), pp. 9505–9. doi: 10.1073/pnas.93.18.9505.

Schauder, S. *et al.* (2001) 'The LuxS family of bacterial autoinducers: biosynthesis of a novel quorum-sensing signal molecule.', *Molecular microbiology*, 41(2), pp. 463–76. Available at: http://www.ncbi.nlm.nih.gov/pubmed/11489131 (Accessed: 27 June 2019).

Schembri, M. A. *et al.* (2003) 'Differential expression of the *Escherichia coli* autoaggregation factor antigen 43.', *Journal of bacteriology*. American Society for Microbiology (ASM), 185(7), pp. 2236–42. doi: 10.1128/jb.185.7.2236-2242.2003.

Schilling, J. D., Mulvey, M. A. and Hultgren, S. J. (2001) 'Structure and Function of *Escherichia coli* Type 1 Pili: New Insightinto the Pathogenesis of Urinary Tract Infections', *The Journal of Infectious Diseases*. Narnia, 183(s1), pp. S36–S40. doi: 10.1086/318855.

Serra, D. O. *et al.* (2013) ‘Microanatomy at cellular resolution and spatial order of physiological differentiation in a bacterial biofilm.’, *mBio*. American Society for Microbiology, 4(2), pp. e00103-13. doi: 10.1128/mBio.00103-13.

Serra, D. O., Richter, A. M. and Hengge, R. (2013) ‘Cellulose as an Architectural Element in Spatially Structured *Escherichia coli* Biofilms’, *Journal of Bacteriology*, 195(24), pp. 5540–5554. doi: 10.1128/JB.00946-13.

Sheldon, R. A. and Woodley, J. M. (2018) ‘Role of Biocatalysis in Sustainable Chemistry’, *Chemical Reviews*, 118(2), pp. 801–838. doi: 10.1021/acs.chemrev.7b00203.

Shi, W. *et al.* (1993) ‘Mechanism of adverse conditions causing lack of flagella in *Escherichia coli*.’, *Journal of Bacteriology*, 175(8), pp. 2236–2240. doi: 10.1128/jb.175.8.2236-2240.1993.

Shimazaki, J. *et al.* (2012) ‘l-Tryptophan prevents *Escherichia coli* biofilm formation and triggers biofilm degradation’, *Biochemical and Biophysical Research Communications*, 419(4), pp. 715–718. doi: 10.1016/j.bbrc.2012.02.085.

Shin, H.-D. *et al.* (2010) ‘Escherichia coli Binary Culture Engineered for Direct Fermentation of Hemicellulose to a Biofuel’, *Applied and Environmental Microbiology*, 76(24), pp. 8150–8159. doi: 10.1128/AEM.00908-10.

Simm, R. *et al.* (2004) ‘GGDEF and EAL domains inversely regulate cyclic di-GMP levels and transition from sessility to motility’, *Molecular Microbiology*, 53(4), pp. 1123–1134. doi: 10.1111/j.1365-2958.2004.04206.x.

Singh, S. *et al.* (2017) ‘Understanding the Mechanism of Bacterial Biofilms Resistance to Antimicrobial Agents.’, *The open microbiology journal*. Bentham Science Publishers, 11, pp. 53–62. doi: 10.2174/1874285801711010053.

Singh, V. *et al.* (2015a) ‘Therapeutic implication of L-phenylalanine aggregation mechanism and its modulation by D-phenylalanine in phenylketonuria’, *Scientific Reports*. Nature Publishing Group, 4(1), p. 3875. doi: 10.1038/srep03875.

Sledjeski, D. D. and Gottesman, S. (1996) ‘Osmotic shock induction of capsule synthesis in *Escherichia coli* K-12.’, *Journal of bacteriology*. American Society for Microbiology Journals, 178(4), pp. 1204–6. doi: 10.1128/jb.178.4.1204-1206.1996.

Sledjeski, D. and Gotresman, S. (2003) 'A small RNA acts as an antisilencer of the H-NS-silenced rcsA gene of *Escherichia coli* (DsrA/lon/transcription initiation/capsule

synthesis)', *Biochemistry Communicated by Sankar Adhya*. Available at: https://www.pnas.org/content/pnas/92/6/2003.full.pdf (Accessed: 17 June 2019).

Sleutel, M. *et al.* (2017) 'Nucleation and growth of a bacterial functional amyloid at single fiber resolution', *Nature chemical biology*. Europe PMC Funders, 13(8), p. 902. doi: 10.1038/NCHEMBIO.2413.

Smith, Daniel R *et al.* (2017) 'The Production of Curli Amyloid Fibers Is Deeply Integrated into the Biology of *Escherichia coli*.', *Biomolecules*. Multidisciplinary Digital Publishing Institute (MDPI), 7(4). doi: 10.3390/biom7040075.

Son, M. S. and Taylor, R. K. (2012) 'Growth and Maintenance of *Escherichia coli* Laboratory Strains', in *Current Protocols in Microbiology*. Hoboken, NJ, USA: John Wiley & Sons, Inc. doi: 10.1002/9780471729259.mc05a04s27.

Soutourina, O. *et al.* (1999) 'Multiple Control of Flagellum Biosynthesis in *Escherichia coli*: Role of H-NS Protein and the Cyclic AMP-Catabolite Activator Protein Complex in Transcription of the flhDC Master Operon', *Journal of Bacteriology*. American Society for Microbiology (ASM), 181(24), p. 7500. Available at: https://www.ncbi.nlm.nih.gov/pmc/articles/PMC94207/ (Accessed: 20 June 2019).

Sperandio, V. *et al.* (2003) 'Bacteria-host communication: The language of hormones', *Proceedings of the National Academy of Sciences*, 100(15), pp. 8951–8956. doi: 10.1073/pnas.1537100100.

Sperandio, V., Torres, A. G. and Kaper, J. B. (2002) 'Quorum sensing *Escherichia coli* regulators B and C (QseBC): a novel two-component regulatory system involved in the regulation of flagella and motility by quorum sensing in *E. coli*.', *Molecular microbiology*, 43(3), pp. 809–21. Available at: http://www.ncbi.nlm.nih.gov/pubmed/11929534 (Accessed: 27 June 2019).

Stella, S. *et al.* (2006) 'Environmental Control of the In vivo Oligomerization of Nucleoid Protein H-NS', *Journal of Molecular Biology*. Academic Press, 355(2), pp. 169–174. doi: 10.1016/J.JMB.2005.10.034.

Stevenson, G. *et al.* (1996) 'Organization of the *Escherichia coli* K-12 Gene Cluster Responsible for Production of the Extracellular Polysaccharide Colanic Acid', *Journal of Bacteriology*. Available at: http://jb.asm.org/ (Accessed: 6 June 2019).

Stewart, P. S. (2014) 'Biophysics of biofilm infection.', *Pathogens and disease*. NIH Public Access, 70(3), pp. 212–8. doi: 10.1111/2049-632X.12118.

Stock, A. M., Robinson, V. L. and Goudreau, P. N. (2000) 'Two-Component Signal Transduction', *Annual Review of Biochemistry*. Annual Reviews 4139 El Camino Way, P.O. Box 10139, Palo Alto, CA 94303-0139, USA , 69(1), pp. 183–215. doi: 10.1146/annurev.biochem.69.1.183.

Stoodley, P. et al. (1997) 'Consensus model of biofilm structure', Biofilms: community interactions and control, edited by Wimpenny, J.W.T., Handley, P.S., Gilbert, P., Lappin-Scott, H.M., and Jones, M. BioLine, Cardiff, UK.

Stout, V. (1996) 'Identification of the promoter region for the colanic acid polysaccharide biosynthetic genes in *Escherichia coli* K-12.', *Journal of Bacteriology*, 178(14), pp. 4273–4280. doi: 10.1128/jb.178.14.4273-4280.1996.

Stout, V. and Gottesman, S. (1990) 'RcsB and RcsC: a two-component regulator of capsule synthesis in *Escherichia coli*.', *Journal of Bacteriology*, 172(2), pp. 659–669. doi: 10.1128/jb.172.2.659-669.1990.

Surette, M. G. and Bassler, B. L. (1998) 'Quorum sensing in *Escherichia coli* and *Salmonella typhimurium*', *Proceedings of the National Academy of Sciences*, 95(12), pp. 7046–7050. doi: 10.1073/pnas.95.12.7046.

Taga, M. E., Miller, S. T. and Bassler, B. L. (2003) 'Lsr-mediated transport and processing of AI-2 in *Salmonella typhimurium*.', *Molecular microbiology*, 50(4), pp. 1411–27. Available at: http://www.ncbi.nlm.nih.gov/pubmed/14622426 (Accessed: 27 June 2019).

Tashiro, Y. *et al.* (2014) 'Low concentrations of ethanol stimulate biofilm and pellicle formation in *Pseudomonas aeruginosa*', *Bioscience, Biotechnology, and Biochemistry*. Taylor & Francis, 78(1), pp. 178–181. doi: 10.1080/09168451.2014.877828.

Thomas, W. E. *et al.* (2002) 'Bacterial Adhesion to Target Cells Enhanced by Shear Force', *Cell*. Cell Press, 109(7), pp. 913–923. doi: 10.1016/S0092-8674(02)00796-1.

Thomen, P. *et al.* (2017) 'Bacterial biofilm under flow: First a physical struggle to stay, then a matter of breathing.', *PloS one*. Public Library of Science, 12(4), p. e0175197. doi: 10.1371/journal.pone.0175197.

Tong, X. *et al.* (2016) 'Rapid enzyme regeneration results in the striking catalytic longevity of an engineered, single species, biocatalytic biofilm', *Microbial Cell Factories*. BioMed Central, 15(1), p. 180. doi: 10.1186/s12934-016-0579-3.

Tseng, C.-P. (2006) ‘Regulation of fumarase (fumB) gene expression in *Escherichia coli* in response to oxygen, iron and heme availability: role of the arcA, fur, and hemA gene products’, *FEMS Microbiology Letters*. Narnia, 157(1), pp. 67–72. doi: 10.1111/j.1574-6968.1997.tb12754.x.

Tsoligkas, A. N. *et al.* (2011) ‘Engineering Biofilms for Biocatalysis’, *ChemBioChem*. John Wiley & Sons, Ltd, 12(9), pp. 1391–1395. doi: 10.1002/cbic.201100200.

Tsoligkas, A. N. *et al.* (2012) ‘Characterisation of spin coated engineered *Escherichia coli* biofilms using atomic force microscopy’, *Colloids and Surfaces B: Biointerfaces*. doi: 10.1016/j.colsurfb.2011.09.007.

Tuson, Hannah H and Weibel, D. B. (2013) ‘Bacteria-surface interactions.’, *Soft matter*. NIH Public Access, 9(18), pp. 4368–4380. doi: 10.1039/C3SM27705D.

Ueda, A. and Wood, T. K. (2009) ‘Connecting quorum sensing, c-di-GMP, pel polysaccharide, and biofilm formation in *Pseudomonas aeruginosa* through tyrosine phosphatase TpbA (PA3885).’, *PLoS pathogens*. Public Library of Science, 5(6), p. e1000483. doi: 10.1371/journal.ppat.1000483.

Urbanowski, M. L., Lostroh, C. P. and Greenberg, E. P. (2004) ‘Reversible acyl-homoserine lactone binding to purified *Vibrio fischeri* LuxR protein.’, *Journal of bacteriology*, 186(3), pp. 631–7. doi: 10.1128/jb.186.3.631-637.2004.

Vianney, A. *et al.* (2005) ‘*Escherichia coli* tol and rcs genes participate in the complex network affecting curli synthesis’, *Microbiology*, 151(7), pp. 2487–2497. doi: 10.1099/mic.0.27913-0.

Vidal, O. *et al.* (1998) ‘Isolation of an *Escherichia coli* K-12 mutant strain able to form biofilms on inert surfaces: involvement of a new ompR allele that increases curli expression.’, *Journal of bacteriology*. American Society for Microbiology (ASM), 180(9), pp. 2442–9. Available at: http://www.ncbi.nlm.nih.gov/pubmed/9573197 (Accessed: 12 March 2019).

Waldron, D. E., Owen, P. and Dorman, C. J. (2002) ‘Competitive interaction of the OxyR DNA-binding protein and the Dam methylase at the antigen 43 gene regulatory region in *Escherichia coli*.’, *Molecular microbiology*, 44(2), pp. 509–20. Available at: http://www.ncbi.nlm.nih.gov/pubmed/11972787 (Accessed: 4 June 2019).

Wall, E., Majdalani, N. and Gottesman, S. (2018) 'The Complex Rcs Regulatory Cascade', *Annual Review of Microbiology*, 72(1), pp. 111–139. doi: 10.1146/annurev-micro-090817-062640.

Walters, M., Sircili, M. P. and Sperandio, V. (2006) 'AI-3 Synthesis Is Not Dependent on luxS in *Escherichia coli*', *Journal of Bacteriology*, 188(16), pp. 5668–5681. doi: 10.1128/JB.00648-06.

Wang, L. C. *et al.* (2012) 'The inner membrane histidine kinase EnvZ senses osmolality via helix-coil transitions in the cytoplasm', *The EMBO Journal*, 31(11), pp. 2648–2659. doi: 10.1038/emboj.2012.99.

Wang, X. *et al.* (2005) 'CsrA post-transcriptionally represses *pgaABCD* , responsible for synthesis of a biofilm polysaccharide adhesin of *Escherichia coli*', *Molecular Microbiology*. John Wiley & Sons, Ltd (10.1111), 56(6), pp. 1648–1663. doi: 10.1111/j.1365-2958.2005.04648.x.

Wang, X. *et al.* (2006) 'In Vitro Polymerization of a Functional *Escherichia coli* Amyloid Protein', *Journal of Biological Chemistry*, 282(6), pp. 3713–3719. doi: 10.1074/jbc.M609228200.

Wang, X., Hammer, N. D. and Chapman, M. R. (2008) 'The molecular basis of functional bacterial amyloid polymerization and nucleation.', *The Journal of biological chemistry*. American Society for Biochemistry and Molecular Biology, 283(31), pp. 21530–9. doi: 10.1074/jbc.M800466200.

Wang, X., Preston, J. F. and Romeo, T. (2004) 'The pgaABCD locus of *Escherichia coli* promotes the synthesis of a polysaccharide adhesin required for biofilm formation.', *Journal of bacteriology*, 186(9), pp. 2724–34. doi: 10.1128/jb.186.9.2724-2734.2004.

Weatherspoon-Griffin, N. *et al.* (2014) 'The CpxR/CpxA Two-component Regulatory System Up-regulates the Multidrug Resistance Cascade to Facilitate *Escherichia coli* Resistance to a Model Antimicrobial Peptide *'. JBC Papers in Press. doi: 10.1074/jbc.M114.565762.

Weber, H. *et al.* (2005) 'Genome-Wide Analysis of the General Stress Response Network in *Escherichia coli*: S-Dependent Genes, Promoters, and Sigma Factor Selectivity', *Journal of Bacteriology*, 187(5), pp. 1591–1603. doi: 10.1128/JB.187.5.1591-1603.2005.

Weber, H. *et al.* (2006) 'Cyclic-di-GMP-mediated signalling within the S network of *Escherichia coli*'. doi: 10.1111/j.1365-2958.2006.05440.x.

Weigel, W. A. and Demuth, D. R. (2016) 'QseBC, a two-component bacterial adrenergic receptor and global regulator of virulence in *Enterobacteriaceae* and *Pasteurellaceae*', *Molecular Oral Microbiology*, 31(5), pp. 379–397. doi: 10.1111/omi.12138.

Weiss-Muszkat, M. *et al.* (2010) 'Biofilm Formation by and Multicellular Behavior of *Escherichia coli* O55:H7, an Atypical Enteropathogenic Strain', *Applied and Environmental Microbiology*, 76(5), pp. 1545–1554. doi: 10.1128/AEM.01395-09.

White-Ziegler, C. A. *et al.* (2008) 'Low temperature (23 C) increases expression of biofilm-, cold-shock- and RpoS-dependent genes in *Escherichia coli* K-12', *Microbiology*, 154(1), pp. 148–166. doi: 10.1099/mic.0.2007/012021-0.

White-Ziegler, C. A. and Davis, T. R. (2009) 'Genome-wide identification of H-NS-controlled, temperature-regulated genes in *Escherichia coli* K-12.', *Journal of bacteriology*. American Society for Microbiology Journals, 191(3), pp. 1106–10. doi: 10.1128/JB.00599-08.

White, A. P. *et al.* (2003) 'Extracellular polysaccharides associated with thin aggregative fimbriae of *Salmonella enterica* serovar enteritidis.', *Journal of bacteriology*. American Society for Microbiology (ASM), 185(18), pp. 5398–407. doi: 10.1128/jb.185.18.5398-5407.2003.

Whitman, W. B., Coleman, D. C. and Wiebe, W. J. (1998) 'Prokaryotes: the unseen majority.', *Proceedings of the National Academy of Sciences of the United States of America*, 95(12), pp. 6578–83. Available at: http://www.ncbi.nlm.nih.gov/pubmed/9618454 (Accessed: 5 March 2019).

Winn, M. *et al.* (2012) 'Biofilms and their engineered counterparts: A new generation of immobilised biocatalysts', *Catalysis Science & Technology*. The Royal Society of Chemistry, 2(8), p. 1544. doi: 10.1039/c2cy20085f.

Wolfe, A. J. *et al.* (2003) 'Evidence that acetyl phosphate functions as a global signal during biofilm development', *Molecular Microbiology*. John Wiley & Sons, Ltd (10.1111), 48(4), pp. 977–988. doi: 10.1046/j.1365-2958.2003.03457.x.

Wolfe, A. J. (2005) 'The Acetate Switch', *Microbiol. Mol. Biol. Rev.* American Society for Microbiology, 69(1), pp. 12–50. doi: 10.1128/MMBR.69.1.12-50.2005.

Wong, S. Y. *et al.* (2012) 'Drastically Lowered Protein Adsorption on Microbicidal Hydrophobic/Hydrophilic Polyelectrolyte Multilayers', *Biomacromolecules*, 13(3), pp. 719–726. doi: 10.1021/bm201637e.

Wood, J. M. (1999) 'Osmosensing by bacteria: signals and membrane-based sensors.', *Microbiology and molecular biology reviews : MMBR*. American Society for Microbiology (ASM), 63(1), pp. 230–62. Available at: http://www.ncbi.nlm.nih.gov/pubmed/10066837 (Accessed: 17 September 2019).

Wood, T. K. *et al.* (2006) 'Motility influences biofilm architecture in *Escherichia coli*', *Applied Microbiology and Biotechnology*, 72(2), pp. 361–367. doi: 10.1007/s00253-005-0263-8.

Wookey, P. J. and Pittard, A. J. (1988) 'DNA sequence of the gene (tyrP) encoding the tyrosine-specific transport system of *Escherichia coli*.', *Journal of Bacteriology*. American Society for Microbiology Journals, 170(10), pp. 4946–4949. doi: 10.1128/JB.170.10.4946-4949.1988.

van der Woude, M. W. and Henderson, I. R. (2008) 'Regulation and Function of Ag43 (Flu)', *Annual Review of Microbiology*, 62(1), pp. 153–169. doi: 10.1146/annurev.micro.62.081307.162938.

Wu, C. *et al.* (2012) 'Quantitative analysis of amyloid-integrated biofilms formed by uropathogenic *Escherichia coli* at the air-liquid interface.', *Biophysical journal*. The Biophysical Society, 103(3), pp. 464–71. doi: 10.1016/j.bpj.2012.06.049.

Wu, C. *et al.* (2013) 'Disruption of Escherichia coli amyloid-integrated biofilm formation at the air-liquid interface by a polysorbate surfactant.', *Langmuir : the ACS journal of surfaces and colloids*. NIH Public Access, 29(3), pp. 920–6. doi: 10.1021/la304710k.

Wuertz, S., Okabe, S. and Hausner, M. (2004) 'Microbial communities and their interactions in biofilm systems: an overview.', *Water science and technology : a journal of the International Association on Water Pollution Research*, 49(11–12), pp. 327–36. Available at: http://www.ncbi.nlm.nih.gov/pubmed/15303758 (Accessed: 11 June 2019).

Xavier, K. B. and Bassler, B. L. (2005) 'Regulation of uptake and processing of the quorum-sensing autoinducer AI-2 in *Escherichia coli*.', *Journal of bacteriology*.

American Society for Microbiology (ASM), 187(1), pp. 238–48. doi: 10.1128/JB.187.1.238-248.2005.

Xing, S.-F. *et al.* (2015) 'D-amino acids inhibit initial bacterial adhesion: thermodynamic evidence.', *Biotechnology and bioengineering*. NIH Public Access, 112(4), pp. 696–704. doi: 10.1002/bit.25479.

Yamamoto, K. *et al.* (2000) 'Negative regulation of the bolA1p of *Escherichia coli* K-12 by the transcription factor OmpR for osmolarity response genes', *FEMS Microbiology Letters*. John Wiley & Sons, Ltd (10.1111), 186(2), pp. 257–262. doi: 10.1111/j.1574-6968.2000.tb09114.x.

Yamamoto, K. *et al.* (2012) 'Involvement of flagella-driven motility and pili in *Pseudomonas aeruginosa* colonization at the air-liquid interface.', *Microbes and environments*, 27(3), pp. 320–3. doi: 10.1264/jsme2.me11322.

Yang, K. *et al.* (2014) 'The Role of the QseC Quorum-Sensing Sensor Kinase in Epinephrine-Enhanced Motility and Biofilm Formation by *Escherichia coli*', *Cell Biochemistry and Biophysics*, 70(1), pp. 391–398. doi: 10.1007/s12013-014-9924-5.

Yang, L. *et al.* (2011) 'Distinct roles of extracellular polymeric substances in *Pseudomonas aeruginosa* biofilm development', *Environmental Microbiology*, 13(7), pp. 1705–1717. doi: 10.1111/j.1462-2920.2011.02503.x.

Yang, Y. *et al.* (2015) 'Relation between chemotaxis and consumption of amino acids in bacteria.', *Molecular microbiology*. Wiley-Blackwell, 96(6), pp. 1272–82. doi: 10.1111/mmi.13006.

Yanofsky, C., Horn, V. and Gollnick, P. (1991) 'Physiological studies of tryptophan transport and tryptophanase operon induction in *Escherichia coli*.', *Journal of bacteriology*. American Society for Microbiology Journals, 173(19), pp. 6009–17. doi: 10.1128/jb.173.19.6009-6017.1991.

Yao, Y. *et al.* (2006) 'Structure of the *Escherichia coli* Quorum Sensing Protein SdiA: Activation of the Folding Switch by Acyl Homoserine Lactones', *Journal of Molecular Biology*, 355(2), pp. 262–273. doi: 10.1016/j.jmb.2005.10.041.

Yoshida, T. *et al.* (2006) 'Transcription Regulation of *ompF* and *ompC* by a Single Transcription Factor, OmpR', *Journal of Biological Chemistry*, 281(25), pp. 17114–17123. doi: 10.1074/jbc.M602112200.

Zhang, T. *et al.* (2007) ‘Improved performances of *E. coli*-catalyzed microbial fuel cells with composite graphite/PTFE anodes’, *Electrochemistry Communications*. Elsevier, 9(3), pp. 349–353. doi: 10.1016/J.ELECOM.2006.09.025.

Zhang, X.-S., García-Contreras, R. and Wood, T. K. (2007) ‘YcfR (BhsA) influences *Escherichia coli* biofilm formation through stress response and surface hydrophobicity.’, *Journal of bacteriology*. American Society for Microbiology (ASM), 189(8), pp. 3051–62. doi: 10.1128/JB.01832-06.

Zhao, K., Liu, M. and Burgess, R. R. (2007) ‘Adaptation in bacterial flagellar and motility systems: from regulon members to ’foraging’-like behavior in *E. coli*.’, *Nucleic acids research*. Oxford University Press, 35(13), pp. 4441–52. doi: 10.1093/nar/gkm456.

Zheng, D. *et al.* (2004) ‘Identification of the CRP regulon using in vitro and in vivo transcriptional profiling.’, *Nucleic acids research*. Oxford University Press, 32(19), pp. 5874–93. doi: 10.1093/nar/gkh908.

Zhou, Y. and Gottesman, S. (2006) ‘Modes of regulation of RpoS by H-NS.’, *Journal of bacteriology*. American Society for Microbiology (ASM), 188(19), pp. 7022–5. doi: 10.1128/JB.00687-06.

Zobell, C. E. *et al.* (1943) ‘The Effect of Solid Surfaces upon Bacterial Activity.’, *Journal of bacteriology*. American Society for Microbiology Journals, 46(1), pp. 39–56. Available at: http://www.ncbi.nlm.nih.gov/pubmed/16560677 (Accessed: 6 March 2019).

Zogaj, X. *et al.* (2001) ‘The multicellular morphotypes of *Salmonella typhimurium* and *Escherichia coli* produce cellulose as the second component of the extracellular matrix.’, *Molecular microbiology*, 39(6), pp. 1452–63. Available at: http://www.ncbi.nlm.nih.gov/pubmed/11260463 (Accessed: 14 May 2019).

8 APPENDICES

APPENDIX 1 SEQUENCING DATA

Position	Ref Allele Forward Strand	Alt Allele Fwd Strand	Average Depth	No calls	Homozygous calls	Het calls	Mutation Type	Mutation Strength	Mutation Type2	Codon Substitution	Amino Acid Substitution	Locus Tag	Gene	PHL644h	PHL644	Discriminatory	Maximum Frequency	Comments
75949	G	A	82	0	1	1	SYNONYMOUS CODING	LOW	SILENT	agC/agT	S450	BN896_RS00350	HTH-type transcriptional regulator sgrR	A	G/A	Y	78.12	Silent mutations
75952	C	T	81	0	1	1	SYNONYMOUS CODING	LOW	SILENT	gaG/gaA	E449			T	C/T	Y	77.42	
276948	G	A	85	0	0	1							upstream of mhpT	G/A		Y	13.64	No evidence in literature to link to motility or biofilms
276955	T	C	81	0	0	1								T/C		Y	10.94	
276956	G	A	82	0	0	1								G/A		Y	13.85	
276962	T	C	85	0	0	1								T/C		Y	13.43	
276969	T	C	87	0	0	1								T/C		Y	13.43	
276976	AGAC	A	86	0	0	1								AGAC/A		Y	13.64	
276986	GCGT	G	79	0	0	1								GCGT/G		Y	15.25	
277005	CG	C	81	0	0	1								CG/C		Y	13.33	
277029	A	G	96	0	0	1								A/G		Y	13.11	
277050	A	G	93	0	0	1								A/G		Y	14.29	
277105	GC	G	85	0	0	1								GC/G		Y	12.31	
277113	C	T	88	0	0	1								C/T		Y	20	
277130	A	G	98	0	0	1									A/G	Y	15.08	
277151	G	A	92	0	0	1									G/A	Y	10.43	
410583	T	C	89	0	0	1							intergentic region		T/C	Y	11.3	Between the ends of two genes - higA family addiction module antidote protein - and copper-exporting P-type ATPase copA
480792	T	C	158	0	1	1	NON SYNONYMOUS CODING	MODERATE	MISSENSE	Aca/Gca	T29A	BN896_RS02400	Prophage DLP12 serum resistance lipoprotein borD	T/C	C	Y	75.54	DLP12 removal deletion leads to decreased biofilm formation in E. coli K-12.
480794	T	G	157	0	1	1	NON SYNONYMOUS CODING	MODERATE	MISSENSE	cAg/cCg	Q28P			T/G	G	Y	75.96	

																		(Wang et al. 2010)
886558	T	TG	85	0	0	1	FRAME SHIFT	HIGH		cgg/Gcgg	R27A?	BN896_RS24500	Hypothetical		T/TG	Y	10.09	No evidence in literature to link to motility or biofilms
886566	G	A	86	0	0	1	NON SYNONYMOUS CODING	MODERATE	MISSENSE	Gag/Aag	E29K				G/A	Y	10.09	
1156894	C	T	55	0	0	1	NON SYNONYMOUS CODING	MODERATE	MISSENSE	Ggc/Agc	G29S	BN896_RS05760	Small toxic polypeptide ldrB	C/T		Y	15.91	No evidence in literature to link to motility or biofilms
1318309	A	G	178	0	1	1	SYNONYMOUS CODING	LOW	SILENT	gaA/gaG	E244	BN896_RS23165	stfR - Rac prophage side tail fiber protein	A/G	G	Y	76.17	Rac removal and also stfR deletion led to decreased biofilm formation in E. coli K-12 in M9C medium. (Wang et al. 2010)
1318312	G	A	181	0	1	1	SYNONYMOUS CODING	LOW	SILENT	gcG/gcA	A245			G/A	A	Y	75.52	
1318380	G	A	190	0	1	1	NON SYNONYMOUS CODING	MODERATE	MISSENSE	gGa/gAa	G268E			G/A	A	Y	75.21	
1318417	C	T	180	0	1	1	SYNONYMOUS CODING	LOW	SILENT	aaC/aaT	N280			C/T	T	Y	75	
1320595	A	T	116	0	0	1	SYNONYMOUS CODING	LOW	SILENT	gcA/gcT	A1006			A/T		Y	12.22	stfR mutant made more biofilm in LB glucose medium than wt (Domka 2007)
1320599	A	G	135	0	0	1	NON SYNONYMOUS CODING	MODERATE	MISSENSE	Aca/Gca	T1008A			A/G		Y	12.38	
1320601	A	T	137	0	0	1	SYNONYMOUS CODING	LOW	SILENT	acA/acT	T1008			A/T		Y	11.93	Rac removal led to increased biofilm formation in K-12 in LB and M9C-glu. (Liu et al. 2015)
1320608	G	C	128	0	0	1	NON SYNONYMOUS CODING	MODERATE	MISSENSE	Gtg/Ctg	V1011L			G/C		Y	12.38	
1321149	T	C	78	0	0	1	SYNONYMOUS CODING	LOW	SILENT	gaT/gaC	D70	BN896_RS06650	tfrA - Rac prophage tail fiber assembly protein	T/C		Y	12.9	Rac removal led to increased motility in E. coli K-12 (Liu et al. 2015). This effect was shown to be not caused by IS insertion at flhDC.
1354730	T	C	87	0	0	1	SYNONYMOUS CODING	LOW	SILENT	ggT/ggC	G270	BN896_RS06795	Hypothetical	T/C		Y	16.46	Silent mutations
1354739	G	A	85	0	0	1	SYNONYMOUS CODING	LOW	SILENT	gcG/gcA	A273			G/A		Y	18.42	
1354799	C	T	78	0	0	1	SYNONYMOUS CODING	LOW	SILENT	atC/atT	I293			C/T		Y	12.12	
1421790	A	C	58	0	0	1	NON SYNONYMOUS CODING	MODERATE	MISSENSE	aaA/aaC	K70N	BN896_RS07110	pptA	A/C		Y	12	No evidence in literature to link to motility or biofilms
2420909	T	C	29	0	0	1	NON SYNONYMOUS	MODERA	MISSENSE	Ttt/Ctt	F58L	BN8	Hypothetical	T/C		Y	19.35	No evidence in literature

							CODING	TE				96 R S247 10						to link to motility or biofilms
2420911	T	G	28	0	0	1	NON SYNONYMOUS CODING	MODERATE	MISSENSE	ttT/ttG	F58L			T/G		Y	16.67	
2742602	G	T	12	0	1	1							upstream of 23S rRNA	T	G/T	Y	90.91	No evidence in literature to link to motility or biofilms
2742607	C	T	12	0	1	1							upstream of 23S rRNA	T	C/T	Y	90	
2841331	T	C	4	0	1	0							Upstream of rbsR		C	Y	100	RbsR is a pleiotrpoic regulator of motility in Serratia (Lee et al., 2017).
3177000	A	G	43	0	0	1							Upstream of ftsY		A/G	Y	12	No evidence in literature to link to motility or biofilms
3336379	C	T	61	0	0	1	NON SYNONYMOUS CODING	MODERATE	MISSENSE	tCt/tTt	S105F	BN896_RS16450	30S ribosomal protein S8	C/T		Y	13.33	No evidence in literature to link to motility or biofilms
3355811	TCGAAA	T	78	0	0	1							Upstream of 23S rRNA	TCGAAA/T		Y	17.31	No evidence in literature to link to motility or biofilms
4427131	A	C	34	0	0	1	SYNONYMOUS CODING	LOW	SILENT	acA/acC	T69	BN896_RS21900	IS1 family transposase		A/C	Y	11.11	Silent mutation

References for Appendix table:

Domka J, Lee J, Bansal T, Wood TK. (2007) Temporal gene-expression in *Escherichia coli* K-12 biofilms. Environ Microbiol. 9:332-46.

Lee CM, Monson RE, Adams RM, Salmond GPC. (2017) The LacI-Family Transcription Factor, RbsR, Is a Pleiotropic Regulator of Motility, Virulence, Siderophore and Antibiotic Production, Gas Vesicle Morphogenesis and Flotation in Serratia. Front Microbiol. 8:1678. doi: 10.3389/fmicb.2017.01678.

Liu X, Li Y, Guo Y, Zeng Z, Li B, Wood TK, Cai X, Wang X. (2015) Physiological Function of Rac Prophage During Biofilm Formation and Regulation of Rac Excision in *Escherichia coli* K-12. Sci Rep. 5:16074. doi: 10.1038/srep16074.

Wang X, Kim Y, Ma Q, Hong SH, Pokusaeva K, Sturino JM, Wood TK. (2010) Cryptic prophages help bacteria cope with adverse environments. Nat Commun. 1:147. doi: 10.1038/ncomms1146.